

Androgenic switch in barley microspores

Simone de Faria Maraschin

Cover: Cell walls of barley androgenic embryos
Designed by Peter Hock

Printed by: Ridderprint, Ridderkerk, The Netherlands

ISBN: 90-5335-046-2

Androgenic switch in barley microspores

Proefschrift

Ter verkrijging van
de graad van Doctor aan de Universiteit Leiden,
op gezag van de Rector Magnificus Dr. D.D. Breimer,
hoogleraar in de faculteit der Wiskunde en
Natuurwetenschappen en die der Geneeskunde,
volgens besluit van het College voor Promoties
te verdedigen op woensdag 9 februari 2005
te klokke 15:15 uur

door

Simone de Faria Maraschin

geboren te Laguna (Brazilië) in 1976

Promotiecomissie

Promotor: Prof. Dr. H.P. Spaink

Co-promotor: Dr. M. Wang

Referent: Prof. Dr. E. Matthys-Rochon (CNRS, Lyon, Frankrijk)

Overige leden: Prof. Dr. E. van der Meijden
Prof. Dr. P.J.J. Hooykaas
Dr. S. de Pater

“Androgenic switch in barley microspores” by Simone de Faria Maraschin

Reproduction of color prints was financially supported by the Leiden University Foundation.

*Para minha família
Pai, Mãe, Jorge e Ângela
Que saudades!*

Contents	Page
Outline of thesis	9
Chapter 1 Androgenic switch in microspores	13
Chapter 2 Time-lapse tracking of barley androgenesis reveals position- determined cell death within pro-embryos	45
Chapter 3 Programmed cell death during the transition from multicellular structures to globular embryos in barley androgenesis	65
Chapter 4 14-3-3 proteins in barley androgenesis	87
I. 14-3-3 isoforms and pattern formation during barley microspore embryogenesis	89
II. Tissue-specific expression of 14-3-3 isoforms during barley microspore and zygotic embryogenesis	111
III. Cell death and 14-3-3 proteins during the induction of barley microspore embryogenesis	119
Chapter 5 cDNA array analysis of stress-induced gene expression in barley androgenesis	135
Summary	163
Samenvatting	169
<i>Curriculum vitae</i>	175
Publications	177
Color supplement	179

Outline of thesis

Barley androgenesis represents an attractive system to study stress-induced cell differentiation and is a valuable tool for efficient plant breeding. The switch from the pollen developmental pathway towards the androgenic route involves several well-described morphological changes. However, little is known about the pathways leading to embryo formation and about the transcriptome of androgenic microspores. By combining molecular, biochemical and cytological techniques, the research described in this thesis aimed to identify new 'bio-markers' for barley androgenesis induction and embryo development. The concept of a 'bio-marker' is not a single gene, protein, metabolite or phenotype. It refers to the concept of understanding biological events, such as gene expression profiles or morphological changes at certain biological states.

As shown by several experiments, microspore embryogenic development is divided into three main characteristic, overlapping phases: acquisition of embryogenic potential by stress, initiation of cell divisions and pattern formation. The main molecular and cellular events that characterize the different commitment phases of microspores into embryos are reviewed in chapter 1. This chapter presents an overview of the progress that the research on androgenesis induction has made in the recent years, emphasizing the phase of microspore embryogenic potential acquisition and initiation of cell divisions. In addition, this chapter draws a parallel between the molecular and cellular biology of androgenic development with that of the two most extensively studied model systems, somatic and zygotic embryogenesis.

In chapter 2, the developmental pathways of stressed microspores are elucidated by time-lapse tracking. This chapter describes the identification of embryogenic microspores and of a position-determined cell death process in the transition from multicellular structures to globular embryos.

In chapter 3, the cell death process that takes place during microspore embryo formation is characterized as programmed cell death. This study provides evidence for a role of the vegetative cell in the formation of globular embryos and for the programmed elimination of the generative derivatives during exine wall rupture.

Chapter 4 is composed of three parts, each concerning different aspects of the expression and tissue-specificity of three isoforms of the 14-3-3 family of regulatory proteins (14-3-3A, 14-3-3B and 14-3-3C). In part I, the differences between the spatial and temporal expression of the individual isoforms during microspore-derived embryo development in parallel to zygotic embryogenesis are presented. In part II, the specific expression of the 14-3-3C isoform is demonstrated to be restricted to the L₂ layer of the shoot apical meristem in microspore-derived and zygotic embryos, as well as to L₂ layer-derived cells of *in vitro* shoot meristematic cultures. In part III, a link is established between the post-translational

modification of the 14-3-3A isoform and the programmed cell death of anther walls and non-embryogenic microspores during androgenesis induction.

Finally, chapter 5 describes the use of an array approach in combination with multivariate data analysis in the identification of gene expression profiles associated with the induction of androgenesis. This chapter shows that pollen-related genes are down-regulated during the reprogramming of microspores, providing molecular evidence that stress acts in blocking pollen development. In addition, it reveals that genes involved in proteolysis, sugar and starch hydrolysis, stress responses, inhibition of programmed cell death and signaling are up-regulated during barley androgenesis induction.

Chapter 1

Androgenic switch in microspores

Submitted

Simone de Faria Maraschin, Wessel de Priester, Herman P. Spaink, Mei Wang

Abstract

Embryogenesis in plants is a unique process in the sense that it can be initiated from a wide range of cells other than the zygote. Upon stress, microspores or young pollen grains can be switched from their normal pollen development towards an embryogenic pathway, a process called androgenesis. Androgenesis represents an important tool for research in plant genetics and breeding, since androgenic embryos can germinate into completely homozygous, double haploid plants. From a developmental point of view, androgenesis is a rewarding system for understanding the process of embryo formation from single, haploid microspores. Androgenic development can be divided into three main characteristic phases: acquisition of embryogenic potential, initiation of cell divisions and pattern formation. The aim of this review is to provide an overview of the main cellular and molecular events that characterize these three commitment phases. Molecular approaches such as differential screening and cDNA array have been successfully employed in the characterization of the spatiotemporal changes in gene expression during androgenesis. These results suggest that the activation of key regulators of embryogenesis, such as the *BABY BOOM* transcription factor, is preceded by the stress-induced reprogramming of cellular metabolism. Reprogramming of cellular metabolism includes the repression of gene expression related with starch biosynthesis and the induction of proteolytic genes (e.g. components of the 26S proteasome, metalloprotease, cysteine and aspartic proteases) and stress-related proteins (e.g. *GST*, *HSP*, *BI-1*, *ADH*). The combination of cell tracking systems with biochemical markers has allowed us to determine the key switches in the developmental pathway of microspores, as well as to identify programmed cell death as a feature of successful androgenic embryo development. The mechanisms of androgenesis induction and embryo formation are discussed in relation to other biological systems, in special zygotic and somatic embryogenesis.

Embryogenesis in higher plants

Embryogenesis has evolved as a successful strategy for the reproduction of higher multicellular organisms. Zygotic embryogenesis in animals and plants starts with the fusion of the haploid female and male gametes, giving rise to a diploid zygote. The zygote possesses the ability to initiate embryogenesis, a developmental program that leads to the establishment of an embryo with the basic features of the adult body plan. This widely conserved mechanism of reproduction has, however, major differences between animal and plant

kingdoms, as plant embryos can develop *in vivo* or *in vitro* from a wide range of cell types other than the zygote (Mordhorst et al., 1997). The development of techniques and protocols to asexually produce plant embryos has had a huge technological and economical impact on agricultural systems, and nowadays these biotechnologies represent an integral part in the breeding programs of agronomically important crops.

Figure 1 provides an overview of the distinct types of cells that can undergo embryogenic development in higher plants. During *in vivo* development, maternal apomixis refers to the asexual formation of a seed from the maternal tissues of the ovule, avoiding the processes of meiosis and fertilization (Koltunow, 1993). Maternal apomictic embryos develop from a somatic cell within the ovule (apospory) or from an unreduced embryo sac derived from the megaspore mother cell (diplospory). In either cases, apomictic embryo development is independent of pollination, but in some species this might be required for the initiation of endosperm development and the production of viable seeds (Koltunow et al., 1998). Another type of apomictic development has been reported to occur in the gymnosperm *Cupressus dupreziana*, where embryos develop from unreduced pollen grains. This type of apomixis is referred to as paternal apomixis (Pichot et al., 2001). Because apomixis offers the possibility of the fixation and indefinite propagation of a desired genotype, there has been a great deal of interest in genetically engineering this ability. Nevertheless, so far it has not been possible to manipulate the apomictic trait for clonal reproduction via seeds (Bicknell and Koltunow, 2004). Clonal propagation is usually achieved via the induction of *in vitro* somatic embryogenesis, a process that is defined as the regeneration of a whole plant from undifferentiated somatic cells in culture. Induction of somatic embryogenesis is usually achieved by a stress and/or hormone treatment of somatic cells. Depending on the donor tissue and the induction treatment conditions, embryos may develop either directly from single cells or indirectly through an intermediary callus phase (Zimmerman, 1993). Additional routes to *in vitro* embryogenesis are defined by the ability of male and female gametes to irreversibly switch from their gametophytic pathway towards an embryogenic route. While androgenesis refers to the development of embryos from microspores or immature pollen grains (Touraev et al., 1997), gynogenesis refers to the development of embryos from unfertilized ovaries *in vitro* or *in vivo* (Gémes-Jushász et al., 2002; Musial et al., 2001). In contrast to apomixis and somatic embryogenesis, which lead to clonal propagation of a specific genotype, androgenic and gynogenic plants reflect the product of meiotic segregation. Thus, they have the remarkable characteristic of possessing only one set of chromosomes, and therefore are haploid plants.

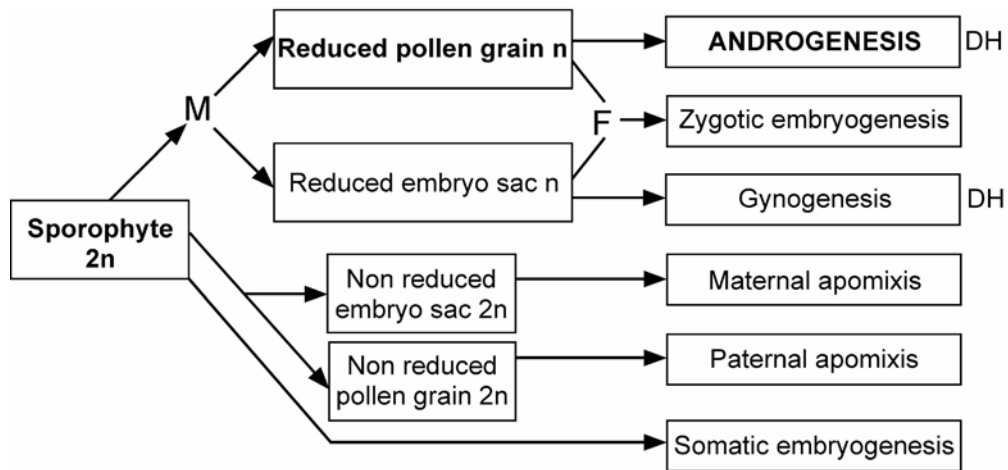


Figure 1. Overview of the different types of cells that can undergo embryogenic development in higher plants. *F* fertilization, *DH* double haploid, *M* mitosis.

Androgenesis as a double haploidization tool for efficient plant breeding

For breeding purposes, the evaluation of diversity in genetic pools and the establishment of homozygous lines are of critical importance. Homozygosity is traditionally achieved by performing time-consuming and labor-intensive backcrosses (Morrison and Evans, 1988). Haploid plants derived from microspores opened a new dimension for the production of homozygous lines due to the large amount of microspores that are produced by a single plant. Due to the colchicine-induced or spontaneous process of chromosome doubling that takes place during the early stages of embryo development, fertile double haploid plants can be easily regenerated within a short period of time (Wang et al., 2000). The production of double haploids via androgenesis represents, in this context, a powerful technique both for the production of hybrid seeds and the evaluation of genetic diversity. Though androgenesis is a naturally occurring process in some species, the *in vivo* frequency is very low (Rammana, 1974; Rammana and Hermsen, 1974; Koul and Karihaloo, 1977). Efficient androgenesis is usually induced by the application of a stress treatment to whole plants *in vivo* or tillers, buds, anthers and isolated microspores *in vitro* (Touraev et al., 1997). Since the first description of androgenesis in *in vitro*-cultured anthers of *Datura innoxia* by Guha and Maheshwari (1964), improvement of the conditions for androgenesis induction and microspore culture have resulted in the regeneration of double haploids of many plant species. However, many agronomically important crops are recalcitrant to androgenesis (Wang et al., 2000). Further use of this technology is largely hampered by the poor understanding of the mechanisms that render microspore cells embryogenic. *In vitro* embryogenesis systems, here represented by androgenesis, are excellent model systems to

study the developmental aspects of embryogenesis induction and embryo formation from single, haploid microspores. As shown by several experiments, embryogenic development during androgenesis is divided into three main characteristic, overlapping phases: in phase I, acquisition of embryogenic potential by stress involves repression of gametophytic development and leads to the dedifferentiation of the cells; in phase II, cell divisions lead to the formation of multicellular structures (MCSs) contained by the exine wall; in phase III, embryo-like structures (ELs) are released out of the exine wall and pattern formation takes place. A time-line of the three different phases during androgenic development in the model species barley is shown in Figure 2a. The aim of this review is to provide an overview of the main molecular and cellular events that characterize the different commitment phases of microspores into embryos, and to highlight their similarities and differences with the two most extensively studied model systems, somatic and zygotic embryogenesis. Special emphasis is given to the initial stages of microspore embryogenic potential acquirement and the initiation of cell divisions.

Androgenesis induction: the role of stress

Owing to their high regeneration efficiencies, barley (*Hordeum vulgare* L.), rapeseed (*Brassica napus* L.), tobacco (*Nicotiana* spp) and wheat (*Triticum aestivum* L.) have been considered model species to study the mechanisms of stress-induced androgenesis (Touraev et al., 1997). However, with the recent advances in protocol design, molecular and morphological studies are now possible in other plant species, such as maize (*Zea mays*; Magnard et al., 2000) and pepper (*Capsicum annum* L.; Bárány et al., 2001). Lessons learned from these advanced model systems suggest that androgenesis can be efficiently triggered within a relatively wide developmental window. During pollen development, the responsive period for androgenesis is represented by the stages that surround the asymmetrical division of the uninucleate microspores, resulting in a polarized pollen grain containing a generative cell embedded in the large vegetative cytoplasm. The vegetative and generative cells differ markedly, as the small condensed generative cell will undergo an

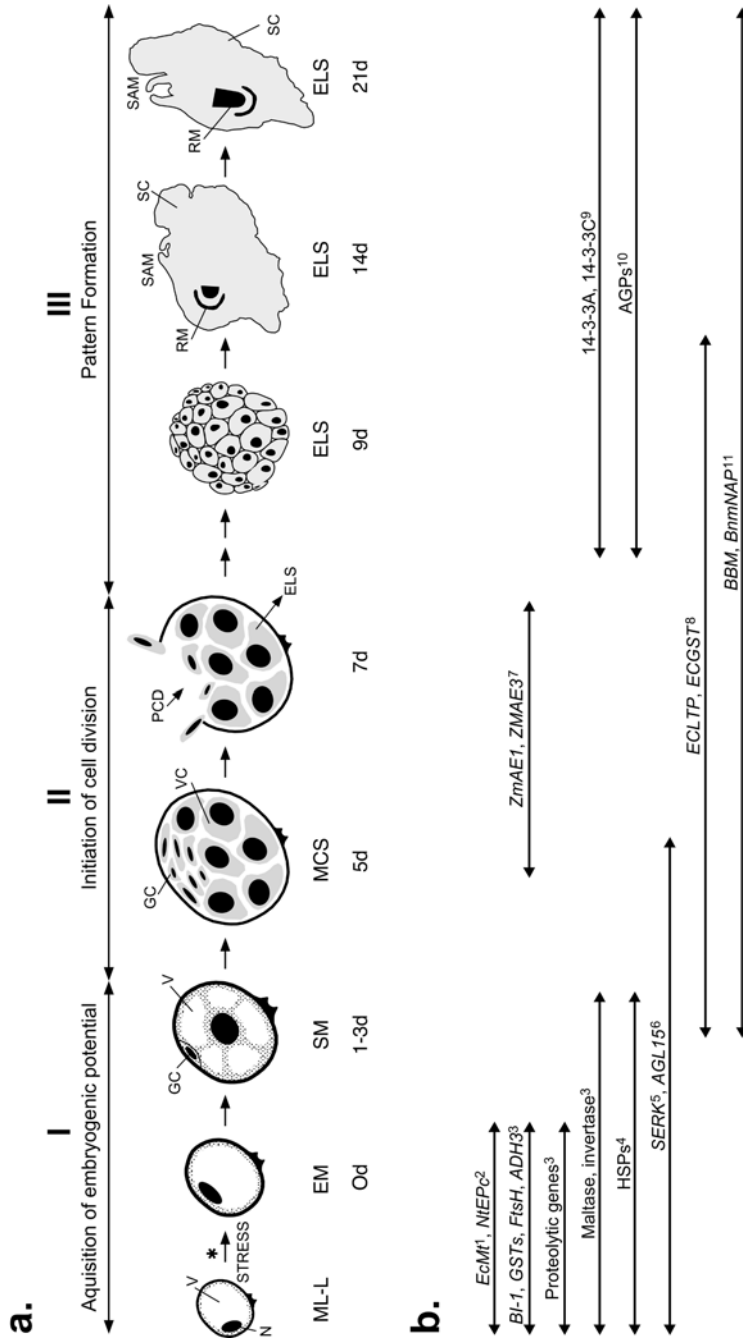


Figure 2. Cellular and molecular aspects of androgenesis. (a) Time-line of *in vitro* androgenic development in the model species barley illustrating the three different phases of embryogenic development. ELS embryo-like structure, EM enlarged microspore, GC generative cell, MCS multicellular structure, ML-L mid-late to late uninucleate microspore, N nucleus, PCD programmed cell death, RM root meristem, SAM shoot apical meristem, SC scutellum, SM star-like microspore, V vacuole, VC vegetative cell. (b) Based on gene expression data collected from barley androgenesis and other androgenic model species, the gene expression programs associated with each phase are displayed underneath the time-line. Reynolds and Crawford (1996);² Kyo et al. (2000);³ Maraschin et al. (2004c);⁴ Pechan et al. (1991), Cordewener et al. (1994, 1997), Zarsky et al. (1995), Smykal and Pechan (2000), Bárányi et al. (2001);⁵ Baudino et al. (2001);⁶ Perry et al. (1999);⁷ Magnard et al. (2000);⁸ Vrienten et al. (1999);⁹ Maraschin et al. (2003a);¹⁰ Borderies et al. (2004);¹¹ Boutillier et al. (1994, 2002).

additional mitotic division to produce two sperm cells, while the vegetative cell will start an intense program of accumulation of storage products, namely starch and lipids to drive further pollen maturation (Bedinger, 1992; McCormick, 1993). It is widely accepted that when the vegetative cytoplasm of binucleate pollen starts to accumulate starch, androgenesis can be no longer triggered (Touraev et al., 1997; Binarova et al., 1997).

Another important postulation based on practical experience is that the stress treatment which is needed to efficiently switch the developmental fate of microspores greatly varies depending on the plant species and the species genotype. In barley, higher regeneration efficiencies are obtained when microspores at the mid-late to late (ML-L) uninucleate stage are subjected to starvation and osmotic stress, which is achieved by incubating anthers in a mannitol solution (Hoekstra et al., 1992). In wheat and tobacco, higher induction rates are achieved by a period of starvation in combination with heat shock (Touraev et al., 1996a,b), whereas a heat shock treatment alone is sufficient to induce androgenesis in rapeseed and pepper (Custers et al., 1994; Bárány et al., 2001). However, other types of stresses applied within the responsive developmental window have been demonstrated to trigger androgenesis at lower rates. They consist of subjecting cells to colchicine (Barnabás et al., 1991; Zhao et al., 1996; Obert and Barnabás, 2004), nitrogen starvation (Kyo and Harada, 1986), auxin (Reynolds and Kitto, 1992; Hoekstra et al., 1996), chemicals, gamma irradiation (Pechan and Keller, 1989; Zheng et al., 2001) and cold treatment (Gaillard et al., 1991; Kasha et al., 2001). Since so many stress factors can trigger the reprogramming of microspores into embryos, it is likely that initiation of androgenesis is induced by converging signaling pathways, although, of course, different stress signals may trigger the same downstream pathways. An analogous situation may be found during the induction of somatic embryogenesis, where the transition of somatic cells to an embryogenic state is regulated by different classes of hormones, namely auxin, cytokinins and abscisic acid (ABA; de Vries et al., 1988; Filonova et al., 2000; Nishiwaki et al., 2000), as well as by wounding, osmotic stress, starvation and heavy metal ions (Ikeda-Iwai et al., 2003). During zygotic embryogenesis, however, stress *per se* is not directly involved with zygotic embryogenic competence. The ability of the zygote to initiate embryogenesis appears to be related to an increase in the endogenous auxin levels after fertilization (Ribnicky et al., 2001). Interestingly, reactive oxygen species (ROS) are second messengers during auxin- and stress-induced embryogenesis (Nagata et al., 1994). Mitogen-activated protein kinase (MAPK) cascades may link auxin signaling to oxidative stress responses and cell cycle regulation (reviewed by Hirt, 2000), and a MAPK has been reported to be activated via stress-related ABA signaling (Knetsch et al., 1996). Thus, it is likely that downstream

regulatory proteins, such as MAPKs, play an important role in bridging the gap between embryogenesis induction in different types of cells.

Morphological changes associated with embryogenic microspores

Upon mannitol treatment to induce barley androgenesis, microspores enlarge, and this has been correlated with embryogenic potential acquirement during induction of androgenesis in many crop species (Hoekstra et al., 1992; Touraev et al., 1996a,b). Embryogenic microspores are characterized by the presence of a large central vacuole, and a clear cytoplasm (Hoekstra et al., 1992; Maraschin et al., 2003a; Huang, 1986). In other embryogenic systems, such as carrot (*Daucus carota* L.) somatic embryogenesis, competent cells are present among a subpopulation of enlarged vacuolated cells (Schmidt et al., 1997; McCabe et al., 1997), and during zygotic embryogenesis plant egg cells show a rapid increase in volume after fertilization (Mansfield and Briarty, 1991; Møl et al., 1994). However, after the induction of somatic embryogenesis in *Dactylis glomerata* and Norway spruce (*Picea abies* L. Karst), enlarged cells are not competent to become embryos. In these species, it is a subpopulation of small, cytoplasm rich cells that become embryogenic (Somleva et al., 2000; Filonova et al., 2000). This indicates that besides cell size, other morphological markers are associated with embryogenic potential. During androgenesis, one of these markers is the degree of cytoplasmic dedifferentiation of enlarged cells. Initiation of cell division from stressed microspores has been correlated with specific ultrastructural changes, including organelle-free regions in the cytoplasm, a significant decrease in the number and size of starch granules and lipid bodies, and an overall decline in the number of ribosomes (Rashid et al., 1982; Huang 1986; Telmer et al., 1995; Maraschin et al., 2004a). Specifically in barley, these cytoplasmic changes are associated with the presence of a thin intine layer, contrasting to the thick intine layer displayed by pollen cells (Maraschin et al., 2004a). Based on these morphological observations, it has been proposed that stress leads to the dedifferentiation of microspores by the repression of gametophytic development. There are two known pathways in eukaryotic cells that lead to cytoplasmic remodeling, the ubiquitin-26S proteasomal system, which is the major cellular pathway for the degradation of short- and long-lived molecules, and autophagy, which is the primary intracellular mechanism for degrading and recycling organelles via the lysosomes. Though these pathways are developmentally regulated, they are also activated upon stress conditions, e.g., starvation, heat shock and low temperatures (Levine and Klionsky, 2004). During the initial steps of androgenesis induction in tobacco, cytoplasmic organelles undergo programmed destruction,

a process that has been shown to be mediated by the lysosomes (Sunderland and Dunwell, 1974). However, not only autophagy seems to take place in cytoplasm remodeling during the dedifferentiation phase of microspores, as genes coding for enzymes involved in the ubiquitin-26S proteosomal pathway are induced in stressed enlarged barley microspores (Maraschin et al., 2004c).

Following cytoplasm dedifferentiation, the nucleus migrates towards the center of the cell, while the large central vacuole is divided into fragments, interspersed by radially oriented cytoplasmic strands. The resulting morphology, often called star-like structure because of its radial polarity, has been described in several androgenic model systems, including barley, wheat, rapeseed and tobacco (Maraschin et al., 2004a; Indrianto et al., 2001; Zaki and Dickinson, 1991; Touraev et al., 1996a,b). During pollen development, the peripheral nuclear position is maintained by microtubules and actin filaments (Hause et al., 1992). Since the treatment of uninucleate microspores using colchicine or cytochalasin D is sufficient to trigger androgenesis by displacing the microspore nucleus towards the center of the cell, it has been proposed that cytoskeleton rearrangements are involved in androgenesis induction (Zaki and Dickinson, 1991; Barnabás et al., 1991; Zhao et al., 1996; Gervais et al., 2000; Obert and Barnabás, 2004). One of the proposed models for the role of cytoskeleton rearrangements in androgenesis induction is related to the symmetrical divisions that are observed following central positioning of the nucleus (Zaki and Dickinson, 1991). According to Simmonds and Keller (1999), this symmetrical division is important in establishing consolidated cell walls via the formation of continuous preprophase bands, a crucial step in the formation of a multicellular organism. However, induction of maize androgenesis by colchicine does not lead to symmetric divisions of the microspore nucleus (Barnabás et al., 1999). These results indicate that the role of cytoskeleton inhibitors in androgenesis induction is not restricted to the induction of symmetric divisions, but it is likely to involve the induction of radial polarity in the microspores. At the early binucleate stage, after the asymmetric pollen division, androgenesis in rapeseed can be efficiently triggered by a heat shock treatment at 32°C (Custers et al., 1994), and in late binucleate pollen by an extra heat shock treatment at 41°C (Binarova et al., 1997). Interestingly, heat shock leads to cytoskeleton rearrangements and central positioning of the vegetative nucleus (Zhao and Simmonds, 1995; Binarova et al., 1997), as do cold (Wallin and Stromberg, 1995; Sopory and Munchi, 1996). Though it is not yet known whether starvation leads to cytoskeleton rearrangements, starvation leads to the displacement of the nucleus towards the center of the cell (Indrianto et al., 2001; Touraev et al. 1996a,b; Maraschin et al., 2004a).

Cell tracking studies on barley and wheat revealed that star-like morphology represents the transition from a dedifferentiated state to the initiation of cell divisions, and

therefore corresponds to the first morphological change associated with microspore embryogenic potential (Indrianto et al., 2001; Maraschin et al., 2004a). Further ultrastructural studies of barley star-like structures revealed that the vegetative nucleus migrates to the middle of the structure, while the generative cell remains attached to the intine (Fig. 3). Following the central positioning of the vegetative nucleus, both generative and vegetative cells start to divide (Maraschin et al., 2004a,b). In agreement with the hypothesis that central nuclear positioning is related to initiation of cell divisions, star-like structures are a characteristic morphology following hormone or heat treatment to induce somatic embryogenesis in *Chichorium* (Dubois et al., 1991; Blervacq et al., 1995) and have been reported in isolated egg cells in culture (Kranz et al., 1995). Nevertheless, star-like morphology *per se* does not assure that a cell will ultimately commit to the embryogenic pathway. According to Indrianto et al. (2001), the occurrence of star-like morphology is part of a dynamic process, where the time of occurrence will depend on the type of stress applied and the stage of microspore development. In barley androgenesis, enlarged microspores acquire star-like morphology within the first days after the onset of culture. Successful embryo formation, however, is restricted to a group of enlarged microspores that has the tendency to display star-like structures relatively later than the majority (Maraschin et al., 2004a). These results suggest that the period of star-like occurrence after the onset of culture is related to the embryogenic pathway of microspores.

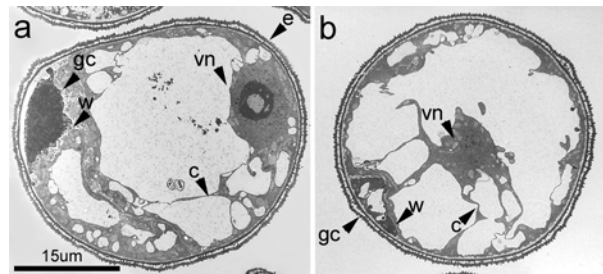


Figure 3. Formation of star-like structure during initiation of barley androgenesis. (a) Asymmetric division of an enlarged microspore showing a small, condensed generative cell embedded in the cytoplasm of the large vegetative cell. The cell wall that separates the generative cell from the vegetative cytoplasm is attached to the intine, while the large vacuole in the vegetative cell is interspersed by cytoplasmic strands. (b) Evolution of star-like structure showing central positioning of the vegetative nucleus, while the generative cell remains attached to the intine. The vegetative cytoplasm shows numerous cytoplasmic strands radially oriented. c cytoplasmic strands, e exine wall, gc generative cell, v vacuole, vn vegetative nucleus, w cell wall.

Gene expression programs during acquisition of microspore embryogenic potential

The analysis of biochemical and molecular changes during stress treatment to induce androgenesis has been a central point of research towards understanding the mechanisms involved in the reprogramming of microspores into embryos (reviewed by Touraev et al., 1997; Mordhorst et al., 1997). Most of the genes identified to be differentially expressed during stress treatment to induce androgenesis are involved with stress hormones, cellular protection from stress, sucrose-starch metabolism and proteolysis. These results indicate that acquisition of androgenic potential largely relies on dedifferentiation, a process whereby existing transcriptional and translational profiles are probably erased or altered in order to block pollen development and trigger the embryogenic route. The gene expression programs that are associated with acquisition of embryogenic competence during androgenesis are highlighted in Figure 2b.

Hormone modulated gene expression

It is known that plant cells produce ABA in response to certain stresses such as osmotic shock, salinity, cold and hypoxia (Zeevaart et al., 1998). During androgenesis induction in barley by a mannitol stress treatment, higher regeneration efficiencies have been correlated to increasing levels of osmotic stress and ABA (Hoekstra et al., 1997). Upon initiation of wheat androgenesis, Reynolds and Crawford (1996) isolated a gene encoding an early cysteine labeled class II metallothionein protein (*EcMt*). The expression of the *EcMt* gene is detected as early as 6h after the onset of induction in auxin-containing media. The promoter region of the *EcMt* gene from wheat contains an ABA responsive element (ABRE), and its up-regulation during androgenesis is closely related to the peak of endogenous ABA production (Reynolds and Crawford, 1996). Further evidence has indicated that Ca^{+2} takes part in the ABA signaling transduction leading to *EcMt* gene expression, a process that might involve calmodulin (Reynolds, 2000). Members of the *ALCOHOL DEHYDROGENASE (ADH)* family are among the genes whose expression is modulated by ABA (Macnicol and Jacobsen, 2001). Interestingly, the induction of *ADH3* during stress treatment to induce barley androgenesis is correlated with high regeneration efficiencies, which in turn are associated with increased ABA levels (Maraschin et al., 2004c; van Bergen et al., 1999). Though it is not yet known whether *EcMt* and *ADH3* play regulatory roles during the acquisition of embryogenic potential, their relation to ABA suggests that an ABA signaling cascade may play important roles in the activation of specific gene expression programs during initiation of androgenesis by stress. Kyo et al. (2000) isolated an embryogenic pollen-abundant phosphoprotein (NtEPc) from nitrogen starved tobacco microspores. *NtEPc*

encodes a protein that shows moderate homology to several type-1 copper binding glycoproteins and to an early nodulin. *NtEPC* expression is restricted to the period of microspore stress treatment, and is induced by low pH and inhibited by cytokinin. These results indicate that, besides ABA signaling, other hormonal signaling cascades are likely to take part in the reprogramming of gene expression during androgenesis induction.

Genes involved in cytoprotection

Members of the heat shock protein (HSP) family have been reported to be highly expressed during initiation of androgenesis by heat and starvation (Pechan et al., 1991; Cordewener et al., 1994, 1997; Zarsky et al., 1995; Smykal and Pechan, 2000; Bárány et al., 2001), as well as during the initiation of somatic embryogenesis by auxin (Kitamiya et al., 2000). These results have led to the hypothesis that increased levels of HSPs may be associated with the acquisition of embryogenic potential. However, androgenesis in rapeseed can be induced by colchicine without altering the levels of HSPs (Zhao et al., 2003), suggesting that alterations in HSP subcellular localization may be associated with their regulatory roles. In agreement with this hypothesis, the phase of the cell cycle (Milarsky and Morimoto, 1986; Suzuki and Watanabe, 1992), and a heat shock treatment to induce rapeseed androgenesis (Cordewener et al., 1997; Binarova et al., 1997) have been reported to control HSP nuclear shuttling. Due to their chaperone activity, it is possible that HSPs play indirect roles in triggering androgenesis via controlling the subcellular localization of other key regulatory proteins, and/or via providing a higher level of thermotolerance (Schöffl et al., 1998). Another major component of stress-induced androgenesis appears to be related to the induction of *GLUTATHIONE S-TRANSFERASE (GST)*. *GST* genes encode proteins that are involved in several processes, including the detoxification of xenobiotics and protection from oxidative stress (Marrs, 1996). Members of the *GST* gene family are up-regulated during the initial stages of androgenic development in barley (Vrienten et al., 1999), as well as during auxin-induced somatic embryogenesis (Nagata et al., 1994; Thibaud-Nissen et al., 2003). Nagata et al. (1994) found that the induction of *GST* genes during somatic embryogenesis is auxin-regulated, indicating that ROS act as signaling molecules involved in inducing stress-related genes and hormone responses (Desikan et al., 1998; Pasternak et al., 2002). In agreement with this hypothesis, increased levels of ROS have been reported to enhance somatic embryogenesis in many plant species (Luo et al., 2001; Pasternak et al., 2002; Caliskan et al., 2004; Ganesan and Jayabalan, 2004). In barley, optimal androgenesis induction is obtained by a mannitol treatment of anthers. When mannitol is omitted during stress treatment, suboptimal regeneration efficiencies are achieved (Hoekstra et al., 1992; van Bergen et al., 1999). The levels of *GST* expression in barley microspores subjected to

optimal and suboptimal stress treatments to induce androgenesis were found to be independent of the embryogenic potential associated with each treatment (Maraschin et al., 2004c). These results suggest that the roles of *GST* genes during acquisition of embryogenic potential are likely to be associated with protecting the cell against the harmful effects of ROS. However, one cannot exclude that the redox status of cells and the glutathione content have important roles in developmental processes, especially in triggering cell division.

Genes involved in sucrose-starch metabolism

Gene expression during pollen development is separated into two phases: transcripts of the “early” phase are detected from meiosis until the first pollen mitosis, whereas transcripts from the “late” phase accumulate from the first pollen mitosis on (Mascarenhas, 1990). Genes involved in starch biosynthesis belong to the class of “late” genes, as starch accumulation takes place after the first pollen mitosis. *In vivo*, the repression of genes involved in starch biosynthesis has been reported to block pollen development (Datta et al., 2001; 2002). A similar mechanism may contribute to blocking gametophytic development during androgenesis induction *in vitro*. An array approach has shown that key genes involved in starch biosynthesis, such as sucrose synthase 1 (SS1), phosphoglucosyltransferase (PGM), UDP-glucose 4-epimerase, glucose-1-phosphate adenylyltransferase (AGPase B), UTP-glucose-1-phosphate uridylyltransferase (UGPase) and granule-bound starch synthase (GBSS1) are down-regulated in microspores following a mannitol treatment to induce barley androgenesis. The down-regulation of starch biosynthetic genes was shown to be parallel to the induction of a maltase and an invertase gene, which are involved in starch and sucrose breakdown, respectively (Maraschin et al., 2004c). These findings provide molecular evidence to support the hypothesis that the repression of starch biosynthesis plays an important role in blocking gametophytic development during androgenesis induction.

Proteolytic genes

Proteomics approaches have demonstrated that microspores show altered synthesis, phosphorylation and glycosylation of proteins upon stress treatment to induce androgenesis (Kyo and Harada, 1990; Pechan et al., 1991; Garrido et al., 1993; Cordewener et al., 1994; Říhová et al., 1996). Many of these reports reveal that stressed microspores show an overall decrease in the protein levels, leading to the hypothesis that down-regulation of pollen specific proteins or increased protein breakdown might play an important role in the dedifferentiation phase of microspores. This is in agreement with the fact that blocking pollen

specific gene transcription has a beneficial effect in initiating androgenesis (Harada et al., 1986).

In plant cells, starvation leads to the transcription activation of the so-called “famine genes”, which encode proteins associated with the degradation of cellular components and with nutrient remobilization. During starvation, genes involved in carbohydrate remobilization are up-regulated in concert with enzymes involved in nitrogen recycling (Lee et al., 2004). Nitrogen recycling involves the degradation of proteins for nitrogen relocation, a process that comprises different classes of plant proteases and the ubiquitin-26S proteasome proteolytic pathway (Smalle and Vierstra, 2004; Beers et al., 2004). In somatic embryogenesis, cell dedifferentiation is accompanied by an increase in gene expression of proteases and proteins related to the ubiquitin-26S proteasome proteolytic pathway (Jamet et al., 1990; Thibaud-Nissen et al., 2003; Mitsushashi et al., 2004; Stasolla et al., 2004). Mannitol stress to induce barley androgenesis leads to the induction of genes involved with proteolysis, including a 20S proteasome catalytic subunit, a 26S regulatory particle, cysteine protease 1 precursor, phytepsin precursor (aspartic protease) and the metalloprotease FtsH (Maraschin et al., 2004c). These results indicate that proteases might be important for nitrogen relocation upon sugar depletion, a process that might result in the selective destruction of proteins associated with the previous differentiated state. This is in agreement with the role of the FtsH metalloprotease in protein turn over, as it is involved in degrading photosystem II reaction center D1 protein upon its irreversible photooxidative damage (Lindahl et al., 2000). In Arabidopsis, a mutational approach has shown that *FtsH* genes are needed for the formation of normal, green chloroplasts (Yu et al., 2004). Chloroplast biogenesis is an important factor for the production of green plants from microspores, since in many species microspores often give rise to albino plants, reducing their use in plant breeding (Jähne and Lörz, 1995). Though it is not yet known whether the *FtsH* metalloprotease plays a role in chloroplast biogenesis during androgenesis initiation, these results indicate that protein turn over may play important regulatory roles during dedifferentiation processes.

Increasing evidence links proteolysis to several aspects of cellular regulation, including hormone signaling and cell cycle regulation (reviewed by Hellman and Estelle, 2004). The plant cell cycle is regulated by changes in the specificity and subcellular localization of cyclin-dependent kinases (CDKs), which in turn are modulated by cyclins, CDK-activating and -inhibiting kinases and several CDK inhibitors (Criqui and Geschink, 2002). The half-life of many of these modulators is affected by the ubiquitin-26S proteasome proteolytic pathway (Geschink et al., 1998; Lee et al., 2003; Capron et al., 2003; Catellano et al., 2001; Ahn et al., 2004). Normal pollen development is characterized by tightly regulated events in the cell cycle. After the asymmetric division, the vegetative cell becomes arrested in

the G₁ phase of the cell cycle, while the generative cell progresses into mitosis and divides again to produce two sperm cells. Induction of androgenesis by stress is able to overcome this developmentally regulated cell cycle arrest, as the vegetative cell re-enters S-phase during stress treatment, and microspores progress into G₂/M transition in culture (Touraev et al., 1996a). In this sense, the induction of components of the ubiquitin pathway and protease gene expression (Maraschin et al., 2004c) may be related to the regulation of mitotic progression during acquisition of microspore embryogenic potential. This hypothesis is further supported by the fact that proteolytic genes are activated prior to cell division-related genes during acquisition of embryogenic potential in somatic embryogenesis (Thibaud-Nissen et al., 2003; Stasolla et al., 2004).

Gene expression programs during initiation of cell division

Master regulators of gene expression

As depicted above, differential screening approaches following stress treatment to induce androgenesis resulted in the identification of several genes and proteins associated with sucrose-starch metabolism, stress responses, proteolysis and cytoprotection. Nevertheless, none of these approaches resulted in the identification of key regulatory genes clearly involved in the acquisition of microspore embryogenic potential, i.e., transcription factors and regulatory proteins. It is only when the stress-induced dedifferentiation phase is over that such genes are expressed, thus correlating with the period of MCS formation at the onset of culture (Fig. 2b). *BABY BOOM (BBM)*, a member of the AP2/ERF family of transcription factors, is the first gene identified so far to have a putative function in coordinating the phase of cell division initiation during androgenesis. The *BBM* cDNA has been isolated from rapeseed MCSs, and is preferentially expressed during androgenesis and zygotic embryogenesis. Ectopic expression of *BBM* in rapeseed and Arabidopsis revealed that *BBM* can lead to the spontaneous formation of somatic embryos on the leaves of young seedlings, however older plants do not show the same response (Boutilier et al., 2002). This suggests that a relatively undifferentiated cell state is important so that *BBM* can trigger embryogenic development, further supporting the idea that a period of dedifferentiation precedes cell division during induction of androgenesis and somatic embryogenesis. Another regulatory protein thought to play a role in cell division initiation during embryogenesis is *AGAMOUS-like 15 (AGL15)*, a member of the MADS-domain family of transcription factors. Though the developmental role of *AGL15* is still unclear, *AGL15* has been shown to be

translocated to the nucleus upon initiation of cell divisions during zygotic and somatic embryogenesis, apomixis and androgenesis (Perry et al., 1999).

The *LEAFY COTYLEDON* genes, *LEAFY COTYLEDON1 (LEC1)*, *LEAFY COTYLEDON2 (LEC2)* and *FUSCA3 (FUS3)*, have been isolated from Arabidopsis mutant screen analysis and encode transcription factors involved in zygotic embryogenic development (Harada, 2001). Though mutant analysis indicates that *LEC1*, *LEC2* and *FUS3* play a role in embryo maturation during later stages of embryogenesis, overexpression of *LEC1* and *LEC2* triggers somatic embryogenesis in vegetative tissues like *BBM* does (Bäumlein et al., 1994; Parcy et al., 1997; Lotan et al., 1998; Nambara et al., 2000; Stone et al., 2001). Therefore, it has been proposed that *LEC* transcription factors play key regulatory roles in coordinating the phase of embryogenic competence acquisition as well as the morphogenesis and maturation phases of embryogenesis (Harada, 2001). Similarly, *WUSCHEL (WUS)*, a homeodomain protein that promotes a vegetative-to-embryonic transition (Zuo et al., 2002), is also involved in specification of shoot and floral meristems during zygotic embryogenesis (Mayer et al., 1998). This indicates that the acquisition of embryogenic competence and embryo development are controlled by a spatial and temporal reprogramming of regulatory genes. The *PICKLE (PKL)* gene encodes a CHD3 protein, a chromosome remodeling factor which is ubiquitously expressed in Arabidopsis. During post-embryonic growth, *PKL* inhibits embryonic traits via transcriptional repression of seed storage proteins (Ogas et al., 1997) and *LEC* genes (Ogas et al., 1999; Rider et al., 2003), and therefore is a master regulator of embryogenesis. Though it is not yet known whether *PKL* plays a role in androgenesis, transcripts coding for seed storage proteins, such as members of the napin seed storage protein family, correlate with the initiation of androgenesis in rapeseed (Boutilier et al., 1994). This suggests a possible role for chromatin remodeling in the coordination of transcription during the context of a stress-induced developmental switch, especially in the de-repression of gene expression programs associated with microspore embryogenic development.

The *SOMATIC EMBRYOGENESIS RECEPTOR-LIKE KINASE (SERK)* was first isolated from auxin-induced embryogenic carrot cell cultures and encodes a Leu-rich repeat (LRR) transmembrane receptor-like kinase (RLK). In somatic and zygotic embryogenesis, *DcSERK* is transiently expressed during initiation of embryogenic development up to the globular stage (Schmidt et al., 1997). Ectopic expression of *AtSERK1*, the Arabidopsis homologue of *DcSERK*, has been reported to increase the efficiency of somatic embryogenesis initiation in Arabidopsis seedlings, indicating that higher levels of *AtSERK1* are sufficient to confer embryogenic competence in culture (Hecht et al., 2001). Interestingly, high levels of *ZmSERK1* are detected in maize microspores at the competent stage for

androgenesis induction and during initiation of MCS formation, indicating that a *SERK*-dependent signaling pathway might be involved in the acquisition of embryogenic competence and initiation of embryogenic development in microspores (Baudino et al., 2001). Similarly, initiation of somatic and zygotic embryogenesis takes place only from cell clusters expressing the *EP2* gene, which encodes a lipid transfer protein whose homologue *ECLTP* has been also demonstrated to accompany the initiation of barley androgenesis (Sterk et al., 1991; Toonen et al., 1997; Vrienten et al., 1999).

Cell-cell communication and secreted signal molecules

Differential screening approaches have resulted in the identification of two endosperm-specific genes, *ZmAE1* and *ZmAE3*, in maize androgenic MCSs (Magnard et al., 2000). During *in vivo* zygotic embryo development, *ZmAE1* and *ZmAE3* are both transiently expressed during initiation of endosperm development in the embryo surrounding region. During androgenesis, expression of *ZmAE1* and *ZmAE3* is detected only in 5-7 days-old MCSs, a period that coincides with the differentiation of a large cellular domain that shows coenocytic organization similar to that of the endosperm initials (Magnard et al., 2000). The identification of these genes is of particular interest since it suggests that androgenic MCS development requires endosperm-like functions which might be needed for the establishment of interactions that probably exist *in planta* between embryo and endosperm. In agreement with this hypothesis, the development of carrot somatic embryos relies on the presence of several secreted proteins (de Vries et al., 1988; van Engelen et al., 1991; van Hengel et al., 1998). EP3, an endochitinase protein secreted by non-embryogenic cells during carrot somatic embryogenesis, is also expressed in the endosperm during zygotic embryo development (van Hengel et al., 1998). In somatic embryogenesis, chitinase-modified arabinogalactan proteins (AGPs) present in the extracellular matrix have been demonstrated to control plant cell fate (van Hengel et al., 2001). Recently, it has been shown that androgenic MCSs progressively secrete proteins in culture which can sustain *in vitro* zygotic embryo development (Paire et al., 2003). Further characterization of the extracellular proteins secreted during maize androgenesis revealed that several proteins are glycosylated, including distinct AGPs. Interestingly, chitinases and other pathogen-related proteins are also transiently secreted into the media, and these conditioned media were able to rescue embryo development in tunicamycin-treated MCSs arrested at the multicellular stage (Borderies et al., 2004). This indicates that progression of embryogenesis relies on the perception of external signals which might be crucial for the activation of specific spatiotemporal developmental programs during the making of an embryo.

Pattern Formation

During zygotic embryo development, an initial asymmetric division establishes the apical-basal axis of the embryo via a reversal of auxin distribution during early embryogenesis (Jürgens, 2001; Friml et al., 2003). This opposes androgenic embryo development, where the establishment of an apical-basal axis takes place from the globular stage onwards (Maraschin et al., 2003a; Hause et al., 1994). During androgenesis, the first signs of pattern formation are visualized by periclinal divisions of the cells that surround the ELSs, leading to epidermis differentiation (Telmer et al., 1995; Yeung et al., 1996). Following epidermis differentiation, rapeseed ELSs proceed through heart- and torpedo-shape stages, in a similar way as zygotic embryos (Hause et al., 1994). An analogous situation is observed during somatic embryogenesis, where somatic embryo development parallels zygotic embryogenesis from the globular stage onwards (Zimmerman, 1993). The genetic analysis of zygotic embryonic pattern formation has been recently reviewed (Laux et al., 2004). The stereotyped sequence of embryonic developmental stages between different embryogenesis systems suggests that analogous molecular mechanisms of embryo patterning are shared between them (Dodeman et al., 1997). Further evidence to support this hypothesis is the similar spatial and temporal regulation of members of the 14-3-3 family of regulatory proteins prior to pattern formation in barley androgenic and zygotic embryos. In barley androgenesis, the expression of 14-3-3A in the outer layer of ELSs precedes epidermis differentiation, while polarized 14-3-3C expression is correlated to the establishment of the scutellum during acquisition of bilateral symmetry. In the late embryogenesis stage, 14-3-3C expression is restricted to the scutellum and to a group of cells underneath the L₁ layer of the shoot apical meristem, prior to L₂ layer specification in both androgenic and zygotic embryos (Maraschin et al., 2003a; Testerink et al., 1999).

The gene expression programs that are associated with each phase during androgenesis are highlighted in Figure 2b, providing a comprehensive overview of the molecular mechanisms involved in microspore embryo formation.

Is there a role for PCD during androgenesis?

Programmed cell death (PCD) is a genetically controlled mechanism that envisages the organized destruction of specific cell types and tissues (Lam, 2004). Zygotic and somatic plant embryogenesis are intimately associated with PCD, as this process is involved in the elimination of unneeded structures within the embryos (Mordhorst et al., 1997) and is

essential for correct embryo patterning (Bohskov et al., 2004; Suarez et al., 2004). Nevertheless, a role for PCD during androgenesis has not been explored until very recently. Studies on barley androgenesis indicate that PCD takes place at least in two levels: during induction of androgenesis by stress, and during the transition from MCSs into globular embryos.

PCD during androgenesis induction

One experimental approach to test the reversibility of initial stages of PCD has shown that agents which promote an oxidative burst can induce star-like morphology in tobacco protoplasts. After removal of the PCD inducing agents, star-like structures were able to recover from the stress and start cell divisions (O'Brien et al., 1998). In animal systems, PCD signals are mediated by pleiotropic signal transductions, indicating that these pathways also have roles in cell proliferation and differentiation (Green and Beere, 2001). The most common form of animal PCD, apoptosis, is regulated by a family of cysteine proteases called caspases. The caspase cascade is triggered by cytochrome *c* release from mitochondria, a process that involves several members of the Bcl-2 family of proteins (Bad, Bcl-xL and Bax). Upon PCD stimuli, Bad is translocated from the cytoplasm to the mitochondria, where it associates with Bcl-xL and leads to cytochrome *c* release. Bax, in its turn, is a pro-apoptotic factor that is thought to accelerate this process (Gallagher et al., 2001). Members of the regulatory family of 14-3-3 proteins have been implicated in apoptosis signaling through their interaction with Bad, thereby preventing its translocation into the mitochondria and interaction with Bcl-xL. Recently, the proteolytic cleavage of the C-terminus of the human 14-3-3 ϵ isoform has been shown to weaken its affinity to Bad, thereby leading to Bad translocation into the mitochondria and activation of the PCD pathway (Won et al., 2003). During androgenesis induction in barley, the proteolytic cleavage of the C-terminus of the 14-3-3A isoform is specifically associated with a population of non-enlarged microspores that dies during stress treatment (Maraschin et al., 2003a,b). The death of these cells displays characteristics of PCD, as visualized by the formation of DNA laddering (Fig. 4). On the other hand, the population composed of enlarged microspores, which have acquired embryogenic potential, does not display DNA laddering neither 14-3-3A processing (Fig. 4; Maraschin et al., 2003a,b). These enlarged microspores are characterized by the expression of the *BAX INHIBITOR 1 (BI-1)* gene (Maraschin et al., 2004c), the plant homologue of the human *BI-1* gene capable of suppressing Bax- and stress-induced PCD in plants (Kawai-Yamada et al., 2001; Chae et al., 2003). This indicates that a stress treatment to induce barley androgenesis activates PCD in non-enlarged microspores, while in enlarged ones it leads to the induction of cell divisions. Since most stress agents used to trigger androgenesis

can induce PCD (Lam, 2004), it is likely that cell divisions may be induced by signaling pathways that cross-talk with those activated by PCD (Kuriyama and Fukuda, 2002). The final result might be related to the regulatory roles played by proteins like *BI-1* and 14-3-3A. Interestingly, the processed form of 14-3-3A is also associated with PCD in barley tapetum upon normal pollen development (Wang et al., 1999; Maraschin et al., 2003b).

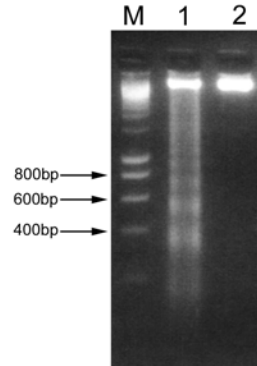


Figure 4. Conventional electrophoresis of DNA isolated from enlarged and non-enlarged microspores after 4 days mannitol treatment to induce barley androgenesis. *lane 1* PCD in non-enlarged microspores as demonstrated by the formation of ~180 bp DNA laddering, *lane 2* enlarged microspores with embryogenic competence, *M* marker DNA.

Since PCD plays important roles that are associated with the development and function of multicellular organisms (Lam, 2004), how can single cells such as microspores benefit from PCD? Answers for this question may arise from unicellular organisms, such as yeast (*Saccharomyces cerevisiae*). Aging and stress can induce many yeast cells within a colony to die, a process that displays hallmarks of PCD and is controlled by molecular mechanisms that parallel animal and plant PCD (Madeo et al., 2002a). A rapid, active suicide of these cells would spare metabolic energy for neighboring cells, at the same time that it neatly destroys cells without any damage to the environment (Madeo et al., 2002b). As in yeast 'altruism', stress during barley androgenesis induction could possibly trigger the programmed removal of the 'weakest' cells, represented by the population of non-enlarged microspores, thereby contributing to the survival of the fittest, enlarged microspores. It will be a challenge to explore how the cell fate of enlarged microspores can be affected by PCD of the non-enlarged ones during barley androgenesis induction.

PCD during the transition from MCSs to globular embryos

The formation of MCSs from star-like microspores involves different developmental pathways that are defined by the symmetry of the first division and the fate of the daughter cells. The asymmetric division of the microspore nucleus resulting in a generative and a

vegetative cell characterizes the A-pathway. In the A-pathway, MCSs are formed from repeated divisions of the vegetative cell concomitantly to the death of the generative cell. In the B pathway, it is the symmetric division of the microspore nucleus that gives rise to MCSs (Sunderland, 1974). An alternative route to androgenesis is defined by the independent divisions of the generative and vegetative cells, giving rise to heterogeneous MCSs with two distinct cellular domains. Because heterogeneous MCSs originate from an initial asymmetric division, this pathway is regarded as a modification of the A-pathway (Sunderland et al., 1979). All the above mentioned developmental pathways occur in most androgenic species, and the preponderance of one pathway over the other has been linked to the developmental stage of the cells and the type of stress applied (Sunderland et al., 1979; Říhová and Tupý, 1999; Kasha et al. 2001; Kim et al., 2004; Zaki and Dickinson, 1991). In rapeseed, MCSs are usually formed by the A- or B-pathway, and the early divisions of embryogenic microspores inside the exine wall appear to be random rather than regular (Hause et al., 1994; Telmer et al., 1995; Yeung et al., 1996). However, recent evidence shows that embryogenic microspores follow a very controlled pattern of cell divisions in wheat and maize, leading to the formation of specific cell domains within the exine: a cellularized domain composed of small cells, and a large domain composed of multinucleate cells. These domains have been compared to meristematic and endosperm initials during zygotic embryogenesis (Magnard et al., 2000; Bonet and Olmedilla, 2000). Though the vegetative and generative origins of these domains have not yet been established, small and large cell domains in barley MCSs developed via the modified A-pathway arise from divisions of the generative and vegetative cells, respectively (Maraschin et al., 2004a). The establishment of a cell tracking system has been crucial in determining that exine wall rupture in these embryos always takes place at the generative domain located at the opposite side of the pollen germ pore. During exine wall rupture, the generative cell domain is eliminated by PCD, and globular embryos are originated entirely from the vegetative domain (Maraschin et al., 2004b). In zygotic embryogenesis, the symmetry of the first division influences the differentiation and fate of the daughter cells, as the terminal cell gives rise to most structures of the embryo proper, while the suspensor is derived from the basal cell. In most species, the suspensor is eliminated by PCD in later stages of zygotic embryo development and it is not present in the mature seed (Jürgens, 2001). During carrot somatic embryogenesis, an initial asymmetric division also appears to seal the fate of the daughter cells, as the cytoplasm rich cell differentiates into the embryo, and the vacuolated suspensor cell is eliminated by PCD (McCabe et al., 1997). These results highlight the importance of an asymmetrical division during the initial steps of plant embryogenesis in defining different developmental fates, most probably by a

mechanism that involves differential accumulation of mRNAs, morphogens and distribution of organelles (Weterings et al., 2001; Friml et al., 2003; Bhalerao and Bennett, 2003).

During somatic embryogenesis in Norway spruce (*Picea abies* L. Karst), PCD is involved in the transition phase from pro-embryogenic masses to somatic embryo, and in the elimination of the embryo suspensor (Filonova et al., 2000). In this plant species, PCD is essential for correct embryo patterning and involves the activation of a caspase-6-like and a metacaspase protease (Bohzkov et al., 2004; Suarez et al., 2004). Despite the fact that canonical caspases have not yet been identified in plants, dying plant cells display caspase-like activity and a caspase-related family of proteins, called metacaspases, has been identified (Lam and del Pozo, 2000; Uren et al., 2000). During barley androgenesis, an increase in caspase-3-like activity has been correlated to PCD during the elimination of the generative cell domain in the transition from MCSs to globular embryos. PCD of the generative domain precedes exine wall rupture and is a condition for the release of globular embryos out of the exine wall (Maraschin et al., 2004b). It is conceivable that PCD might have a role in sculpting globular embryos by promoting exine wall removal and therefore allowing further embryonic development. Further molecular characterization of the events leading to the elimination of the generative cell domain in barley androgenic MCSs will help to elucidate the roles of PCD in exine wall rupture and in the transition from MCSs to globular embryos.

Concluding remarks

In recent years, there has been a considerable increase in the amount of information concerning the cellular and molecular aspects involved in androgenesis induction and embryo formation. The establishment of cell tracking systems has played a crucial role in pointing out the main morphological characteristics of embryogenic microspores, as well as in revealing the developmental pathways of induced microspores. The combination of cell tracking systems with biochemical and molecular markers has the potential to reveal more about the role of PCD both during androgenesis induction and pattern formation in microspore embryos. Due to the lack of genetic tools for the dissection of the signaling pathways leading to androgenesis induction, differential screening methods have often been used. These approaches have resulted in the identification of genes that are markers of a developmental switch, or are capable themselves of inducing embryogenic development. However, these genes are often expressed after the activation of gene expression programs associated with stress-response and cell metabolism. This is not altogether surprising, as the

activation of master regulators of embryogenesis, such as transcription and chromatin remodeling factors, is likely to involve several distinct signaling pathways which may be regulated by stress-induced proteolysis, oxidative burst and changes in the cell metabolism. Therefore, holistic approaches such as the integration of genomics, proteomics and metabolomics, from the perspective of systems biology, have a great potential in revealing the interaction between different signaling cascades involved in triggering androgenesis. In terms of plant breeding, the key for increased regeneration efficiency during androgenesis will largely depend on the control of two main developmental switches, defined as the induction of microspore cell division and their ultimate commitment to the embryogenic pathway.

Literature cited

- Ahn JW, Lim JH, Kim, GT, Pai HS (2004) Phytochemicals control the proliferation and differentiation fates of cells in plant organ development. *Plant J* 38: 969-981
- Bárány I, Testillano PS, Mitykó J, Risueno MC (2001) The switch of the microspore program in *Capsicum* involves HSP70 expression and leads to the production of haploid plants. *Int J Dev Biol* 45:39-40
- Barnabás B, Pfahler PL, Kovács G (1991) Direct effect of colchicine on the microspore embryogenesis to produce dihaploid plants in wheat (*Triticum aestivum* L.). *Theor Appl Genet* 81: 675-678
- Barnabás B, Obert B, Kovács G (1999) Colchicine, an efficient genome-doubling agent for maize (*Zea mays* L.) microspores cultured in anthero. *Plant Cell Rep* 18: 858-562
- Baudino S, Hansen H, Brettschneider R, Hecht VFG, Dresselhaus T, Lörz H, Dumas C, Rogowsky PM (2001) Molecular characterisation of two novel maize LRR receptor-like kinases, which belong to the *SERK* gene family. *Planta* 213: 1-10
- Bäumlein H, Misera S, Luerben H, Kölle K, Horstmann C, Wobus U, Muller AJ (1994) The *FUS3* gene of *Arabidopsis thaliana* is a regulator of gene expression during late embryogenesis. *Plant J* 6: 379-387
- Bedinger P (1992) The remarkable biology of pollen. *Plant Cell* 4: 879-887
- Beers EP, Jones AM, Dickerman AW (2004) The S8 serine, C1A cysteine and A1 aspartic protease families in *Arabidopsis*. *Phytochem* 65: 43-58
- Bhalerao RP, Bennett MJ (2003) The case of morphogens in plants. *Nat Cell Biol* 5: 939-943
- Bicknell RA, Koltunow AM (2004) Understanding apomixis: recent advances and remaining conundrums. *Plant Cell* 16: 228-245
- Binarova P, Hause G, Cenklóva V, Cordewener JHG, van Lookeren Campagne MM (1997) A short severe heat shock is required to induce embryogenesis in late bicellular pollen of *Brassica napus* L. *Sex Plant Reprod* 10: 200-208
- Blervacq AS, Dubois T, Dubois J, Vasseur J (1995) First divisions of somatic embryogenic cells in *Chicorium* hybrid "474". *Protoplasma* 186: 163-168
- Bonet FJ, Olmedilla A (2000) Structural changes during early embryogenesis in wheat pollen. *Protoplasma* 211: 94-102
- Borderies G, Béché M, Rossignol M, Lafitte C, Le Deunff, Beckert M, Dumas C, Matthys-Rochon E (2004) Characterization of proteins secreted during maize microspore culture: arabinogalactan proteins (AGPs) stimulate embryo development. *Eur J Cell Biol* 83: 205-212

- Boutillier K, Offringa R, Sharma VK, Kieft H, Ouellet T, Zhang L, Hattori J, Liu CM, van Lammeren AAM, Miki BLA, Custers JBM, van Lookeren Campagne MM (2002) Ectopic expression of BABY BOOM triggers a conversion from vegetative to embryogenic growth. *Plant Cell* 14: 1737-1749
- Boutillier KA, Ginés MJ, DeMoor JM, Huang B, Baszczynski CL, Iyer VN, Miki BL (1994) Expression of the BrmNAP subfamily of napin genes coincides with the induction of *Brassica* microspore embryogenesis. *Plant Mol Biol* 26: 1711-1723
- Bozhkov PV, Filonova LH, Suarez MF, Helmersson A, Smertenko AP, Zhivotovsky, von Arnold S (2004) VEIDase is a principal caspase-like activity involved in plant programmed cell death and essential for embryonic pattern formation. *Cell Death Differ* 11: 175-182
- Caliskan M, Turet M, Cuming AC (2004) Formation of wheat (*Triticum aestivum* L.) embryogenic callus involves peroxide-generating germin-like oxalate oxidase. *Planta* 219: 132-140
- Capron A, Serralbo O, Fulop K, Fruigier F, Parmentier Y, Dong A, Lecureuil A, Guerche P, Kondorosi E, Scheres B, Genschik P (2003) The *Arabidopsis* APC/C: molecular and genetic characterization of the APC2 subunit. *Plant Cell* 15: 2370-2382
- Catellano MM, del Pozo JC, Ramirez-Parra E, Brown S, Gutierrez C (2001) Expression and stability of *Arabidopsis* CDC6 are associated with endoreplication. *Plant Cell* 13: 2671-2686
- Chae HJ, Ke N, Kim HR, Chen S, Gozik A, Dickman M, Reed JC (2003) Evolutionary conserved cytoprotection provided by Bax inhibitor-1 homologs from animals, plants, and yeast. *Gene* 323: 101-113
- Cordewener JHG, Busink R, Traas JA, Custers JBM, Dons HJM, van Lookeren Campagne MM (1994) Induction of microspore embryogenesis in *Brassica napus* L. is accompanied by specific changes in protein synthesis. *Planta* 195: 50-56
- Cordewener JHG, Hause G, Görger E, Busink R, Hause B, Dons HJM, van Lammeren AAM, van Lookeren Campagne MM, Pechan P (1997) Changes in synthesis and localization of members of the 70-kDa class of heat-shock proteins accompany the induction of embryogenesis in *Brassica napus* L. microspores. *Planta* 196: 747-755
- Criqui MC, Genschik P (2002) Mitosis in plants: how far we have come at the molecular level? *Curr Opin Plant Biol* 5: 487-493
- Custers JBM, Cordewener JHG, Nöllen Y, Dons JJM, van Lookeren Campagne MM (1994) Temperature controls both gametophytic and sporophytic development in microspore cultures of *Brassica napus*. *Plant Cell Rep* 13: 267-271
- Datta R, Chamusco KC, Chourey PS (2002) Starch biosynthesis during pollen maturation is associated with altered patterns of gene expression in maize. *Plant Physiol* 130: 1645-1656
- Datta R, Chourey PS, Pring DR, Tang HV (2001) Gene-expression analysis of sucrose-starch metabolism during pollen maturation in cytoplasmic male-sterile and fertile lines in sorghum. *Sex Plant Reprod* 14: 127-134
- de Vries S, Booi H, Meyerink P, Huisman G, Wilde HD, Thomas TL, van Kammen A (1988) Acquisition of embryogenic potential in carrot cell-suspension cultures. *Planta* 176: 196-204
- Desikan R, Reynolds A, Hancock JT, Neill SJ (1998) Harpin and hydrogen peroxide both initiate programmed cell death but have differential effects on defense gene expression in *Arabidopsis thaliana* suspension cultures. *Biochem J* 330: 115-120
- Dodeman VL, Ducreux G, Kreis M (1997) Zygotic embryogenesis versus somatic embryogenesis. *J Exp Bot* 48: 1493-1509
- Dubois T, Guedira M, Dubois J, Vasseur J (1991) Direct somatic embryogenesis in leaves of *Chicorium*. A histological and SEM study of early stages. *Protoplasma* 162: 120-127
- Filonova LH, Bozhkov PV, Brukhin VB, Daniel G, Zhivotovsky B, von Arnold S (2000) Two waves of programmed cell death occur during formation and development of somatic embryos in the gymnosperm, Norway spruce. *J Cell Sci* 113: 4399-4411

- Friml J, Vieten A, Sauer M, Weijers D, Schwarz H, Hamann T, Offringa R, Jürgens G (2003) Efflux-dependent auxin gradients establish the apical-basal axis of Arabidopsis. *Nature* 426: 147-153
- Gaillard A, Vergne P, Beckert M (1991) Optimization of maize microspore isolation and culture conditions for reliable plant regeneration. *Plant Cell Rep* 10: 55-58
- Gallaher BW, Hille R, Raile K, Kiess W (2001) Apoptosis: live or die – hard work either way! *Horm Metab Res* 33: 511-519
- Ganesan M, Jayabalan N (2004) Evaluation of haemoglobin (erythrogen): for improved somatic embryogenesis and plant regeneration in cotton (*Gossypium hirsutum* L. cv. SVPR 2). *Plant Cell Rep* 23: 181-187
- Garrido D, Eller N, Heberle-Bors E, Vicente O (1993) *De novo* transcription of specific mRNAs during the induction of tobacco pollen embryogenesis. *Sex Plant Reprod* 6: 40-45
- Gémes-Jushász A, Balogh P, Ferenczy A, Kristof Z (2002) Effect of optimal stage of female gametophyte and heat treatment on *in vitro* gynogenesis induction in cucumber (*Cucumis sativus* L.). *Plant Cell Rep* 21: 105-111
- Gervais G, Newcomb W, Simmonds DH (2000) Rearrangement of the actin filament and microtubule cytoskeleton during induction of microspore embryogenesis in *Brassica napus* L. cv Topas. *Protoplasma* 213: 194-202
- Geschink P, Criqui MC, Parmentier Y, Derevier A, Fleck J (1998) Cell cycle-dependent proteolysis in plants: identification of the destruction box pathway and metaphase arrest produced by the proteasome inhibitor MG132. *Plant Cell* 10: 2063-2075
- Green DR, Beere HM (2001) Mostly dead. *Nature* 412: 133-135
- Guha S, Maheshwari SC (1964) *In vitro* production of embryos from anthers of *Datura*. *Nature* 204: 497
- Harada H, Kyo M, Imamura J (1986) Induction of embryogenesis and regulation of the developmental pathway in immature pollen of *Nicotiana* species. *Curr Top Devel Biol* 20: 397-408
- Harada JJ (2001) Role of *Arabidopsis* *LEAFY COTYLEDON* genes in seed development. *J Plant Physiol* 158: 405-409
- Hause B, van Veenendaal WL, Hause G, van Lammeren AA (1994) Expression of polarity during early development of microspore-derived and zygotic embryos of *Brassica napus* L. cv Topas. *Bot Acta* 107: 407-415
- Hause G, Hause B, van Lammeren AAM (1992) Microtubular and actin filament configurations during microspore and pollen development in *Brassica napus* cv. Topas. *Can J Bot* 70: 1369-1376
- Hecht V, Vielle-Calzada JP, Hartog MV, Schmidt ED, Boutilier K, Grossniklaus U, de Vries SC (2001) The *Arabidopsis* somatic embryogenesis receptor kinase 1 gene is expressed in developing ovules and embryos and enhances embryogenic competence in culture. *Plant Physiol* 127: 803-816
- Hellmann H, Estelle M (2004) Plant development: regulation by protein degradation. *Science* 297: 793-797
- Hirt H (2000) Connecting oxidative stress, auxin, and cell cycle regulation through a plant mitogen-activated protein kinase. *Proc Natl Acad Sci USA* 97: 2405-2407
- Hoekstra S, van Bergen S, van Brouwershaven IR, Schilperoort RA, Heidekamp F (1996) The interaction of 2,4-D application and mannitol pretreatment in anther and microspore culture of *Hordeum vulgare* L. cv. Igri. *J Plant Physiol* 148: 696-700
- Hoekstra S, van Bergen S, van Brouwershaven IR, Schilperoort RA, Wang M (1997) Androgenesis in *Hordeum vulgare* L.: effects of mannitol, calcium and abscisic acid on anther pretreatment. *Plant Sci* 126: 211-218
- Hoekstra S, van Zijderveld MH, Louwerse JD, Heidekamp F, van der Mark F (1992) Anther and microspore culture of *Hordeum vulgare* L. cv. Igri. *Plant Sci* 86: 89-96
- Huang B (1986) Ultrastructural aspects of pollen embryogenesis in *Hordeum*, *Triticum* and *Paeonia*. In: Hu H, Hongyuan Y (eds) *Haploids of higher plants in vitro*. Springer-Verlag, Berlin Heidelberg, pp 91-117

- Ikeda-Iwai M, Umehara M, Satoh S, Kamada H (2003) Stress-induced somatic embryogenesis in vegetative tissues of *Arabidopsis thaliana*. *Plant J* 34: 107-114
- Indrianto A, Barinova I, Touraev A, Heberle-Bors E (2001) Tracking individual wheat microspores *in vitro*: identification of embryogenic microspores and body axis formation in the embryo. *Planta* 212: 163-174
- Jähne A, Lörz H (1995) Cereal microspore culture. *Plat Sci* 109: 1-12
- Jamet E, Durr A, Parmentier Y, Criqui MC (1990) Is ubiquitin involved in the dedifferentiation of higher plant cells? *Cell Differ Dev* 29: 37-46
- Jürgens, G (2001) Apical-basal pattern formation in *Arabidopsis* embryogenesis. *EMBO J* 20: 3609-3616
- Kasha KJ, Hu TC, Oro R, Simion E, Shim YS (2001) Nuclear fusion leads to chromosome doubling during mannitol pretreatment of barley (*Hordeum vulgare* L.) microspores. *J Exp Bot* 52: 1227-1238
- Kawai-Yamada M, Jin L, Yoshinaga K, Hirata A, Uchimiya H (2001) Mammalian Bax-induced plant cell death can be down-regulated by overexpression of *Arabidopsis* Bax-inhibitor-1. *Proc Natl Acad Sci USA* 98: 12295-12300
- Kim M, Kim J, Yoon M, Choi DI, Lee KM (2004) Origin of multicellular pollen and pollen embryos in cultured anthers of pepper (*Capsicum annum*). *Plant Cell Tiss Org* 77: 63-72
- Kitamiya E, Suzuki S, Sano T, Nagata T (2000) Isolation of two genes that were induced upon the initiation of somatic embryogenesis on carrot hypocotyls by high concentrations of 2,4-D. *Plant Cell Rep* 19: 551-557
- Knetsch ML, Wang M, Snaar-Jagalska BE, Heimovaara-Dijkstra S (1996) Abscisic acid induced mitogen-activated protein kinase activation in barley aleurone protoplasts. *Plant Cell* 8: 1061-1067
- Koltunow AM, Johnson SD, Bicknell RA (1998) Sexual and apomictic development in *Hieracium*. *Sex Plant Reprod* 11: 213-230
- Koltunow AM (1993) Apomixis: embryo sacs and embryos formed without meiosis or fertilization in ovules. *Plant Cell* 5: 1425-1437
- Koul AK, Karihaloo JL. (1977) *In vivo* embryoids from anthers of *Narcissus bioflorus* curt. *Euphytica* 26: 97-102
- Kranz E, von Wiegen P, Lörz H (1995) Early cytological events after induction of cell division in egg cells and zygote development following *in vitro* fertilization with angiosperm gametes. *Plant J* 8: 9-23
- Kuriyama H, Fukuda H (2002) Developmental programmed cell death in plants. *Curr Opin Plant Biol* 2: 568-573
- Kyo K, Harada H (1990) Specific phosphoproteins in the initial period of tobacco pollen embryogenesis. *Planta* 182: 58-63
- Kyo M, Harada H (1986) Control of the developmental pathway of tobacco pollen *in vitro*. *Planta* 168: 427-432
- Kyo M, Miyatake H, Mamezuka K, Amagata K (2000) Cloning of cDNA encoding NtPEc, a marker protein for the embryogenic differentiation of immature tobacco pollen grains cultured *in vitro*. *Plant Cell Physiol* 41: 129-137
- Lam E, del Pozo O (2000) Caspase-like protease involvement in the control of plant cell death. *Plant Mol Biol* 44: 417-428
- Lam E (2004) Controlled cell death, plant survival and development. *Nat Rev Mol Cell Biol* 5: 305-315
- Laux T, Würschum T, Breuninger H (2004) Genetic regulation of embryonic pattern formation. *Plant Cell* 16: 190-202
- Lee EJ, Koizumi N, Sano H (2004) Identification of genes that are up-regulated in concert during sugar depletion in *Arabidopsis*. *Plant Cell Environ* 27: 337-345
- Lee SS, Cho HS, Yoon GM, Ahn JW, Kim HH, Pai HS (2003) Interaction of NtCDPK1 calcium-dependent protein kinase with NtRpn3 regulatory subunit of the 26S proteasome in *Nicotiana tabacum*. *Plant J* 33: 825-840

- Levine B, Klionsky DJ (2004) Development by self-digestion: molecular mechanisms and biological functions of autophagy. *Dev Cell* 6: 463-477
- Lindahl M, Spetea C, Hundal T, Oppenheim AB, Adam Z, Andersson B (2000) The thylakoid FtsH protease plays a role in the light-induced turnover of the photosystem II D1 protein. *Plant Cell* 12: 419-431
- Lotan T, Ohto M, Yee KM, West MAL, Lo R, Kwong RW, Yamagishi K, Fischer RL, Goldberg RB (1998) *Arabidopsis LEAFY COTYLEDON1* is sufficient to induce embryo development in vegetative cells. *Cell* 93: 1195-1205
- Luo JP, Jiang ST, Pan LJ (2001) Enhanced somatic embryogenesis by salicylic acid of *Astragalus adsurgens* Pall.: relationship with H₂O₂ production and H₂O₂-metabolizing enzyme activities. *Plant Sci* 161: 125-132
- Macnicol PK, Jacobsen JV (2001) Regulation of alcohol dehydrogenase gene expression in barley aleurone by gibberellin and abscisic acid. *Physiol Plant* 111: 533-539
- Madeo F, Herker E, Maldener C, Wissing S, Lächelt S, Herlan M, Fehr M, Lauber K, Sigrist SJ, Wesselborg S, Fröhlich KU (2002a) A caspase-related protease regulates apoptosis in yeast. *Mol Cell* 9: 911-917
- Madeo F, Engelhardt S, Herker E, Lehmann N, Maldener C, Proksch A, Wissing S, Fröhlich KU (2002b) Apoptosis in yeast: a new model system with applications in cell biology and medicine. *Curr Genet* 41: 208-216
- Magnard JL, Le Deunff E, Domenech J, Rogowsky PM, Testillano PS, Rougier M, Risueño MC, Vergne P, Dumas C (2000) Genes normally expressed in the endosperm are expressed at early stages of microspore embryogenesis in maize. *Plant Mol Biol* 44: 559-574
- Mansfield SG, Briarty LG (1991) Early embryogenesis in *Arabidopsis thaliana*. II. The developing embryo. *Can J Bot* 69: 461-476
- Maraschin SF, Lamers GEM, de Pater BS, Spaink HP, Wang M (2003a) 14-3-3 isoforms and pattern formation during barley microspore embryogenesis. *J Exp Bot* 51: 1033-1043
- Maraschin SF, Lamers GEM, Wang M (2003b) Cell death and 14-3-3 proteins during the induction of barley microspore androgenesis. *Biologia* 58: 59-68
- Maraschin SF, Vennik M, Lamers GEM, Spaink HP, Wang M (2004a) Time-lapse tracking of barley androgenesis reveals position-determined cell death within pro-embryos. *Planta*, *in press*
- Maraschin SF, Gaussand G, Pulido A, Olmedilla A, Lamers GEM, Korthout H, Spaink HP, Wang M (2004b) Programmed cell death during the transition from multicellular structures to globular embryos in barley androgenesis. *Planta*, *in press*
- Maraschin SF, Caspers M, Potokina E, Wülfert F, Corredor- Adámez M, Graner A, Spaink HP, Wang M (2004c) cDNA array analysis of stress-induced gene expression in barley androgenesis. *Submitted*
- Marrs K (1996) The functions and regulation of glutathione S-transferases in plants. *Annu Rev Plant Physiol Plant Mol Biol* 47: 127-158
- Mascarenhas JP (1990) Gene activity during pollen development. *Annu Rev Plant Physiol Plant Mol Biol* 41: 317-338
- Mayer KFX, Schoof H, Haecker A, Lenhard M, Jürgens G, Laux T (1998) Role of *WUSCHEL* in regulating stem cell fate in the *Arabidopsis* shoot meristem. *Cell* 95: 805-815
- McCabe P, Valentine TA, Forsberg S, Pennell RI (1997) Soluble signals from cells identified at the cell wall establish a developmental pathway in carrot. *Plant Cell* 12: 2225-2241
- McCormick S (1993) Male gametophyte development. *Plant Cell* 5: 1265-1275
- Milarsky KL, Morimoto RI (1986) Expression of human HSP70 during the synthetic phase of the cell cycle. *Proc Natl Acad Sci USA* 83: 9517-9521
- Mitsushashi W, Yamashita T, Toyomasu T, Kashiwagi Y, Konnai T (2004) Sequential development of cysteine proteinase activities and gene expression during somatic embryogenesis in carrot. *Biosci Biotechnol Biochem* 68: 705-713

- Mòl R, Matthys-Rochon E, Dumas C (1994) The kinetics of cytological events during double fertilization in *Zea mays* L. *Plant J* 5: 197-206
- Mordhorst AP, Toonen MAJ, de Vries SC (1997) Plant Embryogenesis. *Crit Rev Plant Sci* 16: 535-576
- Morrison RA, Evans DA (1988) Haploid plants from tissue culture: new plant varieties in a shortened time frame. *Biotechnology* 6: 684-690
- Musial K, Bohanec B, Przywara L (2001) Embryological study on gynogenesis in onion (*Allium cepa* L.). *Sex Plant Reprod* 13: 335-341
- Nagata T, Ishida S, Hasezawa S, Takahashi Y (1994) Genes involved in the dedifferentiation of plant cells. *Int J Dev Biol* 38: 321-327
- Nambara E, Hayama R, Tsuchiya Y, Nishimura M, Kawaide H, Kamiya Y, Naito S (2000) The role of *ABI3* and *FUS3* loci in *Arabidopsis thaliana* on phase transition from late embryo development to germination. *Dev Biol* 220: 412-423
- Nishiwaki M, Fujino K, Koda Y, Masuda K, Kikuta Y (2000) Somatic embryogenesis by the simple application of abscisic acid to carrot (*Daucus carota* L.). *Planta* 211: 756-759
- O'Brien IEW, Baguley BC, Murray BG, Morris BAM, Ferguson IB (1998) Early stages of the apoptotic pathway in plant cells are reversible. *Plant J* 13: 803-814
- Obert B, Barnabás B (2004) Colchicine induced embryogenesis in maize. *Plant Cell Tiss Org* 77: 283-285
- Ogas J, Cheng JC, Sung ZR, Somerville C (1997) Cellular differentiation regulated by gibberellin in the *Arabidopsis thaliana pkl* mutant. *Science* 277: 91-94
- Ogas J, Kaufmann S, Henderson J, Somerville C (1999) PICKLE is a CHD3 chromatin-remodeling factor that regulates the transition from embryonic to vegetative development in *Arabidopsis*. *Proc Natl Acad Sci USA* 96: 13839-13844
- Paire A, Devaux P, Lafitte C, Dumas C, Matthys-Rochon E (2003) Proteins produced by barley microspores and their derived androgenic structures promote *in vitro* zygotic maize embryo formation. *Plant Cell Tiss Org* 73:167-176
- Parcy F, Valon C, Kohara A, Misera S, Giraudat J (1997) The *ABSCISIC ACID-INSENSITIVE3*, *FUSCA3*, and *LEAFY COTYLEDON1* loci act in concert to control multiple aspects of *Arabidopsis* seed development. *Plant Cell* 9: 1265-127
- Pasternak T, Prinsen E, Ayaydin F, Miskolczi P, Potters G, Asard H, van Onckelen H, Dudits D, Fehér (2002) The role of auxin, pH and stress in the activation of embryogenic cell division in leaf protoplast-derived cells of alfalfa (*Medicago sativa* L.). *Plant Physiol* 129: 1807-1819
- Pechan M, Keller AW (1989) Induction of microspore embryogenesis in *Brassica napus* by gamma irradiation and ethanol stress. *In vitro* 25: 1073-1074
- Pechan PM, Bartels D, Brown DCW, Schell J (1991) Messenger-RNA and protein changes associated with induction of *Brassica* microspore embryogenesis. *Planta* 184: 161-165
- Perry SE, Lehti MD, Fernandez DE (1999) The MADS-domain protein AGAMOUS-like 15 accumulates in embryonic tissues with diverse origins. *Plant Physiol* 120: 121-129
- Pichot C, Maâtaoui M, Raddi S, Raddi P (2001) Surrogate mother for endangered *Cupressus*. *Nature* 412: 39
- Rammana MS, Hermsen JGTH (1974) Embryoid formation in the anthers of some interspecific hybrids in *Solanum*. *Euphytica* 23: 423-427
- Rammana MS (1974) The origin and *in vivo* development of embryoids in the anthers of *Solanum* hybrids. *Euphytica* 23: 623-632
- Rashid A, Siddiqui AW, Reinert J (1982) Subcellular aspects of origin and structure of pollen embryos of *Nicotiana*. *Protoplasma* 113: 202-208
- Reynolds TL, Crawford RL (1996) Changes in abundance of an abscisic acid-responsive, early cysteine-labeled metallothionein transcript during pollen embryogenesis in bread wheat (*Triticum aestivum*). *Plant Mol Biol* 32: 823-826

- Reynolds TL, Kitto SL (1992) Identification of embryoid-abundant genes that are temporally expressed during pollen embryogenesis in wheat anther cultures. *Plant Physiol* 100: 1744-1750
- Reynolds TL (2000) Effects of calcium on embryogenic induction and the accumulation of abscisic acid, and an early cysteine-labeled metallothionein gene in androgenic microspores of *Triticum aestivum*. *Plant Sci* 150: 201-207
- Ribnicky DM, Cohen JD, Hu WS, Cooke TJ (2001) An auxin surge following fertilization in carrots: a mechanism for regulating plant totipotency. *Planta* 214: 505-509
- Rider SD, Henderson JT, Jerome RE, Edenberg HJ, Romero-Severson J, Ogas J (2003) Coordinate repression of regulators of embryonic identity by *PICKLE* during germination in *Arabidopsis*. *Plant J* 35: 33-43
- Říhová L, Čapková V, Tupý J (1996) Changes in glycoprotein patterns associated with male gametophyte development and with induction of pollen embryogenesis in *Nicotiana tabacum* L. *J Plant Physiol* 147: 573-581
- Říhová L, Tupý J (1999) Manipulation of division symmetry and developmental fate in cultures of potato microspores. *Plant Cell Tiss Org* 59: 135-145
- Schmidt EDL, Guzzo F, Toonen MAJ, de Vries SC (1997) A leucine-rich repeat containing receptor-like kinase marks somatic plant cells competent to form embryos. *Development* 124: 2049-2062
- Schöffl F, Prändl R, Reindl A (1998) Regulation of the heat shock response. *Plant Physiol* 117: 1135-1141
- Simmonds DH, Keller WA (1999) Significance of preprophase bands of microtubules in the induction of microspore embryogenesis of *Brassica napus*. *Planta* 208: 383-391
- Smalle J, Vierstra RD (2004) The ubiquitin 26S proteasome proteolytic pathway. *Annu Rev Plant Biol* 55: 555-590
- Smykal P, Pechan PM (2000) Stress, as assessed by the appearance of sHsp transcripts, is required but no sufficient to initiate androgenesis. *Physiol Plant* 110: 135-143
- Somleva MN, Schmidt EDL, de Vries SC (2000) Embryogenic cells in *Dactylis glomerata* L. (Poaceae) explants identified by cell tracking and by *SERK* expression. *Plant Cell Rep* 19: 718-726
- Sopory SK, Munchi M (1996) Anther culture. In vitro haploid production in higher plants (eds Monhanjain SM, Sopory SK and Veilleux, RE. Kluwer Academic Publishers, Dordrecht, pp 145-176
- Stasolla C, Bozhkov PV, Chu TM, van Zyl L, Egertsdotter U, Suarez MF, Craig D, Wolfinger RD, von Arnold S, Sederoff RR (2004) Variation in transcript abundance during somatic embryogenesis in gymnosperms. *Tree Physiol* 24: 1073-1085
- Sterk P, Booj H, Schellekens GA, van Kammen A, de Vries SC (1991) Cell-specific expression of the carrot EP2 lipid transfer protein gene. *Plant Cell* 3: 907-921
- Stone SL, Kwong LW, Yee KM, Pelletier J, Lepiniec L, Fischer RL, Goldberg RB, Harada JJ (2001) *LEAFY COTYLEDON2* encodes a B3 domain transcription factor that induces embryo development. *Proc Natl Acad Sci USA* 98: 11806-11811
- Suarez MF, Filonova LH, Smertenko A, Savenkov EI, Clapham DH, von Arnold S, Zhivotovsky B, Bozhkov PV (2004) Metacaspase-dependent programmed cell death is essential for plant embryogenesis. *Curr Biol* 14: 339-340
- Sunderland N, Dunwell JM (1974) Anther and pollen culture. In: Street HE (ed) *Plant tissue and cell culture*. Blackwell Scientific Publications, Oxford, pp 223-265
- Sunderland N, Roberts M, Evans LJ, Wildon DC (1979) Multicellular pollen formation in cultured barley anthers. I. Independent division of the generative and vegetative cells. *J Exp Bot* 30: 1133-1144
- Sunderland N (1974) Anther culture as a means of haploid induction. In: Kasha KJ (ed) *Haploids in higher plants: advances and potential*. University of Guelph, Canada, pp 91-122
- Suzuki K, Watanabe M (1992) Augmented expression of HSP72 protein in normal human fibroblasts irradiated with ultraviolet light. *Biochem Biophys Res Commun* 186: 1257-1264

- Telmer CA, Newcomb W, Simmonds DH (1995) Cellular changes during heat shock induction and embryo development of cultured microspores of *Brassica napus* cv. Topas. *Protoplasma* 185: 106-112
- Testerink C, van der Meulen RM, Oppedijk BJ, de Boer AH, Heimovaara-Dijkstra S, Kijne JW, Wang M (1999) Differences in spatial expression between 14-3-3 isoforms in germinating barley embryos. *Plant Physiol* 121: 81-87
- Thibaud-Nissen F, Shealy RT, Khanna A, Vodkin LO (2003) Clustering of microarray data reveals transcript patterns associated with somatic embryogenesis in soybean. *Plant Physiol* 132: 118-136
- Toonen MA, Verhees JA, Schmidt EDL, van Kammen A, de Vries SC (1997) AtLTP1 luciferase expression during carrot somatic embryogenesis. *Plant J* 12: 1213-1221
- Touraev A, Pfosser M, Vicente O, Heberle-Bors E (1996a) Stress as the major signal controlling the developmental fate of tobacco microspores: towards a unified model of induction of microspore/pollen embryogenesis. *Planta* 200: 144-152
- Touraev A, Indrianto A, Vicente O, Wratschko O, Heberle-Bors E (1996b) Efficient microspore embryogenesis in wheat (*Triticum aestivum* L.) induced by starvation at high temperature. *Sex Plant Reprod* 9: 209-215
- Touraev A, Vicente O, Heberle-Bors E (1997) Initiation of microspore embryogenesis by stress. *Trends Plant Sci* 2: 297-302
- Uren AG, O'Rourke K, Aravind L, Pisabarro MT, Seshagiri S, Koonin EV, Dixit VM (2000) Identification of paracaspases and metacaspases: two ancient families of caspase-like proteins, one of which plays a key role in MALT lymphoma. *Mol Cell* 6: 961-967
- van Bergen S, Kottenhagen MJ, van der Meulen RM, Wang M (1999) The role of abscisic acid in induction of androgenesis: a comparative study between *Hordeum vulgare* L. cvs Igri and Digger. *J Plant Growth Regul* 18: 135-143
- van Engelen FA, Sterk P, Booij H, Cordewener JHG, Rook W, van Kammen A, de Vries SC (1991) Heterogeneity and cell type-specific localization of a cell wall glycoprotein from carrot suspension cells. *Plant Physiol* 96: 705-712
- van Hengel AJ, Tadesse Z, Immerzeel P, Schols H, van Kammen A, de Vries SC (2001) *N*-Acetylglucosamine and glucosamine-containing arabinogalactan proteins control somatic embryogenesis. *Plant Physiol* 125: 1880-1890
- van Hengel AJ, Guzzo F, van Kammen A, de Vries SC (1998) Expression pattern of the carrot EP3 endochitinase genes in suspension cultures and in developing seeds. *Plant Physiol* 117: 43-53
- Vrienten PL, Nakamura T, Kasha KJ (1999) Characterization of cDNAs expressed in the early stages of microspore embryogenesis in barley (*Hordeum vulgare*) L. *Plant Mol Biol* 41: 455-463
- Wallin M, Stromberg E (1995) Cold-stable and cold-adapted microtubules. *Int Rev Cytol* 157: 1-31
- Wang M, van Bergen S, van Duijn B (2000) Insights into a key developmental switch and its importance for efficient plant breeding. *Plant Physiol* 124: 523-530
- Wang M, Hoekstra S, van Bergen S, Lamers GEM, Oppedijk BJ, van der Heijden MW, de Priester W, Schilperoort RA (1999) Apoptosis in developing anthers and the role of ABA in this process during androgenesis in *Hordeum vulgare* L. *Plant Mol Biol* 39: 489-501
- Weterings K, Apuya NR, Bi Y, Fischer RL, Harada JJ, Goldberg RB (2001) Regional localization of suspensor mRNAs during early embryo development. *Plant Cell* 13: 2409-2425
- Won J, Kim DY, La M, Kim D, Meadows DG, Joe CO (2003) Cleavage of 14-3-3 protein by caspase-3 facilitates Bad interaction with Bcl-x(L) during apoptosis. *J Biol Chem* 278: 19347-19351
- Yeung EC, Rahman MH, Thorpe TA (1996) Comparative development of zygotic and microspore-derived embryos in *Brassica napus* L. cv Topas. I. Histodifferentiation. *Int J Plant Sci* 157: 27-39
- Yu F, Park S, Rodermeil SR (2004) The *Arabidopsis* FtsH metalloprotease gene family: interchangeability of subunits in chloroplast oligomeric complexes. *Plant J* 37: 864-876

- Zaki MAM, Dickinson HG (1991) Microspore-derived embryos in *Brassica*: the significance of division symmetry in pollen mitosis I to embryogenic development. *Sex Plant Reprod* 4: 48-55
- Zarsky V, Garrido D, Eller N, Tupy J, Vicente O, Schöffl F, Heberle-Bors E (1995) The expression of a small heat shock gene is activated during induction of tobacco pollen embryogenesis by starvation. *Plant Cell Environ* 18: 139-147
- Zeevaart JAD, Creelman RA (1988) Metabolism and physiology of abscisic acid. *Annu Rev Plant Physiol Plant Mol Biol* 39: 439-473
- Zhao JP, Simmonds DH, Newcomb W (1996) Induction of embryogenesis with colchicine instead of heat in microspores of *Brassica napus* L. cv Topas. *Planta* 189: 433-439
- Zhao JP, Simmonds DH (1995) Application of trifluralin to embryogenic microspores to generate haploid plants in *Brassica napus*. *Physiol Plant* 95: 304-309
- Zhao JZ, Newcomb W, Simmonds D (2003) Heat-shock proteins 70k Da and 19k Da are not required for induction of embryogenesis of *Brassica napus* L. cv. Topas. *Plant Cell Physiol* 44: 1417-1421
- Zheng MY, Liu W, Weng Y, Polle E, Konzak C (2001) Culture of freshly isolated wheat (*Triticum aestivum* L.) microspores with inducer chemicals. *Plant Cell Rep* 20: 685-690
- Zimmerman JL (1993) Somatic embryogenesis. *Plant Cell* 5: 1411-1423
- Zuo J, Niu QW, Frugis G, Chua NH (2002) The *WUSCHEL* gene promotes vegetative-to-embryonic transition in *Arabidopsis*. *Plant J* 30: 349-359

Chapter 2

Time-lapse tracking of barley androgenesis reveals position-determined cell death within pro-embryos

Planta 2004, in press

Simone de Faria Maraschin, Marco Vennik, Gerda E.M. Lamers, Herman P. Spaink, Mei Wang

Abstract

Following abiotic stress to induce barley (*Hordeum vulgare* L.) androgenesis, the development of 794 enlarged microspores in culture was monitored by time-lapse tracking. In total, 11% of the microspores tracked developed into embryo-like structures (type-I pathway), 36% formed multicellular structures (type-II pathway) and 53% of the microspores followed gametophytic divisions, accumulated starch and died in the first days of tracking (type-III pathway). Despite the microspore fate, enlarged microspores showed similar morphologies directly after stress treatment. Ultrastructural analysis, however, revealed two morphologically distinct cell types. Cells with a thin intine layer and an undifferentiated cytoplasm after stress treatment were associated with type-I and type-II pathways, whereas the presence of differentiated amyloplasts and a thick intine layer were associated with the type-III pathway. Tracking revealed that the first morphological change associated with embryogenic potential was a star-like morphology, which was a transitory stage between uninucleate vacuolated microspores after stress and the initiation of cell division. The difference between type-I and type-II pathways was observed during the time they displayed the star-like morphology. During the transition phase, embryo-like structures in the type-I pathway were always released out of the exine wall at the opposite side of the pollen germ pore, whereas in the type-II pathway multicellular structures were unable to break the exine and to release embryo-like structures. Moreover, by combining viability studies with cell tracking, we show that release of embryo-like structures was preceded by a decrease in viability of the cells positioned at the site of exine wall rupture. These cells were also positively stained by Sytox orange, a cell death indicator. Thereby, we demonstrate, for the first time, that a position-determined cell death process marks the transition from a multicellular structure into an embryo-like structure during barley androgenesis.

Introduction

During androgenesis, haploid microspores initially determined to form gametes are reprogrammed to divide and to form embryos, which develop similarly to their somatic and zygotic counterparts (Mordhorst et al., 1997). As a result of frequent chromosome doubling, microspore-derived embryos develop into double haploid plants, providing advantages for both fundamental and applied research (Wang et al., 2000).

Since it was first described in *in vitro*-cultured anthers of *Datura innoxia* by Guha and Maheshwari (1964), improvement of the conditions for androgenesis induction and

microspore culture have resulted in the regeneration of double haploids of many plant species (Reynolds, 1997). Due to the high regeneration efficiencies, rapeseed (*Brassica napus* L.), tobacco (*Nicotiana* spp), wheat (*Triticum aestivum* L.) and barley (*Hordeum vulgare* L.) are considered model systems for androgenesis studies (Touraev et al., 1997). These species offer the possibility for the identification of the genes involved in androgenesis induction and for the development of molecular markers. However, only a few marker genes have been identified so far. Among these, members of the family of heat-shock proteins, napin seed storage proteins and the *BABY BOOM* gene have been shown to correlate with *Brassica* androgenesis initiation (Smykal and Pechan, 2000; Boutilier et al., 1994; 2000).

One of the most pertinent problems in the search for suitable molecular markers for microspore embryogenic competence is the heterogeneity of stressed microspore populations, which are composed of embryogenic and non-embryogenic cells (Pechan and Smykal, 2001). Therefore, the identification and isolation of the competent microspores following stress treatment is of great importance. Time-lapse tracking offers the possibility to follow the developmental pathway from single cells to embryos in detail (Krens et al., 1998). This technique has been employed in the identification of morphological traits for the induction of embryogenesis in many plant cell cultures, such as barley and tobacco protoplasts, single suspension cells of carrot (*Daucus carota* L.), leaf explants from *Dactylis glomerata* L. and pro-embryogenic masses of Norway spruce (*Picea abies* L. Karst; Golds et al., 1992; Toonen et al., 1994; Somleva et al., 2000; Filonova et al., 2000a). The identification of cells competent to form embryos in carrot somatic embryogenesis has helped the development of robust embryogenic marker genes, such as the *SOMATIC EMBRYOGENESIS RECEPTOR-LIKE KINASE* (*SERK*) and the *EP2* gene, which encodes a lipid-transfer protein (Schmidt et al., 1997; Sterk et al., 1991).

In the field of androgenesis, an efficient system of tracking heat-stressed wheat microspores to the embryo stage has been developed by Indrianto et al. (2001), whose findings indicate that a star-like morphology is correlated with embryogenic competence. Single-cell tracking of barley microspores following cold or heat stress to induce androgenesis revealed that only enlarged microspores with a rich cytoplasm and granular appearance were able to develop into embryos (Bolik and Koop, 1991; Kumlehn and Lörz, 1999). So far, the highest regeneration efficiencies from barley microspores have been obtained by the incubation of anthers containing uninucleate microspores in mannitol solution for 4 days at 25°C. After stress treatment, an average of 20–60% of the microspores appear as enlarged, highly vacuolated cells, an indication of embryogenic potential acquirement (Hoekstra et al., 1992). However, only 7% of these enlarged microspores have been reported to develop into embryo-like structures (Maraschin et al., 2003). In order to gain more

information on the morphology of the enlarged cells that ultimately contribute to embryo formation during barley androgenesis following mannitol and starvation treatment, ultrastructural studies and time-lapse tracking of isolated enlarged microspores immobilized in a thin layer of agarose were carried out. Time-lapse tracking was coupled to viability studies, and the successive developmental stages from single barley microspores to embryos were determined, resulting in the elaboration of a fate map of barley microspore embryogenesis. We demonstrate that the star-like morphology indicates a developmental process, and its time of occurrence is associated with the embryogenic potential of barley microspores. Moreover, we report, for the first time, that the transition from a multicellular structure to an embryo-like structure is accompanied by cell death.

Materials and methods

Androgenesis induction, microspore culture and time-lapse tracking

Donor plants of barley (*Hordeum vulgare* L. cv Igri, Landbouw Bureau Wiersum, The Netherlands) were grown in a phytotron under conditions described previously (Hoekstra et al., 1992). Pre-treatment consisted of incubation of anthers containing mid-late to late uninucleate microspores in 0.37 M mannitol solution for 4 days in the dark, at 25°C (Hoekstra et al. 1992). After pre-treatment, microspores were isolated by gentle blending in 0.37 M mannitol solution for 30 s using a commercial blender at medium power (Waring), filtered through 110 µm nylon meshes and collected by centrifugation at 800 rpm for 5 min. The number of enlarged and non-enlarged microspores was estimated in a population of 300 cells in three independent experiments ($n=3$). The enlarged microspores were separated from the non-enlarged ones by a sucrose gradient (Maraschin et al. 2003). The enlarged microspores were plated in medium I (Hoekstra et al., 1992) at a density of $2 \cdot 10^4$ enlarged microspores per ml, and cultured for 7 days (Hoekstra et al., 1993) for viability studies of multicellular structures (MCSs) or immobilized for time-lapse tracking. Microspores were immobilized onto sterilized 500 µm nylon meshes in 8-well Lab-Tek II chambers (Nalgene Nunc International). For immobilization, each well held 200 µl of medium I (Hoekstra et al., 1992) containing 0.6% (w/v) of low-melting-type agarose (Hispanagar) and $2 \cdot 10^4$ enlarged microspores per ml. The thin layer of immobilized microspores was covered by 500 µl of medium I per well and the cultures were incubated at 25°C in the dark for 28 days for embryo development. After 1 week of culture, 250 µl of fresh medium I was added to each well. Fluorescein diacetate (FDA; Sigma) was used to assay MCS viability during cell tracking. FDA was used at a final concentration of $1 \cdot 10^{-4}$ g.ml⁻¹ and was added at day 0 of tracked cultures. The development

of 794 enlarged microspores was followed in three independent experiments ($n=3$). The immobilized microspores were observed using an inverted Olympus microscope coupled to a Nikon DXM 1200 digital camera. The position of each microspore was determined using the nylon mesh as a reference guide. Digital images were generated at days 0, 1, 2, 3, 4, 6, 8, 10, 14, 16 and 28 of culture using both light and fluorescence microscopy. The microspores were characterized into different types according to their developmental pathways. After 28 days of culture, embryos ranging from 0.5 to 1 mm were transferred to regeneration medium (Hoekstra et al., 1992).

Transmission electron microscopy

Enlarged microspores after stress treatment were assayed for ultrastructural studies. Microspores were fixed in a mixture of 2 % (w/v) glutaraldehyde and 2.5 % (w/v) paraformaldehyde in 0.1 M sodium cacodylate buffer, pH 7.3 for 3 h at room temperature. Microspores were immobilized in 1 % (w/v) low-melting type agarose (Hispanagar) and the resulting pellets were returned to fixative solution overnight at 4 °C. Pellets were washed 10 min in 0.1 M sodium cacodylate buffer, pH 7.3, and placed in 1 % (w/v) OsO₄ in 0.1 M sodium cacodylate buffer, pH 7.3 for 1 h at room temperature. Following post-fixation, pellets were washed 10 min in 0.1 M sodium cacodylate buffer, pH 7.3, and dehydrated at room temperature through a graded ethanol series as follows: 70 %, 80 %, 90 %, 96 %, 100 % (v/v). After dehydration, pellets were placed in propylene oxide for 30 min. The resin was infiltrated by incubation in 1:1 (v:v) mixture of propylene oxide:Epon (Agar Scientific) for 2 h, followed by incubation in Epon overnight at room temperature. Embedding was in Epon and polymerization took place at 55 °C for 48 h. Ultrathin sections were made using an ultramicrotome (Ultracut, Leica), stained for 10 min in 2 % (w/v) uranyl acetate in 50 % (v/v) ethanol and for 10 min in 0.4 % (w/v) lead citrate, followed by thorough washes in deionized filtered water. Electron micrographs were made using a Jeol 100 CX electron microscope. Pictures were taken at 60 kV on a Kodak 5302 FGP-film.

Cell viability and cell death staining of MCSs

MCSs at day 7 of liquid cultures were stained for cell death with 1 µM of Sytox orange (Molecular Probes) and for cell viability with $4 \cdot 10^{-2}$ µg.ml⁻¹ of FDA. MCSs were observed using a Leica DM IRBE confocal microscope. An argon and a krypton laser were used for visualization of the FDA and the Sytox orange signal, respectively.

Experimental data

Mean values \pm SD of the different developmental pathways were calculated as percentages of the relative frequency of each pathway identified. Significance of the differences in mean values was tested with a Student's *t*-test.

Results

Stress-induced developmental pathways identified by time-lapse tracking

Following mannitol and starvation stress, $51.6\pm 4.8\%$ ($n=3$) of the isolated microspores were composed of enlarged, vacuolated cells with yellow/red interference of the exine wall. These enlarged cells were cultured in a thin layer of agarose for development of embryo-like structures (ELSs). The fate of 794 enlarged cells was followed by time-lapse tracking in three independent experiments ($n=3$). Developmental stages were observed at different time-points and the microspores were characterized according to their developmental pathways. This system yielded $10.9\pm 4.2\%$ ELSs released out of the exine wall. These ELSs were capable of regenerating into a new plantlet when transferred to germination medium (data not shown). When enlarged microspores are cultured at the same density in liquid medium, 7% of the microspores develop into ELSs (Maraschin et al., 2003). This suggests that the immobilized cultures are comparable to the liquid system.

Mainly three types of developmental pathway were identified (Fig. 1). Developmental type I, or the embryogenic pathway, represented $10.9\pm 4.2\%$ of the microspores tracked. This group comprised the microspores that followed sporophytic cell divisions, formed multicellular structures (MCSs) and were capable of releasing ELSs out of the exine wall of microspores (Fig. 1a–e). MCSs ruptured the exine wall of microspores after 10.5 ± 1.1 days of cell tracking (Fig. 1e). In the liquid culture system, MCSs usually rupture the exine wall of microspores after 7–8 days of culture (van Bergen et al., 1999), thus immobilized cultures display a 2- to 3-day delay compared to liquid ones. Developmental type II ($36.2\pm 2.4\%$) was also represented by microspores that followed sporophytic cell divisions, formed MCSs but showed shrinkage of the whole structure and died in an asynchronous way. Death occurred mostly between days 7 and 10 of culture, prior to the time of exine wall rupture in the type-I developmental pathway (Fig. 1f–j). Eventually, dead material was extruded from the exine wall of these MCSs (Fig. 1j). Microspores grouped into developmental type III ($52.9\pm 4.5\%$) did not display sporophytic divisions and died soon after initiation of culture (Fig. 1k–n). In order to identify the morphological characteristics of embryogenic microspores at an early developmental stage, microspore morphology at day 0

of tracking from type-I, -II and -III developmental pathways was analyzed. Cells were characterized by the presence of a big central vacuole, surrounded by a narrow strip of cytoplasm in which one nucleus was present. Differences were observed in the nuclear position relative to the pore (0–180°), the exine wall light interference (yellow to red) and in the cytoplasm granularity (Fig. 1a,f,k). However, none of these traits was exclusive to any of the developmental types identified. The first morphological change associated with sporophytic development was nuclear migration towards the middle of the microspore. This phenomenon was observed between days 0 and 3 of tracking in 60% of the microspores following developmental types I and II (Fig. 1a–c, f,g). Central localization of the nucleus was observed concomitantly with fragmentation of the large central vacuole, which was interspersed with centripetally oriented cytoplasmic strands. In both developmental types, the acquisition of a star-like morphology of the cells was always followed by sporophytic divisions. By monitoring the evolution of the star-like morphology over a period of 24 h, it was possible to observe that sporophytic divisions commenced characteristically at the side opposite to the pollen germ pore (Fig. 2a–e). In the first 2 h, the centrally located nucleus migrated towards the side opposite to the pollen germ pore (Fig. 2a–c), followed by nuclear division after 4 h (Fig. 2d). After 24 h, more than half of the space contained by the exine was filled by three visible nuclei (Fig. 2e). However, there seemed to be a difference in the time of appearance of the star-like morphology between developmental types I and II (Fig. 1c,g; Table 1). In developmental type II, 85.4±2.5% of the microspores displayed the star-like morphology in the first 24 h of tracking, whereas only 65.4±4.8% of the microspores following the type-I pathway showed the star-like morphology in the same period ($P<0.06$). Microspores following developmental type III were never found to display the star-like morphology. In most cases, microspores displayed gametophytic divisions and died soon after initiation of tracking, indicating that these microspores were still committed to the pollen developmental pathway (Fig. 1k-n). A comparison of developmental types I, II and III is shown in Table 1.

Subcellular differences in enlarged microspores after stress treatment

At day 0 of tracking, irrespective of their developmental pathway, enlarged microspores showed similar morphologies at the light-microscopy level (Fig. 1a,f,k). Ultrastructural studies of enlarged cells at day 0 of culture were carried out using transmission electron microscopy (TEM). Based on their cytological characteristics, mainly two types of enlarged microspore could be identified. One type of microspore showed a large nucleus close to the exine wall and a narrow strip of cytoplasm surrounding the vacuole.

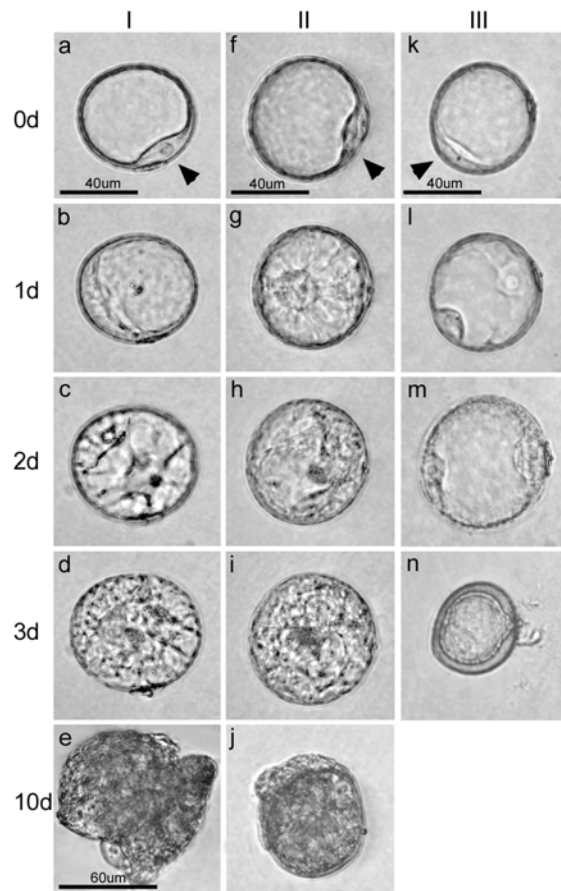


Figure 1. Developmental pathways of stressed enlarged barley microspores in culture, as determined by time-lapse tracking. According to their type of development, microspores were grouped into type I (a–e); type II (f–j) and type III (k–n). *Arrowheads* in (a), (f) and (k) indicate the position of the nucleus in relation to the pollen germ pore: 0°, 0° and 90–180°, respectively. Each developmental type is summarized in Table 1.

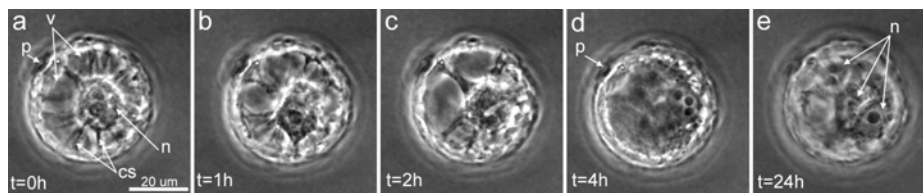


Figure 2. Evolution of a star-like morphology in developmental type I barley microspores, as monitored over a period of 24 h. The star-like morphology was observed from 1 to 2 days of culture by phase contrast. Images were taken every hour from several star-like structures, and representative examples are shown. *cs* cytoplasmic strands, *n* nucleus, *p* germ pore, *v* vacuole.

The intine was present as a thin layer immediately underneath the exine wall (Fig. 3a–c). In another type of vacuolated microspore with the nucleus close to the exine wall, an organelle-rich cytoplasm, filled with differentiated amyloplasts, and a thick intine layer were present (Fig. 3d–f). Amyloplasts containing starch granules were often associated with microspores with a thick intine layer (Fig. 3d–f), but were never found in microspores that had a thin intine layer (Fig. 3a–c). In the latter, only a few organelles were present, such as rough endoplasmic reticulum, mitochondria and undifferentiated proplastids (Fig. 3b,c).

When mid-late to late uninucleate microspores were allowed to further develop in the mother plant for 4 days, they displayed gametophytic cell divisions and developed into binucleate pollen. TEM analysis of these binucleate pollen grains following normal gametophytic development revealed that these cells possess a thick intine layer and an organelle-rich cytoplasm (Fig. 3g–i). The cytoplasm contained numerous mitochondria, Golgi apparatus, rough and smooth endoplasmic reticulum and starch granules in the differentiated amyloplasts (Fig. 3h,i). This cytoplasmic morphology was similar to that observed in the type of enlarged cell with a thick intine layer, indicating that, morphologically, the latter showed signs of gametophytic development (Fig. 3d–f), which, however, was less advanced than for binucleate pollen, as starch granules were much smaller and less numerous.

Table 1. Characterization of developmental types by time-lapse tracking of stressed barley (*Hordeum vulgare*) microspores. The development of 794 enlarged microspores was followed in three independent experiments ($n=3$). The presence or absence of the characteristic is indicated by + or –, respectively. The percentage of star-like structures in developmental types I and II was calculated with respect to the total number of star-like structures visualized in each developmental pathway

Microspore pathways	Cells tracked	Relative frequency (%)	MCS	Cells displaying star-like structure				ELS
				Relative frequency (%)			Total	
				0-1d	1-2d	2-3d		
Type I	90	10.9±4.2	+	65.4±4.8	93.4±4	100	54	+
Type II	286	36.2±2.4	+	85.4±2.5 ^a	96.7±2 ^b	100	171	-
(I+II)	376	47.1±4.5						
Type III	418	52.9±4.5	-		-	-		-

^aMean value significantly different ($P<0.06$) from value of the star-like-structure frequency in the first day of culture of developmental type I

^bMean value not significantly different ($P>0.06$) from value of the star-like-structure frequency in the second day of culture of developmental type I

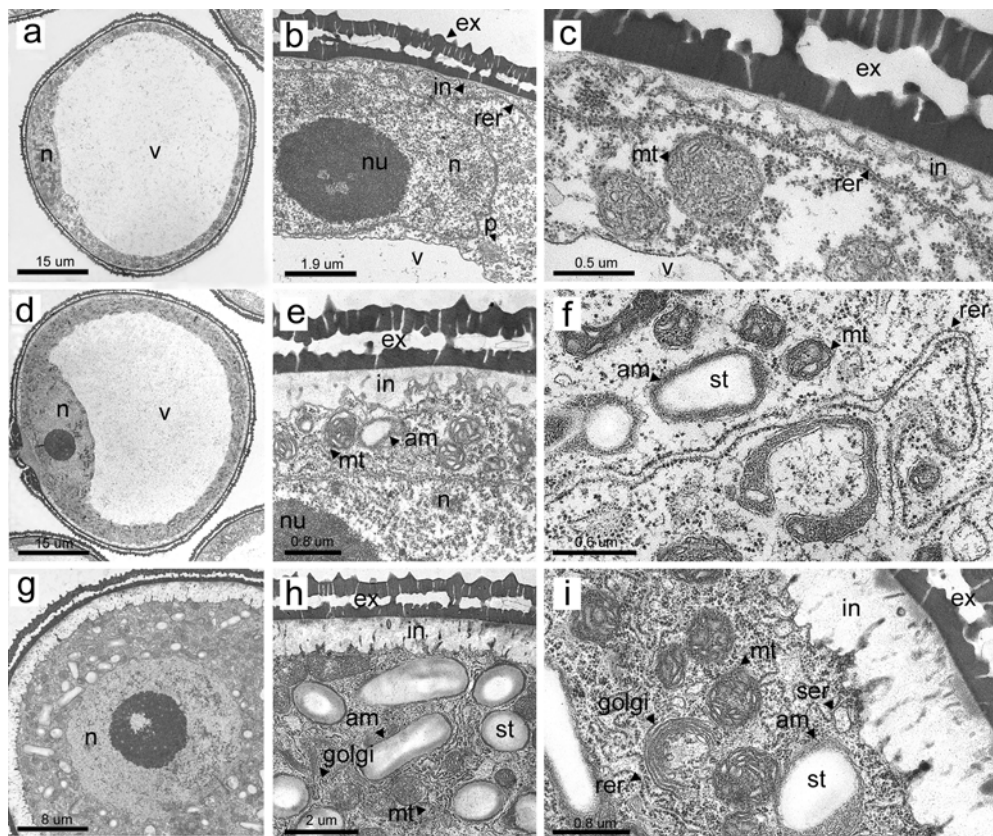


Figure 3. TEM analysis of stressed enlarged barley microspores at day 0 of culture and of binucleate pollen. (a–c) Enlarged microspores with a thin intine layer. (d–f) Enlarged microspores with a thick intine layer. (g–i) Binucleate pollen. *am* amyloplast, *ex* exine wall, *in* intine layer, *mt* mitochondria, *nu* nucleolus, *n* nucleus, *golgi* Golgi apparatus, *p* proplastid, *rer* rough endoplasmic reticulum, *ser* smooth endoplasmic reticulum, *st* starch, *vn* vegetative nucleus.

Cell viability of developmental type-I and type-II MCSs

Both developmental types I and II gave rise to MCSs and together accounted for $47.1 \pm 4.5\%$ of the tracked microspores, in an estimated ratio of 1:5 (I:II). However, microspores following developmental type II never released ELSs out of the exine wall of microspores, indicating that this is a crucial step in the androgenic process of barley. In order to gain more information on the fate of MCSs following developmental types I and II, viability studies were coupled to time-lapse tracking. To do so, FDA was added to the immobilized cultures and observed until the time of exine wall rupture. The FDA concentration used during tracking did not affect the growth rate or the morphology of the cells, suggesting that this FDA concentration is not toxic for microspore-derived embryo development (data not shown).

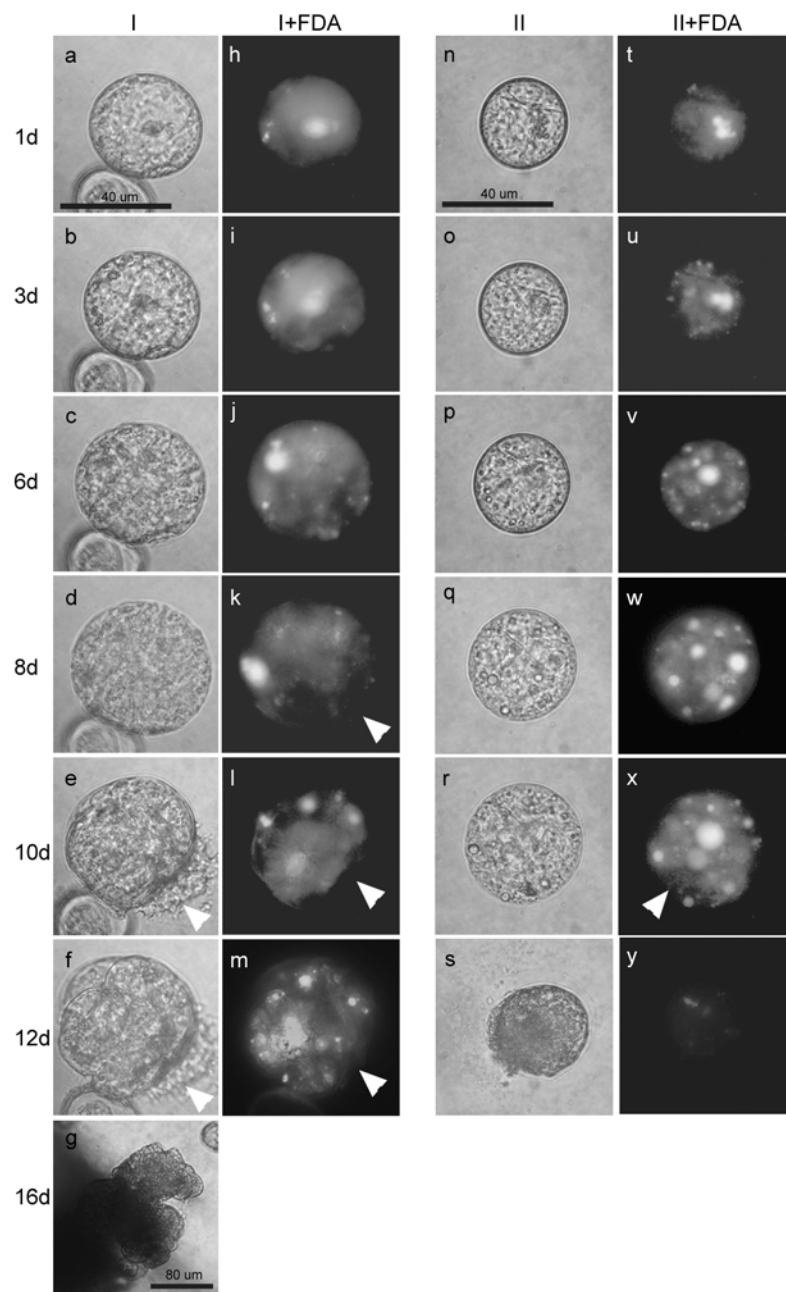


Figure 4. Developmental types I (a–m) and II (n–y), as visualized by light microscopy (brightfield; columns *I* and *II*) and fluorescence microscopy after staining with FDA (columns *I+FDA* and *II+FDA*). *Arrowheads* in (e) and (f) indicate the point of exine wall rupture, and in (k–m) and (x) indicate an MCS domain with lower intensity of FDA staining. The *shadow* in (g) corresponds to the mesh used in tracking experiments.

Figure 4 shows representative examples of developmental type I (Fig. 4a–m) and type II (Fig. 4n–y) observed by brightfield and fluorescence microscopy. During the first sporophytic divisions, MCSs following developmental types I and II were evenly stained by FDA, indicating viability of the whole structure (Fig. 4h–j, t–w). However, 2–3 days prior to exine wall rupture in MCSs following developmental type I, some domains were unstained by FDA near the area of exine wall break, opposite to the pollen germ pore (Fig. 4k, arrowhead). In the brightfield image, the FDA-unstained areas displayed further cell shrinkage and dead cell material was released out of the exine wall of microspores (Fig. 4e–f, l–m, arrowheads). In developmental type II, FDA-unstained domains were observed immediately prior to MCS death, about 2–4 days later than observed for MCSs following the type-I developmental pathway (Fig. 4x, arrowhead).

In order to confirm that the areas unstained by FDA represented dead cells within MCSs following the type-I developmental pathway, confocal laser scanning microscopy (CLSM) analysis of Sytox orange in combination with FDA staining was used. Sytox orange is a cell death indicator, which will only stain the nuclei of cells with damaged membranes. These studies were performed in liquid cultures of enlarged microspores due to the impossibility of using CLSM in agarose-immobilized cultures. In this system, exine wall rupture was observed after 7–8 days of culture (van Bergen et al., 1999). Therefore, FDA/Sytox orange analysis in MCSs was performed after 7 days of liquid culture. Figure 5 shows a confocal z-series of a 7 days-old MCS displaying one domain unstained by FDA, at the point of exine wall rupture (Fig. 5a,b, arrowheads). The same domain is positively stained by Sytox orange (Fig. 5c), indicating that the cells surrounding the point of exine wall break are dead.

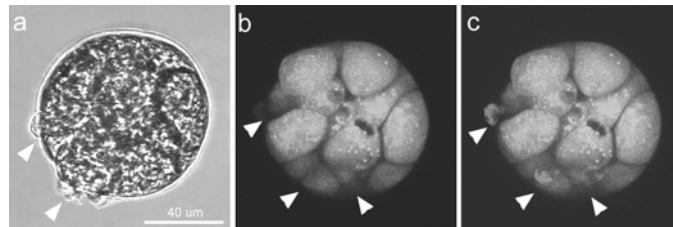


Figure 5. Brightfield image (a) and CLSM (b,c) of MCSs at the stage of exine wall rupture, stained by FDA and Sytox orange. (a) Exine wall rupture in a 7 days-old MCS grown in liquid culture. The site of exine wall rupture is marked by *arrowheads*. (b) The same MCS displayed in (a) showing FDA-unstained cells at the point of exine wall rupture (*arrowheads*). (c) The FDA-unstained cells are stained by Sytox orange (*arrowheads*).

Discussion

Morphology of microspores following androgenesis in barley

Using time-lapse tracking, mainly three developmental pathways were observed and their frequencies quantified: type I, which was the embryogenic pathway (11%); type II, which displayed sporophytic divisions, but failed to make the transition from an MCS into an ELS (36%); and type III, which degenerated in the first days of culture (53%). By tracking back these microspores to day 0 of culture, it was found that no typical morphology was associated with any of the developmental types described. Nevertheless, ultrastructural analysis of enlarged microspores by TEM revealed two distinct types of microspore. One type displayed a thin intine layer and an undifferentiated cytoplasm, while the other showed a thick intine layer and a starch-rich cytoplasm, and thus resembled developing pollen grains. Starch accumulation in the pollen amyloplasts marks the commitment to the pollen developmental pathway (McCormick, 1993). Our observations indicate that the enlarged cells that evolved to pollen morphology after stress treatment were still committed to the gametophytic pathway, probably representing the developmental type III identified by time-lapse tracking. On the other hand, microspores with undifferentiated cytoplasm have been associated with the repression of the gametophytic pathway, as reported for induced tobacco, rapeseed and wheat microspores (Rashid et al., 1982; Telmer et al., 1995; Indrianto et al., 2001). Prior to induction of androgenesis, barley uninucleate microspores are characterized by the lack of specialized morphological structures in the cytoplasm and a thin intine layer (Huang, 1986). This suggests that, in barley, the microspores with undifferentiated cytoplasm and a thin intine layer after stress treatment are probably associated with the repression of the gametophytic pathway (developmental types I and II). The maintenance of a thin intine layer after stress treatment may represent an early morphological marker for induced microspores in barley.

Tracking showed that the first developmental change associated with dividing microspores (developmental types I and II) was a star-like morphology, which was characterized as a transitory stage between vacuolated microspores after stress treatment and the initiation of cell division. The occurrence of a star-like morphology appears to be correlated with embryogenic potential in other androgenic systems, such as tobacco, wheat and rapeseed (Zaki and Dickinson, 1991; Touraev et al., 1997). Though very well documented, the cellular and molecular mechanisms implicated in the central positioning of the microspore nucleus prior to its divisions are not yet clear. Increasing evidence indicates that actin filament rearrangements play a role in the division symmetry (Gervais et al., 2000) and the presence of microtubule preprophase bands was shown to be important to the

symmetrical division of heat-shocked rapeseed microspores following central localization of the nucleus (Simmonds and Keller, 1999). Though the symmetry of the first division could not be verified in this study, subsequent divisions following the star-like morphology were shown to occur at the side opposite to the pollen germ pore, at the site where the generative cell is located during normal pollen development. At the stage when the dividing cells started to fill the exine cavity, they resembled very much the morphology of the cytoplasm-rich microspores previously identified by single-cell tracking as being embryogenic (Bolik and Koop, 1991; Kumlehn and Lörz, 1999).

Although the star-like morphology appears to be a morphological marker for the initiation of cell division in stressed microspores, a star-like morphology *per se* does not assure that a microspore will ultimately commit to the embryogenic pathway. According to Indrianto et al. (2001), the occurrence of a star-like morphology is a dynamic process, in which the time of occurrence will depend on the type of stress applied and the stage of microspore development. In barley, microspores of developmental type I displayed the tendency to form a star-like morphology relatively later than type-II microspores. Our results indicate that the different microspore developmental pathways may reflect differences in the microspore developmental stage during the period of stress treatment.

Transition from MCSs to ELSs during androgenesis in barley

One of the main events that distinguishes androgenesis from other embryogenic systems (zygotic, somatic and apomictic) is the fact that the first divisions of induced microspores are confined by the exine wall (Mordhorst et al., 1997). Therefore, during androgenesis, embryo development relies upon rupture of the exine wall that surrounds the dividing cells. We have demonstrated that 47% of the microspores tracked were induced to divide and to form MCSs (developmental types I and II). However, only MCSs following the type-I developmental pathway were successful in making the transition from an MCS to an ELS, while MCSs from the type-II developmental pathway degenerated and died. These results indicate that successful embryo formation during androgenesis might be a two-step process. The first step would be the induction of cell divisions in those microspores that have acquired the star-like morphology after stress treatment (developmental pathways I and II). Successful ELS release out of the exine wall and further embryo formation would represent a second step that would involve the perception of other, as yet unknown, developmental cues. It is known that barley microspore embryos can progressively secrete glycosylated proteins and arabinogalactan-proteins in the course of culture, which allow the development of maize immature zygotic embryos *in vitro* (Paire et al., 2003). Though little is known about the mode of action of these secreted molecules in microspore embryo formation, these findings indicate

that stress alone does not support the embryogenic route and reinforce the idea that a second trigger might be involved. The question raised is whether developmental type II can be shifted into type I by manipulating the stress and/or culture conditions. Plant regeneration has been reported to increase as a result of application of abscisic acid during pre-treatment and by the use of ovary co-culture in low-response barley cultivars, though that seems not to be the case in the highly responsive cv. Igri (van Bergen et al., 1999; Li and Devaux, 2001). In terms of breeding, it will be a challenge to determine which conditions need to be optimized in order to favor type-I development.

During androgenesis, the process of exine wall rupture has been widely accepted as a passive event that occurs by mechanical rupture due to the growing size of the dividing cells during the transition from MCSs to ELSs (Raghavan, 1986). By time-lapse tracking, we have observed that exine wall rupture always occurs at the side opposite to the pollen germ pore. In wheat, exine wall rupture has been reported to occur opposite to the site of starch granule accumulation (Indrianto et al., 2001). MCSs from monocots such as barley, maize and wheat are known to possess two domains with different cellular organizations (Sunderland and Huang, 1985; Huang, 1986; Bonet and Omedilla, 2000; Magnard et al., 2000; Ramírez et al., 2001; Testillano et al., 2002). In contrast, the divisions that take place inside the exine wall appear to be random in rapeseed microspores and no defined site of exine wall rupture has been reported (Telmer et al., 1995; Yeung et al., 1996). The highly organized structure of microspore-derived MCSs from monocots and the reports of a defined site for exine wall rupture indicate that exine rupture might be a controlled process rather than a passive event.

Further evidence that may support this idea is the finding that the cells on the side opposite to the pollen germ pore die prior to exine wall rupture. During androgenesis, the death of specific cell types has been described within microspore-derived MCSs from many plant species. Depending on the type of developmental pathway, the vegetative or the generative nucleus divides and the undivided nucleus degenerates and dies, a process that envisages the elimination of undesired cells (Raghavan, 1986). Barley MCSs are known to have diverse origins, and both vegetative and generative cell origins have been reported (Sunderland et al., 1979). Though the vegetative or generative origin of the dying cells on the side opposite to the pollen germ pore is not yet known, the side opposite to the pollen germ pore is where the generative nucleus is positioned after the first pollen mitosis during normal pollen development (Huang, 1986). This suggests that this may be a position-determined cell death. Clear examples of position-determined cell death are found during xylem formation (Bhalerao and Bennett, 2003) and during both female gametophyte development and fertilization. During megasporogenesis, only the chalazal-most megaspore survives while the

other three undergo cell death (Drews et al., 1998), whereas during fertilization only the synergid that is located on the side close to the placenta where pollen tubes turn into the ovule degenerates (Wu and Cheung, 2000). In both cases, cell death has been shown to present features of programmed cell death (PCD), a genetically regulated process that occurs upon plant development both *in vivo* and *in vitro* and responds to positional and temporal cues (Wu and Cheung, 2000). Developmental uses of PCD comprise a wide range of purposes, mostly associated with shape remodeling of the plant body plan (Pennell and Lamb, 1997). During *in vitro* somatic embryogenesis in Norway spruce, PCD takes place during the transition phase from pro-embryogenic mass to somatic embryo (Filonova et al., 2000b) and has recently been demonstrated to be essential for correct embryo pattern formation (Bozhkov et al., 2004). In our system, successful embryogenesis relied on position-determined cell death, which preceded the release of ELSs out of the exine wall of MCSs. Our immediate aim will be to investigate whether PCD is involved in the execution of exine wall rupture and further embryogenic development during barley androgenesis.

Acknowledgements

We are grateful to Sandra van Bergen (TNO Department of Applied Plant Sciences, The Netherlands) for technical assistance and valuable discussion and Dr. Wessel de Priester (Institute of Biology Leiden, Leiden University, The Netherlands) for critical reading of the manuscript.

References

- Bhalerao RP, Bennett MJ (2003) The case of morphogens in plants. *Nat Cell Biol* 5: 939-943
- Bolik M, Koop HU (1991) Identification of embryogenic microspores of barley (*Hordeum vulgare* L.) by individual selection and culture and their potential for transformation by microinjection. *Protoplasma* 162: 61-68
- Bonet FJ, Olmedilla A (2000) Structural changes during early embryogenesis in wheat pollen. *Protoplasma* 211: 94-102
- Boutilier KA, Ginés MJ, DeMoor JM, Huang B, Baszczynski CL, Iyer VN, Miki BL (1994) Expression of the BnmNAP subfamily of napin genes coincides with the induction of *Brassica* microspore embryogenesis. *Plant Mol Biol* 26: 1711-1723
- Boutilier K, Offringa R, Sharma VK, Kieft H, Ouellet T, Zhang L, Hattori J, Liu CM, van Lammeren AAM, Miki BLA, Custers JBM, van Lookeren Campagne MM (2002) Ectopic expression of *BABY BOOM* triggers a conversion from vegetative to embryogenic growth. *Plant Cell* 14: 1737-1749

- Bozhkov PV, Filonova LH, Suarez MF, Helmersson A, Smertenko AP, Zhivotovsky, von Arnold S (2004) VEIDase is a principal caspase-like activity involved in plant programmed cell death and essential for embryonic pattern formation. *Cell Death Differ* 11: 175-182
- Drews GN, Lee D, Christensen CA (1998) Genetic analysis of female gametophyte development and function. *Plant Cell* 10: 5-17
- Filonova LH, Bozhkov PV, von Arnold S (2000a) Developmental pathway of somatic embryogenesis in *Picea abies* as revealed by time-lapse tracking. *J Exp Bot* 51: 249-264
- Filonova LH, Bozhkov PV, Brukhin VB, Daniel G, Zhivotovsky B, von Arnold S (2000b) Two waves of programmed cell death occur during formation and development of somatic embryos in the gymnosperm, Norway spruce. *J Cell Sci* 113: 4399-4411
- Gervais G, Newcomb W, Simmonds DH (2000) Rearrangement of the actin filament and microtubule cytoskeleton during induction of microspore embryogenesis in *Brassica napus* L. cv Topas. *Protoplasma* 213: 194-202
- Golds TJ, Babczinsky J, Rauscher G, Koop HU (1992) Computer-controlled tracking of single cell development in *Nicotiana tabacum* L. and *Hordeum vulgare* L. protoplasts embedded in agarose/alginate films. *J Plant Physiol* 140: 582-587
- Guha S, Maheshwari SC (1964) *In vitro* production of embryos from anthers of *Datura*. *Nature* 204: 497
- Hoekstra S, van Zijderveld MH, Louwerse JD, Heidekamp F, van der Mark F (1992) Anther and Microspore culture of *Hordeum vulgare* L. cv. Igri. *Plant Sci* 86: 89-96
- Hoekstra S, van Zijderveld MH, Heidekamp F, van der Mark F (1993) Microspore culture of *Hordeum vulgare* L.: the influence of density and osmolarity. *Plant Cell Rep* 12: 661-665
- Huang B (1986) Ultrastructural aspects of pollen embryogenesis in *Hordeum*, *Triticum* and *Paeonia*. In: Hu H, Hongyuan Y (eds) *Haploids of higher plants in vitro*. Springer-Verlag, Berlin Heidelberg, pp 91-117
- Indrianto A, Barinova I, Touraev A, Heberle-Bors E (2001) Tracking individual wheat microspores *in vitro*: identification of embryogenic microspores and body axis formation in the embryo. *Planta* 212: 163-174
- Krens FA, Verhoeven HA, van Tunen AJ, Hall RD (1998) The use of an automated cell tracking system to identify specific cell types competent for regeneration and transformation. *In vitro Cell Dev Biol Plant* 34: 81-86
- Kumlehn J, Lörz H (1999) Monitoring sporophytic development of individual microspores of barley (*Hordeum vulgare* L.). In: Clement C, Pacini E, Audran JC (eds) *Anther and Pollen: from biology to biotechnology*. Springer-Verlag, Berlin Heidelberg, pp 183-189
- Li H, Devaux P (2001) Enhancement of microspore culture efficiency of recalcitrant barley genotypes. *Plant Cell Rep* 20: 475-481
- Magnard JL, Le Deunff E, Domenech J, Rogowsky PM, Testillano PS, Rougier M, Risueño MC, Vergne P, Dumas C (2000) Genes normally expressed in the endosperm are expressed at early stages of microspore embryogenesis in maize. *Plant Mol Biol* 44: 559-574
- Maraschin SF, Lamers GEM, de Pater BS, Spaink HP, Wang M (2003) 14-3-3 isoforms and pattern formation during barley microspore embryogenesis. *J Exp Bot* 51: 1033-1043
- McCormick S (1993) Male gametophyte development. *Plant Cell* 5: 1265-1275
- Mordhorst AP, Toonen MAJ, de Vries SC (1997) Plant Embryogenesis. *Crit Rev Plant Sci* 16: 535-576
- Paire A, Devaux P, Lafitte C, Dumas C, Matthys-Rochon E (2003) Proteins produced by barley microspores and their derived androgenic structures promote *in vitro* zygotic maize embryo formation. *Plant Cell Tiss Org* 73:167-176
- Pechan PM, Smykal P (2001) Androgenesis: affecting the fate of the male gametophyte. *Physiol Plant* 111: 1-8
- Pennell RI, Lamb C (1997) Programmed cell death in plants. *Plant Cell* 9: 1157-1168

- Raghavan V (1986) Pollen Embryogenesis. In: Barlow PW, Green PB, Wylie CC (eds) Embryogenesis in Angiosperms. Cambridge University Press, Cambridge, pp 153-189
- Ramírez C, Testillano PS, Castillo AM, Vallés MP, Coronado MJ, Cistué L, Risueño MC (2001) The early microspore embryogenesis pathway in barley is accompanied by concrete ultrastructural and expression changes. *Int J Dev Biol* 45: 57-58
- Rashid A, Siddiqui AW, Reinert J (1982) Subcellular aspects of origin and structure of pollen embryos of *Nicotiana*. *Protoplasma* 113: 202-208
- Reynolds TL (1997) Pollen Embryogenesis. *Plant Mol Biol* 33: 1-10
- Simmonds DH, Keller WA (1999) Significance of preprophase bands of microtubules in the induction of microspore embryogenesis of *Brassica napus*. *Planta* 208: 383-391
- Schmidt EDL, Guzzo F, Toonen MAJ, de Vries SC (1997) A leucine-rich repeat containing receptor-like kinase marks somatic plant cells competent to form embryos. *Development* 124: 2049-2062
- Smykal PM, Pechan P (2000) Stress, as assessed by the appearance of sHsp transcripts, is required but not sufficient to initiate androgenesis. *Physiol Plant* 110: 135-143
- Somleva MN, Schmidt EDL, de Vries SC (2000) Embryogenic cells in *Dactylis glomerata* L. (Poaceae) explants identified by cell tracking and by SERK expression. *Plant Cell Rep* 19: 718-726
- Sterk P, Booi H, Schellekens GA, van Kammen A, de Vries SC (1991) Cell-specific expression of the carrot EP2 lipid transfer protein gene. *Plant Cell* 3: 907-921
- Sunderland N, Huang B (1985) Barley anther culture. The switch of programme and albinism. *Hereditas* 3: 27-40
- Sunderland N, Roberts M, Evans LJ, Wildon DC (1979) Multicellular pollen formation in cultured barley anthers. I. Independent division of the generative and vegetative cells. *J Exp Bot* 30: 1133-1144
- Telmer CA, Newcomb W, Simmonds DH (1995) Cellular changes during heat shock induction and embryo development of cultured microspores of *Brassica napus* cv. Topas. *Protoplasma* 185: 106-112
- Testillano PS, Ramírez C, Domenech J, Coronado MJ, Vergne P, Matthys-Rochon E, Risueño MC (2002) Young microspore-derived maize embryos show two domains with defined features also present in zygotic embryogenesis. *Int J Dev Biol* 46: 1035-1047
- Toonen MAJ, Hendriks T, Schmidt EDL, Verhoeven HA, van Kammen A, de Vries SC (1994) Description of somatic-embryo-forming single cells in carrot suspension cultures employing video cell tracking. *Planta* 194: 565-572
- Touraev A, Vicente O, Heberle-Bors E (1997) Initiation of microspore embryogenesis by stress. *Trends Plant Sci* 2: 297-302
- van Bergen S, Kottenhagen MJ, van der Meulen RM, Wang M (1999) Effects of ABA during the pretreatment of barley anthers on androgenesis of *Hordeum vulgare* L. cultivars Igri and Digger. In: Clement C, Pacini E, Audran JC (eds) Anther and Pollen: from biology to biotechnology. Springer-Verlag, Berlin Heidelberg, pp 191-1999
- Wang M, van Bergen S, van Duijn B (2000) Insights into a key developmental switch and its importance for efficient plant breeding. *Plant Physiol* 124: 523-530
- Yeung EC, Rahman MH, Thorpe TA (1996) Comparative development of zygotic and microspore-derived embryos in *Brassica napus* L. cv Topas. I. Histodifferentiation. *Int J Plant Sci* 157: 27-39
- Wu H, Cheung AY (2000) Programmed cell death in plant reproduction. *Plant Mol Biol* 44: 267-281
- Zaki MAM, Dickinson HG (1991) Microspore-derived embryos in *Brassica*: the significance of division symmetry in pollen mitosis I to embryogenic development. *Sex Plant Reprod* 4: 48-55

Chapter 3

Programmed cell death during the transition from multicellular structures to globular embryos in barley androgenesis

Planta 2004, in press

Simone de Faria Maraschin*, Gwénaél Gaussand*, Amada Pulido, Adela Olmedilla, Gerda E.M. Lamers, Henrie Korthout, Herman P. Spaink, Mei Wang

*Both authors contributed equally for this work.

Abstract

Androgenesis represents one of the most fascinating examples of cell differentiation in plants. In barley, the conversion of stressed uninucleate microspores into embryo-like structures is highly efficient. One of the bottlenecks in this process is the successful release of embryo-like structures out of the exine wall of microspores. In the present work, morphological and biochemical studies were performed during the transition from multicellular structures to globular embryos. Exine wall rupture and subsequent globular embryo formation were observed only in microspores that divided asymmetrically. Independent divisions of the generative and the vegetative nuclei gave rise to heterogeneous multicellular structures, which were composed of two different cellular domains: small cells with condensed chromatin structure and large cells with normal chromatin structure. During exine wall rupture, the small cells died and their death marked the site of exine wall rupture. Cell death in the small cell domain showed typical features of plant programmed cell death. Chromatin condensation and DNA degradation preceded cell detachment and cytoplasm dismantling, a process that was characterized by the formation of vesicles and vacuoles that contained cytoplasmic material. This morphotype of programmed cell death was accompanied by an increase in the activity of caspase-3-like proteases. The orchestration of such a death program culminated with the elimination of the small generative domain, and further embryogenesis was carried out by the large vegetative domain. To date, this is the first report to show evidence that programmed cell death takes part in the development of microspore-derived embryos.

Introduction

The life cycle of flowering plants alternates the dominant diploid sporophytic phase with the short-lived, small-sized structures of the haploid female and male gametophytes, represented by the embryo sac and pollen grains. Microspores, or young pollen grains, have the remarkable ability to switch from their normal gametophytic development towards a sporophytic route. This fascinating example of phase transition during the alternation of generations in plants is called androgenesis (Raghavan, 1986). Androgenesis can be efficiently triggered in several plant species by means of stress treatment around the first pollen mitosis. Androgenic microspores under specific culture conditions are capable to form multicellular structures (MCSs), which differentiate into embryo-like structures (ELs) (Touraev et al., 1997). The successive ELS developmental stages are known to parallel

somatic and zygotic embryogenesis, providing advantages for both fundamental and applied research (Wang et al., 2000).

The initial steps of microspore embryogenesis are, however, unusual to any other embryogenic system, since MCS formation takes place inside the exine wall of microspores (Mordhorst et al., 1997). During the initial phase of microspore embryogenesis, several patterns of cell division have been identified to take place inside the exine wall. The asymmetric division of the microspore nucleus resulting in a generative and a vegetative cell characterizes the A-pathway. In the A-pathway, MCSs are formed from repeated divisions of the vegetative cell, while the generative cell or its derivatives degenerate and die (Sunderland, 1974). This is the most widely spread mechanism of MCS formation during androgenesis and it has been described in several plant species, including most cereals (Raghavan, 1986). In the B pathway, it is the symmetric division of the microspore nucleus that gives rise to MCSs (Sunderland, 1974). The B-pathway is known to play a major role in rapeseed (*Brassica napus* L.), potato (*Solanum tuberosum* L.), tobacco (*Nicotiana tabacum* L) and wheat (*Triticum aestivum* L.) microspore embryogenesis (Zaki and Dickinson, 1991; Říhová and Tupý, 1999; Touraev et al., 1996; Indrianto et al., 2001), and it has been also described among barley MCSs (Sunderland and Evans, 1980). An alternative route to androgenesis is defined by the independent divisions of the generative and vegetative cells, giving rise to MCSs with heterogeneous compositions. This modified version of the A-pathway, also termed E pathway (Raghavan, 1986), has been described in barley, maize, tobacco and pepper (*Capsicum annum* L) MCSs (Sunderland et al., 1979; Pretova et al., 1993; Touraev et al., 1996; Kim et al., 2004). Conversely to the known A and B pathways, in which the roles of the generative and vegetative cell are clearer, in this modified version of the A pathway both generative and vegetative cell appear to contribute equally to embryo formation (Raghavan, 1986).

What leads microspores to give preference to a particular division sequence is not yet clear. Different developmental pathways have been reported to vary according to plant species, and in response to different stress treatments and the microspore developmental stage (Raghavan, 1986; Sunderland et al., 1979; Říhová and Tupý, 1999; Kasha et al., 2001; Kim et al., 2004). In barley, a model species for androgenesis studies, a correlation between the yield of ELSs and the presence of heterogeneous MCSs has been reported in anther cultures of cold-stressed spikes (Sunderland and Huang, 1985). Nevertheless, no link has been established between the microspore developmental pathways that ultimately lead to barley ELSs formation. Recently, the development of mannitol-stressed barley microspores into ELSs has been monitored by time-lapse tracking (Maraschin et al., 2004). Following osmotic and starvation stress, 50 % of the microspores were triggered to divide and to form

MCSs, however only 20 % of the MCSs further developed into ELSs. The development of ELSs was conditioned to a specific type of MCSs that released ELSs characteristically at the opposite side of the pollen germ pore, a process that was marked by the death of the cells situated at exine wall rupture. The elimination of a specific cell type during the transition phase from MCSs to ELSs suggests that this might be an active cell death process. Programmed cell death (PCD) is a genetically programmed process of cell death that occurs during development and in response to environmental triggers in a wide variety of biological systems, including higher plants (Raff, 1998; Lam, 2004). Despite the nature of the PCD signal, animal and plant cells undergoing PCD show several common cytological features that include activation of specific proteases, condensation of chromatin, DNA cleavage into ~180bp internucleosomal fragments and loss of cell shape and integrity (Pennel and Lamb, 1997). In animal cells, PCD is regulated by a conserved family of cysteine proteases that specifically cleave target proteins after an Asp residue. The most prevalent executioner caspase in animal cells is caspase-3 (Thornberry and Lazebnik, 1998). Although caspase-3 proteases have not been yet identified in plants, caspase-3-like activity towards the synthetic fluorogenic caspase-3 substrate *N*-acetyl-DEVD-7-amino-4-methylcoumarin (Ac-DEVD-AMC) has been described and related to PCD (Korthout et al., 2000; Lam and del Pozo, 2000).

In order to investigate whether PCD takes place during the transition from MCSs into ELSs, biochemical and morphological markers for PCD were assayed. During the transition of MCSs into ELSs, the death of the cells at the site of rupture was used as a marker for embryogenic development. With the help of this marker, the developmental pathways that lead to ELS formation during barley androgenesis were investigated. Our results indicate that embryogenic MCSs are formed by the modified A-pathway, and therefore are composed of two different cellular domains, displaying generative and vegetative characteristics. During exine wall rupture, the small cell domain derived from the generative cell was eliminated by PCD, while the large cell domain derived from the vegetative cell contributed to globular embryo formation. This is the first report to show that PCD takes place during the transition from MCSs into ELSs in barley androgenesis.

Materials and methods

Androgenesis induction and microspore culture

Donor plants of barley (*Hordeum vulgare* L. cv Igri, Landbouw Bureau Wiersum, The Netherlands) were grown in a phytotron under conditions described previously (Hoekstra et al., 1992). Pre-treatment consisted of incubation of anthers containing mid-late to late

uninucleate microspores in 0.37 M mannitol solution for 4 days in the dark, at 25°C (Hoekstra et al., 1992). After pre-treatment, microspores were isolated as described previously (Maraschin et al., 2003; 2004). The enlarged microspores were plated in medium I (Hoekstra et al., 1992) at a density of 2.10^4 enlarged microspores. ml^{-1} and cultured for 0-14 days for MCS and ELS development (Hoekstra et al., 1993). Cultures were sieved through appropriate nylon mesh sizes and dividing MCSs and ELSs were collected as previously described (Maraschin et al., 2003).

DAPI staining of nuclei

Nuclear evolution of isolated-microspore cultures was followed by 4',6-diamidino-2-phenylindole (DAPI) staining (Vergne et al., 1987). Fresh MCSs were briefly fixed in Carnoy (70% ethanol (v/v): acetic acid, 3:1), after which they were rinsed in 70% (v/v) ethanol and stained for 10 min in $1\text{mg}\cdot\text{ml}^{-1}$ DAPI aqueous solution containing 1% (v/v) Triton X-100. Squashed material was studied under UV light with a Zeiss Axioplan microscope.

Cell viability and cell death staining of MCSs

MCSs and ELSs at different stages of culture were stained for cell death with Sytox orange (Molecular Probes) and for cell viability with fluorescein-diacetate (FDA, Sigma) as described previously (Maraschin et al., 2004). MCSs were observed using a Leica DM IRBE confocal microscope. An argon (488nm) and a krypton (568 nm) laser were used for visualization of the FDA (Ex 488nm, Em 502-540) and the Sytox orange (Ex 568, Em 570-610) signals, respectively. The percentage of ELSs released out of the exine wall was determined in three ($n=3$) independent experiments by estimating the relative amount of ELSs which showed FDA/ Sytox orange positive domains within 300 MCSs per experiment (Maraschin et al., 2004).

Terminal deoxynucleotidyl transferase-mediated dUTP nick end labelling (TUNEL)

MCSs and ELSs from different developmental stages were fixed in 2% (w/v) glutaraldehyde in 10 mM NaH_2PO_4 , 120 mM NaCl, 2.7 mM KCl, pH 7.4 (phosphate-buffered saline, PBS) overnight at room temperature. After dehydration at room temperature in a graded series of 70 %, 90 %, 96 % and 100 % (v/v) ethanol, samples were embedded in Technovit (Heraeus Kulzer). Sections (2 μm) were attached on Biobond (Biocell) coated slides. TUNEL assay was done using an *in situ* cell death detection kit (Roche) according to manufacturer's instructions. Following TUNEL reaction, cross-sections were stained with Sytox orange for visualization of nuclei (Maraschin et al., 2004). Samples were observed using a Zeiss Axioplan confocal microscope with a MRC 1024 ES Biorad module. An argon/

krypton laser (488/568nm) was used for the visualization of the TUNEL (Ex 488 nm, Em 522 DF 32) and the Sytox orange (Ex 568, Em 605 DF 32) signals.

DNA isolation and electrophoresis

Genomic DNA was isolated from MCSs and ELSs from different developmental stages that were frozen in liquid nitrogen immediately after sampling. Samples were ground with a mortar and pestle to a fine powder and DNA was isolated as described previously (Wang et al., 1999). Five µg of genomic DNA/ lane were separated on a 2 % (w/v) agarose gel containing 1 % (w/v) ethidium bromide in 0.2 M tris-acetate, 0.05 M EDTA pH 8.3 at 50 V for 4 h, along with a Smart DNA ladder (Eurogentec).

Protein isolation and caspase-3-like assay

MCSs and ELSs at different time points of culture were frozen in liquid nitrogen and were used to obtain cytosolic protein extracts. Samples were ground in 500 µl ice-cold extraction buffer containing 100 mM HEPES (pH 7.2), 10% (w/v) sucrose, 0.1% (w/v) CHAPS, 5 mM DTT and 10⁻⁶ % (v/v) NP40 using a glass mortar and pestle. Subsequently, the homogenate was incubated on ice for 15 min and centrifuged two times for 10 min at 13000 rpm at 4°C to pellet cell debris. The supernatant was cleared by filtration over a 0.22 µm Millex syringe driven filter unit (Millipore). For *in vitro* caspase-3-like activity, 75 µl of cytosolic extracts containing 5 µg of proteins were mixed to 25 µl of the synthetic fluorogenic caspase-3 substrate *N*-acetyl-DEVD-7-amino-4-methylcoumarin (Ac-DEVD-AMC, 75 µM) or with a mix of caspase-3 substrate Ac-DEVD-AMC and inhibitor (Ac-DEVD-CHO, 250 µM). The measurements were performed every 10 min for 2 h at room temperature in triplicates for each sample in three independent experiments (*n*=3). Substrate cleavage was detected in a Perkin Elmer fluorescence spectrometer LS50B at an excitation wavelength of 380 nm and an emission wavelength of 460 nm. The standard setting used an excitation and an emission slit value of 5.0. Kinetics of substrate hydrolysis was tested to be linear throughout the 2 h reactions.

Transmission electron microscopy (TEM)

MCSs and ELSs fixation, dehydration and embedding procedures were performed as described previously (Maraschin et al., 2004). Ultrathin sections were made using an ultramicrotome (Ultracut, Leica), stained for 10 min in 2 % (w/v) uranyl acetate in 50 % (v/v) ethanol, and for 10 min in 0.4 % (w/v) lead citrate, followed by thorough washes in deionized filtered water. Electron micrographs were made using a Jeol 100 CX electron microscope. Pictures were taken at 60 kV on a FGP- film (Kodak 5302).

Scanning electron microscopy (SEM)

MCSs and ELSs from different developmental stages were fixed in a mixture of 2 % (w/v) paraformaldehyde and 2.5 % (v/v) glutaraldehyde in 0.1 M sodium cacodylate buffer, pH 7.3, for 3 h at room temperature. Samples were dehydrated through a graded series of 50 %, 70 %, 90 %, 96 % and 100 % (v/v) acetone and dried using a Bal-Tec CPD 030 critical point drier. The samples were then mounted on stubs, coated with gold on a Polaron SEM coating unit E5100 and observed using a Jeol 6400 scanning electron microscope.

Experimental data

Data presented on morphological analysis of developing MCSs were representative of at least 300 MCSs observed per time point in three independent experiments ($n=3$). Mean values \pm SD of the daily frequencies of exine wall rupture were calculated as percentages. Significance of the differences in mean values of the specific caspase-3-like activities was tested with a Student's *t*-test.

Results

Mannitol treatment induces the formation of homogeneous and heterogeneous MCSs with different fates in culture

In order to investigate the developmental pathways by which mannitol-treated barley microspores develop into MCSs, the degree of DNA condensation in the nucleus was used as a marker to distinguish cells with vegetative and generative origins (Sunderland, 1974). During pollen and androgenic development, the generative cells are located opposite to the germ pore at the edge of the structure, connected to the intine (Huang, 1986; Sunderland et al., 1979). In the first day of culture, DAPI nuclear staining revealed that both symmetric and asymmetric divisions characterized the initial phase of MCSs formation. While symmetric divisions gave rise to two nuclei with normal chromatin structure (Fig. 1a), asymmetric divisions gave rise to two nuclei with different degrees of chromatin structure (Fig. 1b). In asymmetrically dividing microspores, the small nucleus with intense DAPI staining indicates the generative cell, and the large nucleus with weaker DAPI staining indicates the vegetative cell. Based on these DAPI-staining properties, MCSs with both homogeneous and heterogeneous nuclei composition were observed in 3 days-old cultures (Fig. 1c, indicated by arrows). A close-up of an heterogeneous MCSs shows that the small condensed nuclei formed a file at the edge of the exine wall.

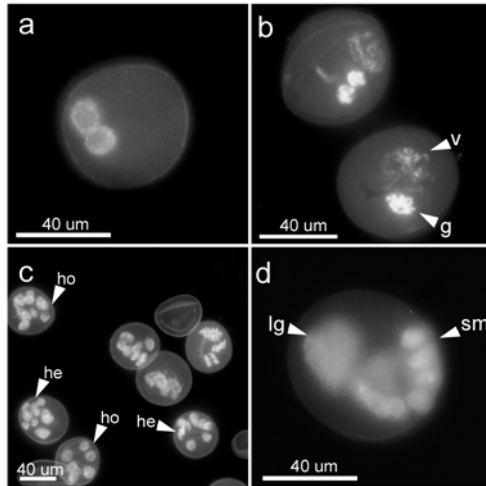


Figure 1. DAPI staining of nuclei in the first days of culture. (a,b) enlarged microspores at the first day of culture illustrating symmetric and asymmetric division of nuclei. (c,d) 3 day-old MCSs with homogeneous and heterogeneous composition. *g* generative nucleus, *lg* large nuclei with normal chromatin structure, *he* heterogeneous, *ho* homogenous, *sm* small condensed nuclei, *v* vegetative nucleus.

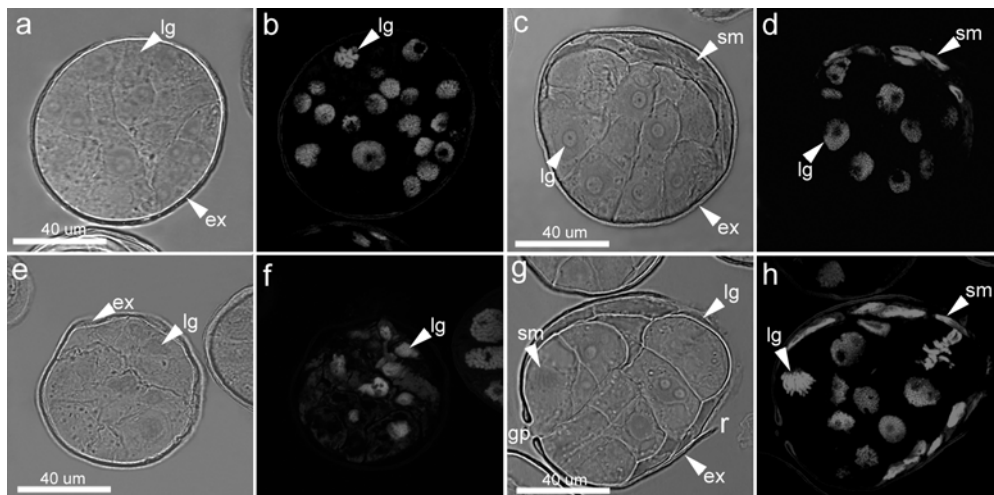


Figure 2. Cross-sections illustrating morphology of homogeneous and heterogeneous 5 and 7 days-old MCSs visualized by DIC and confocal microscopy stained by Sytox orange. (a,b) Homogeneous 5 days-old MCS composed of large cells with round nuclei. (c,d) Heterogeneous 5 days-old MCS displaying two cellular domains. (e,f) Homogeneous 7 days-old MCS displaying shrinkage at the time of exine wall rupture. (g,h) Exine wall rupture in heterogeneous MCS at the site of the small cell domain. *ex* exine wall, *gp* germ pore, *lg* large cell domain, *r* exine wall rupture, *sm* small cell domain.

The degree of chromatin condensation and the position at the edge of the exine wall point out their generative cell origin. At this stage, they divided more frequently than the large nuclei (Fig. 1d).

To better understand the morphology and the fate of the homogeneous and heterogeneous MCSs during the transition phase between MCSs and ELSs, cross-sections of homogeneous and heterogeneous MCSs were analyzed using differential interference contrast (DIC) microscopy and Sytox orange nuclear staining. Prior to exine wall rupture, 5 days-old homogeneous MCSs were composed of cells of equal size with rounded nuclei (Fig. 2a, b). In contrast, in 5 days-old heterogeneous MCSs, the generative domain was composed of small, compact cells with vermiform nuclei showing condensed chromatin structure and dense cytoplasm, while the vegetative domain was composed of large cells with round nuclei and normal chromatin structure (Fig. 2c, d). At the time of exine wall rupture, 7 days-old homogeneous MCSs appeared shrunken and did not develop further (Fig. 2e, f). Interestingly, only heterogeneous MCSs ruptured the exine wall after 7 days of culture. Heterogeneous MCSs displayed exine rupture exclusively at the domain composed of small cells, opposite to the pollen germ pore (Fig. 2g). At the exine wall rupture site, the small cell domain fell apart, while cell divisions were clearly observed within the large cell domain (Fig. 2h).

During microspore embryogenesis, exine wall rupture has been demonstrated to be accompanied by cell death at the site of rupture (Maraschin et al., 2004). In order to establish a link between the localization of the two different morphological domains in heterogeneous MCSs and the dying cells described previously in embryogenic MCSs, cell viability (FDA) and cell death (Sytox orange) staining were performed around the time of exine wall rupture (Fig. 3a-d). During the transition from MCSs to ELSs in 5-7 days-old cultures, Sytox orange-stained cells were located at the edge of the MCSs, at the site of exine wall rupture. This was the same localization as the domain composed of small cells in heterogeneous MCSs with ruptured exine (Fig. 2g, h). This indicates that the small cell domain dies at the time of exine wall rupture. At later stages, few dead cells were observed at the periphery of 9 days-old ELSs, and in most of the 11 days-old ELSs they had been completely eliminated (Fig. 3c, d).

Elimination of the small cell domain by PCD during exine wall rupture

The first PCD marker investigated during exine wall rupture was DNA cleavage. Assessment of *in situ* DNA cleavage was done by TUNEL assay. In liquid cultures, 5 days-old MCS had not yet come out of the exine wall (Fig. 3a). At this stage, some MCSs already showed signs of DNA degradation, as TUNEL-positive nuclei were observed in the small cells with condensed chromatin structure of nuclei. No TUNEL signal was found in the large cell

domain (Fig. 3e-h). After 7 days of culture, most of the MCSs had already ruptured the exine wall. The small cells appeared attached to the boundaries of the ruptured exine and their nuclei were heavily labeled by TUNEL (Fig. 3i-l). Pre-incubation with DNase I prior to TUNEL reaction induced DNA cleavage in both small and large cell domains (Fig. 3m-p), whereas no TUNEL signal was found in negative controls when the transferase was omitted in the TUNEL reaction (data not shown).

In order to investigate the time course analysis of DNA degradation, genomic DNA from 1-8 days-old MCSs was extracted and separated by conventional agarose gel electrophoresis. Extensive DNA degradation could be detected on gel in 7 days-old MCSs and 8 days-old ELSs (Fig. 4a). The apparent 2-days delay in detecting DNA fragmentation on gel compared to the detection of TUNEL-positive nuclei indicates that massive cell death takes place around 7-8 days of culture. In order to determine the dynamics of exine wall rupture, the daily frequency of ELSs released out of the exine wall was determined (Fig. 4b, open bars). An average of $50 \pm 1.52\%$ ($n=3$) of the ELSs were released out of the exine after 7 days of culture, overlapping with the extensive DNA degradation observed in 7 and 8 days-old cultures (Fig. 4a).

To better understand the events leading to DNA degradation during PCD of the small cell domain, caspase-3-like activity towards the synthetic fluorogenic caspase-3 substrate Ac-DEVD-AMC was assayed (Fig. 4b, black bars). A significant increase of the caspase-3-like activity measured in 1-3 days-old MCSs was observed after 4 days of culture ($P < 0.0004$), whereas TUNEL positive nuclei were only detected after 5 days of culture (Fig. 3e-h). The increase in the caspase-3-like activity in 4 and 5 days-old MCSs showed a peak at 6 days of culture ($P < 0.000002$) and significantly decreased thereafter.

The peak of the caspase-3-like activity measured in 6 days-old MCSs extracts preceded the DNA degradation observed after 7 and 8 days of culture (Fig. 4a) and the peak of exine wall rupture in 7 days-old MCSs (Fig. 4b, open bars). The caspase-3-like activity was efficiently inhibited by the specific mammalian caspase-3 inhibitor Ac-DEVD-CHO (Fig. 4b, gray bars). These results suggest that developing barley MCSs contain a caspase-3-like protease or a group of related proteases with the substrate preference and inhibitor specificity similar of mammalian caspase-3.

Morphology of cell dismantling

Since PCD involves specific cellular changes during cell dismantling, the ultrastructure of cell death was investigated by TEM in MCSs and ELSs around the time of exine wall rupture.

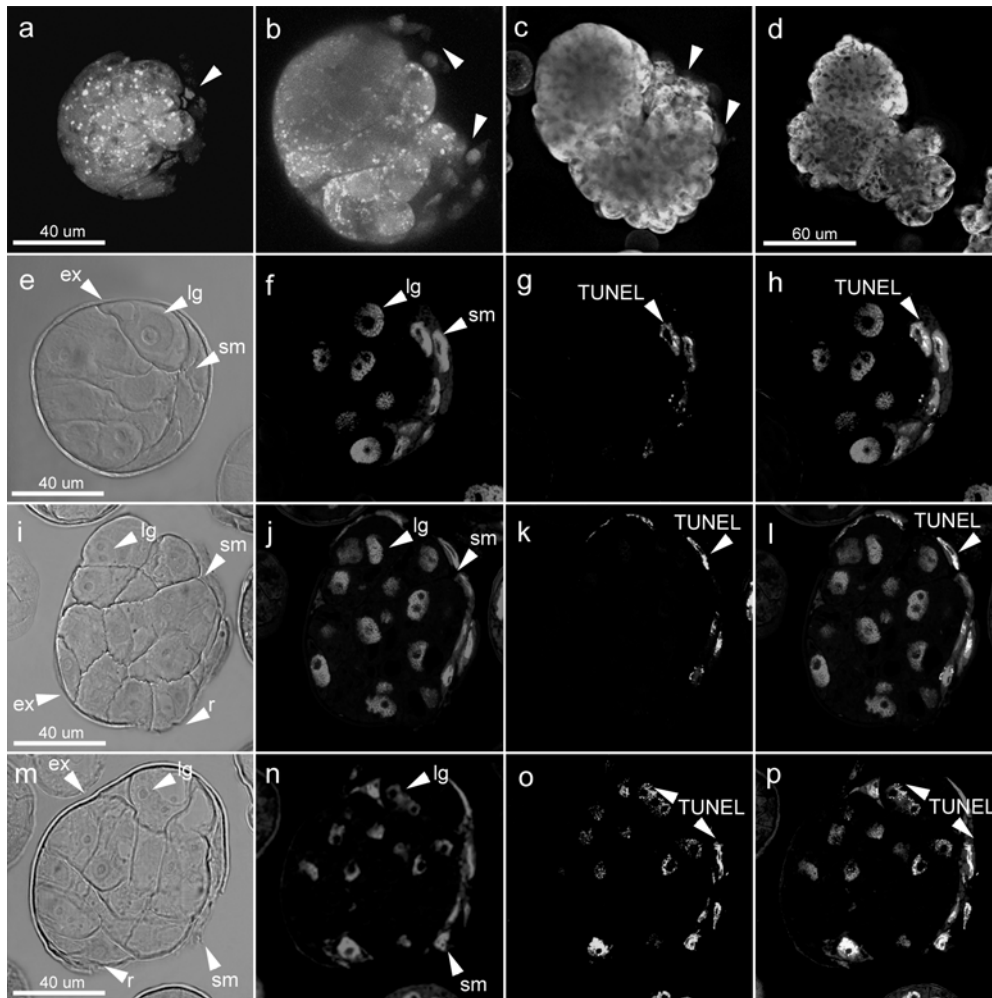


Figure 3. Fate of the different cellular domains during exine wall rupture visualized by FDA/ Sytox orange staining and TUNEL. (a) 5 days-old MCS, (b) 7 days-old MCS, (c) 9 days-old ELS and (d) 11 days-old ELS showing viability of the large cell domain as indicated by FDA staining, whereas the small cells are stained by Sytox orange and are progressively eliminated from the ELS (indicated by arrows). (e-h) Transmitted light image, Sytox orange nuclear staining and TUNEL signal on cross-sections of 5 days-old MCS and (i-l) 7 days-old MCS. (h,l) Are merged images of (f,g) and (j,k), respectively. (m-p) Transmitted light image, Sytox orange nuclear staining and TUNEL signal on a DNase I-treated cross-section of 7 days-old MCS. (p) Is a merged image of (n,o). TUNEL-positive nuclei in the small cell domain are indicated by arrows. *ex* exine wall, *lg* large cell domain, *r* exine wall rupture, *sm* small cell domain.

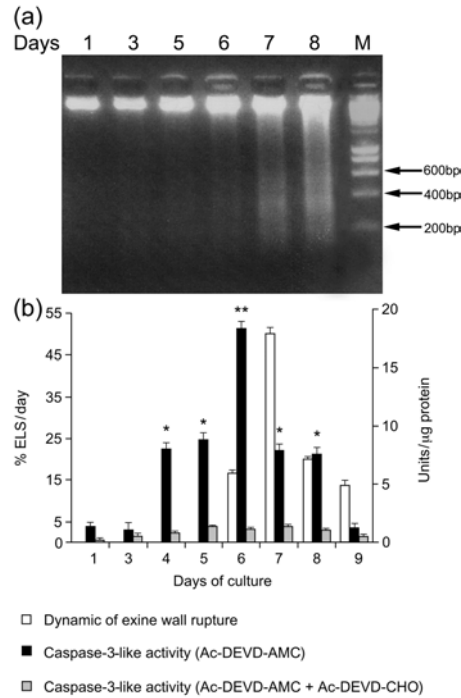


Figure 4. Time course analysis of DNA degradation, exine wall rupture dynamics and caspase-3-like activity. (a) Conventional DNA gel electrophoresis in 1-8 days-old MCSs and ELSs. DNA degradation is observed in 7 days-old MCSs and 8 days-old ELSs. *M*, marker DNA. (b) Dynamics of exine wall rupture (open bars) and caspase-3-like activity in total protein extracts of 1-9 days-old MCSs and ELSs in liquid culture (black bars). (*) Mean value significantly different than value measured at 1 day of culture ($P < 0.0004$). (**) Mean value significantly different from values obtained in all the other samples measured ($P < 0.000002$). Cleavage of the specific animal fluorogenic caspase-3 substrate (Ac-DEVD-AMC) was measured at 460 nm and was efficiently inhibited by the caspase-3 inhibitor (Ac-DEVD-CHO, gray bars) ($n=3$).

One of the most striking differences between the two cellular domains was the electron-dense cytoplasm of the small cells in 5 days-old MCSs prior to exine wall rupture (Fig. 5a). Due to the high density of the cytoplasm, few organelles could be distinguished at this stage. Among these, amyloplasts filled with starch granules, lipid bodies and mitochondria could be recognized. The nucleus showed a very condensed chromatin structure, and the nucleolus was very dense, characteristic of cells with little transcription activity (Fig. 5b).

The first ultrastructural change associated with PCD visualized in the nucleus was the formation of patches of condensed chromatin (Fig. 5c), which differed from the regular organized condensed chromatin structure (Fig. 5b). In the cytoplasm, mitochondria became less electron-dense (Fig. 5c). After exine wall rupture in 7 days-old MCSs, osmiophilic bodies were observed near the cell membranes and in the extracellular space of the dying cells, adjacent to the exine wall (Fig. 5d). Following exine wall rupture, the small cells detached

from the large cell domain (Fig. 5e). The process of cell detachment occurred in an asynchronous way, since it was possible to identify small cells at different stages of cell dismantling in one ELS (data not shown). During cell detachment, the cell walls surrounding the large cells were not removed, but only the ones surrounding the dying cells (Fig. 5e, indicated by arrows). In advanced stages of cell dismantling, the cytoplasm appeared less electron-dense, mitochondria were collapsed and small vesicles were visible. Cytoplasmic material was contained by vesicles and large vacuoles (Fig. 5f-h). Despite the high degree of cytoplasm collapse, the condensed chromatin in the nucleus persisted until later stages of cell dismantling (Fig. 5f). After cell dismantling was completed, cell debris resulting from the disassembly of the small cells remained in contact with the cell wall of the large cell domain in 9 days-old ELSs (Fig. 5i).

The changes in the external morphology of the dividing structures around the time of exine wall rupture were studied by SEM. SEM observations revealed the subsequent stages in exine wall rupture during the transition of MCSs into ELSs (Fig. 6). The first stage was frequently observed after 7 days of culture and represented the rupture of the exine wall at the site of the small cell domain. This rupture generated a crack, exposing the dead small cells to the exine exterior (Fig. 6a). The small cell domain possessed a very compact structure and the cells showed a flattened shape with a smooth surface (Fig. 6a). The second stage in exine wall rupture was often observed in 7-9 days-old cultures. In the second stage, cell dismantling and cell detachment took place in the small cell domain (Fig. 6b-d). This produced a gap within the small-celled domain, which exposed the large cell domain to the exine exterior. The large cell domain possessed loose structure and the cells showed a round shape with a rough surface (Fig. 6b). While the debris of the small cells remained attached to the edges of the opening exine, the crack in the exine further expanded as the large cells divided (Fig. 6b-d). In the third stage, the exine detached from the large, embryogenic cells. During exine detachment, the continuous and smooth pattern of the outer surface of the exine changed, as it became fragmented by its adhesion to the contours of the large cells (Fig. 6e). After the exine wall was detached from the outer surface of the large-celled domain, 11 days-old ELSs resembled zygotic globular embryos (Fig. 6f).

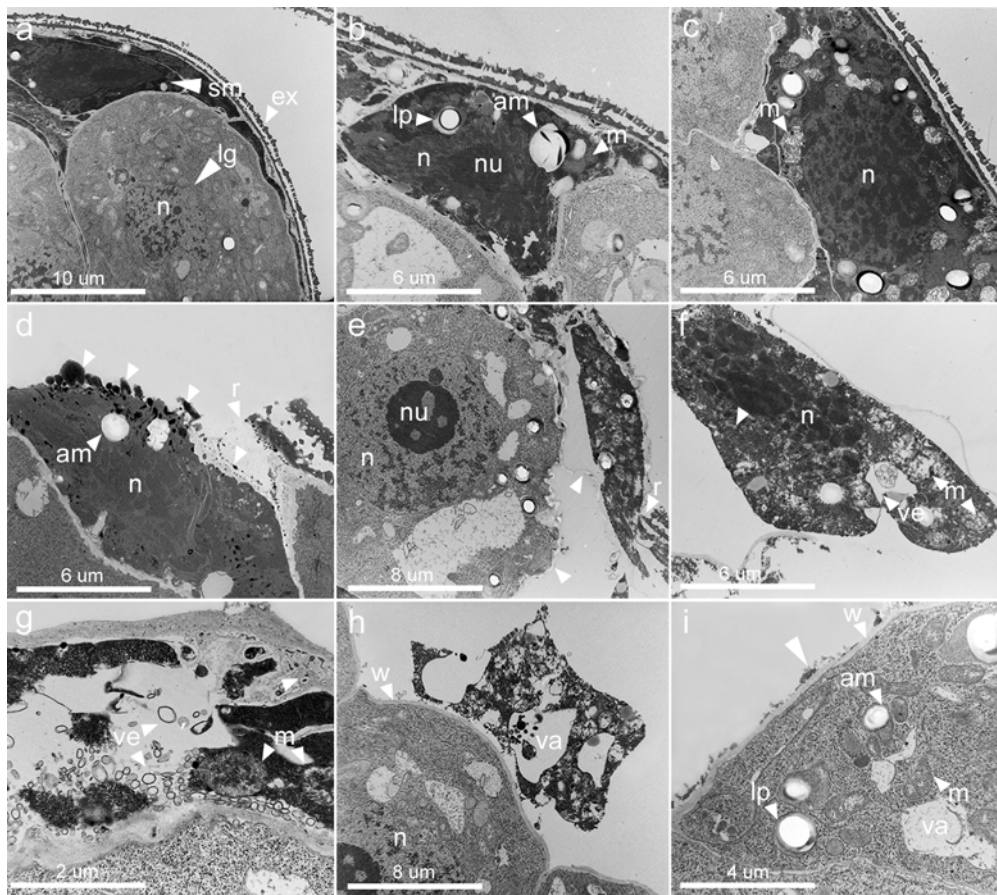


Figure 5. TEM analysis of PCD in MCSs and ELSs. (a-c) 5 days-old MCSs. (a) The cytoplasm of the small cell domain is highly electron-dense compared to the cytoplasm of the large cell domain. (b) A close-up of a small cell illustrates that the cytoplasm of the small cells contains amyloplasts, lipid bodies and mitochondria, while the nucleus shows a high degree of chromatin condensation. (c) The first ultrastructural changes associated with PCD are visualized by the formation of disorganized patches of chromatin in the nucleus and by a decrease in mitochondria electron-density. (d-h) 7 days-old MCSs showing the ultrastructure of the progressive stages of cell dismantling. Arrows in (d) indicate osmiophilic bodies while in (e) indicate cell wall detachment. (i) Region of 9 days-old ELS showing large cell domain after elimination of the small cells. *am* amyloplasts, *ex* exine wall, *lg* large cell domain, *lp* lipid bodies, *m* mitochondrion, *n* nucleus, *nu* nucleolus, *r* exine wall rupture, *sm* small cell domain, *ve* vesicles, *va* vacuole, *w* cell wall.

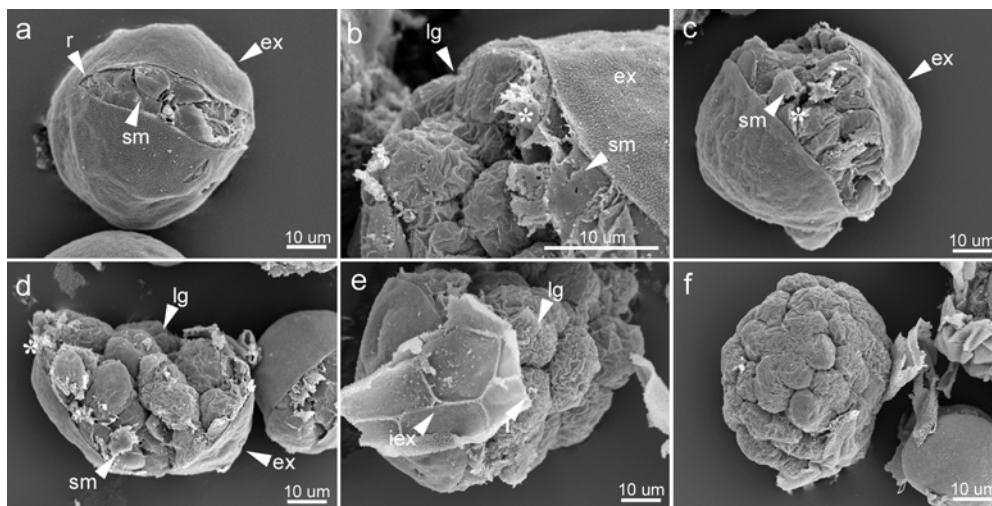


Figure 6. SEM analysis of MCSs and ELSs illustrating the 3 stages of exine wall rupture during the transition from MCSs to globular embryos. (a) Stage one, 7 days-old MCSs: rupture of the exine at the site of the small cell domain, exposing the small cells to the exine exterior. (b-d) Stage two, 7-9 days-old MCSs: cell dismantling and cell detachment of the small cell domain. Cell debris attached to the edges of the opening exine are marked by (*). (e) Stage three, 9 days-old ELS: exine wall detachment from the large cell domain. (f) 11 days-old ELS after exine wall detachment at the stage of globular embryo. *ex* exine wall, *iex* inner side of the exine wall, *lg* large cell domain, *r* exine wall rupture, *sm* small cell domain.

Discussion

Origin and fate of the two different cellular domains in embryogenic MCSs of barley

Cytological observations during the early stages of barley androgenesis revealed that both symmetric and asymmetric divisions result in the formation of MCSs. Symmetric divisions are characterized by the presence of two vegetative-like nuclei and give rise to homogeneous MCSs. On the other hand, asymmetric divisions lead to the formation of heterogeneous MCSs, characterized by a small cell domain with condensed chromatin structure of nuclei and a large cell domain showing normal chromatin structure of nuclei. The morphology of these nuclei resembles that of generative and vegetative nuclei of developing pollen grains (McCormick, 1993). These results indicate that both the B-pathway (Sunderland et al., 1976; Kasha et al., 2001) and the modified version of the A-pathway (Sunderland et al., 1979) contribute to MCS formation during barley androgenesis induced by an anther mannitol treatment. The progression of the embryogenic pathway during the transition of MCSs into ELSs in barley has been reported to occur only from MCSs that display cell death at the site of exine wall rupture (Maraschin et al., 2004). We further demonstrate that cell death takes

place in the small cell domain of heterogeneous MCSs, indicating that they represent the embryogenic MCSs previously described (Maraschin et al., 2004). This is the first report to show that heterogeneous MCSs developed via the modified A-pathway are the real embryogenic MCSs that result in the formation of ELSs in barley androgenesis.

The characterization of the events that resulted in the formation of heterogeneous MCSs indicates that the generative cell divides to give rise to a small cellular domain localized at the opposite side of the pollen germ pore. Cell tracking experiments have shown that the first divisions in embryogenic MCSs of barley take place at the opposite side of the pollen germ pore (Bolik and Koop, 1991; Kumlehn and Lörz, 1999; Maraschin et al., 2004). These findings suggest that the early stages of microspore embryogenesis in barley are marked by the divisions of the generative cell rather than the vegetative cell, which was shown to divide later. In barley, such division patterns have been reported to give rise to heterogeneous MCSs that have been termed 'partitioned units', to denote MCSs composed of different cellular types (Sunderland et al., 1979). Due to the compact cellular organization of the generative domain and the initial free nuclear divisions of the vegetative domain, these domains have been compared to the embryo and endosperm initials in zygotic embryogenesis (Sunderland and Huang, 1985). More recently, embryogenic and endosperm domains have been also described among wheat and maize MCSs (Bonet and Olmedilla, 2000; Magnard et al., 2000). Despite the similarities shared between the small and large cell domains described in the present work and the embryogenic and endosperm initials described previously (Sunderland et al., 1979; Sunderland and Huang, 1985), we show that the small cell domain is eliminated during the process of exine wall rupture and does not contribute to embryo formation, whereas the large cell domain gives rise to ELSs. By SEM, the morphology of ELSs released out of the exine wall resembles that of globular embryos, which showed no apparent signs of pattern formation. Our previous results have shown that pattern formation arises later in culture, when globular embryos released out of the exine wall acquire bilateral symmetry (Maraschin et al., 2003). The expression of the 14-3-3C isoform, a member of the conserved family of 14-3-3 regulatory proteins, has been reported to mark scutellum development during this process (Maraschin et al., 2003). These results indicate that pattern formation is probably not due to the different cellular domains present in MCSs contained within the exine as previously proposed (Sunderland et al., 1979; Sunderland and Huang, 1985). It appears more likely that pattern formation arises after exine wall rupture in globular embryos, a process that might involve new developmental cues.

PCD during the transition from MCSs to globular embryos

During development, uses of PCD include the formation of the plant body plans and specific organ shapes and the removal of unwanted or damaged cells. Three main cytological variants of PCD have been identified in plants (Fukuda, 2000). In apoptotic-like cell death, a process that is analogous to apoptosis in animal PCD, chromatin condensation, nuclear shrinkage and fragmentation, and DNA laddering are known to precede cytoplasm degradation (Pennel and Lamb, 1997). Though this appears to be the classical type of PCD during hypersensitive response and anther tapetum degeneration (Fukuda, 2000; Wang et al., 1999), during the differentiation of tracheary elements it is the vacuolar collapse that precedes nuclear DNA fragmentation (Obara et al., 2001). A third type of cell death morphology has been described within pro-embryos and suspensor cells during somatic embryogenesis of Norway spruce (*Picea abies* L. Karst). In this case, PCD showed apoptotic features concomitantly to autophagy, which was marked by the engulfment of cytoplasmic contents (Filonova et al., 2000).

The morphology of the small cells eliminated by PCD during exine wall rupture presents unique characteristics. Prior to exine wall rupture, the cytoplasm of the small cells is very dense, whereas the nucleus shows condensed chromatin structure. Condensation of nuclear chromatin and an electron-dense cytoplasm have been pointed as morphological markers of plant PCD (Pennel and Lamb, 1997; Domínguez et al., 2001; Aleksandrushkina et al., 2004). However, in the small cell domain of barley MCSs, these characteristics appear to be inherent to their generative cell origin rather than induced by PCD, since they were observed prior to any PCD event had started. The first morphological changes associated with PCD in the nucleus are DNA degradation and the aggregation of chromatin into disorganized patches, however condensed chromatin did not appear marginalized in the nuclear envelope like during pyknosis in most plant PCD events (Pennel and Lamb, 1997). In the cytoplasm, mitochondria became less electron-dense, an indication of mitochondria collapse (Ku et al., 2003). At the exine wall rupture site, osmiophilic bodies were present near the cell membranes and in the extracellular space of the small cells, a morphology that preceded cell detachment and subsequent cytoplasm dismantling. During the PCD events leading to leaf shape remodeling and nucellus degeneration, osmiophilic bodies have been reported near the cell membrane and tonoplast, and in the extracellular space prior to cytoplasm disassembly (Domínguez et al., 2001; Gunawardena et al., 2004). Though the identity of the vesicles heavily stained by osmium has not been identified yet, evidence points out that their presence marks the initiation of the events leading to cytoplasm dismantling during plant PCD.

A remarkable feature of the small dying cells is their detachment from the large cell domain after exine wall rupture. Cell detachment is a characteristic of PCD in the root cap of a wide range of plant species and it is also present during cell death in somatic embryogenic cultures of carrot (*Daucus carota* L.) (Pennel and Lamb, 1997; Willats et al., 2004). After detachment of the small cells from the large cell domain, cell dismantling is characterized by the presence of vesicles and large vacuoles that contain cytoplasmic material. The sequence of events during cytoplasm dismantling in the small cell domain appears to have similarities to the apoptotic-autophagic morphology described during somatic embryogenesis of Norway spruce (Filonova et al., 2000). Apoptotic-autophagic plant PCD is analogous to the cytoplasmic degenerative morphotype of animal PCD where cell death takes place *en masse*, as in the elimination of undesired tissues or complete organs, suggesting overlapping mechanisms of PCD across animal and plant kingdoms (Jones, 2000)

During apoptosis, the most studied case of animal PCD, the first irreversible step in the initiation of the cell death program is the activation of a proteolytic cascade involving caspase proteases. Despite the absence of canonical caspases in plants, dying cells have been reported to have increased proteolytic activities for caspase-1, -3 and -6 (Lam and del Pozo, 2000; Bozhkov et al., 2004). The apparent diversity in the different caspase-like proteases required for PCD in plants is in agreement with their role in animal PCD, since the death of specific cell types and diverse stimuli have been reported to involve different sets of caspases (Raff, 1998). Nevertheless, the most prevalent executioner caspase in animal cells has been pointed to be caspase-3 (Thornberry and Lazebnik, 1998). To date, no plant protease displaying caspase-3-like activity has been so far purified. Recent efforts to purify and characterize the proteases responsible for the caspase-like activities in plant cells has indicated that serine proteases and a vacuolar processing enzyme, which is a cysteine protease, might potentially account for the caspase-like activities upon plant PCD (Coffeen and Wolpert, 2004; Hatsugai et al., 2004). These results suggest that different plant proteases with similar substrate and inhibitor properties of the mammalian caspase-3 might be active during PCD in barley MCSs.

Following activation of the caspase cascade in animal cells, the DNA in the nucleus is cleaved into 180 bp fragments by a caspase-activated DNase (Enari et al., 1998; Sakahira et al., 1998). Upon plant PCD, caspase-like activity has been reported to precede DNA laddering (Lam, 2004), and several DNases have been implicated in this process (Mitler and Lam, 1997; Stein and Hansen, 1999). Though no caspase-activated DNases have been so far identified in plants, the DNA degradation observed during PCD followed the peak of caspase-3-like activity in barley MCSs. This sequence of events points to a possible role of caspase-3-dependent PCD in executing exine wall rupture. Additional roles for the elimination

of the small generative cells by PCD might be associated with sculpting of the microspore embryos, as caspase-6-dependent PCD has been recently demonstrated to be essential for correct embryo pattern formation during *in vitro* somatic embryogenesis in Norway spruce (Bozhkov et al., 2004). The characterization of the molecular events leading to PCD in barley androgenesis will help establishing a causal relation between PCD and exine wall rupture and will shed light on the mechanisms involved in plant PCD regulation. In this regard, biotechnological applications of PCD may be envisaged, since regulation of the PCD processes that take place during microspore and somatic embryogenesis may provide new tools for the manipulation of quality and yield of *in vitro*-developed plant embryos.

Acknowledgements

We are grateful to Dr. Wessel de Priester (Institute of Biology Leiden, Leiden University, The Netherlands) for valuable discussion and critical reading of the manuscript and to Peter Hock for the lay-out of figures.

References

- Aleksandrushkina NI, Zamyatnina VA, Bakeeva LE, Seredina AV, Smirnova EG, Yaguzhinsky LS, Vanyushin BF (2004) Apoptosis in wheat seedlings grown under normal daylight. *Biochemistry (Moscow)* 69: 285-294
- Bolik M, Koop HU (1991) Identification of embryogenic microspores of barley (*Hordeum vulgare* L.) by individual selection and culture and their potential for transformation by microinjection. *Protoplasma* 162: 61-68
- Bonet FJ, Olmedilla A (2000) Structural changes during early embryogenesis in wheat pollen. *Protoplasma* 211: 94-102
- Bozhkov PV, Filonova LH, Suarez MF, Helmersson A, Smertenko AP, Zhivotovsky, von Arnold S (2004) VEIDase is a principal caspase-like activity involved in plant programmed cell death and essential for embryonic pattern formation. *Cell Death Differ* 11: 175-182
- del Pozo O, Lam E (1998) Caspases and programmed cell death in the hypersensitive response of plants to pathogens. *Curr Biol* 8: 1129-1132
- Coffeen WC, Wolpert TJ (2004) Purification and characterization of serine proteases that exhibit caspase-like activity and are associated with programmed cell death in *Avena sativa*. *Plant Cell* 16: 857-873
- Domínguez F, Moreno J, Cejudo FJ (2001) The nucellus degenerates by a process of programmed cell death during the early stages of wheat grain development. *Planta* 213: 352-360
- Enari M, Sakahira H, Yokoyama H, Okawa K, Iwamatsu A, Nagata S (1998) A caspase-activated DNase that degrades DNA during apoptosis, and its inhibitor ICAD. *Nature* 391: 43-50
- Filonova LH, Bozhkov PV, Brukhin VB, Daniel G, Zhivotovsky B, von Arnold S (2000) Two waves of programmed cell death occur during formation and development of somatic embryos in the

- gymnosperm, Norway spruce. *J Cell Sci* 113: 4399-4411
- Fukuda H (2000) Programmed cell death of tracheary elements as a paradigm in plants. *Plant Mol Biol* 44: 245-253
- Hatsugai N, Kuroyanagi M, Yamada K, Meshi T, Tsuda S, Kondo M, Nishimura M, Hara-Nishimura (2004) A plant vacuolar protease, VPE, mediates virus-induced hypersensitive cell death. *Science* 305: 855-858
- Hoekstra S, van Zijderveld MH, Louwerse JD, Heidekamp F, van der Mark F (1992) Anther and Microspore culture of *Hordeum vulgare* L. cv. Igri. *Plant Sci* 86: 89-96
- Hoekstra S, van Zijderveld MH, Heidekamp F, van der Mark F (1993) Microspore culture of *Hordeum vulgare* L.: the influence of density and osmolarity. *Plant Cell Rep* 12: 661-665
- Huang B (1986) Ultrastructural aspects of pollen embryogenesis in *Hordeum*, *Triticum* and *Paeonia*. In: Hu H, Hongyuan Y (eds) *Haploids of higher plants in vitro*. Springer-Verlag, Berlin Heidelberg, pp 91-117
- Gunawardena AHLAN, Greenwood JS, Dengler NG (2004) Programmed cell death remodels lace plant shape during development. *Plant Cell* 16: 60-73
- Indrianto A, Barinova I, Touraev A, Heberle-Bors E (2001) Tracking individual wheat microspores *in vitro*: identification of embryogenic microspores and body axis formation in the embryo. *Planta* 212: 163-174
- Jones A (2000) Does the plant mitochondrion integrate cellular stress and regulate programmed cell death? *Trends Plant Sci* 5: 225-229
- Kasha KJ, Hu TC, Oro R, Simion E, Shim YS (2001) Nuclear fusion leads to chromosome doubling during mannitol pretreatment of barley (*Hordeum vulgare* L.) microspores. *J Exp Bot* 52: 1227-1238
- Kim M, Kim J, Yoon M, Choi DI, Lee KM (2004) Origin of multicellular pollen and pollen embryos in cultured anthers of pepper (*Capsicum annuum*). *Plant Cell Tiss Org* 77: 63-72
- Korthout HAAJ, Berecki G, Bruin W, van Duijn B, Wang M (2000) The presence and subcellular localization of caspase 3-like proteinases in plant cells. *FEBS Lett* 475: 139-144
- Ku S, Yoon H, Suh HS, Chung YY (2003) Male-sterility of thermosensitive genic male-sterile rice is associated with premature programmed cell death of the tapetum. *Planta* 217: 559-565
- Kumlehn J, Lörz H (1999) Monitoring sporophytic development of individual microspores of barley (*Hordeum vulgare* L.). In: Clement C, Pacini E, Audran JC (eds) *Anther and pollen: from biology to biotechnology*. Springer-Verlag, Berlin Heidelberg, pp 183-189
- Lam E (2004) Controlled cell death, plant survival and development. *Nat Rev Mol Cell Biol* 5: 305-315
- Lam E, del Pozo O (2000) Caspase-like protease involvement in the control of plant cell death. *Plant Mol Biol* 44: 417-428
- Magnard JL, Le Deunff E, Domenech J, Rogowsky PM, Testillano PS, Rougier M, Risueño MC, Vergne P, Dumas C (2000) Genes normally expressed in the endosperm are expressed at early stages of microspore embryogenesis in maize. *Plant Mol Biol* 44: 559-574
- Maraschin SF, Lamers GEM, de Pater BS, Spaink HP, Wang M (2003) 14-3-3 isoforms and pattern formation during barley microspore embryogenesis. *J Exp Bot* 51: 1033-1043
- Maraschin SF, Vennik M, Lamers GEM, Spaink HP, Wang M (2004) Time-lapse tracking of barley androgenesis reveals position-determined cell death within pro-embryos. *Planta*, *in press*
- McCormick S (1993) Male gametophyte development. *Plant Cell* 5: 1265-1275
- Mittler R, Lam E (1997) Characterization of nuclease activities and DNA fragmentation induced upon hypersensitive response cell death and mechanical stress. *Plant Mol Biol* 34: 209-221
- Mordhorst AP, Toonen MAJ, de Vries SC (1997) Plant Embryogenesis. *Crit Rev Plant Sci* 16: 535-576
- Obara K, Kuriyama H, Fukuda H (2001) Direct evidence of active and rapid nuclear degradation triggered by vacuole rupture during programmed cell death in *Zinnia*. *Plant Physiol* 125: 615-626
- Pennel RI, Lamb C (1997) Programmed cell death in plants. *Plant Cell* 9: 1157-1168

- Pretova A, de Ruijter NCA, van Lammeren AAM, Schel JHN (1993) Structural observations during androgenic microspore culture of the 4c1 genotype of *Zea mays* L. *Euphytica* 65: 61-69
- Raff M (1998) Cell suicide for beginners. *Nature* 396: 119-122
- Raghavan V (1986) Pollen embryogenesis. In: Barlow PW, Green PB, Wylie CC (eds) *Embryogenesis in angiosperms*. Cambridge University Press, Cambridge, pp 153-189
- Říhová L, Tupý J (1999) Manipulation of division symmetry and developmental fate in cultures of potato microspores. *Plant Cell Tiss Org* 59: 135-145
- Sakahira H, Enari M, Nagata S (1998) Cleavage of CAD inhibitor in CAD activation and DNA degradation during apoptosis. *Nature* 391: 96-99
- Stein JC, Hansen G (1999) Mannose induces an endonuclease responsible for DNA laddering in plant cells. *Plant Physiol* 121: 71-79
- Sunderland N (1974) Anther culture as a means of haploid induction. In: Kasha KJ (ed) *Haploids in higher plants: advances and potential*. University of Guelph, Canada, pp 91-122
- Sunderland N, Roberts M, Evans LJ, Wildon DC (1979) Multicellular pollen formation in cultured barley anthers. I. Independent division of the generative and vegetative cells. *J Exp Bot* 30: 1133-1144
- Sunderland N, Evans LJ (1980) Multicellular pollen formation in cultured barley anthers. II. The A, B and C pathways. *J Exp Bot* 31: 501-514
- Sunderland N, Huang B (1985) Barley anther culture – The switch of programme and albinism. *Hereditas* 3: 27-40
- Thornberry NA, Lazebnik Y (1998) Caspases: enemies within. *Science* 281: 1312-1316
- Touraev A, Pfosser M, Vicente O, Heberle-Bors E (1996) Stress as the major signal controlling the developmental fate of tobacco microspores: towards a unified model of induction of microspore/pollen embryogenesis. *Planta* 200: 144-152
- Touraev A, Vicente O, Heberle-Bors E (1997) Initiation of microspore embryogenesis by stress. *Trends Plant Sci* 2: 297-302
- Vergne P, Delvallée I, Dumas C (1987) Rapid assessment of microspore and pollen development stage in wheat and maize using DAPI and membrane permeabilization. *Stain Technol* 62: 299-304
- Wang M, van Bergen S, van Duijn B (2000) Insights into a key developmental switch and its importance for efficient plant breeding. *Plant Physiol* 124: 523-530
- Wang M, Hoekstra S, van Bergen S, Lamers GEM, Oppedijk BJ, van der Heijden MW, de Priester W, Schilperoort RA (1999) Apoptosis in developing anthers and the role of ABA in this process during androgenesis in *Hordeum vulgare* L. *Plant Mol Biol* 39: 489-501
- Willats WGT, McCartney L, Steele-King CG, Marcus SE, Mort A, Huisman M, van Alebeek GJ, Schols HA, Voragen AGJ, Le Goff A, Bonnin E, Thibault JF, Knox JP (2004) A xylogalacturonan epitope is specifically associated with plant cell detachment. *Planta* 218: 673-681
- Zaki MAM, Dickinson HG (1991) Microspore-derived embryos in *Brassica*: the significance of division symmetry in pollen mitosis I to embryogenic development. *Sex Plant Reprod* 4: 48-55

Chapter 4

14-3-3 proteins in barley androgenesis

I. 14-3-3 isoforms and pattern formation during barley microspore embryogenesis

J Exp Bot (2003) 54: 1033-1043

Simone de Faria Maraschin, Gerda E.M. Lamers, Sylvia de Pater, Herman P. Spaink, Mei
Wang

Abstract

The members of the 14-3-3 isoform family have been shown to be developmentally regulated during animal embryogenesis, where they take part of cell differentiation processes. 14-3-3 isoform-specific expression patterns were studied in plant embryogenic process, using barley (*Hordeum vulgare* L.) microspore embryogenesis as a model system. After embryogenesis induction by stress, microspores with enlarged morphology presented higher viability than non-enlarged ones. Following microspore culture, cell division was only observed among enlarged microspores. Western blot and immunolocalization of three barley 14-3-3 isoforms, 14-3-3A, 14-3-3B and 14-3-3C were carried out using isoform-specific antibodies. The level of 14-3-3C protein was higher in enlarged microspores than in non-enlarged ones. A processed form of 14-3-3A was associated to the death pathway of the non-enlarged microspores. In the early embryogenesis stage, 14-3-3 subcellular localization differed among dividing and non-dividing microspores and the microspore-derived multicellular structures showed a polarized expression pattern of 14-3-3C and a higher 14-3-3A signal in epidermis primordia. In the late embryogenesis stage, 14-3-3C was specifically expressed underneath the L₁ layer of the shoot apical meristem and in the scutellum of embryo-like structures (ELSs). 14-3-3C was also expressed in the scutellum and underneath the L₁ layer of the shoot apical meristem of 21 days after pollination (DAP) zygotic embryos. These results reveal that 14-3-3A processing and 14-3-3C isoform tissue-specific expression are closely related to cell fate and initiation of specific cell type differentiation, providing a new insight into the study of 14-3-3 proteins in plant embryogenesis.

Introduction

The ubiquitous family of 14-3-3 proteins consists of dimeric α -helical pSer/Thr binding proteins that control cellular processes by mediating protein-protein interactions (Yaffe et al., 2001). In animal cells, 14-3-3 proteins have been reported to interact with a wide number of mitotic and apoptotic factors, functioning as mediators of signal transduction cascades involved in cell cycle, differentiation and apoptosis (for a review see Fu et al., 2000). 14-3-3 homologues in plants have been found to interact with key enzymes of the carbon and nitrogen metabolism (Moorhead et al., 1999), from which the best described is the 14-3-3 inhibition of nitrate reductase activity (Bachmann et al., 1996a; Moorhead et al., 1996). 14-3-3 proteins also take part of the plasma membrane H⁺-ATPase regulation (Korthout and de Boer, 1994; Marra et al., 1994; Oecking et al., 1994). Their recent

localization in the chloroplast (Sehnke et al., 2000) and in the nucleus (Bihn et al., 1997) demonstrates their putative involvement in interacting with other metabolic and signaling pathways.

In both animal and plant systems, 14-3-3 regulatory roles are exerted by a family of several highly similar yet distinct protein isoforms. All 14-3-3 isoforms are very conserved in their core region, however the N-terminal dimerization domain and the hyper variable C-terminus show less homology (Wang and Shakes, 1996). In the inner groove of the conserved core lie the amino acids responsible for protein binding, thus different 14-3-3 isoforms interact with their targets probably by common mechanisms (Yaffe et al., 1997). The apparent lack of 14-3-3 isoform-specificity (Lu et al., 1994) seems to be compensated as 14-3-3 genes are differentially regulated at the expression level. In the *Arabidopsis* genome, fifteen 14-3-3 genes have been found (Rosenquist et al., 2001). Tissue-specific expression has been demonstrated for the 14-3-3 χ isoform during *Arabidopsis* plant development (Daugherty et al., 1996). In barley (*Hordeum vulgare* L.), three 14-3-3 isoforms have been cloned: 14-3-3A (GenBank X62388; Brandt et al., 1992), 14-3-3B (GenBank X93170) and 14-3-3C (GenBank Y14200). Upon germination of barley embryos, expression of the 14-3-3C isoform has been shown to be specific to the scutellum and the L₂ layer of the shoot apical meristem (Testerink et al., 1999), whereas the 14-3-3A isoform has been reported to be processed by proteolytic cleavage of the unconserved C-terminus in a isoform- and tissue-specific manner (van Zeijl et al., 2000; Testerink et al., 2001).

In other multicellular organisms, tissue-specific expression of 14-3-3 isoforms is a well described phenomenon that has been often correlated with tissue differentiation during embryogenesis (Watanabe et al., 1993a, b; Roseboom et al., 1994; McConnell et al., 1995; Luk et al., 1998; Siles-Lucas et al., 1998). In *Drosophila* and *Xenopus laevis*, for instance, 14-3-3 ϵ and 14-3-3 ξ expression were prior to the mitogen-activated protein kinase (MAPK) activation during tissue specification in early embryo development (Tien et al., 1999; Kousteni et al., 1997). The same isoforms have been reported to positively regulate Ras-Raf signaling pathway, leading to MAPK cascade activation (Chang et al., 1997; Kockel et al., 1997). Though 14-3-3 proteins have not yet been reported to interact with cell-cycle regulators in plant cells, many cell-cycle regulators are shared by both animal and plant cells, such as MAPKs (Mironov et al., 1997). Allied to this, the conserved 14-3-3 functional homology among eukaryotes (van Heusden et al., 1996) indicates that 14-3-3 may take part of the mechanisms involved in the control of plant cell cycle and differentiation. Since tissue differentiation involves the specific expression of 14-3-3 isoforms during animal embryogenesis, the first step towards elucidation of the role of 14-3-3 isoforms in plant differentiation processes is to understand how different 14-3-3 isoforms are regulated during

the development of plant embryos. Therefore, barley (*Hordeum vulgare* L.) microspore embryogenesis was used as a model system to study 14-3-3 isoform-specific expression patterns.

In barley, a combination of starvation and osmotic stress is able to efficiently induce a microspore developmental switch from the gametophytic to the sporophytic pathway, a process called androgenesis. After acquisition of embryogenic potential, isolated barley microspores can develop into embryo-like structures after 21 days of culture (Hoekstra et al., 1992). Barley androgenesis is a suitable model system to study plant embryogenesis, as embryo development can be easily monitored *in vitro* (Wang et al., 2000). In the present study, western blot analysis and immunolocalization studies of three barley 14-3-3 isoforms were carried out using a set of isoform-specific antibodies that recognizes specifically 14-3-3A, 14-3-3B and 14-3-3C isoforms. This is the first report to show that 14-3-3 isoforms are differentially regulated and processed upon androgenesis induction and embryo pattern formation.

Materials and methods

Androgenesis induction and microspore culture

Donor plants of barley (*Hordeum vulgare* L. cv Igri) were grown in a phytotron under conditions described previously (Hoekstra et al., 1992). Barley anthers containing microspores at mid-late to late uninucleate stage were used for induction of androgenesis. Pre-treatment consisted of anther incubation in 0.37M mannitol solution for 4 days in the dark, at 25°C (Hoekstra et al., 1992). After pre-treatment, microspores were isolated manually from anthers and the number of enlarged and non-enlarged microspores was estimated in 8 independent experiments ($n=8$). Around 300 microspores were counted per experiment. Pre-treated microspores were loaded on a 15% (w/v) sucrose gradient in 0.37M mannitol solution and centrifuged at 125g for 10 minutes for separation of enlarged and non-enlarged cells. Microspores were used for protein isolation, cytological staining or cultured in order to develop embryo-like structures (ELSs). Microspore culture was done according to Hoekstra et al. (1993).

Due to heterogeneity of ELS development during microspore culture, representative stages of ELS development were purified from 0, 3, 8, 14 and 21 days-old cultures by filtration through appropriate mesh sizes. These fractions were used for both immunolocalization studies and western blot analysis. Enlarged microspores from 3 days-old cultures were separated from non-enlarged microspores by filtration through 45µm nylon

mesh, and the fraction bigger than 45 μ m was assayed. Eight days-old cultures were fractionated by filtration through a 110 μ m nylon mesh. The filtrate smaller than 110 μ m comprised enlarged non-dividing structures and dividing microspores inside the exine wall, while the retentate bigger than 110 μ m was mainly composed by ELSs that had just been released from the exine wall. The retentate bigger than 110 μ m was assayed. From 14 days-old cultures, ELSs retained by filtration through 500 μ m nylon mesh were collected. Embryos from 21 days-old cultures ranging 0.5mm-1.0mm were manually harvested from media by forceps.

Immature zygotic embryos

In vivo developed immature zygotic embryos were dissected under binocular microscope from 21 days after pollination (DAP) seeds and used for immunolocalization studies.

Protein isolation and Western analysis

Pre-treated microspores, purified enlarged and non-enlarged microspores and staged-ELSs from 0, 3, 8, 14 and 21 days-old cultures were ground with a glass pestle at room temperature in 60mM Tris pH 6.8, 10% glycerol, 5% β -mercaptoethanol and 2% SDS for total protein extraction. The extracts were boiled for 10 minutes at 95-100°C and centrifuged two times at 15,000g for 10 minutes to collect supernatant. Soluble proteins (10 μ g) were separated on 15% (w/v) SDS-PAGE and blotted onto nitrocellulose membranes. Blots were incubated overnight at 4°C with isoform-specific anti-14-3-3 antibodies (1:20,000). The isoform-specific anti-14-3-3 antibodies were raised against the unconserved C-terminal region of the 14-3-3 proteins and the antibodies were demonstrated to show no cross-reaction (Testerink et al., 1999). Two anti-14-3-3A antibodies, raised against synthetic peptides 237-250 and 251-261 were used (Testerink et al., 1999; Testerink et al., 2001). Unless mentioned otherwise, anti-14-3-3A raised against peptides 237-250 was used for western blot analysis and immunolocalization studies. Anti-14-3-3B and anti-14-3-3C antibodies were raised against peptides 248-262 and 251-262, respectively (Testerink et al., 1999). Bands were visualized by goat anti-rabbit horseradish peroxidase conjugate (Promega), followed by enhanced chemoluminescent detection (ECL) (Amersham). Protein loading was checked by staining protein gels with 0.1% coomassie brilliant blue R-250 (Sigma) in 40% (v/v) methanol and 10% (v/v) acetic acid, followed by incubation in 20% (v/v) methanol and 10% (v/v) acetic acid.

Immunolocalization studies

ELs from 0, 3, 8, 14 and 21 days-old microspore cultures and 21 DAP zygotic embryos were fixed in 4% (w/v) paraformaldehyde in 10mM NaH₂PO₄, 120mM NaCl, 2.7mM KCl, pH 7.4 (Phosphate-buffered saline, PBS) containing 10mM dithiothreitol (DTT) overnight at 4°C. The material was dehydrated at room temperature through a graded ethanol series as follows: 70%, 90%, 96% and 100% (v/v). DTT was present in all dehydration steps at a concentration of 10mM. The resin was infiltrated through a graded series of ethanol: buthyl-methyl-methacrylate (BMM) 3:1, 1:1, 1:3 (v:v) containing 10mM DTT, overnight at 4°C. The plant material was embedded in 100% (v/v) BMM containing 10mM DTT and the resin was polymerized in Beem capsules under UV light for 48 hours at -20°C. Sections (5µm) were attached in 2% 3-aminopropyltriethoxy silane (Sigma) coated slides. After removal of the resin by acetone, proteins were denatured 20 minutes in 0.4% (w/v) SDS, 3mM β-mercaptoethanol, 12mM Tris pH 6.8 and blocked 30 min in 1% (w/v) BSA in PBS buffer. For immunolocalization studies, the antibodies were purified on an affinity column using the synthetic peptides according to Testerink et al. (1999). Primary antibody incubation was carried out overnight at 4°C in 0.01% acetylated BSA (Aurion) in PBS buffer (anti-14-3-3A diluted 1:1,000; anti-14-3-3B diluted 1:5,000 and anti-14-3-3C diluted 1:5,000). Control experiments were performed by omitting the first antibody and, in the case of 14-3-3C, preimmune serum was available which was used in a dilution of 1:5,000 in PBS buffer containing 0.01% acetylated BSA. Sections were developed with goat anti-rabbit alkaline phosphatase conjugate antibody (Promega). The signal was visualized by incubating sections in nitroblue tetrazolium, 5-bromo-4-chloro-3-indolyl phosphate (NBT/BCIP) substrate (Promega). Slides were mounted in 166g.l⁻¹ polyvinylalcohol, 30% (v/v) glycerol in PBS buffer and visualized under light microscope.

Cytological observations and starch staining

Isolated microspores after androgenesis induction were stained for viability with fluorescein diacetate (FDA). FDA can pass through the cell membrane whereupon intracellular esterases cleave off the diacetate group. The fluorescein accumulates in microspores which possess intact membranes so the green fluorescence can be used as a marker of cell viability. Microspores which do not possess an intact cell membrane or an active metabolism may not accumulate the fluorescent product. FDA was used in a final concentration of 0.04 µg.ml⁻¹ in acetone for 10 minutes at room temperature and observed under fluorescence microscope. The number of FDA positive and FDA negative cells was estimated in 8 independent experiments (*n*=8). Around 300 microspores were counted per experiment. Sections of 5µm from 3, 8, 14 and 21 days-old ELs and 21 DAP zygotic

embryos were incubated 1 minute at room temperature in 5.7mM iodine and 43.4mM potassium iodine in 0.2 N HCl (IKI) for staining of starch. Starch staining was observed under light microscope.

Experimental data

Mean values \pm SD are presented unless stated otherwise. Cell enlargement and microspore viability after pre-treatment were correlated using the r correlation coefficient ($P>0.95$) in 8 independent experiments ($n=8$).

Results

14-3-3 expression in microspore developmental switch and androgenesis

Microspores were induced to enter the embryogenic pathway by pre-treating whole anthers in mannitol solution. The anthers were collected at the mid-late to late uninucleate stage of microspore development. After pre-treatment, $18.9 \pm 7\%$ ($n=8$) of the microspores had acquired enlarged morphology (40-60 μm in diameter) and showed red/ blue interference of the exine wall (Fig. 1a, arrow 1; Fig. 1c). The remaining non-enlarged microspore population was composed of cells with 35-40 μm in diameter, showing blue/ black interference of the exine wall (Fig. 1a, arrow 2; Fig 1e). Microspore viability was assayed immediately after pre-treatment and only $19.2 \pm 5\%$ ($n=8$) of the microspores were FDA positive, indicating that they were alive. While the enlarged microspores were usually positively stained for FDA, the non-enlarged microspores were negatively stained for FDA, indicating probably dying cells after pre-treatment (Fig. 1a,b). Due to their difference in size, it was possible to separate these two populations by a sucrose gradient. FDA staining of the two separated microspore populations shows that only the enlarged population contains FDA positive cells (Fig. 1c-f).

The expression of 14-3-3A, 14-3-3B and 14-3-3C isoforms in the pre-treated microspores was studied using isoform-specific antibodies. In these samples, anti-14-3-3A recognized 2 bands, at 30 kD and 28 kD respectively. Anti-14-3-3B detected one band of approximately 31 kD, as well as anti-14-3-3C (Fig. 2a-c; lane 1). In order to know whether there were any differences in 14-3-3 protein levels between enlarged and non-enlarged microspores, 14-3-3 protein expression was analyzed in enlarged and non-enlarged microspores that were separated by a sucrose gradient. 14-3-3A in the enlarged fraction was present mainly as its 30 kD form (Fig. 2a; lane 2), while in the non-enlarged fraction a predominant band of 28 kD was present (Fig. 2a; lane 3).

It has been reported that a 28 kD 14-3-3A band is formed upon proteolytic cleavage of the unconserved C-terminal region of the 14-3-3A 30 kD protein at position Lys 250/ Ala 252, whereas 14-3-3B and 14-3-3C were not processed (van Zeijl et al., 2000; Testerink et al., 2001). In order to confirm whether the 28 kD form detected in non-enlarged microspores was due to the same post-translational event, an anti- 14-3-3A antibody that recognizes the amino acids 251-262 was used. The antibody detected only the 30 kD 14-3-3A form in pre-treated microspores (Fig. 2d). Our results indicate that the 28 kD 14-3-3A band observed in non-enlarged microspores was formed due to loss of the unconserved C-terminus of the protein.

The next step was to investigate whether microspore division and tissue differentiation during culture was also accompanied by a 14-3-3A post-translational event or differences in 14-3-3C protein levels. Western blot analysis was done in dividing structures at 3, 8, 14 and 21 days of microspore culture. At each time-point, multicellular structures were fractionated by filtration in appropriate mesh sizes in order to eliminate dead cells, degenerating microspores and dividing microspores with delayed development. This resulted in homogeneous populations that represented different embryo developmental stages during microspore culture. In these samples, only the 30 kD form of 14-3-3A was present (Fig. 3a). The 28 kD form of 14-3-3A was not detected in dividing structures. No changes in 14-3-3C levels were observed during microspore culture, however anti-14-3-3B recognized an additional slightly higher molecular band in 8-14 days-old ELSs (Fig. 3b,c).

Immunolocalization of 14-3-3 isoforms during embryogenesis: 3 days-old microspores

Although the enlarged microspores were considered to have embryogenic potential, androgenic divisions were observed in only $7.1 \pm 1\%$ ($n=3$) of the enlarged microspores when cultured as isolated cells. Due to this heterogeneity in embryogenic potential, the subcellular localization of the 14-3-3 isoforms was further investigated in the enlarged microspore population. Microspores directly isolated from pre-treated anthers (day 0) presented mainly cytoplasmic localization for the three 14-3-3 isoforms (data not shown). However, after 3 days of further culture, some enlarged microspores presented several division walls and multiple nuclei, while others did not divide. In dividing ones, strong 14-3-3A, 14-3-3B and 14-3-3C expression were mainly detected in the cytoplasm of cells (Fig. 4a-c). 14-3-3 signals in the nucleus were not higher than control background level (Fig. 4d). Incubation of sections with preimmune serum of the rabbit used for immunization with the 14-3-3C peptide revealed no background signal (data not shown). On the other hand, microspores that did not divide only presented a weak 14-3-3 signal in the cytoplasm. In these microspores, 14-3-3B and 14-3-3C isoforms appeared localized in a "dotted" pattern

(Fig. 4f, g; dots are indicated by arrowheads). This pattern was not pronounced for 14-3-3A (Fig. 4e). Concomitantly, the non-dividing microspores were also positively stained with IKI, indicating the presence of starch granules in the cytoplasm (Fig. 4h, starch granules are indicated by arrowheads).

The non-dividing microspores degenerated and died up to 8 days of culture, while dividing cells increased their mass and ruptured the exine wall. Interestingly, western blot analysis in the non-dividing fraction at day 8 of culture revealed the presence of the 28 kD processed form of 14-3-3A (data not shown). This is in agreement with the appearance of the 28 kD processed form of 14-3-3A in non-enlarged microspores with decreased viability directly after pre-treatment (Fig. 2a).

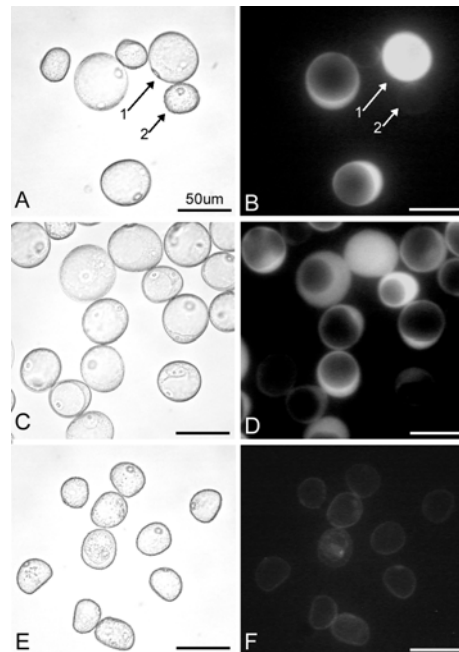


Figure 1. Brightfield image of isolated microspores after 4 days pre-treatment in mannitol solution (a) and under fluorescence microscope stained for FDA (b). The two types of microspores are indicated by arrows: *arrow 1* indicates enlarged microspore and *arrow 2* indicates non-enlarged microspore. The correlation coefficient r between cell enlargement and cell viability of the microspores after pre-treatment was 0.74 ($n=8$, $P>0.95$). Enlarged and non-enlarged microspores were separated by a 15% sucrose gradient. Brightfield image of purified enlarged microspores (c) and under fluorescence microscope stained for FDA (d). Brightfield image of purified non-enlarged microspores (e) and under fluorescence microscope stained for FDA (f).

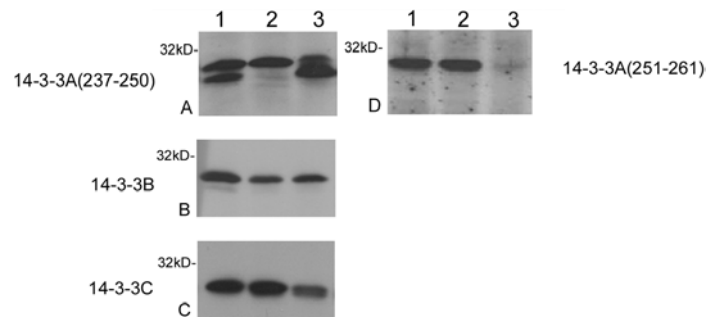


Figure 2. Western blot analysis of 14-3-3A, 14-3-3B and 14-3-3C proteins in microspores after androgenesis induction. 10 μ g per lane of total protein extracts were separated by SDS-PAGE, blotted onto nitrocellulose membranes and incubated with isoform-specific antibodies, followed by enhanced chemoluminescent detection. Lanes were equally loaded as checked by coomassie blue staining (data not shown). Blots were incubated with anti-14-3-3A raised against synthetic peptide 237-250 (a), anti-14-3-3B (b), anti-14-3-3C (c) and anti-14-3-3A raised against synthetic peptide 251-262 (d). *Lane 1* microspores after 4 days pre-treatment in mannitol solution, *lane 2* enlarged microspores and *lane 3* non-enlarged microspores after separation by a 15% sucrose gradient. One representative blot from 4 independent experiments is shown for each 14-3-3 isoform.

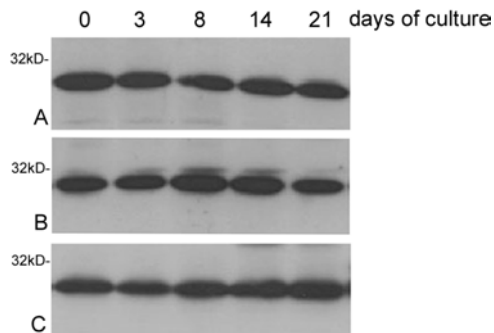


Figure 3. Western blot analysis of 14-3-3A, 14-3-3B and 14-3-3C proteins in ELSs from 0, 3, 8, 14 and 21 days-old cultures. Dividing structures were purified by filtration using appropriate mesh sizes and 10 μ g per lane of total protein extracts were separated by SDS-PAGE. Proteins were blotted onto nitrocellulose membranes and incubated with the isoform-specific antibodies. Signal was detected by enhanced chemoluminescent methods. Lanes were equally loaded as checked by coomassie blue staining (data not shown). Blots were incubated with anti-14-3-3A (a), anti-14-3-3B (b) and anti-14-3-3C (c). One representative blot from 4 independent experiments is shown for each 14-3-3 isoform.

Pattern formation in 8 and 14 days of culture

In 8 days-old cultures, multicellular structures had ruptured the exine wall and were characterized by a mass of undifferentiated cells. After exine wall release, they followed an intensive morphogenetic program. Some of the 14 days-old multicellular structures started to differentiate tissues in the embryo body, with shoot and root meristem formation taking place. At this stage, the scutellum was present as a well-developed structure and the embryo-like structures (ELSs) were surrounded by a differentiated cell layer, the epidermis (Fig. 5).

14-3-3 immunolocalization was studied in multicellular structures derived from 8 and 14 days-old cultures. At day 8 of culture, 14-3-3A signal was distributed all over the multicellular structure, but it showed to be strongest in the outer layer, associated to the differentiation of the epidermis primordia (Fig. 5a). In a later stage of development (14 days-old ELSs), 14-3-3A isoform was detected in scutellum, root and shoot meristems, mesocotyl and in the epidermal tissue. Nevertheless, some cells within the root and shoot meristem showed no 14-3-3A signal (Fig. 5b).

14-3-3B isoform exhibited a mosaic expression in 8 days-old multicellular structures, but no defined pattern was observed. Expression of 14-3-3B isoform in 14 days-old ELSs resembled that of 14-3-3 A, except that 14-3-3B signal was not detected in the epidermis (Fig. 5c,d).

It was quite clear that 14-3-3C expression differed significantly from that of 14-3-3A and 14-3-3B. In multicellular structures derived from 8 days-old cultures, 14-3-3C was often higher expressed in one domain of the embryo, where it appeared associated with cytoplasmic dots. In other domains, 14-3-3C signal was less strong (Fig. 5e). In 14 days-old ELSs, 14-3-3C signal was only detected in scutellum cells, while it was completely absent in all meristematic regions (Fig. 5f). IKI staining in sections of 14 days-old ELSs indicated the presence of starch granules in the cytoplasm of scutellum cells, where 14-3-3B and 14-3-3C were also localized in cytoplasmic dots (data not shown). We could not detect any signal in control experiments (Fig. 5g,h).

21 days-old ELSs and in vivo-developed immature zygotic embryos

At 21 days of culture, most of the ELSs ranging 0.5 – 1.0 mm in culture are capable of germination when transferred to regeneration media (Hoekstra et al., 1992). These ELSs were assayed for immunolocalization studies. At this stage, 14-3-3A was immunolocalized in the scutellum, root and shoot meristems, root cap, leaf primordia, mesocotyl and epidermis. (Fig. 6a,e). 14-3-3B signal was much stronger than that of 14-3-3A and it was found in all embryogenic tissues (Fig. 6b,f). 14-3-3C signal was restricted to scutellum and one group of cells underneath the L₁ layer of the shoot apical meristem (Fig. 6c,g). 14-3-3C was absent from the root meristem and root cap (Fig. 6g), as the signal was not stronger than that observed in control sections incubated only with the secondary antibody (Fig. 6d,h).

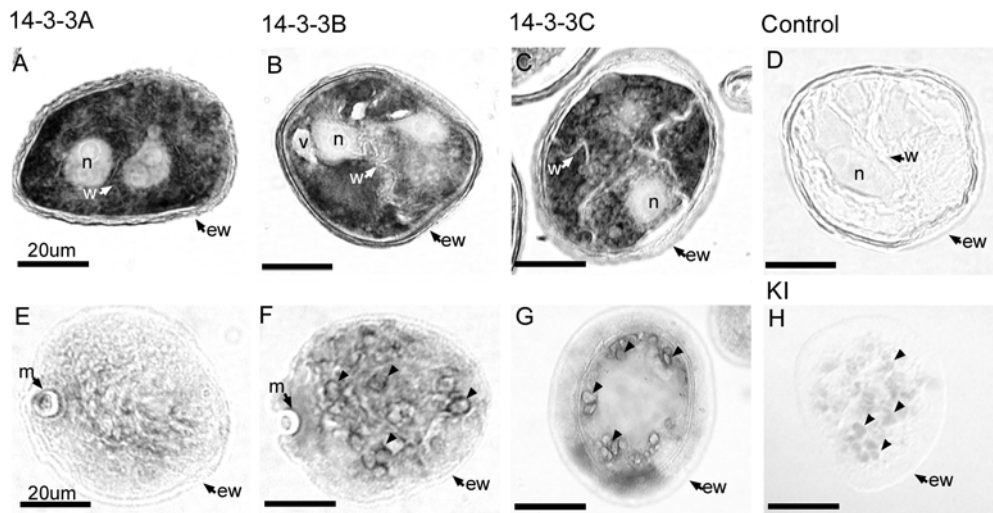


Figure 4. Brightfield image of 14-3-3 immunolocalization in enlarged microspores from 3 days-old cultures. Cross-sections of dividing (a) (b) (c) and non-dividing microspores (e) (f) (g) showing immunolocalization of 14-3-3A, 14-3-3B and 14-3-3C, respectively. Control section of dividing microspore incubated only with secondary antibody (d). Section of a non-dividing microspore stained with ICI observed by differential interference contrast (h). *Arrowheads* in (f) and (g) indicate 14-3-3B and 14-3-3C “dotted” cytoplasmic localization. *Arrowheads* in (h) indicate starch granules. *ew* exine wall, *m* micropore, *n* nucleus, *v* vacuole, *w* dividing wall. 14-3-3 immunolocalization was studied in 3 independent experiments. Sections of at least 10 dividing and non-dividing microspores were studied per experiment. Representative examples are shown for each 14-3-3 isoform.

As ELSs were grown under *in vitro* conditions, 14-3-3 isoforms were studied during normal *in vivo* embryo development. To do so, immature zygotic embryos were assayed at 21 days after pollination (DAP) for 14-3-3 immunolocalization studies. In 21 DAP zygotic embryos, 14-3-3A was expressed in root and shoot meristems, mesocotyl, scutellum, coleoptile and epidermis (Fig. 6i). 14-3-3B isoform seemed to be ubiquitously expressed at this stage, except that some regions within leaf primordia were not stained (Fig. 6j). 14-3-3C signal was detected in scutellum, mesocotyl and underneath the L₁ layer of the shoot apical meristem (Fig. 6k). No signal was detected when first antibody was omitted (Fig. 6l) or, in the case of 14-3-3C, sections of both ELS and immature zygotic embryos were incubated with the preimmune serum (data not shown). Although 21 DAP immature zygotic embryos were at a further developmental stage compared to *in vitro*-developed 21 days-old ELSs, both showed similar 14-3-3 isoform-specific expression patterns.

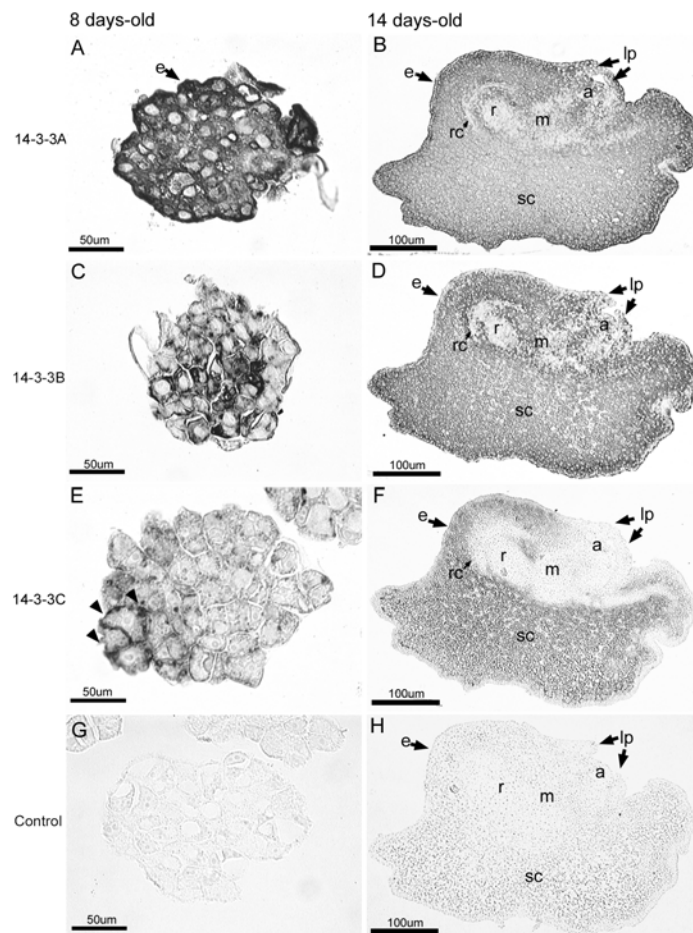


Figure 5. Brightfield image of 14-3-3 immunolocalization in 8 and 14 days-old ELSs. Cross-section of 8 and 14 days-old ELSs were incubated with anti-14-3-3A antibody (a/b), anti-14-3-3B antibody (c/d), anti-14-3-3C antibody (e/f). Control sections were incubated only with secondary antibody (g/h). Incubation of sections with preimmune serum of the rabbit used for immunization with the 14-3-3C peptide revealed no background signal (data not shown). *Arrowheads* in (e) indicate domain of ELS with increased 14-3-3C expression. *a* shoot apical meristem, *e* epidermis, *lp* leaf primordial, *m* mesocotyl, *r* root meristem, *rc* root cap. 14-3-3 immunolocalization was studied in 3 independent experiments. Sections of at least 10 ELS were studied per experiment. Representative examples are shown for each 14-3-3 isoform.

Discussion

Role of 14-3-3 proteins in embryogenic potential acquirement

Androgenesis induction in barley is characterized by two types of morphologically distinct microspores, namely enlarged and non-enlarged cells (Hoekstra et al., 1992). An average of 19% of the microspores showed to have enlarged morphology after pre-treatment.

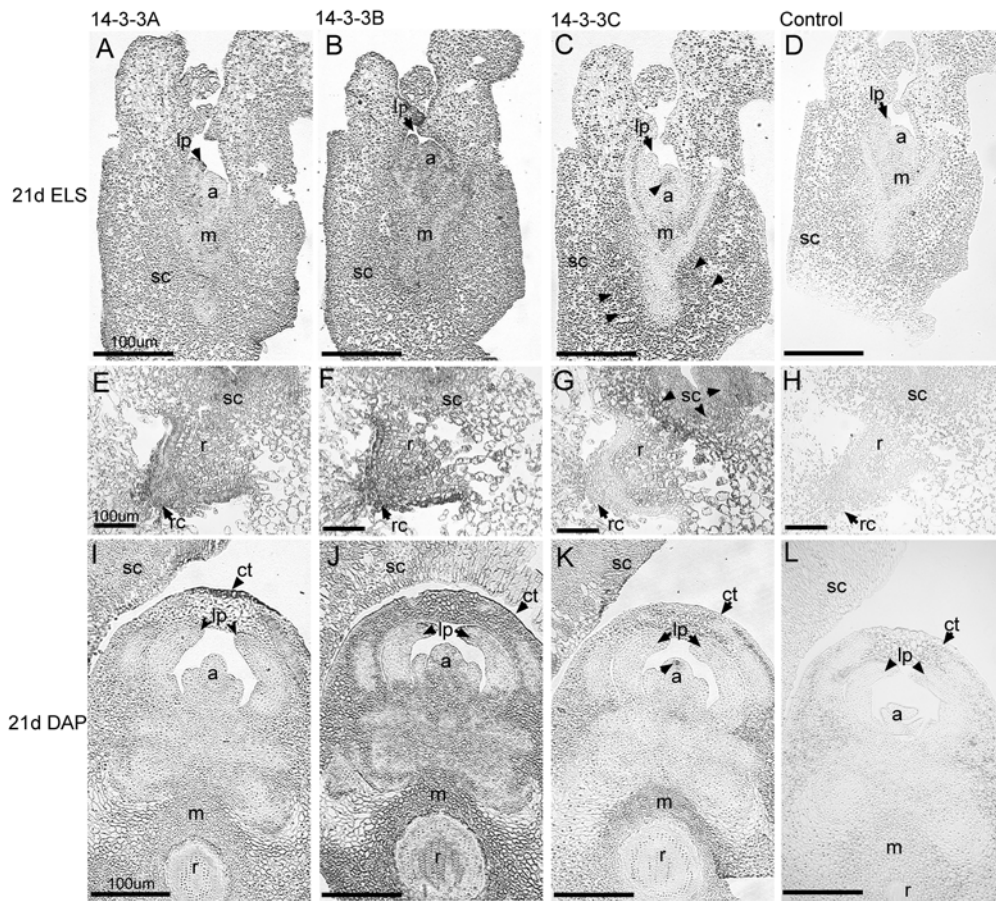


Figure 6. Brightfield image of 14-3-3 immunolocalization in 21 days-old ELs and 21 DAP zygotic embryos. Sections of two different ELs are shown in order to illustrate 14-3-3 expression in shoot (a, b, c, d) and root meristems (e, f, g, h). Sections of 21 days-old ELs were incubated with anti-14-3-3A (a/e), anti-14-3-3B (b/f) and anti-14-3-3C (c/g) antibodies, respectively. Control sections incubated only with secondary antibody (d/h). Sections of 21 DAP zygotic embryo incubated with anti-14-3-3A, anti-14-3-3B and anti-14-3-3C antibodies, respectively (i, j, k). Control section incubated only with secondary antibody (l). *Arrowheads* in (c) and (g) indicate 14-3-3C expression underneath L_1 layer of the shoot apical meristem and in scutellum cells and in (k) 14-3-3C underneath L_1 layer of the shoot apical meristem. A shoot apical meristem, *ct* coleoptile, *lp* leaf primordial, *m* mesocotyl, *r* root meristem, *rc* root cap, *sc* scutellum. 14-3-3 immunolocalization was studied in 3 independent experiments. Sections of at least 5 embryos were studied per experiment. Representative examples are shown for each 14-3-3 isoform.

In previous work, cell enlargement was found in 60% of the microspore population after pre-treatment of barley anthers (Hoekstra et al., 1993). This variation could be due to the different microspore isolation techniques used, as previously reported by Ritala et al. (2001). Cell enlargement was further demonstrated to correlate with cell viability after stress pre-treatment, however androgenic divisions were observed within only 7% of the viable cells. This indicates that only some of the enlarged, viable microspores have acquired embryogenic

potential after pre-treatment. This is supported by the observations made by single-cell tracking experiments in barley microspores (Bolik and Koop, 1991; Kumlehn and Lörz, 1999). 14-3-3 expression analysis showed that enlarged microspores contain mainly the 30 kD form of 14-3-3A and have increased 14-3-3C expression level. Non-enlarged microspores have mainly the processed 28 kD form of 14-3-3A and decreased level of 14-3-3C expression. 14-3-3A processing by proteolytic cleavage at positions Lys 250/ Ala 252 has been previously described in the germination of mature barley embryos (van Zeijl et al., 2000; Testerink et al., 2001). Cell death has been reported to occur in barley scutellum (Lindholm et al., 2000) and aleurone layer during the onset of germination (Wang et al., 1996). In the *in vitro* system studied, 14-3-3A processing was observed in non-enlarged microspores with decreased viability after pre-treatment and in non-dividing cells in culture. The isoform-specific proteolytic cleavage of 14-3-3A may represent the beginning of a total global degradation of the 14-3-3A protein, being related to the cell death pathway of these cells. However, the possibility that processing affects 14-3-3 subcellular localization (van Zeijl et al., 2000) and the functionality of the 14-3-3A isoform cannot be excluded. Recently, both 30 kD and 28 kD forms were found to bind to the plasma membrane H^+ -ATPase in *in vitro* western blot overlay assays (Testerink et al., 2001). Further characterization of the 14-3-3A proteinase will help elucidating the role of the 28 kD processed form of 14-3-3A in relation to cell death. The question raised is whether the low 14-3-3C content in non-enlarged microspores after pre-treatment is also related to cell death of these cells. However, later in culture, the meristematic regions of 14 days-old ELSs also showed decreased 14-3-3C signal in immunolocalization assays. Developing meristems are known to have high division ability (Goldberg et al., 1994). Thus, it is not likely that low 14-3-3C content is related to decreased viability of cells.

After 3 days of further culture of pre-treated enlarged microspores, two sub-populations could be distinguished, dividing and non-dividing cells. In non-dividing cells, starch granules were observed and 14-3-3B and 14-3-3C were mainly localized in cytoplasmic dots. Starch accumulation in pollen amyloplasts marks the commitment to the gametophytic pathway (McCormick, 1993). In the amyloplasts, 14-3-3 proteins have been recently found associated with starch granules and starch synthase III has been proposed as a putative 14-3-3 interacting target (Sehnke et al., 2001). It is possible that 14-3-3B and 14-3-3C signals detected in these dots are associated with starch granule formation in the non-dividing microspores. Dividing cells, however, did not accumulate starch and 14-3-3 isoforms were mainly localized in the cytoplasm. The allocation of different 14-3-3 isoforms inside the cell may play an important role in global 14-3-3 protein interactions. In plants, 14-3-3 proteins form a guidance complex with chloroplast precursor proteins (May and Soll, 2000), facilitating

protein import into the chloroplast. In animal cells, 14-3-3 proteins have been reported to be involved in mitochondrial protein import (Alam et al., 1994) and subcellular compartmentalization of specific targets, by which they can affect cell fate (Muslin et al., 2000). This suggests that the subcellular differences in the localization of the 14-3-3 proteins in dividing and non-dividing microspores may have implications in their different developmental pathways.

Tissue-specific expression of 14-3-3 proteins during in vivo and in vitro embryogenesis

The shift from radial to bilateral symmetry is a crucial event in plant embryogenesis, as it comprises the events involved in the establishment of the scutellum and the embryonic axis (Souter and Lindsey, 2000). During microspore embryogenesis, pattern formation is delineated after the release of undifferentiated multicellular structures from the exine wall of microspores (Yeung et al., 1996). The periclinal divisions of the outer cell layer of globular embryos have been demonstrated to culminate with the first tissue differentiation, the epidermis (Telmer et al., 1995). In barley androgenesis, globular masses of undifferentiated cells were released from exine wall after one week of culture. The uniformly cytoplasmic localization of 14-3-3 isoforms in dividing microspores was progressively changed after exine wall rupture. Prior to epidermis differentiation, 14-3-3A signal was highest in the outer layer of multicellular structures, while 14-3-3C expression was polarized. During further development, 14-3-3C expression was tissue-specific to the scutellum of 14 days-old ELSs, while the epidermis expressed only the 14-3-3A isoform. In other androgenic systems, expression of polarity prior to tissue differentiation has been reported only at the structural and morphological level. Multicellular structures were shown to polarize according to cell size while still inside the exine wall of microspores of *Zea mays* L. and *Triticum aestivum* L. (Magnard et al., 2000; Bonet and Olmedilla, 2000). After exine wall rupture, polarization has been demonstrated by means of spatial differences in starch accumulation in globular embryos of *Triticum aestivum* L. and *Brassica napus* L. (Indrianto et al., 2001; Hause et al., 1994). The spatial differences described here for the expression of 14-3-3 isoforms are among the first biochemical evidences to show pattern formation in androgenesis. Later in development, 14-3-3C isoform was specifically expressed in the scutellum and in one group of cells underneath the L₁ layer of the shoot apical meristem of 21 days-old ELSs. As the same 14-3-3C expression pattern was observed in 21 DAP immature zygotic embryos, this indicates a feature of both *in vivo* and *in vitro* embryogenesis. Testerink et al. (1999) have described L₂ layer-associated 14-3-3C expression in mature barley embryos. These results suggest that the re-expression of 14-3-3C in the shoot apical meristem is likely to occur

during L₂ layer specification, and reinforce the idea that 14-3-3C specific expression is prior to formation of tissues during the embryogenic process of barley.

The highly developmentally regulated expression patterns observed for 14-3-3A and 14-3-3C may be involved in conferring isoform-specific functions *in vivo*, as little isoform-specificity has been so far described (Bachmann et al., 1996b; Rosenquist et al., 2000). In addition, it may reveal yet unexplored functions for plant 14-3-3 isoforms. Spatial and temporal regulation of 14-3-3 isoforms are known to be involved in MAPK activation and tissue differentiation during pattern formation in animal embryogenesis (Tien et al., 1999). It will be a challenge to determine which are the binding partners of 14-3-3A and 14-3-3C during pattern formation and L₂-layer specification in plant embryogenesis, and whether this expression patterns are also followed by activation of MAPK cascade, approximating 14-3-3 functions in animal and plant systems.

Acknowledgments

We are grateful to Sandra van Bergen, Arnoud van Marion and Marco Vennik for technical assistance, and to Dr. Bert van Duijn, Dr. Henrie Korthout and Dr. Jeanine Louwerse for critical reading of the manuscript.

References

- Alam R, Hachiya N, Sakaguchi M, Kawabata S, Iwanaga S, Kitajima M, Mihara K, Omura T (1994) cDNA cloning and characterization of mitochondrial import stimulating factor (MSF) purified from rat liver cytosol. *J Biochem* 116: 416-425
- Bachmann M, Huber JL, Liao PC, Gage DA, Huber SC (1996a) The inhibitor protein of phosphorylated nitrate reductase from spinach (*Spinacia Oleracea*) leaves is a 14-3-3 protein. *FEBS Lett* 387: 127-131
- Bachmann M, Huber JL, Athwal GS, Wu K, Ferl RJ, Huber SC (1996b) 14-3-3 proteins associate with the regulatory phosphorylation site of spinach leaf nitrate reductase in an isoform-specific manner and reduce dephosphorylation of Ser-543 by endogenous protein phosphatases. *FEBS Lett* 398: 26-30
- Bihn EA, Paul AL, Wang SW, Erdos GW, Ferl RJ (1997) Localization of 14-3-3 proteins in the nuclei of arabidopsis and maize. *Plant J* 12: 1439-1445
- Bolik M, Koop HU (1991) Identification of embryogenic microspores of barley (*Hordeum vulgare* L.) by individual selection and culture and their potential for transformation by microinjection. *Protoplasma* 162: 61-68
- Bonet FJ, Olmedilla A (2000) Structural changes during early embryogenesis in wheat pollen. *Protoplasma* 211: 94-102
- Brandt J, Thordal-Christensen H, Vad K, Gregersen PL, Collinge DB (1992) A pathogen-induced gene of barley encodes a protein showing high similarity to a protein kinase regulator. *Plant J* 2: 815-820

- Chang HC, Rubin GM (1997) 14-3-3 ϵ positively regulates Ras-mediated signalling in *Drosophila*. *Genes Dev* 11: 1132-1139
- Daugherty CJ, Rooney MF, Miller PW, Ferl RJ (1996) Molecular organization and tissue-specific expression of an *Arabidopsis* 14-3-3 gene. *Plant Cell* 8: 1239-1248
- Fu H, Subramanian RR, Masters SC (2000) 14-3-3 proteins: structure, function and regulation. *Ann Rev Pharm Toxicol* 40: 617-647
- Goldberg RB, de Paiva G, Yadegari R (1994) Plant Embryogenesis: zygote to seed. *Science* 266: 605-614
- Hause B, van Veenendaal WL, Hause G, van Lammeren AA (1994) Expression of polarity during early development of microspore-derived and zygotic embryos of *Brassica napus* L. cv Topas. *Bot Acta* 107: 407-415
- Hoekstra S, van Zijderveld MH, Louwerse JD, Heidekamp F, van der Mark F (1992) Anther and microspore culture of *Hordeum vulgare* L. cv. Igri. *Plant Sci* 86: 89-96
- Hoekstra S, van Zijderveld MH, Heidekamp F, van der Mark F (1993) Microspore culture of *Hordeum vulgare* L.: the influence of density and osmolarity. *Plant Cell Rep* 12: 661-665
- Indrianto A, Barinova I, Touraev A, Heberle-Bors E (2001) Tracking individual wheat microspores *in vitro*: identification of embryogenic microspores and body axis formation in the embryo. *Planta* 212: 163-174
- Kockel L, Vorbrüggen G, Jäckle H, Mlodzik M, Bohmann D (1997) Requirement for *Drosophila* 14-3-3 ζ in Raf-dependent photoreceptor development. *Genes Dev* 11: 1140-1147
- Korthout HA, de Boer AH (1994) A fusicoccin binding protein belongs to the family of 14-3-3 brain protein homologues. *Plant Cell* 6: 1681-1692
- Kousteni S, Tura F, Sweeney GE, Ramji DP (1997) Sequence and expression analysis of a *Xenopus laevis* cDNA which encodes a homologue of mammalian 14-3-3 zeta protein. *Gene* 190: 279-285
- Kumlehn J, Lörz H (1999) Monitoring sporophytic development of individual microspores of barley (*Hordeum vulgare* L.). In: Clement C, Pacini E, Audran JC (eds) *Anther and Pollen: from biology to biotechnology*. Springer-Verlag, Berlin Heidelberg, pp 183-189
- Lindholm P, Kuitinen T, Sorri O, Guo D, Merits A, Törmäkangas K, Runeberg-Roos P (2000) Glycosylation of phytepsin and expression of dad1, dad2 and ost1 during onset of cell death in germinating barley scutella. *Mech Dev* 93: 169-173
- Lu G, de Vetten NC, Senhke PC, Isobe T, Ichimura T, Fu H, van Heusden PH, Fel RJ (1994) A single *Arabidopsis* GF14 isoform possesses biochemical characteristics of diverse 14-3-3 homologues. *Plant Mol Biol* 25: 659-667
- Luk SCW, Ngai S, Tsui SKW, Chan K, Fung K, Lee C, Waye MMY (1998) Developmental regulation of 14-3-3 ϵ isoform in rat heart. *J Cell Biochem* 68: 195-199
- Magnard JL, Le Deunff E, Domenech J, Rogowsky PM, Testillano PS, Rougier M, Risueño MC, Vergne P, Dumas C (2000) Genes normally expressed in the endosperm are expressed at early stages of microspore embryogenesis in maize. *Plant Mol Biol* 44: 559-574
- Marra M, Fullone MR, Fogliano V, Pen J, Mattei, Masi S, Aducci P (1994) The 30-kilodalton protein present in purified fusicoccin receptor preparations is a 14-3-3-like protein. *Plant Physiol* 106: 1497-1501
- May T, Soll J (2000) 14-3-3 proteins form a guidance complex with chloroplast precursor proteins in plants. *Plant Cell* 12: 53-63
- McConnel JE, Armstrong JF, Hodges PE, Bard JB (1995) The mouse 14-3-3 epsilon isoform, a kinase regulator whose expression pattern is modulated in mesenchyme and neuronal differentiation. *Dev Biol* 169: 218-228
- McCormick S (1993) Male gametophyte development. *Plant Cell* 5: 1265-1275
- Mironov V, Van Montagu M, Inzé D (1997) Regulation of cell division in plants: An *Arabidopsis* perspective. *Prog Cell Cycle Res* 3: 29-41

- Moorhead G, Douglas P, Morrice N, Scarabel M, Aitken A, MacKintosh C (1996) Phosphorylated nitrate reductase from spinach leaves is inhibited by 14-3-3 proteins and activated by fusicoccin. *Curr Biol* 6: 1104-1113
- Moorhead G, Douglas P, Cotellet V, Harthill J, Morrice N, Meek S, Deiting U, Stitt M, Scarabel M, Aitken A, MacKintosh C (1999) Phosphorylation-dependent interactions between enzymes of plant metabolism and 14-3-3 proteins. *Plant J* 18: 1-12
- Muslin AJ, Xing H (2000) 14-3-3 proteins: regulation of subcellular localization by molecular interference. *Cell Signall* 12, 703-709
- Oecking C, Eckerskorn C, Weiler EW. 1994. The fusicoccin receptor of plants is a member of the 14-3-3 superfamily of eukaryotic regulatory proteins. *FEBS Lett* 352: 163-166.
- Ritala A, Mannonen L, Oksman-Caldentey KM (2001) Factors affecting the regeneration capacity of isolated barley microspores (*Hordeum vulgare* L.). *Plant Cell Rep* 20: 403-407
- Roseboom PH, Weller JL, Babila T, Aitken A, Sellers LA, Moffett JR, Namboodiri MA, Klein DC (1994) Cloning and characterization of the epsilon and zeta forms of the 14-3-3 proteins. *DNA Cell Biol* 13: 629-640
- Rosenquist M, Alsterfjord M, Larsson C, Sommarin M (2001) Data mining the *Arabidopsis* genome reveals fifteen 14-3-3 genes. Expression is demonstrated for two out of five novel genes. *Plant Physiol* 127: 142-149
- Rosenquist M, Sehnke P, Ferl RJ, Sommarin M, Larsson C (2000) Evolution of the 14-3-3 protein family: does the large number of isoforms in multicellular organisms reflect functional specificity? *J Mol Evol* 51: 446-458
- Sehnke PC, Henry R, Cline K, Ferl RJ (2000) Interaction of a plant 14-3-3 protein with the signal peptide of a thylakoid-targeted chloroplast precursor protein and the presence of 14-3-3 isoforms in the chloroplast stroma. *Plant Physiol* 122: 235-241
- Sehnke PC, Chung HJ, Wu K, Ferl RJ (2001) Regulation of starch accumulation by granule-associated plant 14-3-3 proteins. *Proc Natl Acad Sci USA* 98: 765-770
- Siles-Lucas M, Felleisen RSJ, Hemphill A, Eilson W, Gottstein B (1998) Stage-specific expression of the 14-3-3 gene in *Echinococcus multilocularis*. *Mol Biochem Parasitol* 91: 281-293
- Souter M, Lindsey K (2000) Polarity and signalling in plant embryogenesis. *J Exp Bot* 51: 971-983
- Telmer CA, Newcomb W, Simmonds DH (1995) Cellular changes during heat shock induction and embryo development of cultured microspores of *Brassica napus* cv. Topas. *Protoplasma* 185: 106-112
- Testerink C, van Zeijl MJ, Drumm K, Palmgren MG, Kijne JW, Wang M (2001) Post-translational modification of barley 14-3-3A is isoform-specific and involves the removal of the hypervariable C-terminus. *Plant Mol Biol* 50: 535-542
- Testerink C, van der Meulen RM, Oppedijk BJ, de Boer AH, Heimovaara-Dijkstra S, Kijne JW, Wang M (1999) Differences in spatial expression between 14-3-3 isoforms in germinating barley embryos. *Plant Physiol* 121: 81-87
- Tien AC, Hsei HY, Chien CT (1999) Dynamic expression and cellular localization of the *Drosophila* 14-3-3 ϵ during embryonic development. *Mech Dev* 81: 209-212
- van Heusden GPH, van der Zanden AL, Ferl RJ, Steensma HY (1996) Four *Arabidopsis thaliana* 14-3-3 protein isoforms can complement the lethal yeast *bmh1 bmh2* double disruption. *FEBS Lett* 391: 252-256
- van Zeijl MJ, Testerink C, Kijne JW, Wang M (2000) Subcellular differences in post-translational modification of barley 14-3-3 proteins. *FEBS Lett* 473: 292-296
- Wang M, Oppedijk BJ, Lu X, van Duijn B, Schilperoort RA (1996) Apoptosis in barley aleurone during germination and its inhibition by abscisic acid. *Plant Mol Biol* 32: 1125-1134
- Wang M, van Bergen S, van Duijn B (2000) Insights into a key developmental switch and its importance for efficient plant breeding. *Plant Physiol* 124: 523-530

- Wang W, Shakes DC (1996) Molecular evolution of the 14-3-3 protein family. *J Mol Evol* 43: 384-398
- Watanabe M, Isobe T, Ichimura T, Kuwano R, Takahashi Y, Kondo H (1993a) Molecular cloning of rat cDNAs for beta and gamma sub-types of 14-3-3 protein and developmental change in expression of their mRNAs in the nervous system. *Mol Brain Res* 17: 135-146
- Watanabe M, Isobe T, Ichimura T, Kuwano R, Takahashi Y, Kondo H (1993b) Developmental regulation of neuronal expression for the eta subtype of the 14-3-3 protein, a putative regulatory protein for protein kinase C. *Dev Brain Res* 73: 225-235
- Yaffe MB, Rittinger K, Volinia S, Caron PR, Aitken A, Leffers H, Gamblin SJ, Smerdon SJ, Cantley LC (1997) The structural basis for 14-3-3:phosphopeptide binding specificity. *Cell* 91: 961-971
- Yaffe MB, Elia AE (2001) Phosphoserine/ threonine-binding domains. *Curr Opin Cell Biol* 13: 131-138
- Yeung EC, Rahman MH, Thorpe TA (1996) Comparative development of zygotic and microspore-derived embryos in *Brassica napus* L. cv Topas. I. Histodifferentiation. *Int J Plant Sci* 157: 27-39

II. Tissue-specific expression of 14-3-3 isoforms during barley microspore and zygotic embryogenesis

Acta Biol Cracov Bot (2003) 45: 103-106

Simone de Faria Maraschin, Jeanine D. Louwerse, Gerda E.M. Lamers, Herman P. Spaink,
Mei Wang

Abstract

The conserved 14-3-3 proteins have been shown to play regulatory roles in eukaryotic cells, including cell cycle control and differentiation. We were interested in the possible involvement of 14-3-3 proteins in the embryogenic process of barley (*Hordeum vulgare* L.). Barley microspore-derived embryo development was used as a model system. Immunolocalization of three barley 14-3-3 isoforms, 14-3-3A, 14-3-3B and 14-3-3C were carried out using isoform-specific antibodies. In immature microspore-derived embryos, 14-3-3C was specifically expressed underneath the L₁ layer of the shoot apical meristem and in the scutellum. Comparative studies showed that 14-3-3C was also expressed underneath the L₁ layer of the shoot apical meristem and in the scutellum of immature zygotic embryos. We further demonstrated that 14-3-3C expression is restricted to L₂ layer-derived cells of *in vitro* shoot meristematic cultures. Our results reveal that 14-3-3C isoform tissue-specific expression is closely related to defined events during differentiation processes in embryogenesis and *in vitro* meristematic cultures.

Introduction

The 14-3-3 proteins constitute a conserved family of 30 kD proteins present in all eukaryotic organisms studied so far. 14-3-3 dimers bind to phosphorylated motifs in a wide number of target proteins. Several biological functions have been attributed to members of the 14-3-3 protein family, as they are directly involved in the transduction of signals related to stress, cell division and differentiation, activation of transcription and apoptosis, amongst others (Sehnke et al., 2002).

14-3-3 functions in eukaryotic cells are exerted by several isoforms, ranging from 2 in *Saccharomyces cerevisiae* to 15 in *Arabidopsis thaliana* (Rosenquist et al., 2001). Though 14-3-3 activity is thought to be conserved among different 14-3-3 isoforms (van Heusden et al., 1996), they appear to be spatially and temporally regulated during development in both plants and animals, suggesting isoform-specific developmental roles. Tissue-specific expression has been described for the 14-3-3 χ isoform during *Arabidopsis thaliana* development (Daugherty et al., 1996), while the 14-3-3C isoform from barley (*Hordeum vulgare* L.) is known to be specifically expressed in the scutellum and in the L₂ layer of the shoot apical meristem (SAM) of germinating zygotic barley embryos (Testerink et al., 1999). In barley, 3 isoforms have been cloned so far: 14-3-3A, 14-3-3B and 14-3-3C (GenBank X62388, X93170 and Y14200). The developmentally regulated expression pattern of the 14-

3-3C isoform in the SAM described by Testerink et al. (1999) prompted us to further investigate 14-3-3 isoform-specific patterns prior to embryo maturation, in both *in vivo* and *in vitro* embryogenesis. With a set of isoform-specific antibodies, we studied 14-3-3 immunolocalization in immature zygotic embryos and embryo-like structures (ELSs) derived from androgenic microspores. In addition, we have investigated 14-3-3 immunolocalization following cell division of the shoot meristem using *in vitro* shoot meristematic cultures (SMCs).

Materials and Methods

Androgenesis induction and microspore culture

Barley (*Hordeum vulgare* L. cv Igri) androgenesis induction and microspore culture were performed according to Hoekstra et al. (1992). Embryo-like structures (ELSs) ranging 0.5-1.0 mm diameter were harvested from media by forceps after 21 days of culture for immunolocalization studies.

Immature zygotic embryos

In vivo developed immature zygotic embryos were dissected under binocular microscope from 21 DAP (days after pollination) seeds for immunolocalization studies.

Shoot meristematic cultures

Shoot meristematic cultures (SMCs) were obtained from mature grains of barley (*Hordeum vulgare* L. cv. Himalaya) germinated according to Louwerse (2002). The material for immunolocalization was obtained from a 16 month-old culture with high regeneration capacity.

Immunolocalization

Fixation and embedding of 21 days-old ELSs, 21 DAP immature zygotic embryos and 16 month-old SMCs was performed as described by Louwerse (2002). Isoform-specific antibodies raised against the C-terminal part of the 14-3-3A, 14-3-3B and 14-3-3C isoforms were used for *in situ* immunolocalization (Testerink et al., 1999).

Results

14-3-3 immunolocalization was first studied in 21 DAP immature zygotic embryos and in 21 days-old ELSs. Although 21 DAP immature zygotic embryos were at a further developmental stage compared to *in vitro*-developed 21 days-old ELSs, both showed similar 14-3-3 isoform-specific expression patterns (Fig. 1). 14-3-3A was immunolocalized in the scutellum, root and shoot meristems, root cap, leaf primordia, mesocotyl and epidermis, while 14-3-3B was found in all embryogenic tissues (data not shown). 14-3-3C expression was markedly different than that of 14-3-3A and 14-3-3B, being restricted to the scutellum, mesocotyl, coleoptile and to one region of the SAM (Fig. 1). Figure 2 shows a magnified view of the 14-3-3 immunolocalization in the SAM. 14-3-3A signal was detected in the leaf primordia and in some of the cells within the SAM, however no defined pattern could be observed (Fig. 2a,e). While 14-3-3B was ubiquitously expressed (Fig. 2b,f), 14-3-3C could only be detected in a group of cells underneath the L₁ layer of the SAM. No signal was detected in control sections that were incubated only with the secondary antibody (Fig. 2d,h).

L₂-layer-specific 14-3-3C expression in the SAM of mature barley embryos has been previously reported (Testerink et al., 1999). Our results suggest that high levels of 14-3-3C are already present underneath the L₁ layer of the SAM before L₂ layer is morphologically differentiated.

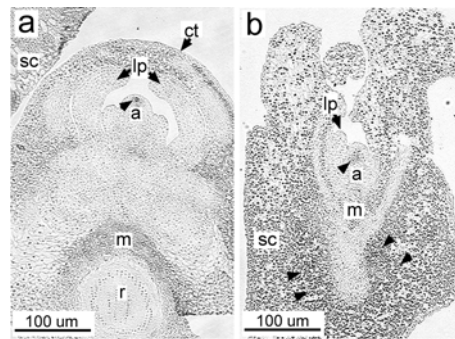


Figure 1. 14-3-3C immunolocalization in 21 DAP zygotic embryos (a) and 21 days-old ELSs (b). Proteins were detected using a secondary alkaline-phosphatase-conjugated antibody followed by incubation in nitroblue tetrazolium, 5-bromo-4-chloro-3-indolyl phosphate (NBT/BCIP) in 5 μ m sections. Arrowheads indicate 14-3-3C expression underneath L₁ layer of the shoot apical meristem and in scutellum cells. a sam, ct coleoptile, lp leaf primordia, m mesocotyl, r root meristem, rc root cap, sc scutellum.

The question raised is whether 14-3-3C specific expression underneath the L₁ layer of developing SAMs is restricted to L₂ layer formation, or whether it is also a feature of further cell division of the L₂ layer during early organogenesis. To answer this question, we studied 14-3-3C immunolocalization in proliferating barley SMCs.

Figure 3a illustrates shoot formation and an adventitious shoot meristem (boxed) in a cross section of a 16 month-old SMC of barley. We observed the presence of L_2 -derived cells as a thick differentiated layer underneath L_1 and above the corpus.

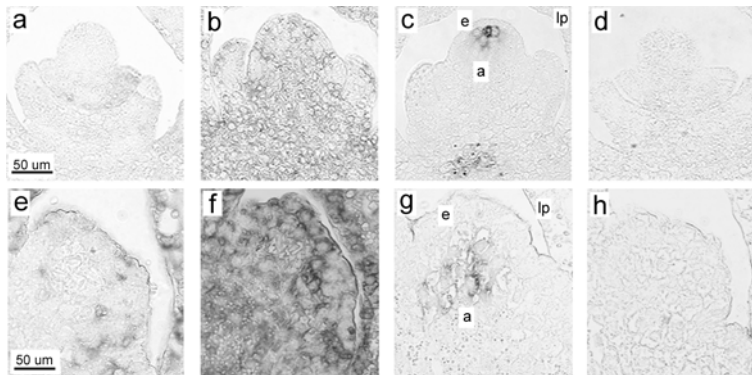


Figure 2. Magnified view of developing SAM of 21 DAP zygotic embryos (a-d) and 21 days-old ELs (e-h) showing immunolocalization of 14-3-3 proteins. 14-3-3A (a,e), 14-3-3B (b, f), 14-3-3C (c, g) and control incubated only with secondary antibody (d, h). a SAM, e epidermis, lp leaf primordia.

While 14-3-3A (Fig. 3b) and 14-3-3B (data not shown) were expressed in all layers within the shoot apical meristem, 14-3-3C expression could mainly be observed in L_2 -layer derived cells (Fig. 3c). No 14-3-3 signal was observed when sections were incubated only with the secondary antibody (Fig. 3d).

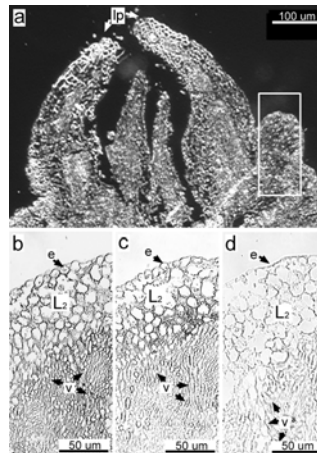


Figure 3. Structure and 14-3-3 immunolocalization in SMCs. A 5 μ m section of a 16 month-old SMC observed by darkfield (a). The equivalent area in the white box is presented in a higher magnification in (b-d). Proteins were detected using a secondary alkaline-phosphatase-conjugated antibody followed by incubation in NBT/BCIP. 14-3-3A (b), 14-3-3C (c) and control incubated only with secondary antibody (d). e epidermis, L_2 L_2 layer-derived cells, v vascular bundles.

Discussion

The developmental programs that lead to embryo formation are thought to be common to both androgenesis and zygotic embryogenesis (Mordhorst et al., 1997). We describe here that 14-3-3 isoform-specific expression patterns are similar during barley zygotic and microspore-derived embryogenesis. Our results are clear evidence for biochemical similarities among these two processes, indicating that the same spatial expression of members of the 14-3-3 family of regulatory proteins might be needed during the formation of barley embryos.

We demonstrate that L₂-layer specification and cell division from the L₂-layer are both accompanied by specific L₂-layer 14-3-3C expression in immature barley embryos and during early organogenesis of SMCs. The L₂ layer of the shoot apical meristem contributes probably to mesophyll formation in adult plants (Jenik and Irish, 2000). This expression pattern of the 14-3-3 C isoform in the SMC points out to specific functions for this isoform associated with the differentiation and function of the L₂ layer.

In other multicellular organisms, tissue-specific expression of 14-3-3 isoforms during embryogenesis is a known phenomenon. For example, in *Drosophila* 14-3-3ε tissue-specific expression was prior to mitogen-activated protein kinase (MAPK) activation in the same tissue during early embryo development (Tien et al., 1999). 14-3-3ε and 14-3-3ξ have been reported to positively regulate Ras-Raf signaling pathway, leading to MAPK cascade activation in *Drosophila* (Chang and Rubin, 1997; Kockel et al., 1997). Recently, Pnueli et al. (2001) have reported the specific expression of at least one 14-3-3 isoform in the SAM of tomato seedlings (*Lycopersicon esculentum* L.). The authors have shown that the same isoform takes part of a signaling system involved in determining SAM vegetative growth potential, a signaling system that is analogous to Raf-1 in animal cells. Further work is needed to address the possible 14-3-3C targets in the L₂-layer. In this regard, SMCs seem to be a suitable system to study 14-3-3C interacting proteins in the shoot meristem of barley.

Acknowledgments

We thank Sandra van Bergen and Arnoud van Marion for technical assistance.

References

- Chang HC, Rubin GM (1997) 14-3-3 ϵ positively regulates Ras-mediated signalling in *Drosophila*. *Genes Dev* 11: 1132-1139
- Daugherty CJ, Rooney MF, Miller PW, Ferl RJ (1996) Molecular organization and tissue-specific expression of an *Arabidopsis* 14-3-3 gene. *Plant Cell* 8: 1239-1248
- Hoekstra S, van Zijderveld MH, Louwerse JD, Heidekamp F, van der Mark F (1992) Anther and Microspore culture of *Hordeum vulgare* L. cv. Igri. *Plant Sci* 86: 89-96
- Jenik PD, Irish VF (2000) Regulation of cell proliferation patterns by homeotic genes during *Arabidopsis* floral development. *Development* 127: 1267-1276
- Kockel L, Vorbrüggen G, Jäckle H, Mlodzik M, Bohmann D (1997) Requirement for *Drosophila* 14-3-3 ζ in Raf-dependent photoreceptor development. *Genes Dev* 11: 1140-1147
- Louwerse JD (2002) Transformation of barley with the maize transposable element *En/Spm*. Ph.D. thesis, Heriot-Watt University, Edinburgh, Scotland
- Mordhorst AP, Toonen MAJ, de Vries SC (1997) Plant Embryogenesis. *Crit Rev Plant Sci* 16: 535-576
- Pnueli L, Gutfinger T, Hareven D, Ben-Naim O, Ron N, Adir N, Lifschitz E (2001) Tomato SP-interacting proteins define a conserved signaling system that regulates shoot architecture and flowering. *Plant Cell* 13: 2687-2702
- Rosenquist M, Alsterfjord M, Larsson C, Sommarin M (2001) Data mining the *Arabidopsis* genome reveals fifteen 14-3-3 genes. Expression is demonstrated for two out of five novel genes. *Plant Physiol* 127: 142-149
- Sehnke PC, DeLille J, Ferl RJ (2002) Consummating signal transduction: The role of 14-3-3 proteins in the completion of signal-induced transitions in protein activity. *Plant Cell* S339-S354
- Testerink C, van der Meulen RM, Oppedijk BJ, de Boer AH, Heimovaara-Dijkstra S, Kijne JW, Wang M (1999) Differences in spatial expression between 14-3-3 isoforms in germinating barley embryos. *Plant Physiol* 121: 81-87
- Tien AC, Hsei HY, Chien CT (1999) Dynamic expression and cellular localization of the *Drosophila* 14-3-3 ϵ during embryonic development. *Mech Dev* 81: 209-212
- van Heusden GPH, van der Zanden AL, Ferl RJ, Steensma HY (1996) Four *Arabidopsis thaliana* 14-3-3 protein isoforms can complement the lethal yeast *bmh1 bmh2* double disruption. *FEBS Lett* 391: 252-256

III. Cell death and 14-3-3 proteins during the induction of barley microspore androgenesis

Biologia (2003) 58: 59-68

Simone de Faria Maraschin, Gerda E.M. Lamers, Mei Wang

Abstract

In the barley (*Hordeum vulgare* L.) anther, tapetum and loculus wall cells undergo programmed cell death (PCD) at the time around the first pollen mitosis, at the uninucleate stage of microspore development. This is the stage where androgenesis is most efficiently induced in barley microspores. Induction of androgenesis is characterized by a switch of the normal pollen developmental pathway towards an embryogenic route via a stress pre-treatment of anthers for 4 days in mannitol solution. We were interested in studying the involvement of members of the 14-3-3 family of regulatory proteins during barley androgenesis induction. With the use of isoform-specific antibodies against the three 14-3-3 isoforms, 14-3-3A, 14-3-3B and 14-3-3C, we have studied their immunolocalization and expression level in anthers. All isoforms were localized in the microspores and in anther wall cells at the induction stage. At this period, 14-3-3A processing was found to take place in tapetum and loculus wall cells, where *in situ* DNA fragmentation was detected by TUNEL assay. After 4 days pre-treatment to induce androgenesis, anther wall cells degenerated and two types of morphologically distinct microspores were observed, enlarged and non-enlarged cells. At this stage, 14-3-3 isoforms were mainly localized in the microspores. 14-3-3A processing was found to be induced by stress and it could only be detected in non-enlarged cells with decreased viability after pre-treatment. Viable enlarged cells and pollen under normal *in vivo* development showed no visible 14-3-3A processing. The identification of 14-3-3A processing in anther wall cells and in microspores with decreased viability represents the first link between the processing of a specific 14-3-3 isoform in cells undergoing death pathway. The implications of this post-translational event in barley anthers are discussed.

Introduction

Programmed cell death (PCD) is a genetically controlled mechanism activated upon normal development or in response to environmental stress (Raff, 1998). It is a tightly regulated process known to involve an intracellular signaling cascade that culminates with the activation of specific proteases and leads to a characteristic apoptotic morphology of cells (Häcker, 2000). The molecular and biochemical events that culminate in the apoptotic morphology, a specific type of PCD, are well characterized for animal cells (Green and Beere, 2001). In plants, these processes are not yet unravelled at the molecular level. Nevertheless, there are some common morphologies present in both animal and plant cells

under PCD. It includes nuclear condensation of chromatin, DNA fragmentation, shrinkage of nucleus and loss of cell shape and integrity (Danon et al., 2000).

In animal cells, proteins involved in the apoptotic pathway are known to be regulated by members of the 14-3-3 protein family (Fu et al., 2000). 14-3-3s are highly conserved dimeric proteins with a subunit mass of approximately 30kD shown to be ubiquitously expressed in eukaryotes. In multicellular organisms, 14-3-3 proteins are present in many isoforms and take part of several processes within the cell. Besides their involvement in the control of apoptosis, 14-3-3s have been reported to participate in the regulation of cell cycle, intracellular signaling, transcription activation, vesicle trafficking and primary metabolism of the eukaryotic cell (van Hemert, 2001). Their regulatory functions arise from their properties to bind phosphopeptide motifs contained in their interacting proteins, which are exerted by the conserved core region of the monomers (Yaffe et al., 1997). The N-terminal dimerization domain and the hyper variable C-terminus, however, show little homology among different isoforms (Wang and Shakes, 1996). No specific functions have been so far described for the unconserved C-terminal region of 14-3-3 proteins.

In barley, three 14-3-3 isoforms have been cloned: 14-3-3A (GenBank X62388; Brandt et al., 1992), 14-3-3B (GenBank X93170) and 14-3-3C (GenBank Y14200). It has been reported that a 14-3-3A 28 kD band is formed by proteolytic cleavage of the unconserved C-terminal region of the 30 kD protein at the positions Lys 250/ Ala 255 upon the germination of barley embryos (van Zeijl et al., 2000; Testerink et al., 2001). During the onset of germination of barley embryos, massive TUNEL positive staining has been observed (unpublished data) and PCD has been described in barley scutellum and aleurone layer (Lindholm et al., 2000; Wang et al., 1996; Wang et al., 1998). It is known that several proteinases become active during barley germination which take part of the breakdown of storage proteins (Gibbons, 1980; Palmer, 1982; Briggs, 1987). Germination-related proteinases and their putative involvement in plant PCD have been recently reviewed by Beers et al. (2000). So far, no causal link has been established between PCD and the processing of 14-3-3A. The concomitant occurrence of PCD and 14-3-3A proteolytic cleavage during germination challenged us to further study this inter-relationship.

A classical example of PCD in plants is the death of anther tissues upon normal pollen development. PCD in anthers concerns two major events, that is the death of anther tapetum around the first pollen mitosis, and the death of specific anther wall layers such as stomium, endothecium and the circular cell cluster upon anther dehiscence (Wu and Cheung, 2000). The tapetum is an anther wall layer in intimate contact with the microspores in the loculus, whose prominent function is nourishing and directing the development of pollen grains (McCormick, 1993). PCD in tapetum has been described by means of condensation of

nuclear chromatin, DNA fragmentation, followed by nucleus and cell shrinkage (Papini et al., 1999; Wang et al., 1999). However, contrasting PCD in tapetum cells that is accomplished during pollen maturation, Wang et al. (1999) described massive PCD in tapetum cells in response to osmotic and starvation stresses upon androgenesis induction in barley microspores. During barley androgenesis induction, microspores are switched from their normal pollen development towards an embryogenic route by pre-treating whole anthers containing microspores at the mid-late to late uninucleate stage of development for 4 days in a mannitol solution (Hoekstra et al., 1992). The starvation and osmotic stresses imposed have been described as the triggers for the developmental switch observed during barley androgenesis (Wang et al., 2000).

We have used barley androgenesis as a model system to study 14-3-3 proteins and to investigate whether 14-3-3A processing was present in the developmental switch of microspores and in the PCD of anther tissues. To do so, isoform-specific antibodies against the three barley 14-3-3 isoforms (Testerink et al., 1999) were used to study 14-3-3 localization and expression levels in barley anthers. For the study of 14-3-3A processing, we have used two 14-3-3A antibodies, which were raised against the synthetic peptides 237-250 and 251-261. The former is able to detect both the 30 kD and the 28 kD forms of 14-3-3A, while the latter detects only the 30 kD unprocessed form of 14-3-3A due to the loss of the antibody recognition site by processing (Testerink et al., 1999; Testerink et al., 2001).

Materials and Methods

Androgenesis induction and microspore isolation

Donor plants of barley (*Hordeum vulgare* L. cv Igri) were grown in a phytotron under conditions described previously (Hoekstra et al., 1992). Barley anthers containing microspores at mid-late to late uninucleate stage were used for induction of androgenesis. Pre-treatment consisted of anther incubation in 0.37 M mannitol solution for 4 days in the dark, at 25°C (Hoekstra et al., 1992). Anther and microspore samples were collected at days 0, 1, 2, 3 and 4 of pre-treatment for various assays. As a control, spikes containing microspores at the mid-late to late uninucleate stage were allowed to stay 4 days longer in the mother plant. After this period, microspores had further developed into binucleate pollen. Isolation of microspores from control and pre-treated anthers was done by manual disruption of the anther tissue with a Teflon pestle to release the microspores. Microspores were then separated from anther tissues by filtration over a 110 µm mesh, and collected by centrifugation at 800 rpm for 5 minutes. Microspore isolation from pre-treated anthers was

carried out in 0.37 M mannitol solution, and microspores from control anthers were isolated in 8.5 % maltose solution. In order to obtain homogeneous populations of enlarged and non-enlarged microspores after anther incubation for 4 days in 0.37 M mannitol, microspores were loaded on a 15 % (w/v) sucrose gradient in 0.37 M mannitol solution and centrifuged at 800 rpm for 10 minutes for separation of enlarged and non-enlarged cells.

Protein isolation and Western analysis

Total protein extracts were prepared from anthers at day 0 and at day 4 of pre-treatment. Protein extracts were obtained from whole anthers gently macerated with the use of a metal pestle in protein extraction buffer at room temperature. Under such isolation conditions, microspores remained intact, which was checked under light microscope. These extracts contained mainly proteins from anther tissue. Protein extracts were prepared from purified enlarged and non-enlarged microspores after 4 days pre-treatment, binucleate pollen and microspores pre-treated for 0, 4 h, 12 h, and 1, 2, 3 and 4 days by vigorous maceration of the cells with a glass pestle in protein extraction buffer at room temperature. Protein extraction buffer consisted of 60 mM Tris pH 6.8, 10 % Glycerol, 5 % β -mercaptoethanol and 2 % SDS. The extracts were heated for 10 min at 95-100°C and centrifuged two times at 14,000 rpm for 10 minutes to collect supernatant. Soluble proteins (10 μ g) were separated on 15 % (w/v) SDS-PAGE and blotted onto nitrocellulose membranes or stained with coomassie brilliant blue 0.1 % (w/v) in 40 % (v/v) methanol and 10 % (v/v) acetic acid. Blots were incubated overnight at 4°C with isoform-specific 14-3-3 antibodies (1:20,000). Two 14-3-3A antibodies, raised against synthetic peptides 237-250 and 251-261 were used (Testerink et al., 1999; Testerink et al., 2001). Anti-14-3-3B and anti-14-3-3C antibodies were raised against peptides 248-262 and 251-262, respectively (Testerink et al., 1999). Bands were visualized by goat anti-rabbit horseradish peroxidase conjugate (Promega), followed by enhanced chemoluminescent detection (ECL) (Amersham).

Immunolocalization studies

Anthers containing microspores at the mid-late to late uninucleate stage and 4 days pre-treated anthers were fixed in 4 % paraformaldehyde in 10 mM NaH_2PO_4 , 120 mM NaCl, 2.7 mM KCl, pH 7.4 (phosphate-buffered saline, PBS) containing 10 mM dithiothreitol (DTT) overnight at 4°C. The material was dehydrated at room temperature through a graded ethanol series as follows: 70 %, 90 %, 96 % and 100 % (v/v). DTT was present in all dehydration steps at a concentration of 10 mM. Infiltration of resin was in ETOH: buthyl-methyl-methacrylate (BMM) 3:1, 1:1, 1:3 (v:v) containing 10 mM DTT, overnight at 4°C. Plant material was embedded in 100 % (v/v) BMM containing 10 mM of DTT and the resin was

polymerised in Beem capsules under UV light for 48 h at -20°C. Sections (5 µm) were attached to 2 % 3-aminopropyltriethoxy silane (Sigma) coated slides. After removal of the resin by acetone, proteins were denatured 20 minutes in 0.4 % (w/v) SDS, 3 mM β-mercaptoethanol, 12 mM Tris pH 6.8 and blocked 30 minutes in 1 % (w/v) bovine serum albumine (BSA) in PBS buffer, pH 7.4. Primary antibody incubation was carried out overnight at 4°C in 0.01 % acetylated BSA (Aurion) in PBS buffer, pH 7.4 (anti-14-3-3A diluted 1:1,000; anti-14-3-3B diluted 1:5,000 and anti-14-3-3C diluted 1:5,000). Sections were developed with alkaline-phosphatase-conjugated goat anti-rabbit antibody (Promega). The signal was visualized by incubating sections in nitroblue tetrazolium/5-bromo-4-chloro-3-indolyl phosphate (NBT/BCIP) substrate (Promega). Control experiments were performed omitting the first antibody. Slides were mounted in a mixture of 166 g/L polyvinylalcohol and 30 % (v/v) glycerol in PBS buffer, pH 7.4 and analyzed by light microscopy.

Terminal deoxynucleotidyl transferase-mediated dUTP nick end labelling (TUNEL)

Anthers at the mid-late to late uninucleate stage and after 4 days incubation in mannitol solution were fixed in 2 % glutaraldehyde in 10 mM NaH₂PO₄, 120 mM NaCl, 2.7 mM KCl, pH 7.4 (phosphate-buffered saline, PBS) overnight at room temperature. After dehydration at room temperature in a graded series of 70 %, 90 %, 96 % and 100 % (v/v) ethanol, samples were embedded in Histo-resin. Sections (2 µm) were attached to Biobond (Biocell) coated slides. TUNEL staining was done using an *in situ* cell death detection kit (Boehringer) and analysed by fluorescence microscopy (Wang et al., 1999). Following TUNEL reaction, nuclear staining was performed by incubating sections in 4'-6-diamidino-2-phenylindole (DAPI) 0.02 mg/ml in water for 5 minutes at room temperature.

FDA staining

Isolated microspores after androgenesis induction were stained for viability with fluorescein diacetate (FDA) 0.04 µg/ml in acetone for 10 minutes at room temperature and analysed by fluorescence microscopy.

Results

14-3-3A processing in pre-treated microspores

Anthers containing microspores at the mid-late to late uninucleate stage were pre-treated in mannitol solution for the induction of androgenesis. We investigated the levels of 14-3-3 expression in isolated microspores at the stage of induction and after 4 days of anther

pre-treatment. Upon androgenesis induction, 14-3-3A, 14-3-3B and 14-3-3C were present at higher levels in the isolated microspores (Fig. 1a-c). Moreover, in extracts of microspores at the uninucleate stage of development, mainly a 30 kD band of 14-3-3A was detected (Fig. 1a; day 0), whereas microspores after pre-treatment displayed both forms of 14-3-3A, a band at 30 kD and a band at 28 kD (Fig. 1a; day 4). This suggested that processing of 14-3-3A in the microspores was taking place during stress pre-treatment. Therefore, we monitored 14-3-3A protein expression during the course of pre-treatment. The 28 kD form of 14-3-3A could already be detected in microspores isolated from anthers that have been pre-treated for 4 hours in mannitol solution (Fig. 2). Interestingly, the 28 kD processed form of 14-3-3A seemed not to be a feature of normal pollen development, as mainly a 30 kD band was detected in extracts of binucleate pollen (Fig. 2; lane B).

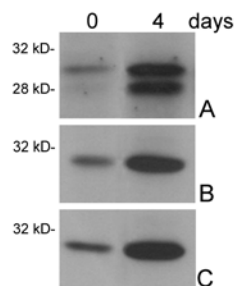


Figure 1. Western blot analysis of 14-3-3 expression in isolated microspores upon androgenesis induction. Microspores were isolated from anthers at day 0 and day 4 of pre-treatment as indicated above the lanes. 10 µg/lane of total protein extracts were separated by SDS-PAGE. Proteins were blotted onto nitrocellulose membranes and incubated with the isoform-specific antibodies. Signal was detected by enhanced chemoluminescent methods. Protein loading was verified by coomassie staining. Blots were incubated with anti 14-3-3A raised against synthetic peptide 237-250 (a), anti-14-3-3B (b) and anti-14-3-3C (c). One representative blot from 4 independent experiments is shown for each 14-3-3 isoform.

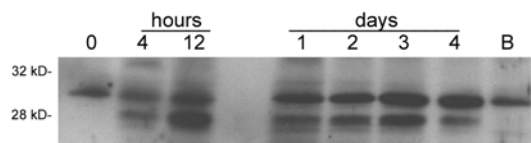


Figure 2. Western blot analysis of 14-3-3A expression in isolated microspores during the course of pre-treatment. Microspores were isolated from anthers at the designated times as indicated above the lanes. 0 microspores at the uninucleate stage, B binucleate pollen. 10 µg/lane of total protein extracts were separated by SDS-PAGE. Proteins were blotted onto nitrocellulose membranes and incubated with anti-14-3-3A raised against synthetic peptide 237-250. Signal was detected by enhanced chemoluminescent methods. Protein loading was verified by coomassie staining. One representative blot from 4 independent experiments is shown.

Upon pre-treatment, 60 % of the microspores appear as enlarged, vacuolated cells. Microspores displaying this morphology have been often reported to have acquired embryogenic potential after pre-treatment, while the remaining microspore population represents non-enlarged cells with no ability to divide during further microspore culture (Hoekstra et al., 1993). We were interested in further investigating whether the 14-3-3A processing was a feature of these two microspore populations. To do so, we separated microspores that have been pre-treated for 4 days by a sucrose gradient in order to obtain isolated fractions of enlarged and non-enlarged cells. In the population of enlarged microspores, 14-3-3A was present as its 30 kD form, while in non-enlarged microspores the 28 kD processed form of 14-3-3A was mainly detected (Fig. 3a). Processing of 14-3-3A by proteolytic cleavage of the unconserved C-terminus of the protein (van Zeijl et al., 2000; Testerink et al., 2001) was confirmed by the use of the 14-3-3A antibody that recognizes the amino acids 251-262. The antibody detected only the 30 kD 14-3-3 A form in enlarged and non-enlarged microspores (Fig. 3b), thus confirming the loss of the unconserved C-terminus of the 14-3-3A protein. FDA staining of the separated enlarged and non-enlarged microspore populations revealed the presence of FDA positive cells only in the enlarged microspore population, indicating that they were alive (Fig. 4a,b). Non-enlarged microspores were negatively stained for FDA and represented probably dying cells after pre-treatment (Fig. 4c,d).

In microspores after pre-treatment, the processing of 14-3-3A was associated to decreased viability of the non-enlarged cells (Fig. 3, 4). The question raised is whether cell death pathway of microspores upon pre-treatment shows features of PCD. We have used the TUNEL reaction (Gavrieli et al., 1992), which labels the 3' ends of DNA strand breaks, to assess *in situ* DNA fragmentation in the anthers upon the induction of androgenesis (Fig. 5).

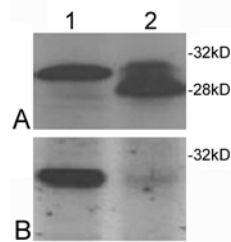


Figure 3. Western blot analysis of 14-3-3A expression in enlarged and non-enlarged microspores after 4 days of mannitol pre-treatment. Microspores were separated by a 15% sucrose gradient. 10 μ g/lane of total protein extracts were separated by SDS-PAGE, blotted onto nitrocellulose membranes and incubated with isoform-specific antibodies, followed by enhanced chemoluminescent detection. Protein loading was verified by coomassie staining. Blots were incubated with anti-14-3-3A raised against synthetic peptide 237-250 (a) and with anti-14-3-3A raised against synthetic peptide 251-262 (b). Lane 1 enlarged microspores and lane 2 non-enlarged microspores. One representative blot from 4 independent experiments is shown for each 14-3-3A antibody.

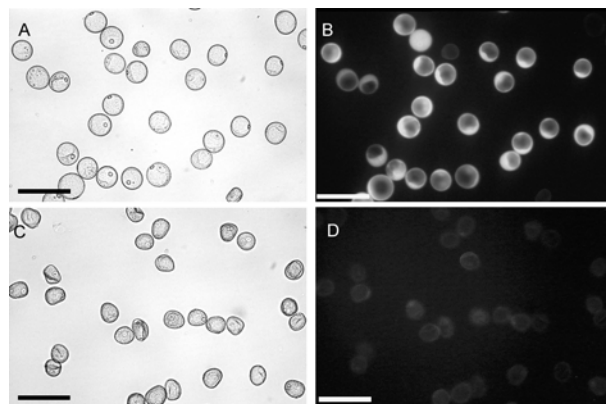


Figure 4. Microspore viability in enlarged and non-enlarged microspores after 4 days of mannitol pre-treatment assessed by FDA staining. The two populations were separated by a 15% sucrose gradient. (a) Enlarged microspores observed by light microscopy and (b) by fluorescence microscopy stained for FDA. (c) Non-enlarged microspores observed by light microscopy and (d) by fluorescence microscopy stained for FDA. Bars: 100 μm .

In anthers containing microspores at the mid-late to late uninucleate stage, TUNEL positive nuclei were observed mainly in anther tapetum, loculus and epidermis (Fig. 5a). Upon stress pre-treatment, we observed occurrence of TUNEL positive nuclei in some microspores, in the epidermal tissue and in the outermost layer of loculus wall cells, whereas anther tapetum and the innermost layer of loculus wall cells had degenerated (Fig. 5b).

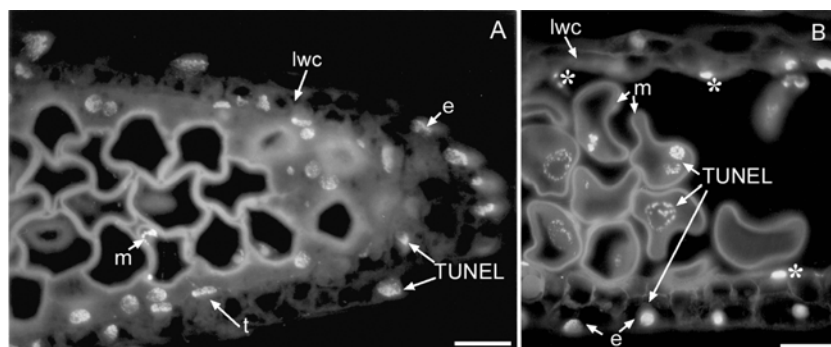


Figure 5. TUNEL detection of nuclear DNA fragmentation in anthers analysed by fluorescence microscopy. (a) TUNEL staining of anthers containing microspores at the mid-late to late uninucleate stage, prior to pre-treatment. (b) TUNEL staining of pre-treated anthers. Typical morphology of TUNEL-positive nuclei are indicated by arrows in (a) and (b). Remains of degenerated tapetum and innermost layer of loculus wall cells are indicated by (*). *e* epidermis, *lwc* loculus wall cells, *m* microspores, *t* tapetum. Sections of at least 5 anthers were studied per treatment in each experiment. TUNEL staining was studied in at least 5 anthers in 3 independent experiments. Representative examples are shown. Bars: 30 μm .

14-3-3 immunolocalization and detection of 14-3-3A processing in anthers

Upon osmotic and starvation stresses, anther wall cells and microspores underwent several morphological changes (Fig. 6). After pre-treatment, the anther tapetum and the innermost layer of loculus wall cells degenerated, while some of the microspores inside the anther appeared as enlarged, vacuolated cells (Fig. 6e-h). We studied the 14-3-3 immunolocalization in freshly isolated barley anthers containing microspores at the verge of mitosis, and investigated their temporal and spatial expression in anthers that have been pre-treated for the induction of androgenesis.

The immunolocalization patterns of the three barley 14-3-3 isoforms, 14-3-3A, 14-3-3B and 14-3-3C are shown in Figure 6. In freshly isolated anthers at the stage of androgenesis induction, 14-3-3 isoforms were present both in the microspores and in the anther wall cells. In the microspores, 14-3-3 signals were mainly detected in the cytoplasm of the cells. In the anther wall, all three isoforms were expressed in tapetum and in the loculus wall cells (Fig. 6a-c), however 14-3-3A signal was stronger in the tapetum layer when compared to that of 14-3-3B and 14-3-3C. After anther pre-treatment for the induction of androgenesis, 14-3-3 immunolocalization was restricted to the microspores. No signal was detected in the outermost layer of loculus wall cells, while the tapetum and the innermost layer of loculus wall cells had degenerated (Fig 6e-g). In pre-treated microspores, 14-3-3 signals were stronger than in untreated microspores, thus confirming the higher protein levels of the 14-3-3 isoforms observed by western blot analysis (Fig. 1). No signal was detected in the control sections incubated only with the secondary antibody (Fig. 6d,h).

Next, we investigated 14-3-3 protein expression levels in anther tissues before and after stress pre-treatment. In extracts of anthers developed to the stage of uninucleate microspores, 14-3-3A was present as a double band, at 30 kD and 28 kD respectively (Fig. 7a; day 0). 14-3-3B and 14-3-3C were present as bands of approximately 31 kD (Fig. 7b,c; day 0). The presence of a 28 kD form of 14-3-3A indicates that processing is a feature of anthers that have developed to the stage of uninucleate microspores.

Within the anther, the tapetum and loculus are most likely to display this post-translational modification, as these are the cell layers where the 14-3-3A isoform was shown to be localized (Fig. 6a). Interestingly, tapetum and loculus wall cells presented TUNEL positive nuclei at the uninucleate stage of microspore development, prior to pre-treatment (Fig. 5a). After pre-treatment, the protein expression level of the three isoforms was markedly lower compared to that of freshly isolated anthers (Fig. 7a-c; day 4), which is probably due to the accelerated degeneration of the anther tapetum and the anther loculus wall cells (Fig. 5b; 6e-g).

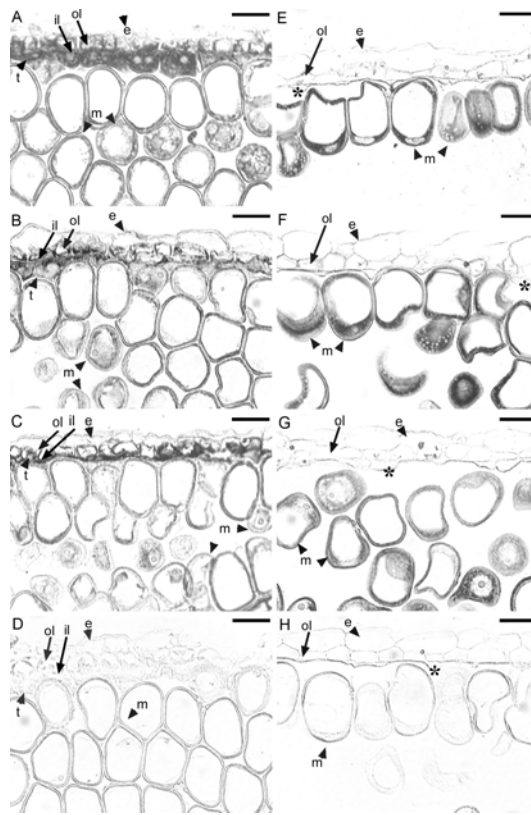


Figure 6. Immunolocalization of 14-3-3 isoforms in anthers analysed by light microscopy. Cross-sections of anthers containing microspores at the mid-late to late uninucleate stage (a) (b) (c) (d) and after 4 days of pre-treatment in mannitol solution (e) (f) (g) (h). (a/e) show immunolocalization of 14-3-3A, (b/f) 14-3-3B and (c/g) 14-3-3C. (d/h) were incubated only with secondary antibody. *e* epidermis, *il* innermost layer of loculus wall cells, *ol* outermost layer of loculus wall cells, *m* microspores, *t* tapetum. Remains of tapetum and innermost layer of loculus wall cells are indicated by (*). 14-3-3 immunolocalization was studied in at least 5 anthers in 3 independent experiments. Representative examples are shown for each 14-3-3 isoform. Bars: 20 μ m.

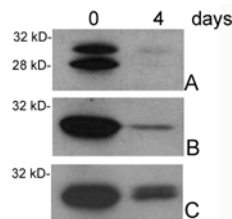


Figure 7. Western blot analysis of 14-3-3 expression in anther tissues upon androgenesis induction. 10 μ g/lane of total protein extracts were separated by SDS-PAGE. Proteins were blotted onto nitrocellulose membranes and incubated with the isoform-specific antibodies. Signal was detected by enhanced chemoluminescent methods. Protein loading was verified by coomassie staining. Blots were incubated with anti 14-3-3A raised against synthetic peptide 237-250 (a), anti-14-3-3 B (b) and anti-14-3-3 C (c). One representative blot from 4 independent experiments is shown for each 14-3-3 isoform.

Discussion

14-3-3A processing during PCD in tapetum upon normal pollen development

In germinating barley embryos, the 14-3-3A isoform is processed into a lower molecular weight form of 28 kD by proteolytic cleavage of the unconserved C-terminus of the protein (van Zeijl et al., 2000; Testerink et al., 2001). TUNEL positive staining has been observed in the germination process of barley (unpublished data). However, no link between processing of 14-3-3A and the death of specific cell types could be established in the above studies. We have demonstrated that both the 30 kD and the 28 kD forms of 14-3-3A were immunolocalized in tapetum and loculus wall cells in developing anthers where the microspores were at the mid-late to late uninucleate stage of pollen development (Fig. 6a, 7A). PCD has been demonstrated to take place in the anther tapetum and loculus wall cells by Wang et al. (1999) and we have shown that these are the cell layers to display DNA fragmentation in TUNEL assay (Fig 5a). Our results consist in the first report showing 14-3-3A processing in cell types dying in a programmed way. It is possible that 14-3-3A processing is linked to a PCD-related proteolytic cleavage.

Several proteinases have been identified during PCD of anther wall cells. In *Solanum melongena*, the expression of a cysteine proteinase mRNA has been correlated to the death of endothecium upon anther dehiscence (Xu and Chye, 1999), whereas accumulation of the transcript encoding a thiol endopeptidase has been described in dehiscent tobacco anthers (Koltunow et al., 1990). The LIM9 serine proteinase, whose putative function is to take part in PCD, is synthesized as a preprotein in the young tapetum and is secreted in the anther loculus, where it is also expressed in the microspores (Taylor et al., 1997). The expression of PCD-related proteinases upon the death of anther wall layers reinforce the idea that 14-3-3A processing is related to a cell death pathway. However, the biological function of the 14-3-3A processing is not yet clear. Both 14-3-3 A 30 kD and 28 kD forms were found to bind to the plasma membrane H⁺-ATPase in *in vitro* gel overlay assays (Testerink et al., 2001), suggesting that the 28 kD is still functional. van Zeijl et al. (2000) observed the 28 kD form of 14-3-3A to accumulate in cytosolic and microsomal fractions of germinating barley embryos, an indication that 14-3-3A processing might affect its subcellular localization. The characterization of the 14-3-3A proteinase will help clarifying whether 14-3-3A processing is accomplished by a PCD-related proteinase and it will shed light on its biological function.

14-3-3A processing during the developmental switch of barley microspores

The processing of 14-3-3A was detected in microspores neither at the uninucleate stage, prior to androgenesis induction, nor at the binucleate stage, when microspores were

allowed to develop for further 4 days in the mother plant (Fig. 1a; 2). This suggests that 14-3-3A processing may not be important for *in vivo* development and it is probably not required for the first pollen mitosis. However, one cannot exclude 14-3-3A processing to take place in the microspores beyond our detection level.

In the microspores, we described 14-3-3A processing to take place upon osmotic and starvation stresses during the switch from the gametophytic pathway towards an embryogenic route (Fig. 1a). The period of dedifferentiation of tobacco microspores is known to be accompanied by phosphorylation of proteins (Kyo and Harada, 1990a; Kyo and Harada, 1990b; Kyo and Ohkawa, 1991) and specific phosphorylation of one of the Hsp70 has been reported during early androgenesis of *Brassica napus* microspores (Cordewener et al., 2000). During cold stress pre-treatment of *Zea mays* anthers, ubiquitination of proteins detected in the microspores have indicated that protein degradation by the ubiquitin-mediated pathway is a biochemical feature of stressed microspores (Alché et al., 2000). These evidences suggest that post-translational events are likely to be associated with the developmental changes brought up by stress during induction of androgenesis. In barley androgenesis, we were able to detect a post-translational event in a specific cell type: while enlarged microspores with embryogenic potential showed mainly the 30 kD form of 14-3-3A, non-enlarged microspores with decreased viability showed mainly the 28 kD processed form of 14-3-3A (Fig. 3). However, processing of 14-3-3A could be already detected in 4 hours pre-treated microspores (Fig. 2), at a stage where no decrease of viability or morphological changes were observed within the microspore population (data not shown). This indicates that the processing of 14-3-3A may be part of an early event involved in cell death of the microspores.

The question raised is whether decrease of viability in non-enlarged is due to PCD induced by stress pre-treatment. In normal development of anthers, PCD of tapetum and loculus wall cells have been reported (Papini et al., 1999; Wang et al., 1999). The massive cell death in these anther wall layers during androgenesis induction in barley indicates that PCD may be accelerated by stress (Wang et al., 1999). Nutrient deprivation and salt stresses have been demonstrated to induce death of cells with characteristic of PCD in *Arabidopsis* cell-suspension cultures and in barley roots (Callard et al., 1996; Katsuhara, 1997). We showed that TUNEL positive nuclei were mainly found within the microspore population in pre-treated anthers, indicating DNA fragmentation to take place upon stress (Fig. 5b). These evidences indicate that cell death of the microspores upon stress pre-treatment display both the same type of 14-3-3A processing and DNA fragmentation showed by anther tapetum and loculus upon developmental PCD. Further investigation of the mechanisms of the death of the non-enlarged microspores displaying the 14-3-3A processing will help characterizing whether PCD is involved.

Acknowledgments

We are grateful to Sandra van Bergen for technical assistance and to Bert van Duijn for critical reading of the manuscript.

References

- Alché JD, Castro AJ, Solymoss M, Timar I, Barnabas B, Rodríguez-García MI (2000) Cellular approach to the study of androgenesis in maize anthers: immunocytochemical evidence of the involvement of the ubiquitin degradative pathway in androgenesis induction. *J Plant Physiol* 155: 146-155
- Beers EP, Bonnie J, Zhao W, Zhao C (2000) Plant proteolytic enzymes: possible roles during programmed cell death. *Plant Mol Biol* 44: 399-415
- Brandt J, Thordal-Christensen H, Vad K, Gregersen PL, Collinge DB (1992) A pathogen-induced gene of barley encodes a protein showing high similarity to a protein kinase regulator. *Plant J* 2: 815-820
- Briggs DE (1987) Endosperm breakdown and its regulation in barley germination. In: Schweigert S (ed), *Food and Science Technology*, Academic Press, London, pp. 441-532
- Callard D, Axelos M, Mazzolini L (1996) Novel molecular markers for late phases of the growth cycle of *Arabidopsis thaliana* cell-suspension cultures are expressed during organ senescence. *Plant Physiol* 112: 705-715
- Cordewener J, Bergervoet J, Liu CM (2000) Changes in protein synthesis and phosphorylation during microspore embryogenesis in *Brassica napus*. *J Plant Physiol* 156: 156-163
- Danon A, Delorme V, Mailhac N, Gallois P (2000) Plant programmed cell death: A common way to die. *Plant Physiol Biochem* 38: 647-655
- Fu H, Subramanian RR, Masters SC (2000) 14-3-3 proteins: structure, function and regulation. *Annu Rev Pharmacol Toxicol* 40: 617-647
- Gibbons GC (1980) On the sequential determination of α -amylase transport and cell breakdown in germinating seeds of *Hordeum vulgare*. *Carlsberg Research Communication* 45: 177-184
- Gavrieli Y, Sherman Y, Ben-Sasson SA (1992) Identification of programmed cell death *in situ* via specific labelling of DNA fragmentation. *J Cell Biol* 119: 493-501
- Green DR, Beere HM (2001) Mostly dead. *Nature* 412: 133-135
- Häcker G (2000) The morphology of apoptosis. *Cell Tissue Res* 301: 5-17
- Hoekstra S, van Zijderveld MH, Heidekamp F, van der Mark F (1993) Microspore culture of *Hordeum vulgare* L.: the influence of density and osmolarity. *Plant Cell Rep* 12: 661-665
- Hoekstra S, van Zijderveld MH, Louwerse JD, Heidekamp F, van der Mark F (1992) Anther and microspore culture of *Hordeum vulgare* L. cv. Igri. *Plant Sci* 86: 89-96
- Katsuhara (1997) Apoptosis-like cell death in barley roots under salt stress. *Plant Cell Physiol* 38: 1091-1093
- Koltunow AM, Truettner J, Cox KH, Wallroth M, Goldberg RB (1990) Different temporal and spatial expression patterns occur during anther development. *Plant Cell* 2: 1201-1224
- Kyo M, Harada H (1990a) Phosphorylation of proteins associated with embryogenic dedifferentiation of immature pollen grains of *Nicotiana rustica*. *J Plant Physiol* 136: 716-722
- Kyo M, Harada H (1990b) Specific phosphoproteins in the initial period of tobacco pollen embryogenesis. *Planta* 182: 58-63

- Kyo M, Ohkawa T (1991) Investigation of subcellular localization of several phosphoproteins in embryogenic pollen grains of tobacco. *J Plant Physiol* 137: 525-529
- Lindholm P, Kuittinen T, Sorri O, Guo D, Merits A, Törmäkangas K, Runeberg-Roos P (2000) Glycosylation of phytepsin and expression of *dad1*, *dad2* and *ost1* during onset of cell death in germinating barley scutella. *Mech Develop* 93: 169-173
- McCormick S (1993) Male Gametophyte Development. *Plant Cell* 5: 1265-1275
- Palmer GH (1982) A reassessment of the pattern of endosperm hydrolysis (modification) in germinated barley. *Journal of the Institute of Brewing* 88: 145-153
- Papini A, Mosti S, Brighigna L (1999) Programmed cell death events during tapetum development of angiosperms. *Protoplasma* 207: 213-221
- Raff M (1998) Cell suicide for beginners. *Nature* 396: 119-122
- Taylor AA, Horsch A, Rzepczyk A, Hasenkampf CA, Riggs CD (1997) Maturation and secretion of a serine proteinase is associated with events of late microsporogenesis. *Plant J* 12: 1261-1271
- Testerink C, van Zeijl MJ, Drumm K, Palmgren MG, Kijne JW, Wang M (2001) Post-translational modification of barley 14-3-3A is isoform-specific and involves the removal of the hypervariable C-terminus. *Plant Mol Biol* 50: 535-542
- Testerink C, van der Meulen RM, Oppedijk BJ, de Boer AH, Heimovaara-Dijkstra S, Kijne JW, Wang M (1999) Differences in spatial expression between 14-3-3 isoforms in germinating barley embryos. *Plant Physiol* 121: 81-87
- van Hemert M (2001) Characterization of the *Saccharomyces cerevisiae* Fin1 protein: a binding partner of the 14-3-3 proteins. PhD thesis. Leiden University, Leiden, 143 pp
- van Zeijl MJ, Testerink C, Kijne JW, Wang M (2000) Subcellular differences in post-translational modification of barley 14-3-3 proteins. *FEBS Lett* 473: 292-296
- Wang M, Hoekstra S, van Bergen S, Lamers GEM, Oppedijk BJ, van der Heijden MW, de Priester W, Schilperoort RA (1999) Apoptosis in developing anthers and the role of ABA in this process during androgenesis in *Hordeum vulgare* L. *Plant Mol Biol* 39: 489-501
- Wang M, Oppedijk BJ, Caspers MPM, Lamers GEM, Boot MJ, Geerlings DNG, Bakhuizen B, Meijer AH, van Duijn B (1998) Spatial and temporal regulation of DNA fragmentation in the aleurone of germinating barley. *J Exp Bot* 325: 1293-1301
- Wang M, Oppedijk BJ, Lu X, van Duijn B, Schilperoort RA (1996) Apoptosis in barley aleurone during germination and its inhibition by abscisic acid. *Plant Mol Biol* 32: 1125-1134
- Wang M, van Bergen S, van Duijn B (2000) Insights into a key developmental switch and its importance for efficient plant breeding. *Plant Physiol* 124: 523-530
- Wang W, Shakes DC (1996) Molecular evolution of the 14-3-3 protein family. *J Mol Evol* 43: 384-398
- Wu H, Cheung AY (2000) Programmed cell death in plant reproduction. *Plant Mol Biol* 44: 267-281
- Xu FX, Chye ML (1999) Expression of cysteine proteinase during developmental events associated with programmed cell death in brinjal. *Plant J* 17: 321-327
- Yaffe MB, Rittinger K, Volinia S, Caron PR, Aitken A, Leffers H, Gamblin SJ, Smerdon SJ, Cantley LC (1997) The structural basis for 14-3-3: phosphopeptide binding specificity. *Cell* 91: 961-971

cDNA array analysis of stress-induced gene expression in barley androgenesis

Submitted

Simone de Faria Maraschin, Martien Caspers, Elena Potokina, Florian Wülfert, Maximiliano Corredor-Adámez, Andreas Graner, Herman P. Spaink, Mei Wang

Abstract

Different aspects of androgenesis induction have been studied in detail, but little is known about the molecular mechanisms associated with this developmental switch. We have employed macroarrays containing 1421 ESTs covering the early stages of barley zygotic embryogenesis to compare the gene expression profiles of stress-induced androgenic microspores with that of uninucleate microspores as they progressed into binucleate stage during pollen development. Principle component analysis defined distinct sets of gene expression profiles that were associated with androgenesis induction and pollen development. During pollen development, uninucleate microspores were characterized by the expression of cell-division related genes and transcripts involved in lipid biosynthesis. Progress into binucleate stage resulted in the significant increase in the level of transcripts associated with starch biosynthesis and energy production. These transcripts were down-regulated in androgenic microspores. These results indicate that stress blocks the expression of pollen-related genes. Induction of androgenesis by stress was marked by the up-regulation of transcripts involved in sugar and starch hydrolysis, proteolysis, stress response, inhibition of programmed cell death and signaling. Further expression analysis of a subset of genes revealed that the induction of *ALCOHOL DEHYDROGENASE 3* and proteolytic genes, such as the metalloprotease *FtsH*, cysteine protease 1 precursor, phytepsin precursor (aspartic protease) and a 26S proteasome regulatory subunit were associated with the androgenic potential of microspores, while the induction of transcripts involved in signaling and cytoprotection were associated with stress responses. Taken together, these expression profiles represent 'bio-markers' associated with the androgenic switch in microspores, providing a substantial contribution towards understanding the molecular events underlying stress-induced androgenesis.

Introduction

Pollen development follows a controlled sequence of events that can be divided into two major processes, microsporogenesis and microgametogenesis (Bedinger, 1992). In barley, microsporogenesis begins with meiosis of pollen mother cells and ends with the formation of haploid microspores. The first pollen mitosis marks the initiation of microgametogenesis, where an asymmetric division gives rise to a condensed generative cell embedded in the large vegetative cytoplasm. While the generative cell undergoes another mitosis to produce two sperm cells, the vegetative cell becomes arrested in the G₁ phase of

the cell cycle and fills up with starch grains and other storage products (McCormick, 1993). The events that take place during the transition between microsporogenesis and microgametogenesis represent a critical point in the commitment to the pollen developmental pathway, since a stress treatment applied around the first pollen mitosis is sufficient to switch the microspores to an embryogenic route of development, a process called androgenesis (Touraev et al., 1997). Due to the haploid nature of pollen cells, androgenesis is a valuable tool to generate double haploids for breeding purposes (Wang et al., 2000). Recent molecular and biochemical approaches have demonstrated that microspore, somatic and zygotic embryos share the expression of several transcription factors and key regulatory proteins (Boutilier et al., 2002; Vrienten et al., 1999; Perry et al., 1999; Baudino et al., 2001). Androgenesis represents, in this context, a convenient model system to address questions concerning plant embryogenesis (Matthys-Rochon, 2002). For both applied and fundamental research, it is of uttermost importance to understand how a highly specialized cell such as the developing pollen grain can be reprogrammed to become embryogenic.

Several types of stress treatments are known to efficiently trigger androgenesis. They usually consist of subjecting whole plants *in vivo* or tillers, buds, anthers and isolated microspores *in vitro* to carbon and nitrogen starvation, heat, cold or osmotic shock (Touraev et al., 1997). Upon stress, the microspores enlarge and the cytoplasm is characterized by the lack of starch and lipid accumulation, the presence of organelle-free regions in the cytoplasm and an overall decrease in the number of ribosomes (Hoekstra et al., 1992; Maraschin et al., 2004; Telmer et al., 1995; Rashid et al., 1982). The nucleus re-enters the cell cycle as DNA replication takes place during stress treatment (Touraev et al., 1996). Both the de-repression of cell cycle arrest and the inhibition of pollen differentiation have been pointed out as important features of androgenesis induction (Touraev et al., 1997). At the molecular level, the induction of several genes marks the reprogramming of microspore towards the androgenic pathway. Stress proteins, such as members of the chaperone family of heat shock proteins (HSP), are induced in rapeseed (*Brassica napus* L.) and tobacco (*Nicotiana* spp) microspores upon heat shock, starvation and colchicine (Zarsky et al., 1995; Smykal and Pechan, 2000). In wheat (*Triticum aestivum* L.), an ABA-responsive, early cysteine labeled class II metallothionein gene has been identified as a marker for acquisition of embryogenic potential, suggesting a role for ABA in androgenesis induction (Reynolds and Crawford, 1996). In rapeseed, androgenesis-related marker genes were first identified in heat-stressed microspores and encode a subfamily of napin genes (Boutilier et al., 1994). It is also from rapeseed microspores that the *BABY BOOM* (*BBM*) gene, a member of the AP2/ERF family of transcription factors, has been identified by Boutilier et al. (2002). Its ectopic expression in *Arabidopsis* and rapeseed suggests that *BBM* plays a role in

vegetative-to-embryonic transition, being the first androgenic-related marker to date to exhibit a putative function in microspore embryogenesis induction. However, holistic approaches to characterize the stress-induced gene expression programs during androgenesis induction have not yet been explored, and there is nearly no information available on the transcriptome associated with this developmental switch.

With the recent development of high-throughput techniques allowing the expression analysis of thousands of expressed sequence tags (ESTs), the analysis of complex networks governing developmental and metabolic processes has become possible (Lee et al., 2002). In an attempt to identify gene expression profiles associated with androgenesis induction in barley (*Hordeum vulgare* L.), macroarrays containing 1421 barley ESTs isolated from a cDNA library covering the first 15 days of seed development were used (Michalek et al., 2002; Sreenivasulu et al., 2002; Potokina et al., 2002). Efficient androgenesis in barley is induced by a combination of starvation and osmotic stress, which is achieved via a mannitol treatment of anthers containing microspores at the mid-late to late (ML-L) uninucleate stage, just prior to the first pollen mitosis (Hoekstra et al., 1992). Following mannitol stress treatment, embryogenic potential is displayed by a population of highly vacuolated, enlarged cells which can be isolated by means of a sucrose gradient (Maraschin et al., 2003). Principle component analysis (PCA) based on array expression data revealed the gene expression profiles that were associated with normal pollen development as ML-L microspores developed into binucleate pollen, and their reprogramming during androgenesis induction. Our results provide a comprehensive overview of the molecular events unfolding in the microspores during their reprogramming and identify cellular processes that have never been so far described in the context of androgenesis.

Material and Methods

Plant material, androgenesis induction and microspore isolation

Donor plants of barley (*Hordeum vulgare* L. cv Igri, Landbouw Bureau Wiersum, The Netherlands) were grown in a phytotron under conditions described previously (Hoekstra et al., 1992). For array experiments, three microspore populations representing different developmental stages were assayed: (1) ML-L uninucleate microspores, (2) early to mid-binucleate pollen and (3) enlarged microspores after androgenesis induction. For isolation of developmental stages 1 and 2, microspores were separated from the anther tissues by gently blending anthers in 8.5 % (w/v) maltose solution. The microspore suspensions were then sieved through appropriate nylon meshes for collection of microspores as previously

described (Maraschin et al., 2003). For isolation of developmental stage 3, anthers containing microspores at the ML-L uninucleate stage were incubated for 4 days in the dark at 25°C in 0.37 M mannitol in CPW basal salt buffer (440 mOsm.kg⁻¹; Hoekstra et al., 1992). After androgenesis induction, microspores were separated from the anther tissues by gentle blending (Maraschin et al., 2004) and the enlarged microspore fraction was isolated by a sucrose gradient (Maraschin et al., 2003). Only the fraction composed of viable, enlarged microspores was used for array experiments. Alternatively, two additional pre-treatment solutions with different osmolarities were used to induce androgenesis: anther pre-treatment in CPW basal salt buffer without addition of mannitol (50 mOsm.kg⁻¹) and anther pre-treatment in deionized water alone (0 mOsm.kg⁻¹; van Bergen et al., 1999). Following stress treatment, enlarged microspores were isolated as described for developmental stage 3. All microspore samples were immediately frozen in liquid nitrogen after isolation.

Total RNA isolation

Total RNA was isolated from microspore samples using Trizol reagent (Invitrogen, Carlsbad, CA, USA) according to manufacturer's instructions.

Macroarray hybridization and data analysis

For array analysis, polyA⁺-RNA purified from 20 µg of total RNA from developmental stages 1, 2 and 3 were used for preparation of ³³P-labeled cDNA probes as previously described (Sreenivasulu et al., 2002). Radioactive-labeled probes were hybridized onto Nylon membranes containing 1421 ESTs selected from barley cv. Barke cDNA libraries of developing caryopsis 1-15 days after flowering (Michalek et al., 2002; Sreenivasulu et al., 2002; Potokina et al., 2002). Sequence and related clone information are available at the IPK Website <http://www.pgrc.ipk-gatersleben.de>. For each microspore stage, two hybridizations were carried out using biological duplos, totalizing six hybridizations. After quantitative removal of the probe, macroarrays were re-used up to three times as described by Sreenivasulu et al. (2004). Radioactive signals on the cDNA macroarrays were detected using a phosphoimager (Fuji BAS, 2000, Fuji Photo Film Co., Ltd, Tokyo, Japan), and the intensities of individual spots and the corresponding local backgrounds were quantified (Array-Vision, Imaging Research, St Catherine's, Ont., Canada). The data were exported to a spreadsheet program for further processing. The local background signals were subtracted from spot-signal intensities. Normalization of spot-signal intensities of individual hybridizations was done based on the total amount of radioactivity bound to the array for each different hybridization. Since each EST on the macroarray was spotted twice, gene filtering was done based on the average spot-signal intensities of the two spots representing

the same EST ($n=2$). Only the gene data with averaged spot-signal intensities equal or greater than five times the average background and a standard error (standard deviation/average spot signal intensity) smaller than 0.3 in at least one of the six hybridizations were further analyzed.

Principle Component Analysis (PCA)

The expression data of the ESTs which showed signals above background level were analyzed by PCA (Matlab version 6, The MathWorks, Inc., Natick, MA, USA; PLS toolbox version 2, Eigenvector Research, Inc., Manson, WA, USA). For PCA analysis, mean centering and level scaling were used to normalize the average spot-signal intensities of the ESTs. Level scaling has been chosen so that up- or down-regulations of similar relative level will get similar weight in the PCA model. The frequency distribution of the ESTs according to the sum of the square root of the average loadings from PC1 and PC2 (distance to origin on the loading plot) was used to identify the ESTs which were differentially expressed. The average sample scores of PC1 and PC2 were used to calculate the optimal orientation of the samples on the two-dimensional plots. The loading plot was subsequently divided in six areas defined by the average between the sample optimal orientations. These criteria were used to assign the ESTs comprised in each area to six different groups. The derived vector component (factor spectra) of the sample loadings of PC1 oriented in the optimal direction of developmental stages 1, 2 and 3 were used to quantify the relative contribution of the ESTs to each of the developmental stages. The expression dynamics of each EST was calculated as a ratio between the maximum and the minimum average spot-signal intensities within the three populations.

cDNA annotation and functional classification of genes

For annotation and functional classification, the sequences of the differentially expressed ESTs were compared to the SwissProt database (Apweiler et al., 2004) using BlastX (Altschul et al., 1997). Protein hits in the SwissProt database with e-value equal or greater than $E-15$ were classified according to their putative functions.

Northern blot analysis

Ten μg of total RNA sample were separated electrophoretically along with a RNA marker (GiboBRL, Gaithersburg, MD, USA) in a 1.5 % (w/v) agarose gel containing 2 % (v/v) formaldehyde, 20 mM 3-(N-morpholino) propanesulfonic acid, 8 mM sodium acetate, 10 mM EDTA, pH 7.0; blotted onto nitrocellulose membranes and hybridized with ^{32}P -labeled cDNA probes as described previously (Menke et al., 1999). The cDNA clones corresponding to the

ESTs HY10G20, HY08C24, HY06G09, HY06J08, HY01C15, HY01O02, HY10N13, HY01B24, HK03G06, HY10O06, HK04B02, HW01H17, HY03O15, HW01K08, HY06J20 were used as probes. The corresponding cDNA inserts were excised from pBK-CMV plasmids by enzymatic digestion with *Bam*HI/ *Xho*I and purified from agarose gels using Qiaquick Gel Extraction kit (QIAGEN, Valencia, CA, U.S.A.) according to manufacturer's instructions. cDNA probes were labeled using Rediprime II kit and purified using Microspin S-200 columns (Amersham Biosciences, Piscataway, NJ, USA) according to manufacturer's instructions.

Results and Discussion

Classification of microspore developmental stages

In order to gain knowledge of the gene expression profiles associated with barley androgenesis induction, three cell populations representing defined developmental stages during pollen and androgenic development were assayed. Stage 1 is represented by ML-L microspores at the verge of the first pollen mitosis. These uninucleate microspores are characterized by the presence of a large central vacuole and an undifferentiated cytoplasm, and represent the responsive stage for androgenesis induction (Fig. 1, stage 1). Stage 2 is represented by early to mid-binucleate pollen, which is the stage when ML-L microspores further develop for 4 days in the mother plant. These cells are characterized by the presence of a small generative cell embedded in the cytoplasm of the large vegetative cell, and by the accumulation of starch granules in the vegetative cytoplasm (Fig. 1, stage 2). The initiation of starch accumulation marks the commitment to the pollen developmental pathway, therefore androgenesis can be no longer triggered at this stage. Stage 3 is represented by enlarged cells, which is the morphology when ML-L microspores are treated in 0.37 M mannitol solution for 4 days. This stress treatment is able to switch 50% of the enlarged microspores towards the androgenic pathway (Maraschin et al., 2004). Nevertheless, still half of the enlarged microspores do not respond to the stress treatment to induce androgenesis, as they accumulate starch and eventually die in culture (Fig. 1, stage 3). Due to the heterogeneity of the microspore population at stage 3, comparisons between the gene expression profiles in the transition from stage 1 to 2 (Fig. 1, bold arrow) and between stage 1 to 3 (Fig. 1, open arrow) were needed in order to distinguish pollen development-related genes from those that were specific to androgenic development.

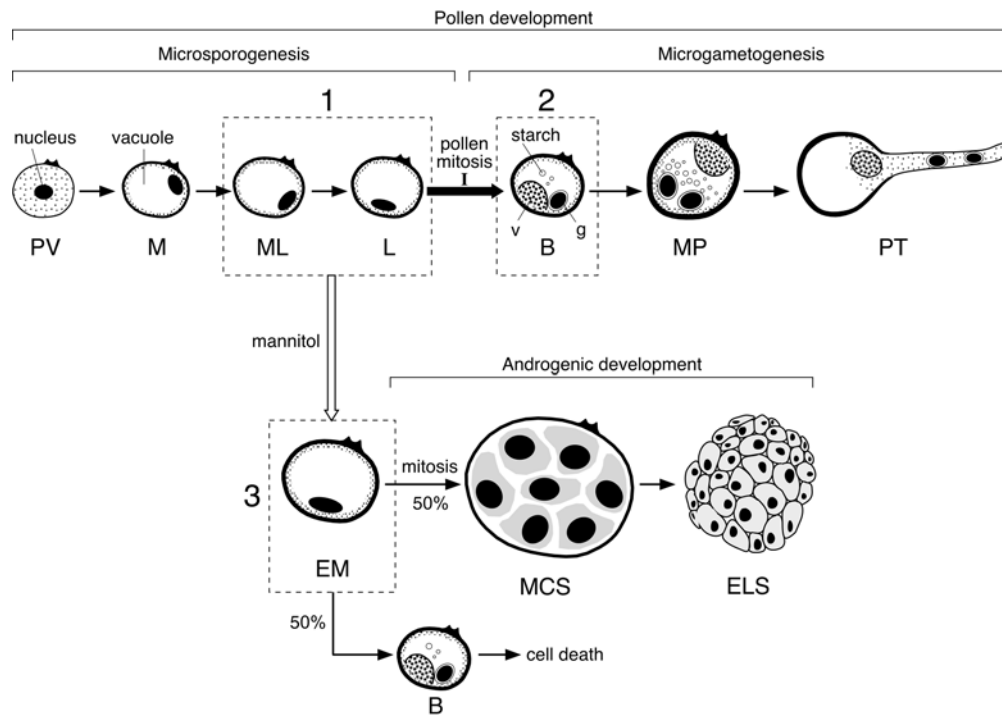


Figure 1. Pollen development and mannitol-induced androgenic development in barley. Developmental stages contained by boxes were assayed for array analysis: (1) ML-L uninucleate microspores, (2) early-mid binucleate pollen and (3) enlarged microspores after mannitol treatment. The relative conversion of enlarged microspores into multicellular structures, as well as the frequency of enlarged microspores that are still committed to the pollen developmental pathway are indicated (Maraschin et al., 2004). Bold arrows indicate transition between stage 1 to 2, while open arrows indicate transition between stage 1 to 3. *PV* pre-vacuolate microspore, *M* mid-uninucleate microspore, *ML* mid-late uninucleate microspore, *L* late uninucleate microspore, *B* binucleate pollen, *MP* mature tricellular pollen, *PT* pollen tube growth, *EM* enlarged microspores, *ELS* embryo-like structure, *MCS* multicellular structure.

PCA analysis of gene expression in microspore at different developmental stages

Poly A⁺-RNA isolated from stages 1, 2 and 3 was used to synthesize ³³P-labeled cDNA probes. ³³P-labeled cDNA probes were hybridized to macroarrays containing 1421 barley ESTs (Michalek et al., 2002; Sreenivasulu et al., 2002). From the 1421 ESTs spotted on the macroarray, 509 ESTs showed signal above background level, from which 418 displayed a standard error smaller than 0.3. The complete data set from six hybridizations comprising the normalized signal intensities from the 418 ESTs was subjected to PCA analysis. The six hybridizations resulted in up to six principle components (PCs) that describe the total variance in the gene expression data. The first PC's are the most important, as the amount of variance captured decreases with increasing PC number. Each PC is based on a data trend or "gene expression profile" that is expressed in the loading vector of that PC. For each sample a score is assigned by the algorithm for this data trend, representing how

important that profile of ESTs is to that respective sample. Differences between samples can therefore be visualized by plotting the scores, while the underlying data trends can be shown in the loading plots.

Figure 2a reveals the major differences between the gene expression data from individual hybridizations. This score plot indicates that the first two components of the expression data (PC1 and PC2) corresponded to the differences in the stage and in the developmental pathway of the cells, respectively, and together accounted for 82 % of the variances found. The relative distances between the biological duplos and between stages 1, 2 and 3 illustrate that the variances between biological duplos were relatively small compared to the variances between developmental stages, indicating a high reproducibility between biological duplos. In order to find the optimal vector orientation of the three developmental stages on the score plot, the PC1 and PC2 scores between duplo hybridizations were averaged. These optimal orientations are indicated by arrows (Fig. 2a). We interpret the PCA results as an indicative of massive re-programming of gene expression during the commitment of ML-L uninucleate microspores to the pollen developmental pathway (transition 1 to 2) or their switch towards the androgenic route (transition 1 to 3).

To reveal which ESTs were primarily responsible for the variances found between the three developmental stages, the 418 ESTs were analyzed based on their average PC1 and PC2 loadings (Fig. 2b). This plot illustrates the contribution of each of the 418 ESTs to the differences between the three developmental stages. In the loading plot, EST distance and orientation from the origin of the plot can be regarded as indicative for the degree of correlation of each EST to one of the three developmental stages according to their optimal directions as deduced from the sample scores (Fig. 2a, b). To reduce the amount of weakly correlated genes, ESTs most close to the origin were discarded (Fig. 2b, outlined by circle). This was done by creating a histogram of the distribution of the ESTs according to their distance to origin in the loading plot (Fig. 2c). Since ESTs that were 0.07 units far from the origin were observed more frequently than it would be expected based on the histogram shape for a normal distribution, they were considered to be differentially expressed between the three developmental stages. The reduced data set was composed of 96 ESTs, whose expression dynamics varied among the three developmental stages by a minimum of 2.0-fold and a maximum of 52-fold. The loading plot was subsequently divided in six areas defined by the average between the sample optimal orientations (Fig. 2b, dashed lines). These criteria were used to group the ESTs comprised in each of the six areas of the loading plot. The ESTs grouped in the same area showed a similar expression profile (Fig. 2d, groups I-VI). This indicates that the position of the ESTs in the loading plot correlates with their expression profiles. Therefore, the ESTs plotted in the positive orientation of developmental stages 1, 2,

and 3 were specifically induced in these cell populations (Fig. 2b,d; groups I, III, V), whereas the ESTs plotted in the opposite direction were down-regulated (Fig. 2b,d; groups II, IV, VI). The relative correlation of each EST to a given group was quantified with the factor spectra of the derivative of the loading of PC1 oriented in the optimal directions of stages 1, 2 and 3 (data not shown). These factor spectra were used to list the ESTs in descending order according to their degree of relevance to each group as shown in Table 1, along with their putative functions based on BlastX hits in the SwissProt database and their expression dynamics between the three developmental stages.

Gene expression profiles associated with ML-L microspores

Gene expression during pollen development has been divided into an early and a late phase, to describe the gene expression programs that are associated with microsporogenesis and microgametogenesis, respectively (Mascarenhas, 1990). In total, 12 ESTs were higher expressed at stage 1 as compared to stages 2 and 3 (Fig. 2d, group I; Table 1, group I). This EST group corresponds to the class of early genes, which are preferentially expressed in ML-L uninucleate microspores prior to the first pollen mitosis. Based on their putative functions, the ESTs in group I were involved with two main processes: preparation for the first pollen mitosis and lipid biosynthesis.

The period that precedes the first pollen mitosis is characterized by an intense activity of synthesis (McCormick, 1991; Mascarenhas, 1990). Interestingly, two ESTs representing nucleoside diphosphate kinase I (NDK I) were highly expressed in stage 1 as compared to stages 2 and 3 (16-fold; Table 1, group I). NDK I is involved in the biosynthetic pathway of nucleotides. This kinase is responsible for the phosphorylation of nucleosides into nucleotides, which are building blocks for several primary and secondary products, nucleic acids and serve as an energy source. In cell culture systems, an increase in nucleotide biosynthesis has been reported as a prerequisite for the initiation of cell division, where intense DNA and RNA synthesis takes place (Stasolla et al., 2003). Synthetic activity in stage 1 is further evidenced by the expression of an EST that shows homology to fibrillarlin (Table 1, group I). Fibrillarlin is a component of a small nuclear ribonucleoprotein particle (snRNP) localized in coiled bodies, which are nuclear subdomains thought to participate in pre-rRNA processing machineries. rRNA genes are known to be actively transcribed in microspores prior to pollen mitosis (Mascarenhas, 1990), and meristematic plant cells entering proliferation activity have increased number of nucleoplasmic coiled bodies (Acevedo et al., 2002). This indicates that the expression of fibrillarlin may be related to pre-rRNA processing that probably takes place in stage 1. Concomitantly to genes involved in the activity of synthesis that precedes mitosis, stage 1 was characterized by the expression of an EST

homologous to a centromere/ microtubule binding protein (CBF 5; Table 1, group I), a gene that is involved in mitotic chromosome segregation (Winkler et al., 1998).

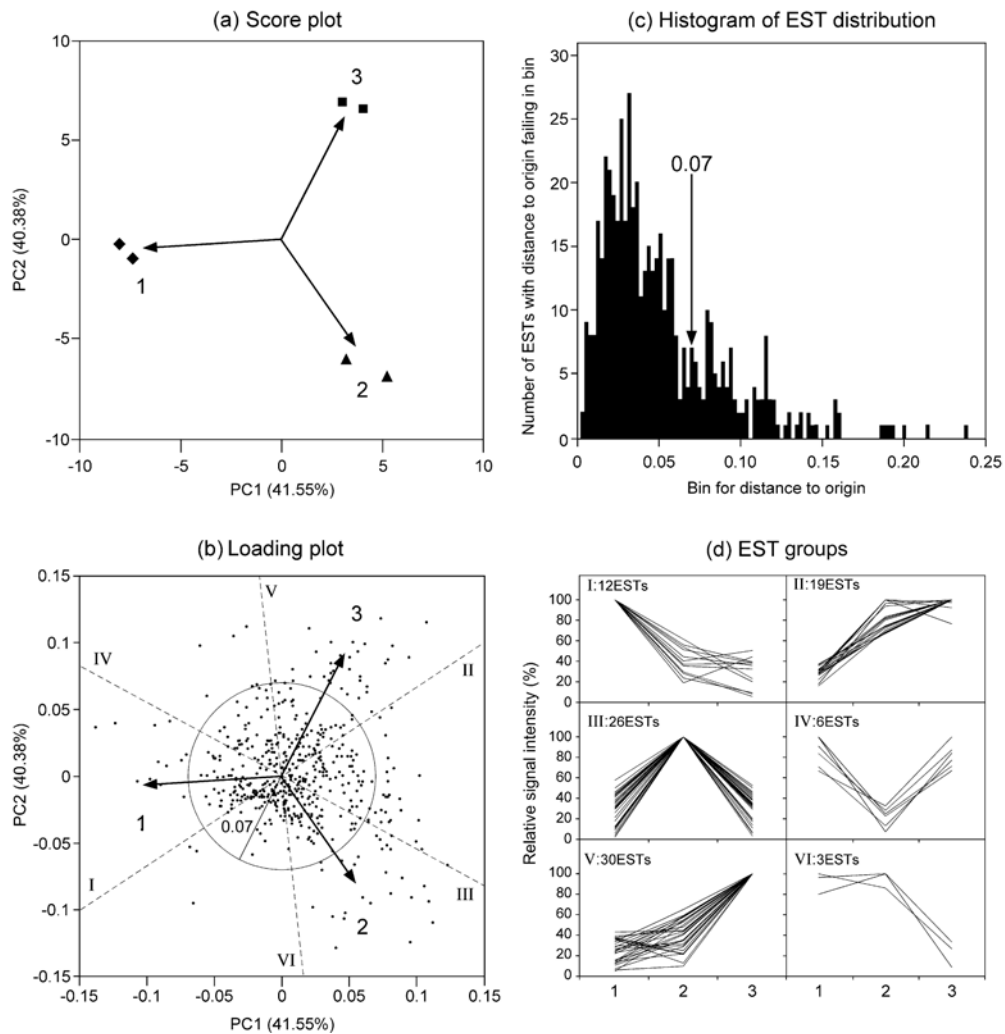


Figure 2. PCA analysis of gene expression in microspores at different developmental stages. (a) Score plot based on gene expression data sets of three developmental stages: (1) ML-L uninucleate microspores, (2) early-mid binucleate pollen and (3) enlarged microspores after mannitol treatment. Biological duplos are represented for each developmental stage. Arrows pointing to 1, 2 and 3 indicate the optimal vector orientation of the three developmental stages based on the average PC1 and PC2 scores between duplo hybridizations. (b) Loading plot displaying the 418 individual ESTs that contributed to the variances between different developmental stages. The ESTs displaying distance to origin greater or equal to 0.07 were considered to be differentially expressed (96 ESTs, out of the circle). Dashed lines indicate the average distance between the optimal orientation of the different cell populations (indicated by arrows), and were used to divide the loading plot into six areas. (c) Histogram of the ESTs distribution according to their distance to origin in the loading plot. (d) Clustering of the 96 differentially expressed ESTs into six different groups representing different expression profiles.

Peroxisomal multifunctional enzyme type II enzyme (Table 1, group I) acts on the peroxisomal beta-oxidation pathway for fatty acids, while cytochrome b5 (Table 1, group I) functions in lipid biosynthesis in plants by its association with fatty acid desaturation and the formation of polyunsaturated lipids (Smith et al., 1992). An isoform of cytochrome b5 has been reported to be induced in anther tapetum and in microspores at the verge of mitosis (Martsinkovskaya et al., 1999). After the first pollen mitosis, pollen cells start to accumulate significant amounts of storage products (Bedinger, 1992), and the cytoplasm of barley binucleate pollen is characterized by the presence of several lipid bodies (Huang, 1986). Our results point out that genes involved with lipid biosynthesis are highly expressed prior to the first pollen mitosis in barley, thus preceding the stage of intensive lipid biosynthesis.

Dynamic of gene expression profiles associated with pollen development

Based on PCA analysis, ESTs associated with pollen development (transition 1 to 2) are represented by the ESTs that were induced specifically in stage 2 (Fig. 2d, group III), as well as by those ESTs that were specifically down-regulated in 3, indicating that the latter were probably important for the transition 1 to 2, but not for stage 3 (Fig. 2d, group VI).

Group VI was composed of three ESTs that encoded cobalamin-independent methionine synthase, rubisco subunit binding protein and a protein with no significant homology (Table 1, group VI). On the other hand, group III was composed of 26 ESTs (Table 1, group III). Based on the putative functions and on the factor spectra of the ESTs grouped in group III, the induction of an EST coding for inositol-3 phosphate synthase (IPS; 16-fold), and of ESTs involved with carbohydrate and energy metabolism were highly correlated with the stage 2.

Most of the ESTs associated with carbohydrate metabolism represented enzymes involved with sucrose metabolism and starch biosynthesis: sucrose synthase 1 (SS1), phosphoglucomutase (PGM), UDP-glucose 4-epimerase, glucose-1-phosphate adenylyltransferase (AGPase B), UTP-glucose-1-phosphate uridylyltransferase (UGPase) and granule-bound starch synthase 1 (GBSS1). Our results are in agreement with Datta et al. (2001; 2002), whose findings indicate that the major transcriptional changes after the first pollen mitosis are the up-regulation of genes involved in the biosynthesis of starch. ESTs involved in energy production were represented by phosphoglycerate kinase, ubiquinol-cytochrome c reductase, cytochrome c oxidase, and ATP synthase (Table 1, group III). While the first is involved in glycolysis, the others are part of the five protein complexes that are involved with electron transport and oxidative phosphorylation. These results indicate that the induction of transcripts involved in electron transport and oxidative phosphorylation might be needed to match the demand of ATP for starch biosynthesis and to fulfill the role of the

vegetative cell as a “powerhouse” to drive further pollen maturation and pollen tube germination (McCormick, 1993). This is further evidenced by the induction of two ESTs coding for an ADP/ATP carrier protein in stage 2 (Table 1, group III).

In addition, stage 2 was characterized by the up-regulation of ESTs homologous to actin 1, Rac-like GTPase and guanine nucleotide binding protein (Table 1, group III). At stage 2, the starch-filling cytoplasm occupies the space of the large central vacuole, and the vegetative nucleus migrates towards the center of the pollen grain (Bedinger, 1992). Actin networks function during the migration of the vegetative nucleus during this process (Zonia et al., 1999). Rac GTPases and guanine nucleotide binding protein are mediators of various signal transduction processes and are particularly involved in the organization of the actin cytoskeleton (Bischoff et al., 1999). During pollen development, GTPases have been proposed to control the asymmetry of the first pollen mitosis and actin-dependent movement of the generative cell (Lin et al., 1996). This indicates that the induction of actin 1, Rac-like GTPase and guanine nucleotide binding protein in stage 2 is probably related to the events that are associated with the first pollen mitosis and vegetative and generative cell functions.

Dynamic of gene expression profiles associated with androgenesis induction

Based on PCA analysis, ESTs associated with androgenesis induction (transition 1 to 3) were represented by the ESTs that were induced in stage 3 (Fig. 2d, group II, V), as well as by those ESTs that were specifically down-regulated in stage 2 (Fig. 2d, group IV).

Group II is represented by 19 ESTs that were induced both in the transition from stage 1 to 3, as well as in the transition 1 to 2 (Fig. 2d, group II). These ESTs represent, therefore, the gene expression profiles that are common to both pollen development and androgenesis induction. ESTs within this group were mainly involved in oxidative phosphorylation and energy production, amino acid metabolism, carbohydrate metabolism, metabolism of complex lipids and protein biosynthesis (Table 1, group II). Since a considerable amount of stage 3 microspores still display characteristics of stage 2 during the initial stages of microspore culture (Maraschin et al., 2004; Fig. 1), it is likely to assume that these ESTs were induced in those microspores that were still committed to the pollen developmental pathway. Therefore, they may represent ESTs that are associated with pollen development rather than with the acquisition of androgenic potential. However, one cannot exclude the possibility that induction of these ESTs is needed for both pollen development and induction of androgenesis.

The 6 ESTs included in group IV are of particular interest because their induction was not important for further pollen development. Therefore, they represent putative candidates for playing a role in androgenesis induction.

Table 1. List of the 96 ESTs differentially expressed between the three microspore developmental stages. ESTs are listed in descending order according to their relative contribution to the EST groups as determined by the factor spectra of the derived vector component of PC1 loading oriented in the optimal direction of stages 1, 2 and 3. ^aEST from the 5' or 3' of the clone. ^bInformation about EST-ID can be found at the IPK Website (<http://www.pgrc.ipk-gatersleben.de>). ^cSimilarity between ESTs and hit proteins was considered significant when the BlastX e-value was equal or greater than E-15. ^dLM, Lipid Metabolism; MCL, Metabolism of Complex Lipids, AAM, Amino Acid Metabolism; CM, Carbohydrate Metabolism; MCC, Metabolism of Complex Carbohydrates; NM, Nucleotide Metabolism; EM, Energy Metabolism; BSM, Biosynthesis of secondary metabolites. ^eDy, dynamics of EST expression between developmental stages 1, 2 and 3. *Number of ESTs showing homology to the same hit proteins

^a GenBank accession number	^b IPK EST ID	^c e-value and BLASTX homology	^d Putative Functions	^e Dy
Group I				
AL510785	HY05P23	9e-15 Peroxisomal multifunctional enzyme type II	LM	11
AL511296	HY07J18	5e-69 Nucleoside diphosphate kinase I, NDK I**	NM	16
AL503494	HW02F11	2e-55 Vacuolar invertase, VI	CM, MCC	3.3
AL510698	HY05L18	4e-65 Cytochrome b5	LM	5.2
AL512102	HY10G13	3e-51 20 kDa chaperonin	Cochaperone	4.8
AL506360	HY02N20	2e-58 Centromere/ microtubule binding protein, CBF5	Cell division	3.1
AL512252	HY10O19	5e-27 Fibrillarin	rRNA processing	2.7
AL511960	HY09O09	6e-16 PPLZ12 protein	Unknown	2.7
AL511726	HY09A06	No significant homology	Unknown	2.5
AL507915	HY07D14	5e-53 Glutamate dehydrogenase	EM, AAM	2.6
AL510697	HY05L17	No significant homology	Unknown	2.5
Group II				
AL510870	HY06E02	No significant homology	Unknown	6
AL507111	HY05I10	e-44 Probable ATP synthase 24 kDa subunit	EM	6.6
AL511334	HY07L16	No significant homology	Unknown	4.6
AL506101	HY02A11	e-22 ATP synthase delta chain	EM	4.8
AL510976	HY06J15	e-109 Glutamate decarboxylase	AAM, CM	3.6
AL511258	HY07H20	No significant homology	Unknown	3.6
AL511115	HY07A18	2e-22 C-4 methyl sterol oxidase	Unclassified	3.6
AL506696	HY03P14	5e-47 Dehydrogenase/ reductase SDR family member 4	MCL	3.4
AL506640	HY03M17	6e-57 S-adenosylmethionine decarboxylase proenzyme	AAM	3.6
AL510968	HY06J04	No significant homology	Unknown	3.7
AL509234	HY01C04	No significant homology	Unknown	3.7
AL499671	HK01I16	No significant homology	Unknown	3.3
AL506048	HY01L10	3e-40 Elongation factor-1 alpha	Protein synthesis	3.7
AL511059	HY06N18	e-101 14-3-3-like protein A (14-3-3A)	Protein interaction	3.2
AL506065	HY01M23	8e-96 L-ascorbate peroxidase	CM	3.5
AL506970	HY04M13	e-20 Transmembrane protein PFT27	Unclassified	3.4
AL507833	HY06P18	3e-45 DnaJ-like protein	Unclassified	2.7
AL506613	HY03L07	No significant homology	Unknown	2.7
Group III				
AL511500	HY08E09	2e-89 Inositol-3-phosphate synthase IPS	MCL, BSM	16

Table 1. Continued

^a GenBank accession number	^b IPK EST ID	^c e-value and BLASTX homology	^d Putative Functions	^e Dy
AL503638	HW02O11	3e-17 UDP-glucose 4-epimerase	NM, MCC	6.7
AL511879	HY09J04	e-68 ATP synthase beta chain	EM	13
AL508462	HY08N11	2e-74 Gluc 1-phosphate adenylyltransferase, AGPaseB***	MCC	9.4
AL506807	HY04E21	e-75 Actin 1	Cytoskeleton	8
AL511872	HY09I18	No significant homology	Unknown	3.7
AL511706	HY08P05	9e-97 ADP/ ATP carrier protein**	EM	4.5
AL506567	HY03I21	e-100 Granule-bound starch synthase I, GBSS1	MCC	3.4
AL511708	HY08P09	e-110 Sucrose synthase 1, SS1	MCC	7.7
AL507123	HY05I22	6e-64 Ferritin 1	Iron storage	4.3
AL511309	HY07K08	7e-16 Tyramine N-feruloyltransferase	Unclassified	4.4
AL511268	HY07I08	e-23 Cytochrome c oxidase	EM	4
AL502305	HW07C09	6e-15 UTP-gluc-1-phosphate uridylyltransferase, UGPase	CM, MCC, NM	2.6
AL511218	HY07F23	e-102 Phosphoglycerate kinase	EM, CM	4
AL506698	HY03P16	4e-97 Phosphoglucomutase, PGM	MCC, CM, BSM	2.7
AL511357	HY07M21	no significant homology	Unknown	3.5
AL508466	HY08N15	6e-34 RAC-like GTP binding protein RHO1	Signaling	3.1
AL507096	HY05G15	e-113 Phospho-2-dehydro-3-deoxyheptonate aldolase 1	AAM	2.6
AL512172	HY10K07	7e-57 Guanine nucleotide-binding protein alpha-1 subunit	Signaling	2.9
AL510976	HY05M10	9e-55 Glutamate decarboxylase 1	AAM, CM	2.8
AL508740	HY09K13	e-81 Cytosolic monodehydroascorbate reductase	CM	2.8
AL506589	HY03J22	2e-81 Ubiquinol cytochrome c reductase***	EM	2.6
Group IV				
AL507141	HY05K18	e-40 Glutathione S-transferase, GST	stress response	3.7
AL507411	HY05H18	2e-82 Alpha glucosidase precursor, maltase	CM, MCC	2.9
AL507431	HY05J18	2e-83 Ubiquitin-specific protease, UBF	Proteolysis	2.7
AL506437	HY03C01	7e-88 Catalase 1	stress response	2.7
AL511519	HY08F08	8e-38 Hypothetical protein At1g60740	Unknown	2.7
AL508576	HY09C18	6e-82 Ubiquitin-conjugating enzyme, UBE2	Proteolysis	2.6
Group V				
AL507319	HY01O02	e-102 Alcohol dehydrogenase 3, ADH3	LM, MCL, AAM	52
AL503324	HW01K08	e-40 Glutathione S-transferase, GST	stress response	18
AL505972	HY01C15	4e-75 Glutathione S-transferase 1, GST class-phi	stress response	19
AL510913	HY06G09	No significant homology	Unknown	5.3
AL499908	HK04B02	No significant homology	Unknown	5.7
AL511473	HY08C24	3e-53 Bax inhibitor-1 (BI-1)**	PCD inhibitor	3.9
AL507702	HY06J20	e-112 Glyceraldehyde-3-phosphate dehydrogenase, GAPD	EM, CM	3.3
AL510971	HY06J08	e-104 20S proteasome subunit alpha-5	Proteolysis	3.5
AL512108	HY10G20	e-105 Ras-related protein RIC2	Signaling	4.9
AL509162	HY10O06	e-66 Phytapsin precursor (aspartic protease)	Proteolysis	3.3
AL511054	HY06N11	8e-53 Fructose-bisphosphate aldolase	EM, CM	2.9

Table 1. Continued

^a GenBank accession number	^b IPK EST ID	^c e-value and BLASTX homology	^d Putative Functions	^e Dy
AL505964	HY01B24	2e-18 26S protease regulatory subunit 8	Proteolysis	3.2
AL499780	HK03G06	2e-30 Cysteine protease 1 precursor**	Proteolysis	3.4
AL511847	HY09H06	e-31 20S proteasome subunit alpha-2	Proteolysis	2.6
AL509296	HY01F11	No significant homology	Unknown	2.6
AL503287	HW01H17	2e-56 Cell wall invertase, CWI	CM, MCC	3.5
AL510859	HY06D13	3e-24 Tryptophanyl-tRNA synthetase	AAM	2.5
AL507218	HY01D11	6e-46 60S ribosomal protein L26A	Protein synthesis	2.4
AL510656	HY05J22	No significant homology	Unknown	2.3
AL511801	HY09E20	No significant homology	Unknown	2.6
AL510614	HY05H16	No significant homology	Unknown	2.5
AL512228	HY10N13	e-90 Filamentous temperature-sensitive protein, FtSH	Proteolysis	3.1
AL506676	HY03O15	4e-86 Dihydrodipicolinate synthase 2	AAM	3.3
AL506034	HY01J20	e-116 Hypothetical protein yiiG	Unknown	2.6
AL508862	HY10A14	e-76 Phospholipid hydroperoxide glutathione peroxidase	stress response	2
AL511543	HY08G13	8e-42 TGF beta-inducible nuclear protein 1	Unclassified	2.7
AL509039	HY10I17	e-54 Hypothetical UPF0204 protein At2g03800	Unknown	2.6
AL508611	HY09E11	No significant homology	Unknown	2.3
Group VI				
AL506629	HY03M03	No significant homology	Unknown	13
AL507142	HY05K19	2E-97 Cobalamin-independent methionine synthase	AAM	3.9
AL511072	HY06O11	3e-78 RuBisCO subunit binding-protein	Unclassified	3

They encode glutathione S-transferase (GST), alpha glucosidase precursor (maltase), ubiquitin-specific protease (UBP), catalase 1, ubiquitin-conjugating enzyme (Ub-E2) and a hypothetical protein (Table 1, group IV). Maltase is the enzyme responsible for the breakdown of maltose in starch granules (Tibbot et al., 1998). This suggests that breakdown of storage products, such as starch, might be an important feature of androgenesis induction. GST and catalase 1 are involved in protecting the cell against the harmful effect of reactive oxygen species (ROS). While GSTs take part in the detoxification of both endogenous and xenobiotic compounds by the formation of glutathione conjugates (Marrs, 1996), catalase 1 is responsible for degrading hydroperoxides into water and oxygen, and is one of the major antioxidant enzymes in plants. Since many types of biotic and abiotic stresses are known to cause oxidative stress, it has been proposed that ROS might be the common secondary stress factor responsible for the induction of antioxidant enzymes (Scandalios et al., 1997). The promoter region of many plant GST genes contains elements responsive to ROS (Chen and Singh, 1999; Garretón et al., 2002). However, in our system, GST and CATALASE 1

were expressed both in stage 1 during microspore development, and in stage 3 during initiation of androgenesis by stress. Therefore, it is likely that these genes are developmentally regulated in microspores. In agreement with this hypothesis, *CATALASE* and *GST* genes have been reported to be spatially and temporally regulated during plant development (Bailly et al., 2004; Marrs, 1996).

The ESTs coding for Ub-E2 and UBP (Table 1, group IV) are components of the ubiquitin/26S proteasome proteolytic pathway. Proteins subjected to degradation are marked with ubiquitin tags and are subsequently targeted to the degradative action of the 26S proteasome (Hellmann and Estelle, 2004). Ub-E2 functions in the enzymatic cascade involved in the conjugation of ubiquitin to target proteins. On the other hand, UBPs belong to a family of proteins involved in deubiquitination of proteins, and therefore have a role in regulating a protein's half-life by reversing the ubiquitin reaction (Smalle and Vierstra, 2004). Regulation of the cell cycle is mediated by the ubiquitin-mediated degradation of mitotic cyclins and the control of the half-life of regulatory factors, which are important for mitotic progression (Harper et al., 2002). In plants, Ub-E2 proteins participate in the formation of the anaphase-promoting complex (APC). Mutations affecting *APC* genes in *Arabidopsis* have demonstrated that the APC is essential for cell cycle progression in plants (Blilou et al., 2002; Capron et al., 2003). Higher mRNA levels of Ub-E2 and UBP in stages 1 and 3 as compared to stage 2 indicate that these ESTs might play a role in stress-induced microspore division by controlling the re-entry into mitosis.

The 30 ESTs comprised in group V represented the most interesting ESTs, since they were up-regulated exclusively during androgenesis induction (Table 1, group V). Therefore, their expression profiles can be regarded as molecular markers for the induction of androgenesis in barley. Based on their factor spectra, the sharp induction of *ALCOHOL DEHYDROGENASE 3 (ADH 3; 52-fold)*, and two *GST* genes (18/19-fold) showed the highest correlation with the stage 3. Other gene expression profiles correlated with this stage were associated with inhibition of programmed cell death (PCD; bax inhibitor, BI-1), ubiquitin-mediated proteolysis and protein degradation (filamentous temperature-sensitive protein, FtsH; 20S proteasome subunit alpha-5 and alpha-2; 26S protease regulatory subunit 8; phytepsin precursor, aspartic protease; cysteine protease 1 precursor) and carbohydrate metabolism (glyceraldehydes-3-phosphate dehydrogenase, GAPD; cell wall invertase, CWI; fructose-biphosphate aldolase). In addition, stage 3 was characterized by the induction of 7 ESTs, which encoded proteins with no known homologies, along with ESTs involved in various functions, such as Ras-related protein RIC2, TGF beta-inducible nuclear protein 1, tryptophanyl-tRNA synthetase, 60S ribosomal protein L26A and dihydropicolinate synthase 2.

Validation of array data

Since the ESTs grouped in group V showed the most interesting expression profiles with regard to androgenesis induction, we wanted to validate their expression profiles obtained by macroarrays using Northern blot analysis. To do so, the expression of the 15 ESTs that were induced in stage 3 by a minimum of 3-fold (Table 1, group V) was further analyzed. Expression is shown for 10 out of the 15 most dynamic ESTs (Fig. 3), since no signal was obtained on Northern blots probed with HW01K08, HK04B02, HY06J22, HW01F04 and HY03O15 cDNAs (data not shown). The blots on figure 3 show that all 10 ESTs representing BI-1, RIC2, ADH3, FtsH, phi-GST, cysteine protease 1 precursor, phytepsin precursor, 20S proteasome subunit alpha-5, 26S proteasome regulatory subunit 8 and EST HY06G09 were induced in stage 3 as compared to 1 and 2, indicating that there was a high consistency between the expression profiles obtained by macroarray and Northern blot analysis.

Gene expression associated with microspore androgenic potential

To explore the possibility that these 10 ESTs were associated with the high embryogenic potential of enlarged microspores treated by a mannitol stress, we further investigated their expression in enlarged microspore populations that had been treated under optimal and sub-optimal conditions for androgenesis induction. Optimal regeneration efficiency in barley (which was set to 100 %) is obtained by a combination of starvation and osmotic shock, achieved by an anther treatment in 0.37 M mannitol in CPW basal salt buffer (Hoekstra et al., 1992). However, starvation alone is sufficient to trigger androgenesis at lower frequencies. The regeneration efficiency drops to 57 % of the optimal when mannitol is omitted in the CPW basal salt buffer during stress treatment. The reduction is even more drastic when the CPW salts are not present, and microspores are treated in deionized water alone, resulting in a drop to 37 % of the optimal (van Bergen et al., 1999).

Figure 4 shows that there were mainly 2 groups of genes based on their expression in enlarged microspores subjected to mannitol, CPW or water treatment. In the first group, up-regulation was independent of the regeneration efficiency, while in the second group induction of gene expression was positively correlated with the regeneration efficiency.

The EST HY06G09 and the ESTs representing BI-1, RIC2, 20S proteasome subunit alpha-5 and a class phi-GST belonged to the first group (Fig. 4, group I). This indicates that induction of these genes is probably not related to the acquisition of androgenic potential, but rather might play a role in stress responses. This is in agreement with the role of GST proteins in protecting the cell against the harmful effects of ROS (Kampranis et al., 2000). Though the cytoprotective roles of *BI-1* are not yet understood at the molecular level, *BI-1*

overexpression has been reported to confer protection against PCD induced by abiotic stresses (Chae et al., 2003). Conversely, antisense-mediated down-regulation of *BI-1* results in accelerated PCD upon carbon starvation (Bolduc and Brisson, 2002). Taken together, these results suggest that induction of *BI-1* and *GST* may contribute for microspore survival upon stress conditions, such as nutrient deprivation and ROS. *RIC2* is a member of the Rab family of small plant GTPases thought to play a role in vesicle trafficking and signal transduction (Bischoff et al., 1999). Since different levels of stress led to similar levels of *RIC2* expression (Fig. 4, group I), it is likely that *RIC2* is involved in stress signaling. The 20S proteasome subunit alpha-5 is a component of the 20S proteasome multicatalytic complex, which, together with the 26S regulatory subunits, forms the 26S proteasome (Shibahara et al., 2002). The induction of 20S proteasome subunit alpha-5 upon mannitol, CPW or water stress (Fig. 4, group I) indicates that ubiquitin-mediated proteolysis is probably a cellular response of microspores to starvation.

The 26S proteasome is involved in many different aspects of cellular regulation, including stress and hormonal responses, cell cycle control, nutrient remobilization and organ differentiation. The ubiquitin/26S proteasome proteolytic pathway is regulated both at the transcriptional and post-translational levels, and one important mechanism of regulation is known to involve the 26S regulatory subunits (Hellmann and Estelle, 2004). Interestingly, in the second group of genes, up-regulation of the 26S proteasome regulatory subunit 8 was positively correlated with the regeneration efficiencies induced by mannitol, CPW and water treatment (Fig. 4, group II). This regulatory subunit showed homology to the regulatory particle ATPase subunit 2 from rice (*RPT2*). *RPT* genes are known to confer ATP dependence and specificity for ubiquitinated substrates to the 26S proteasome (Fu et al., 1999), and the *RPT2a* gene from *Arabidopsis* is known to be essential for proteasome activity and for meristem maintenance (Ueda et al., 2004).

Further evidence to support a role for proteolysis during androgenesis induction is demonstrated by the higher expression of cysteine protease 1 precursor, phytepsin precursor (aspartic protease) and *FtsH* upon mannitol and CPW treatment as compared to water (Fig. 4, group II). The *FtsH* gene encodes a protein that displays both metalloprotease and chaperone activities. In prokaryotes, *FtsH* expression is induced by stress and functional analysis revealed that this protease is involved in several aspects of bacterial growth, like stress responses, cell division and differentiation (Fischer et al., 2002). In plants, *FtsH* has been demonstrated to be the protease involved in degrading photosystem II reaction center D1 protein upon its irreversible photooxidative damage (Lindahl et al., 2000). The *FtsH* EST induced in barley microspores showed homology to the *Arabidopsis FtsH2* isoform. The *Arabidopsis* genome contains 12 members of the *FtsH* family, and a mutational approach

indicated that *FtsH2* is needed for the formation of normal, green chloroplasts (Yu et al., 2004). Chloroplast biogenesis is an important factor for the production of green plants derived from microspores. Treatment of barley anthers in mannitol has been reported to induce not only higher regeneration efficiencies, but also higher green/albino ratios among microspore-derived plants (Caredda et al., 1999). The association between higher levels of *FtsH* expression with mannitol-treated microspores indicates that this protein might play a role in chloroplast biogenesis during the induction of barley androgenesis.

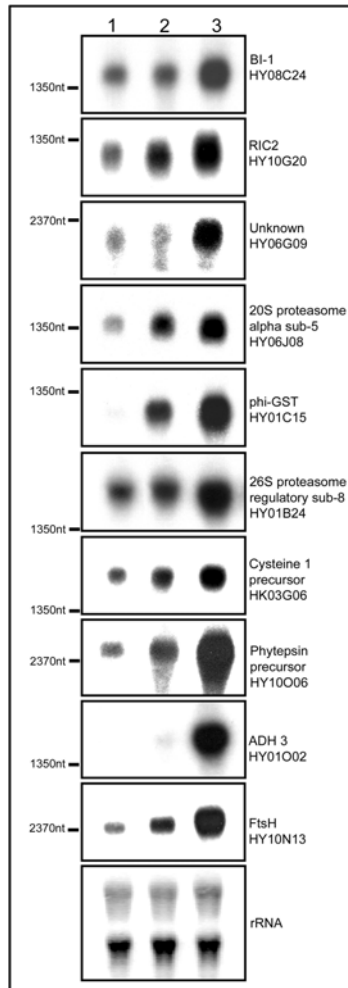


Figure 3. Validation of expression profiles obtained by macroarray using Northern blot analysis. Expression is shown for 10 ESTs whose expression was induced in stage 3 as compared to stages 1 and 2 by a minimum of 3-fold. Ethidium bromide staining of rRNA shows equal RNA loading. *Lane 1* ML-L uninucleate microspores, *lane 2* early-mid binucleate pollen, *lane 3* enlarged microspores after mannitol treatment.

Cysteine and aspartic proteases have been implicated in protein maturation, execution of PCD, germination and tissue remodeling (Beers et al., 2004). Induction of cysteine protease gene expression correlates with somatic embryogenesis induction in carrot and soybean (Mitsuhashi et al., 2004; Thibaud-Nissen et al., 2003) and several proteases are induced during barley and rapeseed zygotic embryogenesis (Dong et al., 2004; Sreenivasulu et al., 2004). During somatic embryogenesis, the expression of cell division-related genes follows the expression of proteolytic genes, the latter being a characteristic of the differentiation phase of somatic cells (Thibaud-Nissen et al., 2003). Recently, a cysteine protease has been demonstrated to be involved in the control of cell differentiation in plants (Ahn et al., 2004). In our system, a drop to 57% of the regeneration efficiency did not result in lower expression levels of both cysteine protease 1 and phytepsin precursor; however, a decrease in their expression levels was clearly visible when the regeneration efficiency dropped to 37 % of the optimal (Fig. 4, group II). During androgenesis induction, several studies have reported that one of the main changes brought by stress is represented by an overall decrease in total protein in the microspores (Říhová et al., 1996; Garrido et al., 1993; Kyo and Harada, 1990). Morphologically, stress leads to the marked repression of gametophytic differentiation, characterized by the degradation of the pollen cytoplasm (Dunwell and Sunderland, 1975; Rashid et al., 1982). Based on these evidences, it has been postulated that androgenesis induction may involve proteolytic degradation of pollen-specific proteins. Our gene expression data represents the first molecular evidence to show that proteolysis may take part of the stress responses leading to the acquisition of microspore embryogenic potential.

In addition, induction of an EST coding for *ADH3* was correlated to the higher regeneration efficiencies of mannitol and CPW as compared to water treatment (Fig. 4, group II). ADH catalyzes the reversible reaction of an aldehyde or ketone into alcohol in a NAD-dependent manner. *ADH* expression has been implicated in the shift from the oxidative pathway to a fermentative one, leading to the induction of glycolytic and fermentative genes (Dat et al., 2004). There are three ADH isoforms in barley, which are mainly regulated at the transcriptional level (Hanson et al., 1984). Gene expression of the barley *ADH1* gene has been demonstrated to be induced by ABA (Macnicol and Jacobsen, 2001). The promoter of the *ADH1* gene contains sequence motifs that closely resemble the ABA response elements found in the *Arabidopsis ADH* promoter (de Bruxelles et al., 1996). ABA is important for mediating plant tolerance to many environmental stresses, and ABA increases with the level of osmotic stress (Zeevaart et al., 1988), being correlated with mannitol-induced androgenesis induction in barley (Wang et al., 1999). However, exogenously applied ABA only led to increased regeneration efficiencies during androgenesis when applied to CPW or

water treatment, indicating that these suboptimal treatments result in lower endogenous ABA levels (van Bergen et al., 1999). Though it is not yet known whether the *ADH3* promoter contains ABA responsive elements, *ADH3* gene expression was correlated with increasing osmotic stress, indicating that this gene might be an indicative for osmotic stress responses associated with barley androgenesis induction.

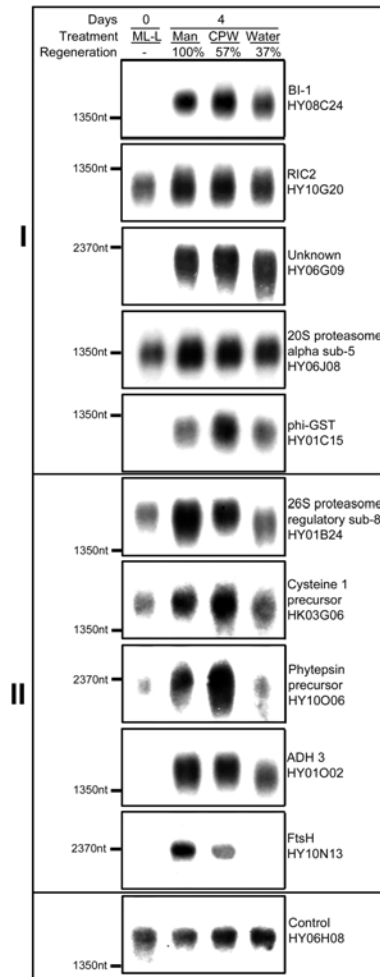


Figure 4. Northern blot analysis of ESTs up-regulated by mannitol stress under optimal and sub-optimal treatments for androgenesis induction. Group I, up-regulation upon stress is independent of regeneration efficiency; group II, up-regulation shows a positive correlation with regeneration efficiency. The EST HY06H08 was equally expressed between the three developmental stages based on array analysis, and was used as a control for RNA loading on Northern blots. *ML-L* ML-L uninucleate microspores; *Man* microspores treated in 0.37 M mannitol in CPW basal salt buffer; *CPW* microspores treated in CPW basal salt buffer alone; *water* microspores treated in deionized water. The regeneration efficiencies associated with each microspore treatment and the duration of treatment are indicated on each lane (van Bergen et al., 1999).

Concluding remarks

In this study, macroarrays were used to gain insight into the gene expression profiles active during the stress-induced reprogramming of microspores from pollen development towards the androgenic pathway. PCA analysis based on gene expression data has proved to be a useful tool to identify 'bio-markers' for androgenesis induction, which can be regarded as a 'fingerprint' associated with this developmental switch. The main transcriptional changes identified upon mannitol treatment to induce androgenesis were represented by the down-regulation of genes involved in starch biosynthesis and the induction of transcripts involved in sugar and starch hydrolysis, cytoprotection, signal transduction, stress responses, and proteolysis. Further expression analysis indicated that the induction of *ADH3* and genes involved with proteolysis were positively associated with the embryogenic potential of microspores. Further research should focus in the role of proteolysis in the regulation of stress-induced androgenesis. This issue is attracting increasing attention as an important regulatory mechanism in cell differentiation and cell cycle progression in plant cells (Geschink et al., 1998; Yanagawa et al., 2002; Hellmann and Estelle, 2004). In addition, the development of microspore stage-specific cDNA arrays will help extending our current knowledge of transcript profiles associated with androgenesis induction. Gene expression profiling by array technology represents only a starting point towards understanding stress-induced androgenesis, as regulation of protein levels, post-translational changes and metabolites are of importance as well. Integration of all these information into a system will represent the ultimate tool in understanding androgenesis induction.

Acknowledgements

The authors are grateful for Dr. Nils Stein for the support and help in facilitating the array hybridizations at the IPK, Germany, Ying Zhang for technical assistance, and Dr. Sylvia de Pater for critical reading of the manuscript.

References

- Acevedo R, Samaniego R, de la Spina SMD (2002) Coiled bodies in nuclei from plant cells evolving from dormancy to proliferation. *Chromosoma* 110: 559-569
- Ahn JW, Lim JH, Kim GT, Pai HS (2004) Phytocalpain controls the proliferation and differentiation fates of cells in plant organ development. *Plant J* 38: 969-981

- Altschul SF, Madden TL, Schäffer AA, Zhang Z, Miller W, Lipman DJ (1997) Gapped BLAST and PSI-BLAST: a new generation of protein database search programs. *Nucleic Acids Res* 25: 3389-3402
- Apweiler R, Bairoch A, Wu CH, Barker WC, Boeckmann B, Ferro S, Gasteiger E, Huang H, Lopez R, Magrane M, Martin MJ, Natale DA, O'Donovan C, Redaschi N, Yeh LS (2004) UniProt: the Universal Protein knowledgebase. *Nucleic Acids Res* 32: 115-119
- Bailly C, Leymarie J, Lehner A, Rousseau S, Côme D, Corbineau F (2004) Catalase activity and expression in developing sunflower seeds as related to drying. *J Exp Bot* 55: 475-483
- Baudino S, Hansen H, Brettschneider R, Hecht VFG, Dresselhaus T, Lörz H, Dumas C, Rogowsky PM (2001) Molecular characterisation of two novel maize LRR receptor-like kinases, which belong to the *SERK* gene family. *Planta* 213: 1-10
- Bedinger P (1992) The remarkable biology of pollen. *Plant Cell* 4: 879-887
- Beers EP, Jones AM, Dickerman AW (2004) The S8 serine, C1A cysteine and A1 aspartic protease families in Arabidopsis. *Phytochem* 65: 43-58
- Bischoff F, Molendijk A, Rajendrakumar CSV, Palme K (1999) GTP-binding proteins in plants. *Cell Mol Life Sci* 55: 233-256
- Bliou I, Frugier F, Folmer S, Serralbo O, Willemsen V, Wolkenfelt H, Eloy NB, Ferreira PCG, Weisbeek P, Scheres B (2002) The *Arabidopsis* *HOBBIT* gene encodes a CDC27 homologue that links the plant cell cycle to progression of cell differentiation. *Genes Dev* 16: 2566-2575
- Bolduc N, Brisson LF (2002) Antisense down regulation of NtBI-1 in tobacco BY-2 cells induces accelerated cell death upon carbon starvation. *FEBS Lett* 532: 111-114
- Boutillier K, Offringa R, Sharma VK, Kieft H, Ouellet T, Zhang L, Hattori J, Liu CM, van Lammeren AAM, Miki BLA, Custers JBM, van Lookeren Campagne MM (2002) Ectopic expression of BABY BOOM triggers a conversion from vegetative to embryogenic growth. *Plant Cell* 14: 1737-1749
- Boutillier KA, Ginés MJ, DeMoor JM, Huang B, Baszczynski CL, Iyer VN, Miki BL (1994) Expression of the BnmNAP subfamily of napin genes coincides with the induction of *Brassica* microspore embryogenesis. *Plant Mol Biol* 26: 1711-1723
- Capron A, Serralbo O, Fulop K, Frugier F, Parmentier Y, Dong A, Lecureuil A, Guerche P, Kondorosi E, Scheres B, Genschik P (2003) The *Arabidopsis* APC/C: molecular and genetic characterization of the APC2 subunit. *Plant Cell* 15: 2370-2382
- Caredda S, Devaux P, Sangwan RS, Clément C (1999) Differential development of plastids during microspore embryogenesis in barley. *Protoplasma* 208: 248-256
- Chae HJ, Ke N, Kim HR, Chen S, Gozik A, Dickman M, Reed JC (2003) Evolutionary conserved cytoprotection provided by Bax inhibitor-1 homologs from animals, plants, and yeast. *Gene* 323: 101-113
- Chen WQ, Singh KB (1999) The auxin, hydrogen peroxide and salicylic acid induced expression of the *Arabidopsis* *GST6* promoter is mediated in part by an ocs element. *Plant J* 19: 667-677
- Dat JF, Capelli N, Folzer H, Bourgeade P, Badot PM (2004) Sensing and signaling during plant flooding. *Plant Physiol Biochem* 42: 273-282
- Datta R, Chamusco KC, Chourey PS (2002) Starch biosynthesis during pollen maturation is associated with altered patterns of gene expression in maize. *Plant Physiol* 130: 1645-1656
- Datta R, Chourey PS, Pring DR, Tang HV (2001) Gene-expression analysis of sucrose-starch metabolism during pollen maturation in cytoplasmic male-sterile and fertile lines in sorghum. *Sex. Plant Reprod* 14: 127-134
- de Bruxelles GL, Peacock WJ, Dennis ES, Dolferus R (1996) Abscisic acid induces the alcohol dehydrogenase gene in Arabidopsis. *Plant Physiol* 111: 381-391
- Dong J, Keller WA, Yan W, Georges F (2004) Gene expression at early stages of *Brassica napus* seed development as revealed by transcript profiling of seed-abundant cDNAs. *Planta* 218: 483-491
- Dunwell JM, Sunderland N (1975) Pollen ultrastructure in anther cultures of *Nicotiana tabacum*. *J Exp Bot* 26: 240-252

- Fischer B, Rummel G, Aldridge P, Jenal U (2002) The FtsH protease is involved in development, stress response and heat shock control in *Caulobacter crescentus*. *Mol Microbiol* 44: 461-478
- Fu H, Doelling JD, Rubin DM, Vierstra RD (1999) Structural and functional analysis of the six regulatory particle triple-A ATPase subunits from the *Arabidopsis* 26S proteasome. *Plant J* 18: 529-539
- Garretón V, Carpinelli J, Jordana X, Holuigue L (2002) The *as-1* promoter element is an oxidative stress-responsive element and salicylic acid activates it via oxidative species. *Plant Physiol* 130: 1516-1526
- Garrido D, Eller N, Heberle-Bors E, Vicente O (1993) *De novo* transcription of specific mRNAs during the induction of tobacco pollen embryogenesis. *Sex Plant Reprod* 6: 40-45
- Geschink P, Criqui MC, Parmentier Y, Derevier A, Fleck J (1998) Cell cycle-dependent proteolysis in plants: identification of the destruction box pathway and metaphase arrest produced by the proteasome inhibitor MG132. *Plant Cell* 10: 2063-2075
- Hanson AD, Jacobsen JV, Zwar JA (1984) Regulated expression of three alcohol dehydrogenase genes in barley aleurone layers. *Plant Physiol* 75: 573-581
- Harper JW, Burton JL, Solomon MJ (2002) The anaphase-promoting complex: it's not just for mitosis anymore. *Genes Dev* 16: 2179-2206
- Hellmann H, Estelle M (2004) Plant development: regulation by protein degradation. *Science* 297: 793-797
- Hoekstra S, van Zijderveld MH, Louwerse JD, Heidekamp F, van der Mark F (1992) Anther and Microspore culture of *Hordeum vulgare* L. cv. Igri. *Plant Sci* 86: 89-96
- Huang B (1986) Ultrastructural aspects of pollen embryogenesis in *Hordeum*, *Triticum* and *Paeonia*. In: Hu H, Hongyuan Y (eds) *Haploids of higher plants in vitro*. Springer-Verlag, Berlin Heidelberg, pp 91-117
- Kampranis SC, Damianova R, Atallah M, Toby G, Kondi G, Tsihchlis PN, Makris AM (2000) A novel plant glutathione S-transferase/ peroxidase suppresses Bax-lethality in yeast. *J Biol Chem* 275: 29207-29216
- Kyo K, Harada H (1990) Specific phosphoproteins in the initial period of tobacco pollen embryogenesis. *Planta* 182: 58-63
- Lee JM, Williams ME, Scott VT, Rafalski JA (2002) DNA array profiling of gene expression changes during maize embryo development. *Funct Integr Genomics* 2: 13-27
- Lin Y, Wang Y, Zhu J, Yang Z (1996) Localization of Rho GTPases implies a role in tip growth and movement of the generative cell in pollen tubes. *Plant Cell* 8: 293-303
- Lindahl M, Spetea C, Hundal T, Oppenheim AB, Adam Z, Andersson B (2000) The thylakoid FtsH protease plays a role in the light-induced turnover of the photosystem II D1 protein. *Plant Cell* 12: 419-431
- Macnicol PK, Jacobsen JV (2001) Regulation of alcohol dehydrogenase gene expression in barley aleurone by gibberellin and abscisic acid. *Physiol Plant* 111: 533-539
- Maraschin SF, Lamers GEM, de Pater BS, Spaink HP, Wang M (2003) 14-3-3 isoforms and pattern formation during barley microspore embryogenesis. *J Exp Bot* 51: 1033-1043
- Maraschin SF, Vennik M, Lamers GEM, Spaink HP, Wang M (2004) Time-lapse tracking of barley androgenesis reveals position-determined cell death within pro-embryos. *Planta*, *in press*
- Marrs K (1996) The functions and regulation of glutathione S-transferases in plants. *Annu Rev Plant Physiol Plant Mol Biol* 47: 127-158
- Martsinkovskaya AI, Poghosyan ZP, Haralampidis K, Murphy DJ, Hatzopoulos P (1999) Temporal and spatial gene expression of cytochrome b5 during flower and fruit development in olives. *Plant Mol Biol* 40: 79-90
- Mascarenhas JP (1990) Gene activity during pollen development. *Annu Rev Plant Physiol Plant Mol Biol* 41: 317-338

- Matthys-Rochon E (2002) Fascinating questions raised by the embryonic development in plants. *Biologia* 57: 1-4
- McCormick S (1993) Male gametophyte development. *Plant Cell* 5: 1265-1275
- McCormick S (1991) Molecular analysis of male gametogenesis in plants. *Trends Genet* 7: 298-303
- Menke FLH, Parchmann S, Mueller MJ, Kijne JW, Memelink J (1999) Involvement of the octadecanoid pathway and protein phosphorylation in fungal elicitor-induced expression of terpenoid indole alkaloid biosynthetic genes in *Cataranthus roseus*. *Plant Physiol* 119: 1289-1296
- Michalek W, Weschke W, Pleissner KP, Graner A (2002) EST analysis in barley defines a unigene set comprising 4,000 genes. *Theor Appl Genet* 104: 97-103
- Mitsushashi W, Yamashita T, Toyomasu T, Kashiwagi Y, Konnai T (2004) Sequential development of cysteine proteinase activities and gene expression during somatic embryogenesis in carrot. *Biosci Biotechnol Biochem* 68: 705-713
- Pechan PM, Bartels D, Brown DCW, Schell J (1991) Messenger-RNA and protein changes associated with induction of *Brassica* microspore embryogenesis. *Planta* 184: 161-165
- Perry SE, Lehti MD, Fernandez DE (1999) The MADS-domain protein AGAMOUS-like 15 accumulates in embryonic tissues with diverse origins. *Plant Physiol* 120: 121-129
- Potokina E, Sreenivasulu N, Altschmied L, Michalek W, Graner A (2002) Differential gene expression during seed germination in barley (*Hordeum vulgare* L.). *Funct Integr Genom* 2: 28-39
- Rashid A, Siddiqui AW, Reinert J (1982) Subcellular aspects of origin and structure of pollen embryos of *Nicotiana*. *Protoplasma* 113: 202-208
- Reynolds TL, Crawford RL (1996) Changes in abundance of an abscisic acid-responsive, early cysteine-labeled metallothionein transcript during pollen embryogenesis in bread wheat (*Triticum aestivum*). *Plant Mol Biol* 32: 823-826
- Říhová L, Čapková V, Tupý J (1996) Changes in glycoprotein patterns associated with male gametophyte development and with induction of pollen embryogenesis in *Nicotiana tabacum* L. *J Plant Physiol* 147: 573-581
- Scandalios JG, Guan LM, Polidoros A (1997) In: J.G. Scandalios (Ed.), *Oxidative Stress and the Molecular Biology of Antioxidant Defenses*, Cold Spring Harbor Lab Press, New York, pp. 343-406.
- Shibahara T, Kawasaki H, Hirano H (2002) Identification of the 19S regulatory subunits from the rice 26S proteasome. *Eur J Biochem* 269: 1474-1483
- Smalle J, Vierstra RD (2004) The ubiquitin 26S proteasome proteolytic pathway. *Annu Rev Plant Biol* 55: 555-590
- Smith MA, Jonsson L, Stryme S, Stobart K (1992) Evidence for cytochrome b5 as an electron donor in ricinoleic acid biosynthesis in microsomal preparations from developing castor bean (*Ricinus communis* L.). *Biochem J* 287: 141-144
- Smykal P, Pechan PM (2000) Stress, as assessed by the appearance of sHsp transcripts, is required but no sufficient to initiate androgenesis. *Physiol Plant* 110: 135-143
- Sreenivasulu N, Altschmied L, Panits R, Hänel U, Michalek W, Weschke W, Wobus U (2002) Identification of genes specifically expressed in maternal and filial tissues of barley caryopses. A cDNA array analysis. *Mol Genet Genom* 266: 758-767
- Sreenivasulu N, Altschmied L, Radchuk V, Gubatz S, Wobus U, Weschke W (2004) Transcript profiles and deduced changes of metabolic pathways in maternal and filial tissues of developing barley grains. *Plant J* 37: 539-553
- Stasolla C, Katahira R, Thorpe T A, Ashihara H (2003) Purine and pyrimidine nucleotide metabolism in higher plants. *J Plant Physiol* 160: 1271-1295
- Telmer CA, Newcomb W, Simmonds DH (1995) Cellular changes during heat shock induction and embryo development of cultured microspores of *Brassica napus* cv. Topas. *Protoplasma* 185: 106-112

- Thibaud-Nissen F, Shealy RT, Khanna A, Vodkin LO (2003) Clustering of microarray data reveals transcript patterns associated with somatic embryogenesis in soybean. *Plant Physiol* 132: 118-136
- Tibbot BK, Henson CA, Skaden RW (1998) Expression of enzymatically active, recombinant barley α -glucosidase in yeast and immunological detection of α -glucosidase from seed tissue. *Plant Mol Biol* 38: 379-391
- Touraev A, Pfosser M, Vicente O, Heberle-Bors E (1996) Stress as the major signal controlling the developmental fate of tobacco microspores: towards a unified model of induction of microspore/pollen embryogenesis. *Planta* 200: 144-152
- Touraev A, Vicente O, Heberle-Bors E (1997) Initiation of microspore embryogenesis by stress. *Trends Plant Sci* 2: 297-302
- Ueda M, Matsui K, Ishiguro S, Sano R, Wada T, Paponov I, Palme K, Okada K (2004) The *HALTED ROOT* gene encoding the 26S proteasome subunit RPT2a is essential for the maintenance of Arabidopsis meristems. *Development* 131: 2101-2111
- van Bergen S, Kottenhagen MJ, van der Meulen RM, Wang M (1999) The role of abscisic acid in induction of androgenesis: a comparative study between *Hordeum vulgare* L. cvs Igri and Digger. *J Plant Growth Regul* 18: 135-143
- Vrienten PL, Nakamura T, Kasha KJ (1999) Characterization of cDNAs expressed in the early stages of microspore embryogenesis in barley (*Hordeum vulgare*) L. *Plant Mol Biol* 41: 455-463
- Wang M, Hoekstra S, van Bergen S, Lamers GEM, Oppedijk BJ, van der Heijden MW, de Priester W, Schilperoort RA (1999) Apoptosis in developing anthers and the role of ABA in this process during androgenesis in *Hordeum vulgare* L. *Plant Mol Biol* 39: 489-501
- Wang M, van Bergen S, van Duijn B (2000) Insights into a key developmental switch and its importance for efficient plant breeding. *Plant Physiol* 124: 523-530
- Winkler AA, Bobok A, Zonneveld BJM, Steensma HY, Hooykaas PJJ (1998) The lysine rich c-terminal repeats of the centromere-binding factor 5 (CBF5) of *Kluyveromyces lactis* are not essential for function. *Yeast* 14: 37-48
- Yanagawa Y, Hasezawa S, Kumagai F, Oka M, Fujimuro M, Naito T, Makino T, Yokosawa H, Tanaka K, Komamine A, Sato T, Nakagawa H (2002) Cell-cycle dependent dynamic change of 26S proteasome distribution in tobacco BY-2 cells. *Plant Cell Physiol* 43: 604-613
- Yu F, Park S, Rodermeil SR (2004) The *Arabidopsis* FtsH metalloprotease gene family: interchangeability of subunits in chloroplast oligomeric complexes. *Plant J* 37: 864-876
- Zarsky V, Garrido D, Eller N, Tupy J, Vicente O, Schöffl F, Heberle-Bors E (1995) The expression of a small heat shock gene is activated during induction of tobacco pollen embryogenesis by starvation. *Plant Cell Environ* 18: 139-147
- Zeevaert JAD, Creelman RA (1988) Metabolism and physiology of abscisic acid. *Annu Rev Plant Physiol Plant Mol Biol* 39: 439-473
- Zonia L, Tupy J, Staiger CJ (1999) Unique actin and microtubule arrays co-ordinate the differentiation of microspores to mature pollen in *Nicotiana tabacum*. *J Exp Bot* 50: 581-594

Summary

For breeding purposes, the evaluation of diversity in genetic pools and the establishment of homozygous lines are of critical importance. Homozygosity has been traditionally achieved by performing time-consuming and labor-intensive backcrosses. However, in the middle 1960's, a new technique came into view: the production of double haploid plants from immature pollen grains (microspores). Prompted by certain stress signals, microspores can be switched from their normal pollen developmental pathway towards an embryogenic route of development, a process that is referred to as androgenesis. Due to the colchicine-induced or spontaneous chromosome doubling during the early stages of microspore embryo development, single haploid microspores give rise to fertile double haploid plants within a short period of time. The production of double haploids via androgenesis represents, nowadays, a powerful technique both for the production of hybrid seeds and the evaluation of genetic diversity.

Stress has been considered the main trigger for the androgenic switch in microspores. Depending on the plant species, and even the plant variety, different stress treatments are required to efficiently induce androgenesis. However, many agronomically important crops are still recalcitrant to androgenesis. Improvement in protocol development has been so far based on trial and error experiences, limiting further use of this biotechnology for breeding purposes. For both applied and fundamental research, it is of uttermost importance to understand how a highly specialized cell such as an immature pollen grain can be reprogrammed to become embryogenic. Barley (*Hordeum vulgare* L.) cv. Igri is considered a model plant for androgenesis studies due to the high regeneration efficiencies that are obtained. Efficient androgenesis in this cultivar is obtained by starvation and osmotic stress at the mid-late to late (ML-L) uninucleate stage of microspore development, which is achieved via a mannitol treatment of anthers.

In this thesis, barley androgenesis was used as a model system to gain insight into the molecular and cellular events that control the developmental switch of microspores into embryos. As shown by several experiments, microspore embryogenic development is divided into three main characteristic, overlapping phases: acquisition of embryogenic potential by stress, initiation of cell divisions and pattern formation. The main molecular and cellular events that characterize the different commitment phases of microspores into embryos are reviewed in chapter 1. This chapter presents an overview of the progress that the research on androgenesis induction has made in the recent years, emphasizing the phase of microspore embryogenic potential acquirement and initiation of cell divisions. In addition, this chapter draws a parallel between the molecular and cellular biology of androgenic development with that of the two most extensively studied model systems, somatic and zygotic embryogenesis. In chapter 2, time-lapse tracking of mannitol-stressed microspores

was used with the objective to identify the morphology of embryogenic cells, and to investigate the stress-induced microspore developmental pathways. Three developmental pathways were identified: developmental type I, or embryogenic pathway, was represented by the microspores that followed embryogenic cell divisions, formed multicellular structures and released globular embryos out of the exine wall; developmental type II was characterized by those microspores that followed embryogenic cell divisions, formed multicellular structures, but died during the transition to globular embryos; developmental type III comprised the microspores that were not triggered and died in the first days of tracking. The first morphological change associated with the embryogenic potential of microspores was represented by the migration of the nucleus towards the center of the cell (star-like structure), which represented a transitory stage between vacuolated enlarged microspores after stress and the initiation of cell divisions. The difference between type I and type II pathways was observed in the time they displayed star-like morphology. By combining viability studies with cell tracking, we showed that the release of globular embryos out of the exine wall in developmental type I was always preceded by the death of the cells positioned at exine wall rupture, which was at the opposite side of the pollen germ pore. This position-determined cell death process was found to be a marker for the transition from multicellular structures into globular embryos during barley androgenesis, as cell death was delayed or absent in developmental type II.

Since the position-determined cell death process during the transition from multicellular structures into globular embryos appeared to be an important step in the commitment of microspores to the embryogenic route, this process was characterized in detail in chapter 3. Morphological analysis of type I multicellular structures showed that these pro-embryos were composed of two different cellular domains: a large vegetative domain, and a small generative domain positioned at the opposite side of the pollen germ pore. During the transition between multicellular structures into globular embryos, the generative cell domain died and this process showed typical features of plant programmed cell death, a genetically controlled mechanism of cell suicide. Hallmarks of programmed cell death such as chromatin condensation, DNA degradation and an increase in the activity of caspase-3-like proteases preceded massive cell death of the generative cell domain. The orchestration of such a death program culminated with the elimination of the small generative domain, and further embryogenesis was carried exclusively by the large vegetative domain. These results show that programmed cell death is an important feature of the embryogenic pathway of barley microspores.

In chapter 4, the expression and tissue-specificity of three members of the 14-3-3 family of regulatory proteins were studied by using isoform-specific antibodies against 14-3-

3A, 14-3-3B and 14-3-3C. This chapter is composed of three parts, each concerning different aspects of 14-3-3 proteins in barley androgenesis. In part I, we demonstrate that androgenic globular embryos show a polarized expression of 14-3-3C, and a higher 14-3-3A expression in epidermis primordia. During later stages of androgenic embryo development, 14-3-3C was found to be specifically expressed in the scutellum and in a group of cells underneath the L₁ layer of the shoot apical meristem, prior to L₂ layer specification. These results suggest that differential expression of 14-3-3A and 14-3-3C precede pattern formation in androgenic embryos. In part II, the specific expression of the 14-3-3C isoform was demonstrated to be restricted to the L₂ layer of the shoot apical meristem in both androgenic and zygotic embryos, as well as to L₂ layer-derived cells of *in vitro* shoot meristematic cultures. In part III, the proteolytic cleavage of the C-terminus of the 14-3-3A isoform was demonstrated to be specific to anther walls and non-embryogenic microspores undergoing programmed cell death during androgenesis induction. Taken together, the results described in chapter 4 indicate that cell fate and pattern formation during barley androgenesis are associated with 14-3-3A post-translational modification and the spatial and temporal regulation of 14-3-3A and 14-3-3C expression.

In chapter 5, we have employed microarray technology in combination with principle component analysis to identify gene expression profiles associated with the switch from pollen development towards the androgenic pathway. During the reprogramming of microspores, pollen-related genes were down-regulated, suggesting that stress acts in blocking pollen development. On the other hand, transcripts involved in sugar and starch hydrolysis, proteolysis, stress responses, inhibition of programmed cell death and signaling were induced. Further expression analysis of a subset of these genes revealed that the induction of genes encoding alcohol dehydrogenase 3 and proteolytic enzymes were associated with the androgenic potential of microspores, while the induction of genes involved in signaling and cytoprotection were probably part of stress responses.

The research described in this thesis has provided a substantial contribution towards understanding the mechanisms of androgenesis induction. The use of a cell tracking system in combination with biochemical markers has been crucial in pointing out the morphology of embryogenic microspores, and in identifying programmed cell death as an integral part of the developmental pathway of androgenic embryos. In addition, the markers identified in this thesis by cDNA array and 14-3-3 expression analyses represent useful tools for further analysis of stress-induced androgenesis and pattern formation in androgenic embryos. Understanding the role of these markers, as well as the role of programmed cell death during exine wall rupture and subsequent pattern formation represents a future challenge for the improvement of quality and yield of androgenic embryos.

Samenvatting

Voor toepassingen in plantenkweek is het van groot belang om de genetische diversiteit in een populatie alsmede de ontwikkeling van homozygote lijnen goed te kunnen beoordelen. Het verkrijgen van homozygote lijnen wordt traditioneel tot stand gebracht door het uitvoeren van terugkruisingen, die echter veel tijd en werkkraft vereisen. In het midden van de zestiger jaren kwam er een nieuwe techniek beschikbaar: de productie van dubbel-haploïde planten afstammend van onvolwassen pollenkorrels, de zogenaamde microsporen. Aangezet door bepaalde ongunstige omgevingsfactoren, kortweg aangeduid als 'stress' aangeduidt, kunnen microsporen hun normale ontwikkelingspatroon verlaten en in plaats daarvan zich ontwikkelen tot embryo's. Dit proces wordt androgenese genoemd (letterlijk: mannelijke schepping). Als gevolg van het spontane proces van verdubbeling van de chromosomen, dat plaats vindt gedurende de vroege stadia van embryo-ontwikkeling, kunnen de individuele microsporen zich in korte tijd ontwikkelen tot dubbel-haploïde planten, die zelf weer in staat zijn zich voort te planten. Tegenwoordig is het verkrijgen van dubbel-haploïde planten als gevolg van androgenese een belangrijke techniek voor zowel het verkrijgen van hybride zaden alsmede voor het beoordelen van genetische diversiteit van een gewas.

Stress wordt meestal beschouwd als de belangrijkste aanleiding voor het aanzetten van de androgene ontwikkeling van microsporen. Afhankelijk van de plantensoort en zelfs de plantenvariëteit zijn verschillende omgevingsfactoren benodigd om het proces dat leidt tot androgenese, efficiënt aan te zetten. Het is echter voor sommige belangrijke landbouwgewassen onmogelijk gebleken ze tot androgenese aan te zetten. Het verbeteren van de protocollen voor de benodigde omgevingsfactoren voor deze gewassen is tot nu gebaseerd op een "probeer maar wat" basis zodat de toepassingen in de plantenkweek tot nu toe sterk beperkt zijn geweest. Voor zowel toegepast als fundamenteel onderzoek is het van het grootste belang om te begrijpen hoe een hooggespecialiseerde cel zoals een onvolwassen pollenkorrel geheel omgeprogrammeerd kan worden tot een embryo. De gerst (*Hordeum vulgare* L.) cultivar Igri wordt beschouwd als een modelplant voor bestudering van androgenese dankzij de hoge efficiëntie van regeneratie die met deze plant kan worden bereikt. Efficiënte androgenese in deze cultivar wordt verkregen door uithongering en hoogsmotische omstandigheden in het middel late- tot late (ML-L) eenkernig stadium van microspore-ontwikkeling. Dit wordt bereikt door een behandeling van de pollendragers (stuifmeeldraden) met een oplossing van een suiker (mannitol).

In dit proefschrift wordt de androgenese van gerst gebruikt als een modelsysteem om meer inzicht te verkrijgen in de moleculaire en cellulaire processen die de omschakeling van de ontwikkeling van een microspore tot een embryo controleren.

De belangrijkste gebeurtenissen op moleculair en cellulair niveau, die karakteristiek zijn voor de verschillende fasen in de ontwikkeling van microsporen naar embryo's, worden middels een overzicht beschreven in hoofdstuk 1. Verder beschrijft dit hoofdstuk de overeenkomsten tussen de moleculaire- en celbiologische aspecten van enerzijds de androgene ontwikkeling en anderzijds die van twee veel bestudeerde modelsystemen, namelijk somatische en zygotische embryogenese. In hoofdstuk 2 is 'time-lapse tracking' van mannitol-behandelde microsporen gebruikt met als doel de morfologie van embryogene cellen te identificeren en vervolgens de ontwikkelingsmechanismen van stress-behandelde microsporen te onderzoeken. De eerste morfologische verandering die geassocieerd is met het embryogene potentieel van microsporen werd vertegenwoordigd door de migratie van de kern naar het centrum van de cel (sterachtige structuur). Dit stadium vertegenwoordigt een overgangsfase tussen gevacuoliseerde en vergrote microsporen na stressbehandeling en de initiatie van celdelingen. Door combinatie van de analyse van de levensvatbaarheid van de aldus onstane structuren en 'cell tracking' experimenten, hebben we laten zien dat positiebepaalde celdood de overgang van multicellulaire structuren in globulaire embryo's tijdens androgenese in gerst markeert. Omdat dit positie-bepaalde celdoodproces tijdens de overgang van multicellulaire structuren in globulaire embryo's een bepalende stap bleek te zijn in de overschakeling van microsporen naar de embryogene ontwikkelingsroute, is dit proces nader gekarakteriseerd in hoofdstuk 3. Tijdens de ontwikkeling van multicellulaire structuren in globulaire embryo's sterft het generatieve celdomein af. Dit proces vertoont bepaalde karakteristieken van geprogrammeerde celdood oftewel een genetisch bepaald mechanisme van zelfdoding door de cel. De resultaten laten zien dat geprogrammeerde celdood een belangrijk aspect is van de embryogene ontwikkelingsroute van gerstmicrosporen. In hoofdstuk 4 is de expressie en de weefselspecificiteit van drie leden (14-3-3A, 14-3-3B en 14-3-3C) van de 14-3-3-familie van regulatie-eiwitten bestudeert met behulp van isoform-specifieke antilichamen. Dit hoofdstuk is samengesteld uit drie onderdelen die elk verschillende aspecten behandelen van 14-3-3-eiwitten in androgenese van gerstmicrosporen. De resultaten, beschreven in dit hoofdstuk, laten zien dat de uitkomst van de ontwikkeling van cellen en patroonvorming gedurende androgenese van gerstmicrosporen geassocieerd is met posttranslationele modificatie van het 14-3-3-eiwit alsmede met ontwikkelingsafhankelijke expressie van de 14-3-3A en 14-3-3C-eiwitten. In hoofdstuk 5 is de 'macro-array' technologie ingezet in combinatie met een specifieke statistische methode, aangeduid als 'principle component analysis', teneinde genexpressieprofielen te karakteriseren die geassocieerd zijn met de omschakeling van de pollenontwikkeling naar de androgene ontwikkelingsroute. Verdere expressie-analyse van een gedeelte van deze genen liet zien dat de inductie van genen coderende voor

alcoholdehydrogenase-3 en een aantal proteolytische enzymen geassocieerd is met het androgene ontwikkelingspotentieel van gerstmicrosporen, terwijl de inductie van genen betrokken bij signaaltransductie en celbescherming waarschijnlijk onderdeel zijn van de respons op stress.

In dit proefschrift wordt een belangrijke vooruitgang in het begrip van de mechanismen, dat aan androgenese van gerstmicrosporen ten grondslag liggen, beschreven. Het gebruik van een techniek die de ontwikkeling van vele cellen tegelijk kan volgen in combinatie met het gebruik van biochemische technieken is hiervoor van groot belang geweest. Dit heeft belangrijke morfologische verschillen aangetoond die het proces van androgenese markeren. Het heeft ook aangetoond dat het proces van gecontroleerde celdood tijdens het uitbreken uit de pollenkorrelwand en de daarop volgende weefselpatroonvorming een belangrijk onderdeel is van androgenese. Daarnaast zijn ook genetische markeringsfactoren geïdentificeerd door de analyse van cDNA en de expressie van het 14-3-3-gen zodat het nu veel makkelijker is geworden om te bepalen wat de gewenste omgevingsfactoren zijn teneinde het proces van androgenese te stimuleren. In de toekomst zal de uitdaging zijn om de functie van deze genetische factoren en geprogrammeerde celdood in het androgenese proces te begrijpen. Dit zal het mogelijk maken een betere kwaliteit en hogere opbrengst van androgenetisch verkregen embryo's te verwezenlijken.

Curriculum vitae

Simone de Faria Maraschin was born on June 21 1976 in Laguna, state of Santa Catarina, Brazil. She attended high school in Porto Alegre, Brazil, at Colégio Jesuíta Anchieta. In March 1994, she started the study of Agriculture Engineering at Universidade Federal do Rio Grande do Sul (UFRGS), Porto Alegre. From June 1996 until February 1999, she dedicated herself to a research training on genetic breeding of *Passiflora* and *Citrus* in the Horticulture Department, Faculty of Agronomy, UFRGS, under the supervision of Prof. Dr. Ana Cunha Dornelles. From March 1999 until December 1999, she was involved in the projects “Rice genetic transformation” and “Chitinase-mediated fungal resistance in plants” as a research trainee in the Laboratory of Plant Molecular Biology, Biotechnology Center, UFRGS, under the supervision of Prof. Dr. Giancarlo Pasquali. On August 21 1999, she graduated in Agricultural Engineering at UFRGS. From March 2000 to August 2004, she worked on her PhD research project in the Center for Phytotechnology, Leiden University/ TNO Institute for Nutrition and Food Research, TNO Department of Applied Plant Sciences, Leiden, The Netherlands, under the supervision of Dr. Mei Wang and Prof. Dr. Herman P. Spaink. From December 2004, she is working as a post-doc in the group of Dr. Pieter Ouwkerk at the Institute of Biology Leiden.

Publications

- Fulgosi H, Soll J, Maraschin SF, Korthout HAAJ, Wang M, Testerink C (2002) 14-3-3 proteins and plant development. *Plant Mol Biol* 50: 1019-1029
- Maraschin SF, Lamers GEM, de Pater BS, Spaink HP, Wang M (2003) 14-3-3 isoforms and pattern formation during barley microspore embryogenesis. *J Exp Bot* 54: 1033-1043
- Maraschin SF, Lamers GEM, Wang M (2003) Cell death and 14-3-3 proteins during the induction of barley microspore androgenesis. *Biologia* 58: 59-68
- Maraschin SF, Louwerse JD, Lamers GEM, Spaink HP, Wang M (2003) Tissue-specific expression of 14-3-3 isoforms during barley microspore and zygotic embryogenesis. *Acta Biol Cracov Bot* 45: 103-106
- Maraschin SF, Vennik M, Lamers GEM, Spaink HP, Wang M (2004) Time-lapse tracking of barley androgenesis reveals position-determined cell death within pro-embryos. *Planta*, *in press*
- Maraschin SF, Gaussand G, Olmedilla A, Pulido A, Lamers GEM, Korthout H, Spaink HP, Wang M (2004) Programmed cell death during the transition from multicellular structures into globular embryos in barley androgenesis. *Planta*, *in press*
- Maraschin SF, Caspers M, Potokina E, Wulfert F, Corredor-Adámez M, Graner A, Spaink HP, Wang M. cDNA array analysis of stress-induced gene expression in barley androgenesis. *Submitted*
- Maraschin SF, Priester W de, Spaink HP, Wang M. Androgenic switch in microspores. *Submitted*
- Kern MF, Maraschin SF, Schrank A, Vainstein MH, Pasquali G. Variable expression levels of a chitinase from *Metarhizium anisopliae* in tobacco plants and its chitinolytic activity against the phytopathogen *Rhizoctonia solani*. *Submitted*

Color Supplement

Chapter 2

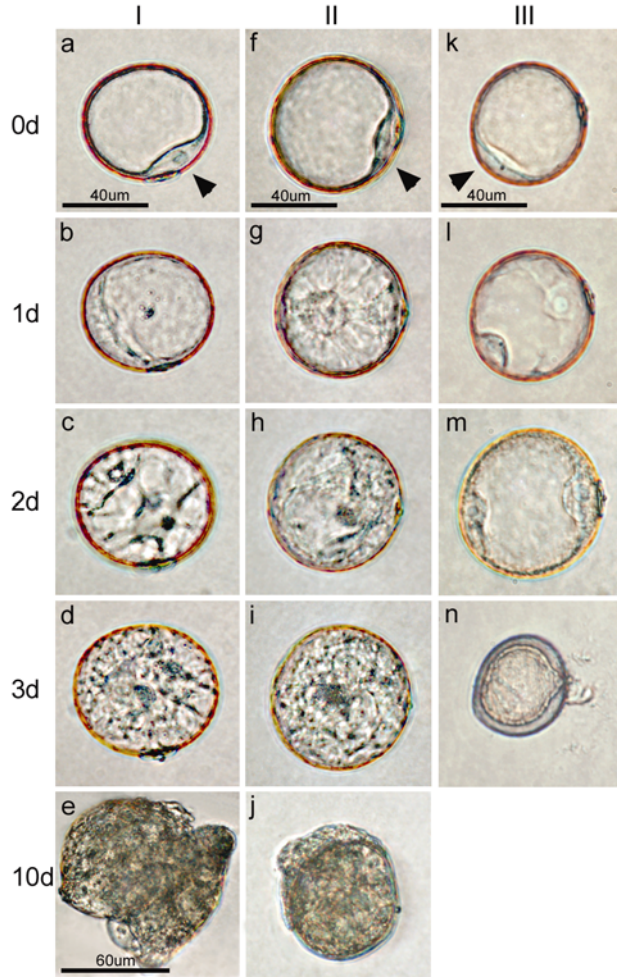


Figure 1

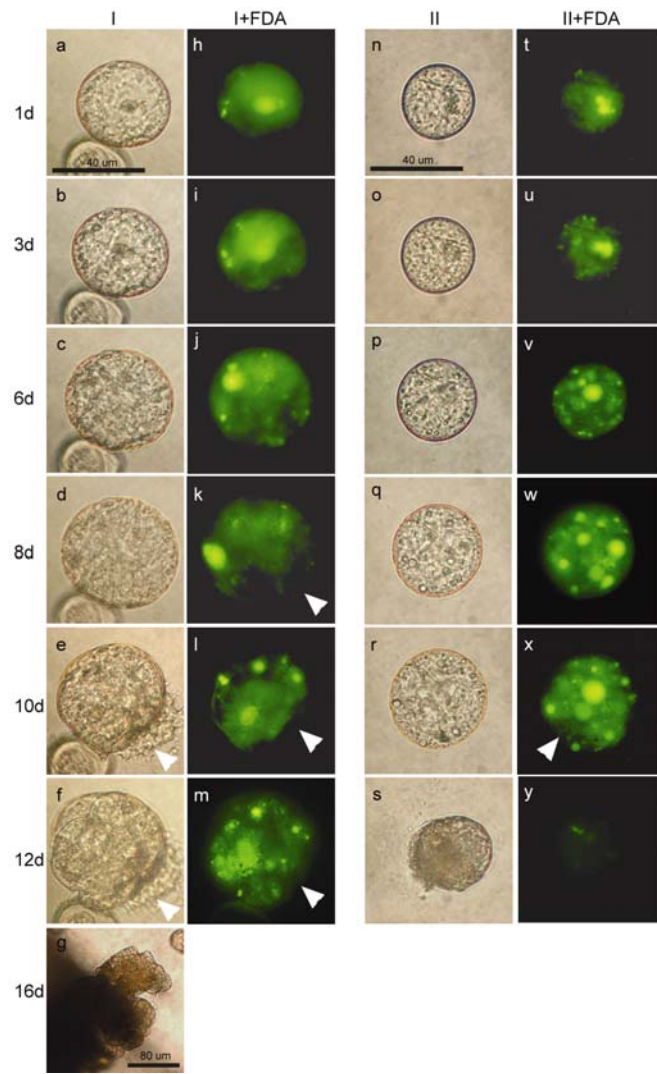


Figure 4

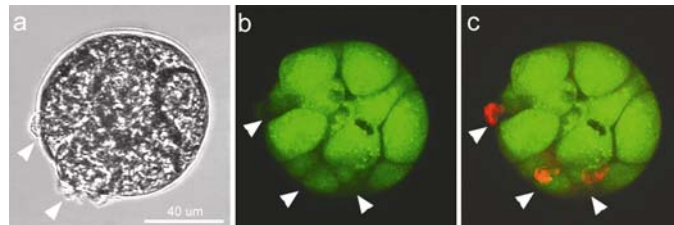


Figure 5

Chapter 3

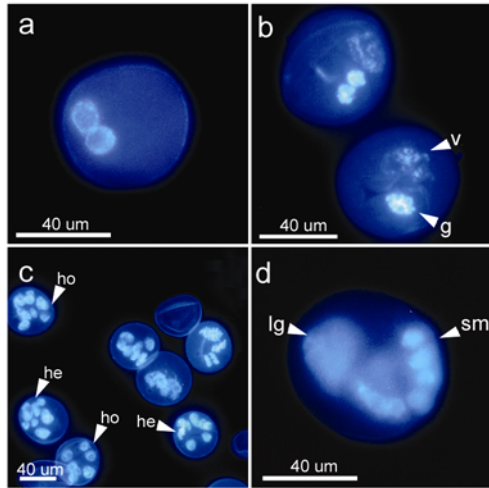


Figure 1

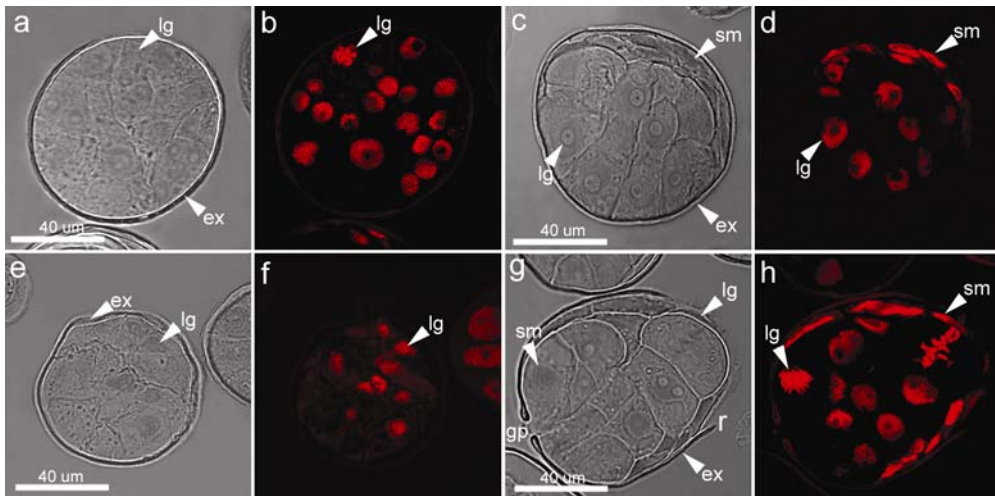


Figure 2

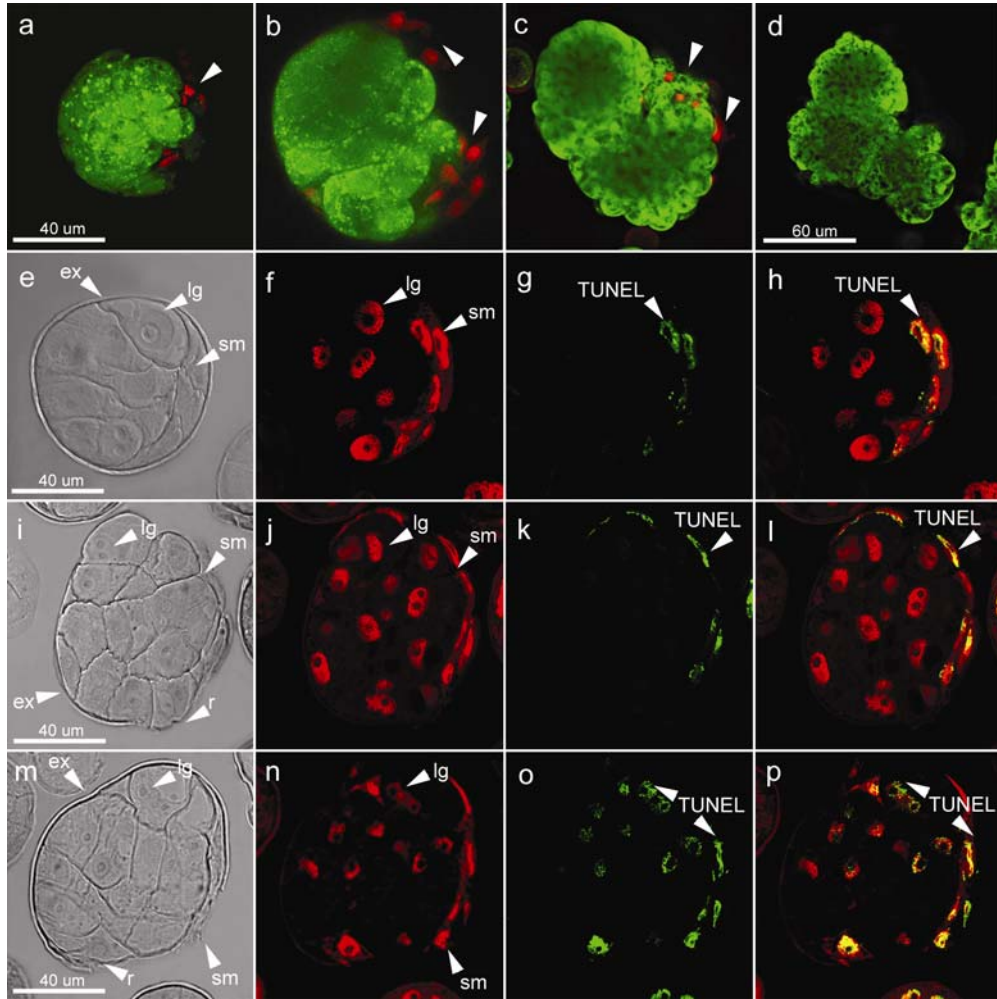


Figure 3

Chapter 4.I

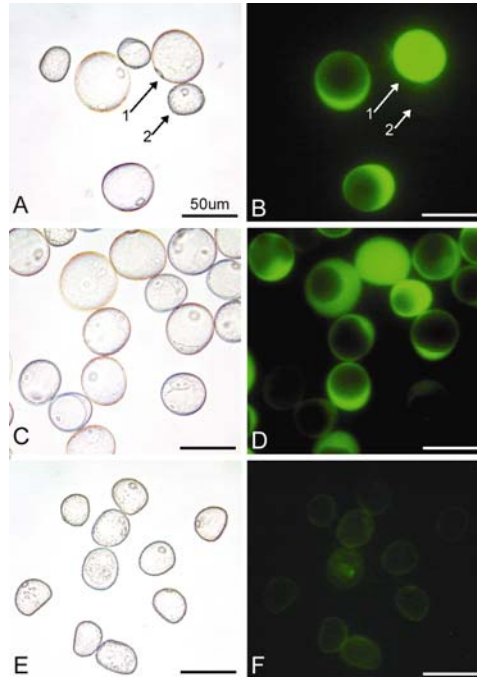


Figure 1

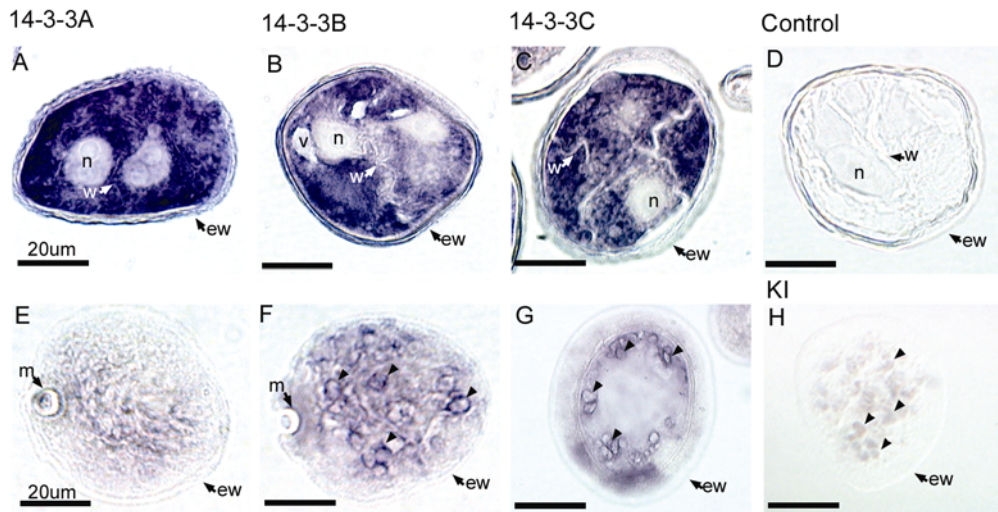


Figure 4

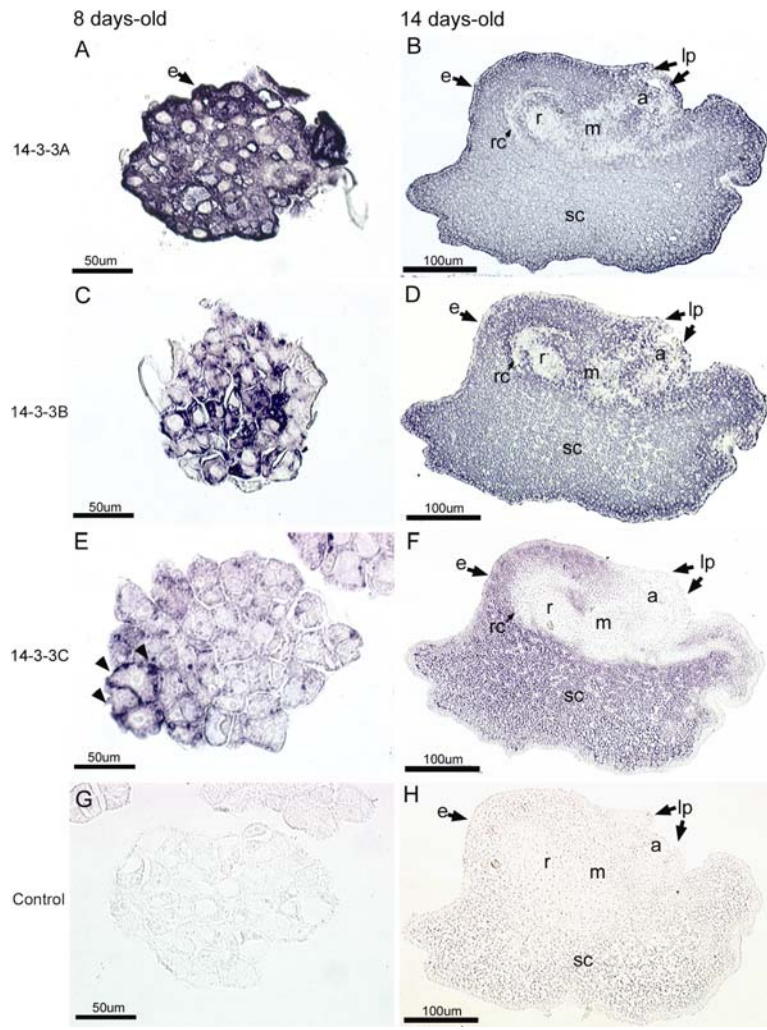


Figure 5

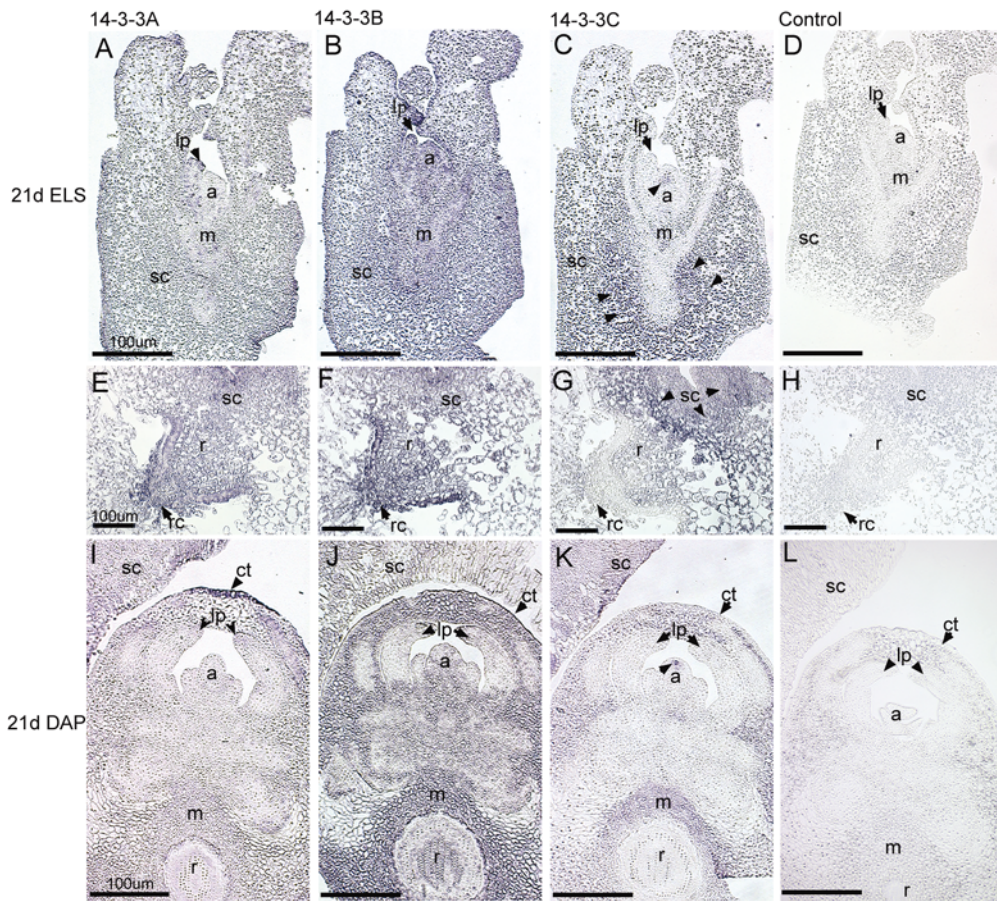


Figure 6

Chapter 4.II

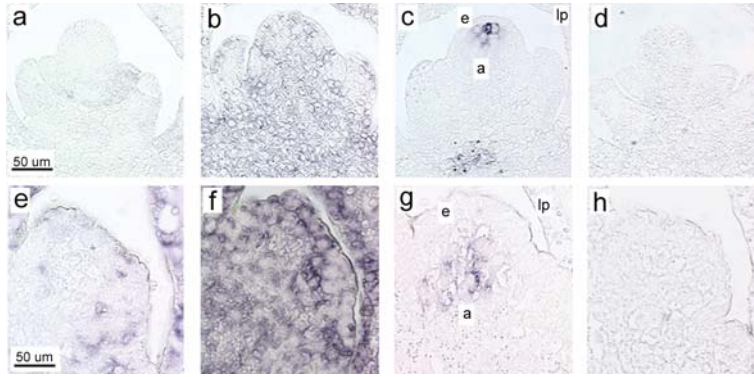


Figure 2

Chapter 4.III

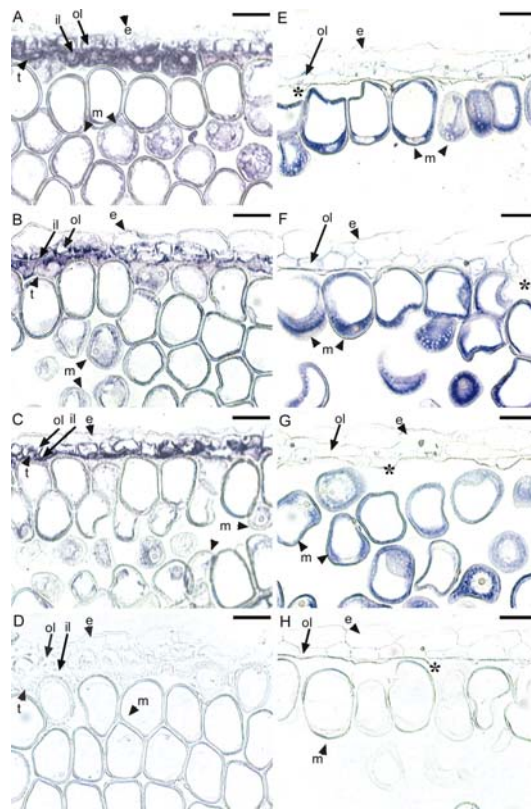


Figure 6

